DISSOLVED ORGANIC CARBON IN AQUITARD ENVIRONMENTS: PROPERTIES, COMPLEXATION, AND TRANSPORT

A Thesis Submitted to the College of
Graduate Studies and Research
In Partial Fulfillment of the Requirements
For the Degree of Doctor of Philosophy
In the Department of Geological Sciences
University of Saskatchewan
Saskatoon

By

THORSTEN N. RESZAT

Keywords: DOC, colloids, transport, complexation, metals

Permission to Use

In presenting this thesis in partial fulfilment of the requirements for a Postgraduate degree from the University of Saskatchewan, I agree that the Libraries of this University may make it freely available for inspection. I further agree that permission for copying of this thesis in any manner, in whole or in part, for scholarly purposes may be granted by the professor or professors who supervised my thesis work or, in their absence, by the Head of the Department or the Dean of the College in which my thesis work was done. It is understood that any copying or publication or use of this thesis or parts thereof for financial gain shall not be allowed without my written permission. It is also understood that due recognition shall be given to me and to the University of Saskatchewan in any scholarly use which may be made of any material in my thesis.

Requests for permission to copy or to make other use of material in this thesis in whole or part should be addressed to:

Head of the Department of Geological Sciences

University of Saskatchewan

114 Science Place

Saskatoon, Saskatchewan

S7N 5E2

ABSTRACT

Clay-rich glacial till aquitards are widespread throughout the northern hemisphere. Due to their low hydraulic conductivity, these geologic units are commonly used to contain wastes. Dissolved Organic Carbon (DOC) in natural environments influences the speciation and mobility of contaminants, such as heavy metals and radionuclides, and is present in high concentrations in clay-rich tills (5 to 150 mg l^{-1}). Detailed knowledge of the influence of DOC on the long-term stability, speciation, and mobility of elements is lacking. Studies in this thesis characterize the properties and function of DOC with respect to element speciation and transport at the King research site, an archetypal clay-till aquitard in Saskatchewan, Canada. Characterization of DOC using Asymmetrical Flow-Field Flow Fractionation (AsFlFFF) with on-line UV and DOC detection demonstrated the molecular weight (M_w) of DOC within the aquitard environment is low, ranging from 1160 to 1286 daltons (Da), and the relative amount of aromatic carbon in aquitard DOC is lower than in surface water DOC. These findings imply the complexation ability of DOC in aquitards is lower than surface water DOC. DOC aromaticity decreased with depth in the aquitard, while M_w remained constant. DOC M_w in other aquitards investigated was comparably low (1470-1630 Da). Coupling AsFlFFF with on-line ICP-MS analysis allowed the identification of Fe, U and Zn associated with the DOC, and demonstrated that <4% of total aqueous elements tested at the King site were complexed with DOC. Experimental and numerical modeling results demonstrate the low masses of metals (Cu, Mn, Mo, Ni, Sr, U and Zn) complexed with the DOC can be attributed to competitive complexation with carbonate and sulphate ligands naturally present in the pore water. The *in-situ* association constant, K_d, for U and Zn as determined by complexation experiments decreased with depth in the aquitard and was attributed to the corresponding decrease in DOC aromaticity. The maximum mass of complexation of U and Zn to DOC takes place at pH 3-6, and decreases above and below this pH range (range tested: pH 1.3-10). These results were supported by geochemical modeling and suggest the complexation of aqueous metals by DOC should be limited in ground water environments of similar chemistries. Laboratory transport studies using double reservoir diffusion cells showed DOC and other similarly sized

colloidal material can diffuse through the matrix at the King site aquitard. The effective pore throat diameter in the matrix media was determined to be 2 - 2.2 nm and travel times of colloids increased with increasing colloidal diameter. Colloids >2 nm were prevented from movement in the till by sieving mechanisms, which suggests bacteria and viruses as well as larger colloids should not migrate through till aquitards. Due to preferential sieving of larger M_w DOC, DOC in aquitard environments is typified by a small diameter compared with surface water DOC, and a small range in hydrodynamic diameter and M_w.

ACKNOWLEDGMENTS

This thesis is a collaborative work, and I am aware that it resulted from the efforts of many people.

I am grateful for my supervisor Dr. M. Jim Hendry, for his guidance and mentoring. His support over the years was invaluable.

I thank my committee and external advisor for their participation in this thesis, which undoubtedly improved this work.

I thank some outstanding professors at this university; especially Dr. Malcolm Reeves and Dr. S. Lee Barbour, whose enthusiasm and expertise in their fields inspired me, instructed me, and helped my growth as a scientist.

I thank many colleagues and friends.

I thank Kristie Bonstrom, for her moral support and understanding during the course of this research. I commend her patience and thank her for humoring my never-ending rambling about the contents of this document.

I especially thank Klaus, Petra, and Tanja, for a lifetime of support and encouragement.

TABLE OF CONTENTS

LIST OF FIGURES

LIST OF TABLES

1.0 INTRODUCTION

1.1 Overview

Dissolved Organic Matter (DOM) is a constituent of the total aqueous carbon pool in ground water and plays an important role in the geochemical and biochemical evolution of ground water (Thurman, 1985a). DOM is usually referred to as DOC (dissolved organic carbon) and is generally comprised of aquatic humic colloids in the form of higher molecular weight humic and fulvic acids and lower molecular weight hydrophilic organic acids (Thurman, 1985a). Operationally defined, DOC is the dissolved fraction of organic carbon that can pass through a 0.45 μm filter (Thurman, 1985b). The majority of organic carbon that is present in this fraction is polymeric organic acids, which are termed humic substances (HS). These organic acids are between 500 and 10,000 daltons (molecular weight) and are complex polyelectrolytes consisting of aromatic and aliphatic carbon chains with carboxylic, phenolic and hydroxyl functional groups (Silverstein et al., 1991; Thurman, 1985a). They typically consist of 50 to 75% of the total dissolved organic compounds in natural waters (Thurman, 1985b). The other fraction of dissolved compounds consists of fatty acids, carbohydrates, amino acids, and hydrocarbons (Kononova, 1966). Larger carbon moieties (>0.45 μm) in natural waters consist of bacteria, phytoplankton and zooplankton (Thurman, 1985b). Figure 1-1 presents a diagram detailing the continuum of organic carbon and other common ground water colloidal material.

The amount of DOC in natural waters varies greatly, from a few mg l^{-1} to hundreds of mg l^{-1}, but generally the highest amounts of DOC are found in organic rich bogs and aquitard environments (Thurman, 1985b). In addition, grassland soils have a higher DOC content than forest soils due to larger quantities of raw material that is available for HS synthesis (Stevenson, 1994). Ground water (aquifers) and seawater contain an average of 0.5 mg l^{-1} up to over 30 mg l^{-1} in swamps and bogs (Thurman,

1985b). Streams and lakes contain an average of 2 to 10 mg l^{-1} (Thurman, 1985b). In some extreme cases, DOC concentrations can be as great as 200 mg l^{-1} in organic- and clay-rich aquitards (Artinger et al., 1998b; Hendry and Wassenaar, 2005a). High DOC concentrations in these waters facilitate their characterization; therefore the majority of the research in this thesis will focus on pore waters from unlithified fine-grained sedimentary aquitard systems, which are widespread throughout North America (Hendry et al., 1986; Husain et al., 2004; Rodvang and Simpkins, 2001; Shaw and Hendry, 1998a). In addition, studies will focus on aquitard systems because they have been suggested as possible repositories for nuclear waste, due to their low hydraulic conductivities (Shaw and Hendry, 1998a; Shaw and Hendry, 1998b).

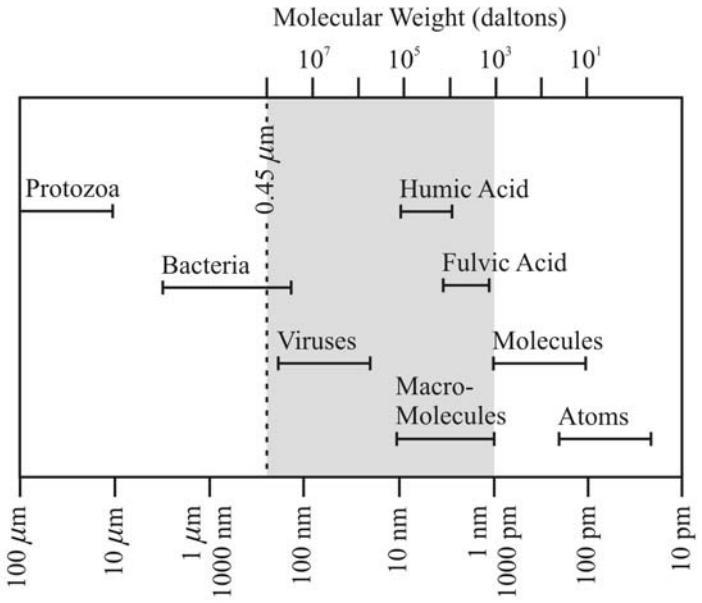

Figure 1-1. The continuum of dissolved, colloidal, and particulate matter within natural waters. Shaded area from 1 – 450 nm is the generally accepted range in colloid size. Adapted from Matthess and Peckdeger, (1985) and Thurman (1985).

The geochemical and transport processes of DOC components in the subsurface are of interest because these humic colloids have been reported to complex and transport heavy metals and radionuclides (Christensen et al., 1996; Lenhart et al., 2000; Mantoura et al., 1978). Dissolved Organic Carbon may also exert an important control on microbial redox processes in ground water systems, buffer the pH of ground waters, and

participate in mineral dissolution/precipitation reactions (Cronan and Aiken, 1985; Deng and Stumm, 1993; Macgowan and Surdam, 1990; Wassenaar et al., 1991). Actinides and radionuclides complex with mobile DOC, and thus metals and radionuclide transport may be facilitated by the presence of DOC in ground waters (Artinger et al., 1998a; Dearlove et al., 1991; McCarthy et al., 1993).

The characterization of DOC properties, primarily molecular weight and reactivity, is necessary when attempting to quantify complexation and transport behavior of DOC in natural and process affected waters.

1.2 Research Objectives

A wealth of knowledge on DOC function in the environment exists. However the majority of experiments are conducted on isolated and extracted DOC in simplified and controlled chemical environments. Information on DOC complexation and structure of DOC in field-based natural systems is lacking. In addition the control on transport of DOC in aquitard environments has not been examined thoroughly. DOC has been studied in surface water environments but has not garnered as much interest in certain ground water environments such as aquitards. Studies on DOC function within a natural system are lacking to a large degree because of the difficulty in characterizing this complex and polymeric substance. The development and application of chromatographic separation systems such as size exclusion chromatography, gel permeation chromatography and field flow fractionation (FFF), and use of a variety of on-line detection systems have made possible the rapid and effective characterization of DOC in its natural environment. The research completed for this thesis relies heavily on Asymmetrical Flow Field-Flow Fractionation (AsFlFFF), a relatively new method in the FFF family of separation methods.

AsFlFFF had a number of advantages over similar separation methods such as size-exclusion chromatography (SEC) for this work. The carrier ionic strength for AsFlFFF is much lower than that required for SEC and can be similar to the sample, which may minimize the possibility of sample alteration during fractionation. Also, the higher ionic strengths needed to prevent interactions of the sample with the SEC resin

are problematic for detection systems because of salt build-up on the cones and plasma loading within ICP-MS detectors. In general there are fewer chemical interactions between the sample and the FFF channel than with the SEC resin, thus making the molecular weight measurements potentially more accurate. Finally, FFF techniques give direct measure of aqueous diffusion coefficient.

The goal of this research was to develop and apply a systematic and scientific approach for characterizing the properties of DOC relevant to contaminant complexation and mobility within ground water environments. This work focuses on DOC in low permeability ground water environments, specifically on a Saskatchewan clay-rich glacial till. The primary research site is the King Site, an aquitard research site 100 km south of Saskatoon, Saskatchewan, Canada. This site was chosen as the focus of the study because the geology and hydrogeology is simple and well characterized, as are the solute transport mechanisms (Hendry and Wassenaar, 1999b; Shaw and Hendry, 1998a), the inorganic geochemistry of the aquitard porewater (Hendry and Wassenaar, 2000b; Hendry et al., 2000), and the microbiology of the aquitard (Lawrence et al., 2000b). In addition, the site is instrumented with high quality piezometers (Wassenaar and Hendry, 1999). DOC concentrations have been monitored at site since 1995, and preliminary research has been conducted on DOC from this site (Hendry et al., 2003b).

This thesis addresses three main issues of importance to determining how DOC migrates in low permeability, clay-rich aquitard environments and if DOC facilitates the transport of metals in these environments. Specifically, the thesis addresses i) the molecular weight and structural characteristics of the DOC, ii) complexation of metals by DOC, and iii) the mobility and transport of DOC in clay-rich aquitards. To achieve these goals, the study took the following approach.

1. Acquisition of samples from several research sites, including the King Site, Warman Site (Saskatchewan), and Chalco Aquitard (Mexico City).

2. Optimization of an AsFlFFF system to separate and characterize DOC in different environments.

3. Modification of a Total Organic Carbon analyzer to operate as an on-line DOC detector with AsFlFFF and UV detection.

4. Characterization of the weight averaged molecular weight (M_w), number averaged molecular weight (M_n), and polydispersity (M_w/M_n) of DOC from sampled ground waters using UV and DOC detection.

5. Determination of the reactivity of DOC from the King Site using coupled UV and DOC detection systems.

6. Development of a method to combine ICP-MS with the AsFlFFF system for on-line detection of metals.

7. Determination of the amount and type of metals complexed to DOC from the King Site ground waters.

8. Using properties of DOC determined in previous experiments to set up a representative complexation model for metal – DOC interactions.

9. Determination of the controls on DOC and other colloid transport and migration within low permeability ground water environments.

The findings of this research are presented in the form of three peer reviewed scientific publications (Chapters 2-4), and a manuscript which is in preparation for submission for publication, and is in manuscript format. All field work (aside from collection of samples from the Chalco Aquitard), instrumentation modifications, laboratory studies, data analysis, modeling and manuscript preparation for Chapters 2, 4, and 5 were performed by the author. The manuscript obtained from work done in Chapter 3 was a collaborative effort by several authors (see reference (Ranville et al., 2007)). This author collected samples, performed all lab experiments, and conducted a portion of the data analysis for this research. Editing of all manuscripts prior to submission was performed by Dr. M. Jim Hendry.

The manuscripts presented in this thesis all follow a logical progression and together fully characterize DOC for the purpose of contaminant complexation and mobility in aquitards.

A method of characterizing DOC using AsFlFFF was used with on-line UV and DOC analysis is presented in Chapter 2. This chapter describes the modification of a conventional Total Organic Carbon (TOC) analyzer for on-line application as a detection system. This was the first successful application of DOC analysis with an AsFlFFF system. This chapter demonstrates that TOC detection is a more effective characterization tool for DOC molecular weight determination that the conventional UV light provides. In addition the coupling of data derived from UV and TOC detection provides valuable insights into the properties of surface water and ground water DOC. The chapter presents the results obtained from humic standards, ground waters, and surface waters. Information on detector modifications and more detailed results not discussed in the manuscript are presented in Appendix 2. The information on structure and reactivity of DOC obtained from experiments in this chapter were instrumental to the application of metal-DOC complexation models in Chapter 4. Chapter 2 was published in *Analytical Chemistry* (Reszat and Hendry, 2005).

Chapter 3 presents the results of a preliminary examination of uranium complexation by DOC from the King Site. Previous studies determined that DOC is one of the primary ligands for metal complexation in natural water samples. This chapter shows that this may not be the case for all DOC and all chemical environments. Results of this experiment showed that DOC from the King Site complexes a minimal amount (<3 %) of uranium present in the clay-rich till. These results were contrary to what was expected. The minimal amount of metal-DOC complexation was more important from a waste disposal point of view than if considerable complexation had occurred. Results from this manuscript showed that more research was necessary to verify the observed data and examine metal-DOC complexation in more detail. This chapter was published in the *Journal of Contaminant Hydrology* (Ranville et al., 2007).

The results from a more detailed investigation of metal-DOC complexation at the King Site are presented in Chapter 4. This study confirms the results presented in Chapter 3 and expands on those findings. It addresses the complexation of a wider range of elements to DOC and does so across a more detailed pore water – depth profile than in Chapter 3. In addition, Chapter 4 also examines the effects of pH on U complexation to DOC and the kinetics of the complexation/dissociation of U and Zn to DOC. Further, in addition to the on-line UV detection method used in Chapter 3, this study applies on-line TOC analysis. It also determines K_d values for U and Zn on the DOC with depth at the research site and provides a potential explanation for these values. Lastly, Chapter 4 provides a comparison between the binding of U and Zn in a natural ground water system to that in an ideal system containing only fulvic acid and elements (with no competitive complexation present). These results may help explain why lab based studies often document considerable metal complexation with DOC while under field conditions this may not be the case. This manuscript is in press in *Ground Water* (Reszat and Hendry, 2007b).

The results of Chapters 3 and 4 show minimal metal – DOC complexation at the King Site. However, facilitated transport of metals by colloids such as DOC may occur in other ground water environments. Colloidal transport has been examined in coarse grained and fractured sediments, and facilitated metal transport has been reported, but the transport of colloids in fine-grained low permeability media has not been performed. Chapter 5 presents the results of laboratory diffusion tests on clay till samples from the King site using a variety of types and diameters of colloids to define the controls on the distribution and migration of DOC in aquitards, and to define what size colloidal material will be able to move through these environments. A pore throat cut-off was determined for the clay-rich till, and it is proposed that the diameter of DOC may be a proxy to estimate the pore throat diameter of low-permeability environments. This manuscript has not been submitted to a journal as of yet.

1.3 References

Artinger, R., Kienzler, B., Schussler, W., and Kim, J.I., 1998a, Effects of humic substances on the Am-241 migration in a sandy aquifer: column experiments with Gorleben groundwater/sediment systems: Journal of Contaminant Hydrology, v. 35, p. 261-275.

Artinger, R., Kienzler, B., Schüßler, W., and Kim, J.I., 1998b, Effects of humic substances on the 241Am migration in a sandy aquifer: Column experiments with the Gorleben groundwater/sediment systems: Journal of Contaminant Hydrology, v. 35, p. 261-275.

Christensen, J.B., Jensen, D.L., and Christensen, T.H., 1996, Effect of dissolved organic carbon on the mobility of cadmium, nickel and zinc in leachate polluted groundwater: Water Research, v. 30, p. 3037-3049.

Cronan, C.S., and Aiken, G.R., 1985, Chemistry and Transport of Soluble Humic Substances in Forested Watersheds of the Adirondack Park, New-York: Geochimica et Cosmochimica Acta, v. 49, p. 1697-1705.

Dearlove, J.P.L., Longworth, G., Ivanovich, M., Kim, J.I., Delakowitz, B., and Zeh, P., 1991, A Study of Groundwater-Colloids and Their Geochemical Interactions with Natural Radionuclides in Gorleben Aquifer Systems: Radiochimica Acta, v. 52-3, p. 83-89.

Deng, Y.W., and Stumm, W., 1993, Kinetics of Redox Cycling of Iron Coupled with Fulvic-Acid: Aquatic Sciences, v. 55, p. 103-111.

Hendry, M.J., Cherry, J.A., and Wallick, E.I., 1986, Origin and Distribution of Sulfate in a Fractured Till in Southern Alberta, Canada: Water Resources Research, v. 22, p. 45-61.

Hendry, M.J., Ranville, J.R., Boldt-Leppin, B.E.J., and Wassenaar, L.I., 2003, Geochemical and transport properties of dissolved organic carbon in a clay-rich aquitard: Water Resources Research, v. 39, p. 1194-1203.

Hendry, M.J., and Wassenaar, L., 2005, Origin and migration of dissolved organic carbon fractions in a clay-rich aquitard: 14C and delta13C evidence: Water Resources Research, v. 41.

Hendry, M.J., and Wassenaar, L.I., 1999, Implications of the distribution of delta-D in pore waters for groundwater flow and the timing of geologic events in a thick aquitard system. Water Resources Research, v. 35, p. 1751-1760.

—, 2000, Controls on the distribution of major ions in pore waters of a thick surficial aquitard: Water Resources Research, v. 36, p. 503-513.

Hendry, M.J., Wassenaar, L.I., and Kotzer, T., 2000, Chloride and chlorine isotopes (Cl-36 and delta Cl-37) as tracers of solute migration in a thick, clay-rich aquitard system: Water Resources Research, v. 36, p. 285-296.

Husain, M.M., Cherry, J.A., and Frape, S.K., 2004, The persistence of a large stagnation zone in a developed regional aquifer, southwestern Ontario: Canadian Geotechnical Journal, v. 41, p. 943-958.

Kononova, M.M., 1966, Soil Organic Matter: Its Nature, Its Role in Soil Formation and in Soil Fertility: London, Pergamon Press, 544 p.

Lawrence, J.R., Hendry, M.J., Wassenaar, L.I., Germida, J.J., Wolfaardt, G.M., Fortin, N., and Greer, C.W., 2000, Distribution and biogeochemical importance of bacterial populations in a thick clay-rich aquitard system: Microbial Ecology, v. 40, p. 273-291.

Lenhart, J.J., Cabaniss, S.E., MacCarthy, P., and Honeyman, B.D., 2000, Uranium(VI) complexation with citric, humic and fulvic acids: Radiochimica Acta, v. 88, p. 345-353.

Macgowan, D.B., and Surdam, R.C., 1990, Carboxylic-Acid Anions in Formation Waters, San Joaquin Basin and Louisiana Gulf-Coast, USA - Implications for Clastic Diagenesis: Applied Geochemistry, v. 5, p. 687-701.

Mantoura, R.F.C., Dickson, A., and Riley, J.P., 1978, Complexation of Metals with Humic Materials in Natural-Waters: Estuarine and Coastal Marine Science, v. 6, p. 387-408.

McCarthy, J.F., Williams, T.M., Liang, L., Jardine, P., Jolley, L.W., Taylor, D.L., Palumbo, A.V., and Cooper, L.W., 1993, Mobility of natural organic matter in a sandy aquifer: Environ. Science and Technology, v. 27, p. 667-676.

Ranville, J.F., Hendry, M.J., Reszat, T.N., Xie, Q., and Honeyman, B.D., 2007, Quantifying uranium complexation by groundwater dissolved organic carbon using asymmetrical flow field-flow fractionation: Journal of Contaminant Hydrology, v. 91, p. 233-246.

Reszat, T.N., and Hendry, M.J., 2005, Characterizing Dissolved Organic Carbon Using Asymmetrical Flow Field-Flow Fractionation with On-Line UV and DOC Detection: Analytical Chemistry, v. 77, p. 4194-4200.

—, 2007, Complexation of Aqueous Elements by DOC in a Clay Aquitard: Ground Water, v. In Press.

Rodvang, S.J., and Simpkins, W.W., 2001, Agricultural contaminants in Quaternary aquitards: A review of occurrence and fate in North America: Hydrogeology Journal, v. 9, p. 44-59.

Shaw, J., and Hendry, M.J., 1998a, Groundwater flow in a thick clay till and clay bedrock sequence in Saskatchewan, Canada: Canadian Geotechnical Journal, v. 35, p. 1041-1052.

Shaw, R.J., and Hendry, M.J., 1998b, Hydrogeology of a thick clay till and Cretaceous clay sequence, Saskatchewan, Canada: Canadian Geotechnical Journal, v. 35, p. 1041-1052.

Silverstein, R.M., Bassler, G.C., and Morrill, T.C., 1991, Spectrometric Identification of Organic Compounds: New York, John Wiley and Sons, 419 p.

Stevenson, F.J., 1994, Humus Chemistry. Genesis, Composition, Reactions: New York, John Wiley & Sons, 496 p.

Thurman, E.M., 1985a, Humic substances in groundwater, *in* MacCarthy, P., ed., Humic substances in soil sediment and water: Geochemistry, isolation, and characterization, John Wiley and Sons, p. 87-103.

—, 1985b, Organic Geochemistry of Natural Waters: Dordrecht, Martinus Nijhoff/Dr W. Junk Publishers, 497 p.

Wassenaar, L.I., Aravena, R., Fritz, P., and Barker, J.F., 1991, Controls on the transport and carbon isotopic composition of dissolved organic carbon in a shallow groundwater system, Central Ontario, Canada: Chemical Geology, v. 87, p. 39-57.

Wassenaar, L.I., and Hendry, M.J., 1999, Improved piezometer construction and sampling techniques to determine pore water chemistry in aquitards: Ground Water, v. 37, p. 564-571.

2.0 CHARACTERIZING DISSOLVED ORGANIC CARBON USING ASYMMETRICAL FLOW FIELD-FLOW FRACTIONATION WITH ON-LINE UV AND DOC DETECTION

2.1 Abstract

A method of characterizing dissolved organic carbon (DOC) by Asymmetrical Flow Field-Flow Fractionation with on-line UV and DOC detection is described and applied to standards and natural water samples. Poly(styrene sulphonate) polymer standards, Suwannee River humic standards, and naturally occurring surface water and ground water DOC were analyzed using this coupled detection technique. Molecular weight determinations in the samples and standards were 6-30% lower with DOC analysis than UV analysis. This difference was attributed to the insensitivity of the latter technique to non-aromatic carbon and suggests the molecular weight determined with the DOC detector is a more accurate representation of the actual molecular weight of the DOC. A normalized intensity comparison (NIC) method was proposed to distinguish differences in the relative amounts of aromatic and aliphatic carbon in DOC by comparing the two detector responses. The NIC method was applied to yield an average aromatic content of the bulk DOC and to detail the aromatic content over a range of molecular weights in a single DOC fraction.

2.2 Introduction

Naturally occurring dissolved organic matter (DOM) is ubiquitous in terrestrial and aquatic environments (Aravena et al., 1995; Crum et al., 1996; McCarthy et al., 1993; Thurman, 1985b). DOM is frequently reported as dissolved organic carbon (DOC, ≤0.45 μm filtrate) and is dominantly comprised of aquatic humic colloids in the form of higher molecular weight humic acids (HA) and fulvic acids (FA), and lower molecular weight hydrophilic organic acids (Thurman, 1985a). Types of DOC (e.g., aquatic FA)

play an important role in the geochemistry of pollutants because they can form metal-ligand complexes (Means et al., 1987), enhance the solubility of non-polar organic contaminants(Chiou et al., 1986), influence colloid stability (Ranville and Macalady, 1997), and participate in redox reactions (Aravena et al., 1995; Crum et al., 1996; Scott et al., 1998; Thurman, 1985b).

If various components of DOC (with different chemistry) are significantly different in molar mass, then the molecular weight of DOC components can be indirectly attributed to distinct structure and functional group concentrations. Determination of the molecular weights of components comprising the DOC yields information on the type of DOC present. This, in turn, can indicate how the DOC will function in the environment. For example, determining the type of DOC present in natural waters can help identify the complexation ability of DOC fractions (Stevenson, 1985). Determining the molecular weight of DOC in ground water systems may also yield valuable insight into the effective porosity of the associated porous media (Hendry et al., 2003).

The molecular weight of DOC has been measured using a variety of methods. The most common of these methods are size exclusion chromatography (Her et al., 2002a; Perminova et al., 2003), gel permeation chromatography (Kim et al., 1990), sequential ultrafiltration (Assemi et al., 2004), and field-flow fractionation (Assemi et al., 2004; Beckett et al., 1987; Benedetti et al., 2002; Dycus et al., 1995; Schimpf and Wahlund, 1997). The field-flow fractionation (FFF) technique is the gentlest method available for separations, being relatively non-destructive to samples. Other advantages include flexibility and ease of use with different carriers and membranes, rapid measurements, minimal cleanup between sample runs, and the widest dynamic operating range in terms of M_w of any separation method.

Identification and molecular weight characterization of DOC is commonly determined using UV detection in the range of 254 and 270 nm. Adsorption is associated with chromophores such as C=C and C=O double bonds, aromatic rings and phenolic functional groups (Silverstein et al., 1991; Thurman, 1985a). However, UV

spectroscopy may not be an accurate method to characterize molecular weights of DOC as the majority of DOC contains unsaturated bonds that can not be resolved with UV detection (Harvey et al., 1983; Malcolm, 1985; Tan, 2003). An alternate approach to UV-based detection systems is to couple a DOC analyzer with HPLC-size exclusion chromatography and gel chromatography (Her et al., 2002a; Her et al., 2002b; Huber and Frimmel, 1994). To date, studies using FFF have used only UV methods for DOC characterization and identification (Beckett et al., 1987; Benedetti et al., 2002; Dycus et al., 1995; Geckeis et al., 2003; Hassellov et al., 1999; Lyven et al., 2003; Thang et al., 2001).

Our primary objective was to develop a method to accurately characterize DOC in surface water and ground water samples by modifying and optimizing a conventional total organic carbon (TOC) analyzer for use with a FFF–UV system. Secondary objectives were to compare results of the FFF-DOC to those of FFF-UV and develop and apply an interpretive method to utilize both continuous DOC and UV data. The objectives were attained using surface water and ground water samples with concentrations of DOC ranging from 18-136 mg l^{-1}.

2.3 Method Development

2.3.1 Instrumentation Setup.

Separation experiments were conducted using an Asymmetrical Flow Field-Flow Fractionation (AsFlFFF) system (model HRFFF 10.000) from Postnova Analytics (FFFractionation, Salt Lake City, Utah). The PC controlled instrumentation consisted of an arrangement of pumps, an AsFlFFF channel, and a vacuum degasser (to remove air bubbles from the carrier solution that may interfere with separation efficiency in the AsFlFFF channel). The AsFlFFF system primarily separates particles by differences in their aqueous diffusion coefficient. Aqueous diffusion coefficient can be related to molecular weight by determining the retention times of known molecular weight standards having properties similar to DOC and through FFF theory (Beckett et al., 1987). Particles, in this case DOC, are detected as they elute from the system after fractionation. The resulting plots of detector intensity vs. time, called fractograms,

consist of two regions: the void peak, which may contain some undifferentiated low molecular weight ligands, and the colloidal peak(s). To ensure organic material of interest was not lost through the membrane into the cross flow during analysis, the AsFlFFF channel was fitted with regenerated cellulose acetate membranes (Millipore Corp.) with a nominal molecular weight cutoff of 1000 daltons (Da). A Rheodyne 100 µL manual sample injection loop was used to inject filtered (<0.45 µm) water samples into the AsFlFFF. The theory and application of AsFlFFF are presented elsewhere (Schimpf and Wahlund, 1997; Wahlund, 2000).

After separation of the DOC with the AsFlFFF, the sample stream was passed through a UV detector (Postnova Analytics, 254 nm). Ultraviolet measurements were made at one second intervals with data acquisition software provided by Postnova Analytics (NovaFFF version 3.14). After UV detection, the sample stream was pumped into a modified TOC analyzer (Sievers 800 Turbo Total Organic Carbon analyzer; Ionics Instrument Business Grp., Boulder CO). This analyzer was selected because: (1) it allowed continuous flow analysis; (2) the time between analyses was rapid (4 sec.), thus allowing the effective resolution of the DOC peaks; and (3) detection limits were in the ppb range, which allowed for analysis of low concentrations DOC waters. Upon entering the TOC analyzer, the sample stream was acidified with 6M phosphoric acid at a flow rate of 1.50 μl min^{-1} using an automated syringe dosing system. All inorganic carbon is removed from the carrier solution and sample using a second vacuum degasser (a modified Sievers Inorganic Carbon Removal (ICR) module). This step was necessary due to the high dissolved carbonate content (i.e., 750 to 780 mg l^{-1} as $CaCO_3$) in the ground water DOC samples being analyzed (Hendry and Wassenaar, 2000). Another syringe dosing system added 15% ammonium persulphate at a flow rate of 0.50 μl min^{-1} to the sample and all of the organics are oxidized to CO_2 gas in a UV reactor. A conductivity sensor is used to measure the amount of CO_2 gas, which diffused through a selective membrane. DOC data were collected at 4 second intervals (maximum detection speed of Turbo TOC analyzer) using the same data acquisition software as for UV detection.

2.3.2 Modifications to the TOC Analyzer.

The TOC analyzer detects DOC via UV/persulphate wet oxidation. The detector contains two channels: an inorganic carbon (IC) channel and a total carbon (TC) channel. TOC is normally determined as the difference between TC and IC. However, for this application, the IC channel was removed to allow analysis of smaller sample volumes, and only the TC signal was collected.

The analyzer is designed for flow rates between 30 to 220 ml min^{-1}. Because sample flow rates from the AsFlFFF system range between 0.5 and 1.5 ml min^{-1}, we retrofitted the TOC analyzer plumbing with 0.05" ID PEEK tubing and 0.1" ID stainless line (Upchurch Scientific). We also disassembled the separate ICR module and placed it inside the TOC analyzer compartment to reduce potential band broadening in the DOC signal because of an increased sample flow path. More detail on the Sievers Turbo TOC analyzer can be found elsewhere (Her et al., 2002b). The TOC analyzer is referred to hereafter as a DOC detector.

2.3.3 System Optimization and Calibration.

We assessed a range of run conditions and 5 possible carrier solutions: tris(hydroxymethyl)aminomethane (Tris – $NH_2C(CH_2OH)_3$), the surfactant FL-70 (both chosen due to use in previous FFF studies (Beckett et al., 1987; Dycus et al., 1995)), potassium hydrogen phthalate ($HOCOC_6H_4COOK$), ammonium acetate ($NH_4C_2H_3O_2$), NaCl, and Na_2SO_4 (last two tested to minimize potential alterations of the DOC attributed to changes in ionic strength or chemical composition of the water-DOC system during the fractionation process). Sodium azide (NaN_3) (0.003M) was added to the carrier solutions during all tests to reduce biological activity in the AsFlFFF channel. All reagents were from Merck Inc. (Darmstadt, Germany). Our objective was to determine conditions that maximized separation of the void peak from the DOC peak in both detectors; the M_w difference between the two regions was determined to be about 500 Da. Three of the carrier solutions tested contained carbon. These carriers increased the baseline of the DOC detector and decreased the sensitivity of the instrument. Optimal separation efficiencies (i.e., peak intensities and retention times on the AsFlFFF

channel) were attained using run conditions outlined in Table 2-1 and carrier compositions of 0.001M NaCl and 0.005M Na_2SO_4 (data not presented). Because the natural ground water samples being analyzed were dominated by Na^+ and SO_4^{2-} (Hendry and Wassenaar, 2000), we selected Na_2SO_4 as the carrier solution for our subsequent experiments. Using a Na_2SO_4 carrier with the instrument conditions as outlined allowed for accurate detection of samples with DOC concentrations as low as 3-4 mg l^{-1} (data not presented). Analysis of waters with DOC lower than this could be accomplished if the samples were pre-concentrated before analysis or if a larger injection loop was used. All calibration and subsequent analyses were performed in triplicate and the fractograms averaged.

Table 2-1: Operating Conditions for the AsFlFFF-DOC-UV system.

Laminar In Flow	5.00 ml min^{-1}
Laminar Out Flow	1.50 ml min^{-1}
Cross Flow	3.50 ml min^{-1}
Cross Flow	70 %
Carrier Solution	0.005*M* Na_2SO_4 + 0.003*M* NaN_3
Injection Volume	100 μl
Channel Length	26 cm
Channel Breadth at L=0 cm	1.4 cm
Channel Breadth at L=26 cm	0.1 cm
Channel Thickness	0.0246 cm
UV Intensity	1.0 A.U.
DOC Acid Flow Rate	1.50 μl min^{-1}
DOC Peroxydisulphate Flow Rate	0.50 μl min^{-1}

Because sodium poly(styrene sulphonate) (PSS) standards have been used to represent DOC in FFF analysis (Beckett et al., 1987; Benedetti et al., 2002; Chin et al., 1994; Dycus et al., 1995; Geckeis et al., 2003; Lyven et al., 2003; Thang et al., 2001), we selected four PSS standards (American Polymer Standards Corp.; weight averaged molecular weight (M_w) of 840, 1430, 4800, and 6500 Da) for system calibration. Standards were prepared to 50 mg l^{-1}. In both DOC and UV fractograms, retention time of the colloidal peak was used to calculate a weight averaged retention time (t_{rw}) in seconds using:

$$t_{rw} = \frac{\sum h_i t_{ri}}{\sum h_i}, \qquad [2\text{-}1]$$

where h_i is the intensity of the detector signal of ith molecule and t_{ri} is the retention time of the ith molecule. We plotted the calculated t_{rw} value against the M_w reported by American Polymer Standards Corp. to create molecular weight calibration curves for both the UV and DOC detectors (log retention time vs. log molecular weight; Figure 2-1).

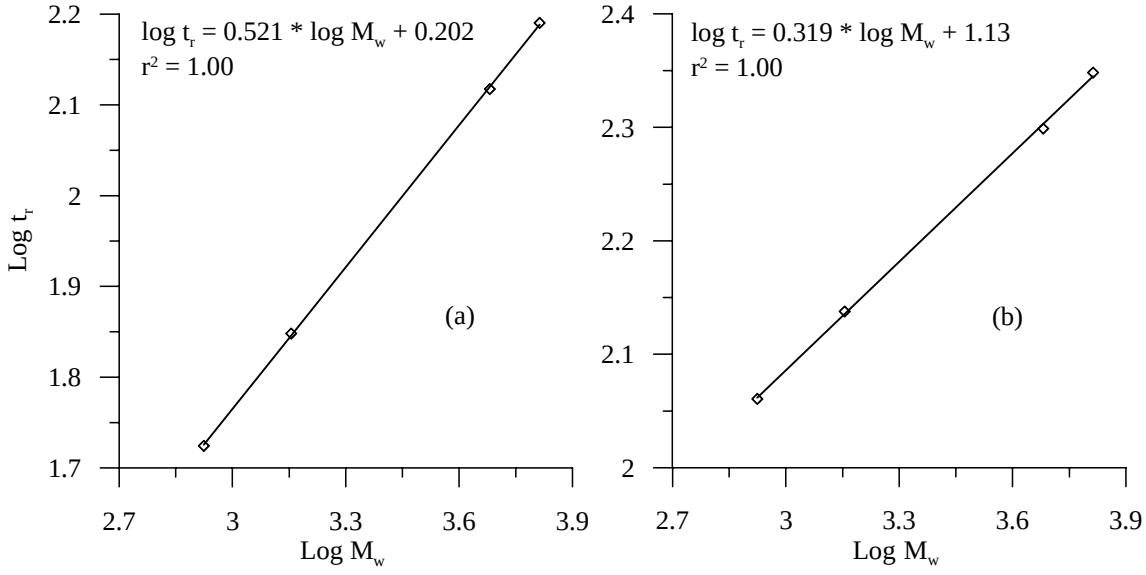

Figure 2-1: Molecular weight calibration curves obtained from sodium poly(styrene sulphonate) standards.

In contrast, calibration curves in previous studies were constructed by plotting the peak maxima obtained from the calibration standards against peak maxima molecular weight (M_p) provided by the calibration standard manufacturer (Benedetti et al., 2002; Chin et al., 1994; Her et al., 2002a). The approach used here removes ambiguity in selecting the most appropriate retention time (t_r) and assigning the correct molecular weight value from raw fractograms for subsequent plotting against the PSS manufacturer's reported molecular weight value. Calibration curves produced with our method had perfect linear regressions (r^2 = 1.00 for both UV and DOC detectors), slightly better than those obtained using peak maximum values (r^2 = 0.97 and 0.98 for UV and DOC, respectively). To facilitate subsequent comparison of results between the two detection systems, we represented fractogram retention times (raw data) on a molecular weight scale, giving us molecular weight distribution curves.

2.3.4 DOC Samples.

We collected ground water samples (n=4), surface water samples (n=2) and Suwannee River humic standards (n=3) for testing. Ground water samples were collected from piezometers completed at 2.2, 3.5, 3.7, and 4.5 m below ground at a thick (80 m) laterally extensive, clay-rich till aquitard (the King site) located in southern Saskatchewan, Canada (51.05 N Lat., 106.5 W Long.). Samples were collected from this site because it is well instrumented, the hydrogeology and hydrochemistry of the aquitard is well understood (Hendry et al., 2003; Hendry and Wassenaar, 1999, 2000; Lawrence et al., 2000; Shaw and Hendry, 1998), and the DOC has already been characterized (Hendry et al., 2003; Ranville et al., 2007). Surface water samples consisted of spring runoff water derived from snowmelt collected at the King site (KSR-2) on March 29, 2004, and river water collected from the organic-rich Hangingstone River (HGSR-1) in a boreal forest in central Alberta, Canada (56.37 N Lat., 111.2 W Long.) on Nov 13, 2003. Suwannee River (SW) humic standards (International Humic Substances Society; Humic Acid (HA - 1S101H), Fulvic Acid (FA - 1S101F), and Natural Organic Matter (NOM - 1S101N)) were prepared to 50 mg l^{-1}.

2.3.5 Molecular Weight Distribution

We determined M_w and number averaged molecular weight (M_n) of PSS 1430 and the 9 DOC samples from the PSS calibration curves. M_w and M_n were calculated using:

$$M_w = \frac{\sum(h_i M_i)}{\sum h_i} \qquad [2\text{-}2a]$$

and

$$M_n = \frac{\sum h_i}{\sum(h_i / M_i)} \qquad [2\text{-}2b]$$

where h_i is the height of the detector signal (or frequency) of *i*th molecule and M_i is the molecular weight of the *i*th molecule from the molecular weight distribution curves calculated from PSSs (Thang et al., 2001). It is assumed that the height of the UV and DOC signals (after baseline correction) is equal to the mass concentrations of the sample. M_w and M_n calculations were performed on the material corresponding only to DOC. Calculations began at the molecular weight that corresponds to the lowest intensity between the void and DOC peak and ended where baseline values were obtained . From these values we determined the degree of polydispersity (M_w/M_n) of the samples (Beckett et al., 1987; Chin et al., 1994). Polydispersity indicates the distribution of individual molecular weights within a sample; a value of 1.00 indicates the sample is homogenous.

2.3.6 Band Broadening

The addition of switching valves and fittings in the DOC detector, introduction of reagents to the DOC sample stream, and additional lengths of tubing between the two detectors created the potential for broadening of the DOC fractograms relative to the UV fractograms (i.e., artificial differences in molecular weight distribution between the two signals). PSS 1,430 (M_w=1430; M_n=1200) was selected to assess the extent of band broadening because its molecular weight scale was closest to that of the DOC in the

samples analyzed. Suwannee River standards were not used to assess band broadening because inherent differences in molecular weight distribution between the DOC and UV signals in these samples were anticipated; these standards contain differing amounts of aliphatic carbon and as such are not totally resolvable with UV analysis. Because of the repetitive structure of the polymers, we assumed fractograms of PSS would result in similar signals using both UV and DOC detectors.

2.3.7 UV and DOC Molecular Weight Distribution Curves

DOC and UV molecular weight distributions of Suwannee River standards and natural water samples all exhibited well defined maxima and tailing (Figures 2-2 and 2-3), typical of UV results from previous studies (Beckett et al., 1987; Benedetti et al., 2002). Comparing ground water samples (Figure 2-3a,b) shows M_p attained at 900 Da with the DOC detector but at 1100 Da with UV detection.

The majority of the lighter molecular weight organic fraction (<900 Da) is not recognized with the UV method for the samples and standards tested, suggesting these organic moieties are predominantly aliphatic. M_w and M_n determined from the DOC distributions (Table 2-2) were consistently less than those determined by UV (DOC values ~77-94% of UV values). The higher molecular weights calculated from UV distributions are attributed to the UV method's inability to detect aliphatic carbon bonds, which are more common in the lower weight fraction of the DOC (Silverstein et al., 1991; Thurman, 1985a). UV determined M_w and M_n of SRHA and SRFA standards were at the upper end of published values (Table 2-3).

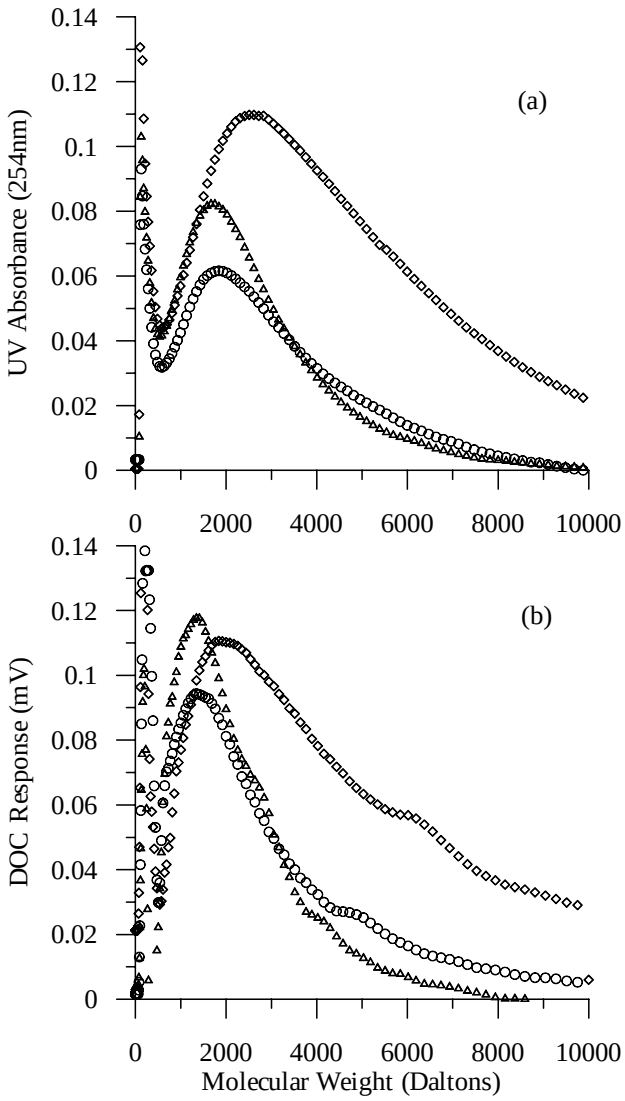

Figure 2-2: Molecular weight distribution curves of Suwannee River Humic Substances analyzed with (a) UV analyzer and (b) DOC detector. Humic Acid (53 mg l^{-1}) are represented by open diamonds; Fulvic Acid (49 mg l^{-1}) by open triangles; Natural Organic Matter (51 mg l^{-1}) by open circles.

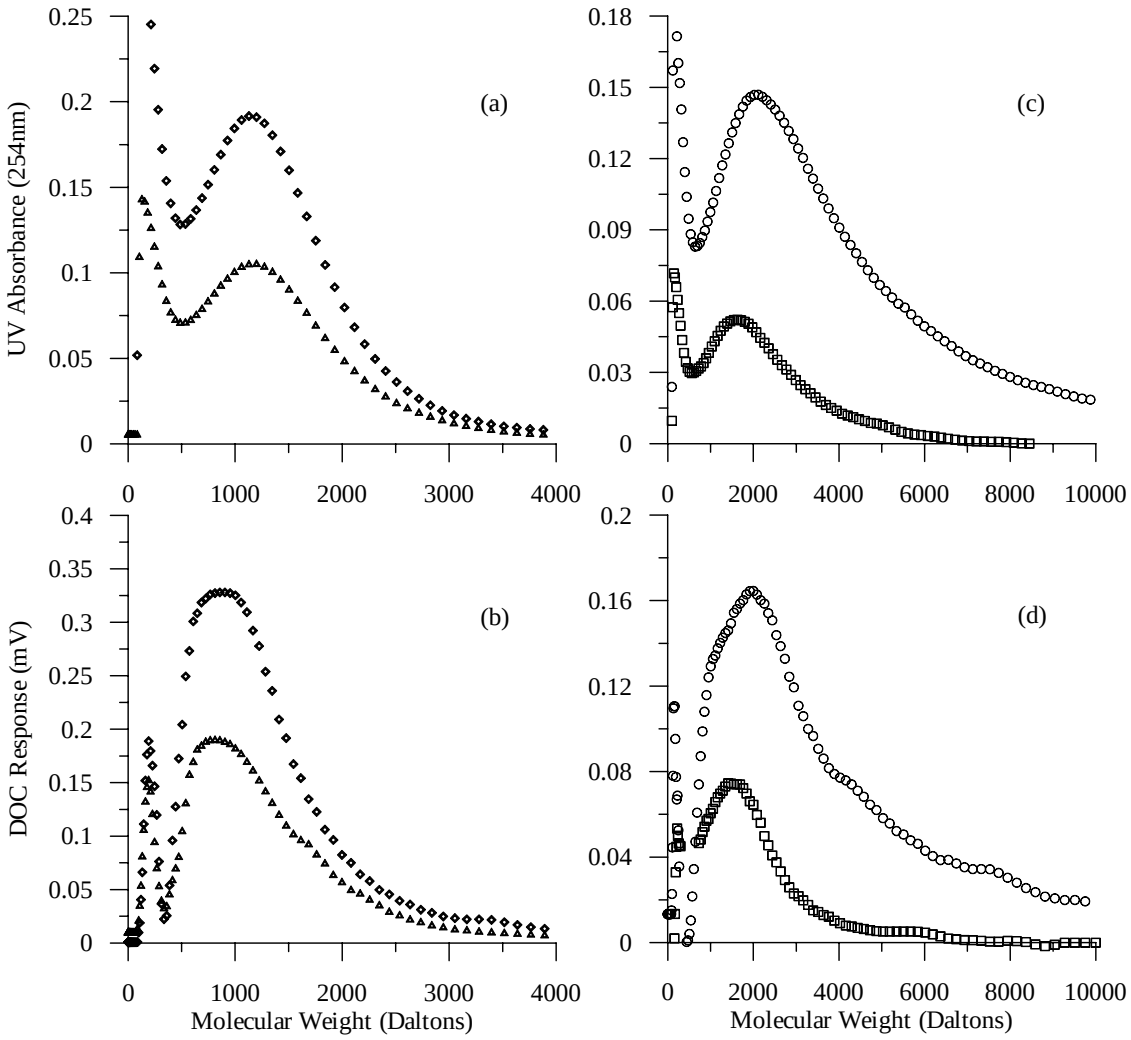

Figure 2-3: Molecular weight distribution curves of natural water samples analyzed with UV analysis (a, c) and DOC detection (b, d). (a) and (b) are King Site ground water samples where 2.2 m sample is represented by open diamonds; and 3.7 m sample by open triangles. (c) and (d) are King Site spring runoff water (KSR-2) and Hangingstone River sample (HGSR-1) where KSR-2 is represented by open circles; and HGSR-1 by open squares.

Table 2-2. Sample analysis results.

Sample	DOC (mg l^{-1})	M_w (UV)	M_n (UV)	M_n/M_w (UV)	M_w (DOC)	M_n (DOC)	M_n/M_w (DOC)	NIC	$SUVA_{254}$ l m·mg^{-1} C
standards									
PSS 1430	---	1461	1228	1.19	1480	1237	1.20	---	---
SRHA	53.0	3792	2389	1.59	3199	2039	1.57	0.99	7.5 (Benedetti et al., 2002)
SRFA	49.0	2364	1658	1.43	1900	1518	1.25	0.70	5.5 (Benedetti et al., 2002)
SRNOM	51.0	2945	1885	1.56	2263	1454	1.56	0.71	n/a
ground waters									
2.2 m	135.5	1382	1101	1.26	1142	891	1.28	0.58	1.88 (Hendry et al., 2003)
3.5 m	136.1	1470	1195	1.23	1285	1037	1.24	0.59	2.00 (Hendry et al., 2003)
3.7 m	74.9	1416	1121	1.26	1160	895	1.30	0.55	n/a
4.5 m	123.6	1486	1207	1.23	1274	1018	1.25	0.58	n/a
surface waters									
KSR-2	38.4	3001	2037	1.47	2784	1679	1.66	0.89	n/a
HGSR-1	18.6	2113	1558	1.36	1839	1465	1.26	0.72	n/a

Table 2-3: Comparison of published molecular weight estimations of Suwannee River Substances using different separation methods. Published M_w and M_n values exhibit a large range in molecular weights; this variability is attributed at least in part to differences in analytical method and method of calibration, although deviation in the reported values using the same separation method still exists.

Sample	M_w	M_n	M_w/M_n	Method; Detection	Ref.
SRFA	1910	1150	1.66	FlFFF; UV	(Beckett et al., 1987)
	1240	1160	1.07	FlFFF; UV	(Benedetti et al., 2002)
		840 (959)		VPO THF (H_20)	(Aiken and Malcolm, 1987)
	2080	1390	1.50	GPC	(Janos, 2003)
	2310	1360	1.70	HP/SEC; UV	(Chin et al., 1994)
	2114 (2114)	1385 (1166)	1.53 (1.81)	HP/SEC; UV (DOC)	(Her et al., 2002a)
	2364 (1900)	1658 (1518)	1.43 (1.25)	This work; UV (DOC)	
SRHA	4390	1580	2.78	FlFFF; UV	(Beckett et al., 1987)
	3153	2247	1.40	FlFFF; UV	(Dycus et al., 1995)
	2090	1320	1.58	FlFFF; UV	(Benedetti et al., 2002)
	3305 (3409)	1934 (1730)	1.71 (1.97)	HP/SEC; UV (DOC)	(Her et al., 2002a)
	3792 (3199)	2389 (2039)	1.59 (1.57)	This work; UV (DOC)	

FlFFF, Flow Field-Flow Fractionation; VPO, vapor pressure osmometry; THF, tetrahydrofuran; GPC, gel permeation chromatography; HP/SEC, high pressure size exclusion chromatography.

2.4 Results and Discussion

Polydispersity values determined from the UV detector data were near the average of reported values (Table 2-3). Polydispersity values calculated from DOC detector data were poorly correlated with those from the UV detector data ($r^2 = 0.65$). This poor correlation was expected due to the diverse range of bond types present in the samples being analyzed. For a given sample, the range in molecular weight of DOC resolved by the UV detector depends on the type of bonding present (aromatic or aliphatic) in the DOC; the range resolved by the DOC detection system reflects the actual range of molecular weight present.

2.4.1 UV-DOC Relationships

We devised a method to compare maximum peak height obtained from UV absorbance and DOC detection. Detector sensitivities were changed between different samples (due to the wide range in sample concentrations); therefore we normalized detector intensities of all analyses prior to comparison. The UV detector has an adjustable range of absorbance units (AU) and sensitivity was increased when samples of low DOC concentration were analyzed. All UV values were normalized to 1.0 AU (0-2.5 V analogue signal), before comparison. Output sensitivity of the DOC detection system was altered between samples by changing the concentration range sent through analogue output. All DOC results were normalized to a concentration of 0-10 ppm total carbon (0-2.5 V analogue signal).

The intensity of the UV peak maxima divided by the DOC peak maxima, or normalized intensity comparison (NIC), is similar to the Specific UV Absorbance ($SUVA_{254}$) approach routinely used to measure aromaticity of DOC (Benedetti et al., 2002; Hendry et al., 2003; Weishaar et al., 2003). $SUVA_{254}$ is determined by dividing the UV absorbance at 254 nm by the bulk DOC concentration. Weishaar et al. observed a strong linear correlation ($r^2 = 0.97$) between specific UV absorbance ($SUVA_{254}$) and the aromatic range (110-160 ppm) of ^{13}C NMR (Weishaar et al., 2003); this positive relationship suggests $SUVA_{254}$ is a good indicator of aromaticity in DOC. Because the calculation for NIC is based on the same parameters as $SUVA_{254}$ (i.e., both are

essentially an indication of the UV absorbance at 254 nm related to DOC concentration), NIC should also yield information on the aromaticity of the DOC, with larger NIC values suggesting greater aromatic carbon content. An NIC of 1.00 indicates the same intensity of UV and DOC molecular weight distributions, with the majority, or all, of the carbon in the sample identifiable with UV detection.

The advantage of using NIC over $SUVA_{254}$ is that $SUVA_{254}$ is a bulk measurement, using concentration and total absorbance values of DOC in the bulk solution, not just organic matter of interest (i.e., the humic and fulvic fractions). NIC allows a direct comparison to be made of absorbance and concentration of a given DOC fraction in a solution. The term NIC is proposed here to avoid confusion between values obtained from this on-line method and the $SUVA_{254}$ method. The peak maxima between UV and DOC molecular weight distribution curves are not at the same molecular weight in most samples. Therefore this comparison is not of exactly the same DOC size fraction. The peak maximum UV absorbance is, however, very close in molecular weight to the peak maximum DOC intensity. Therefore trends in NIC are similar to a comparison of intensities at the same molecular weights.

The NIC, or aromaticity, of the Suwannee River standards increased in the order SRFA < SRNOM < SRHA (Table 2-2). The NIC of SRFA and SRNOM were 71% and 72% of the SRHA value. This suggests similar structural characteristics between SRFA and SRNOM, with both having less aromatic content than the SRHA. NIC values for the ground waters were less than for SRFA, indicating less aromaticity in the DOC of these samples. AsFlFFF characterization of two ground water samples (2.2 and 3.7 m BG; Figure 2-3) show a corresponding less intense UV absorbance as compared to DOC detection. The stream sample, HGSR-1, had an average NIC value of 0.72, within the range of SRHA and SRNOM. Surface runoff water for the King Site (KSR-2) had an average NIC value of 0.89, which approaches the high value obtained from SRHA. Greater NIC values for the surface samples compared to ground water samples was anticipated because ground water DOC is reported to contain greater amounts of aliphatics than surface waters (Thurman, 1985a). This can be explained by two hypotheses. One would be that kerogen is the source of DOC in the ground waters,

which is generally higher in aliphatic carbon. The other hypothesis being that in the anaerobic environment of the ground waters, microbes use DOC as a source of oxygen, therefore lowering the oxygen content in the DOC (Thurman, 1985a). Aromaticity of the samples as determined by $SUVA_{254}$ measurements matched the order determined by NIC (SRHA > SHFA > ground water).

NIC values exhibit a strong linear correlation with molecular weight ($r^2 = 0.96$ for M_w and $r^2 = 0.92$ for M_n). If NIC reflects aromaticity, as suggested above, this relationship indicates aromaticity is a function of molecular weight for DOC. E_4/E_6 ratios (ratio of absorbance at 465 and 665 nm), used to determine characteristics of HA and FA, also exhibit a relationship between degree of aromaticity and molecular weight (Chen et al., 1977; Kononova, 1966; Thurman, 1985a). Thurman (1985) shows humic acids in ground waters have a consistently lower E_4/E_6 ratio than fulvic acids (Thurman, 1985a).

2.4.2 Molecular Weight Specific NIC Analysis

The strong linear correlation between molecular weight and NIC values suggests a change in the chemical composition of DOC (increasing aromaticity) over the range of molecular weights in samples. To substantiate this molecular weight trend, we performed continuous molecular weight specific NIC analysis (NIC_c) on all samples. We divided UV absorbance by DOC intensity at a given molecular weight, resulting in a continuum of NIC_c values over the entire range of measurable molecular weights in a sample. The NIC_c increased with increased molecular weight in all ground water and surface water samples. The NIC_c values for SRNOM and a representative ground water sample (Figure 2-4) increased from 0.53 to 0.95 from 600 to 5200 Da and from 0.52 to 0.96 from 600 to 2900 Da, respectively. All NIC_c values became unstable as the peak intensities approached baseline values, at about 5000 Da for SRNOM, and at 2500 Da for the 2.2 m ground water sample. The NIC_c profiles exhibited the same trend to increasing aromatic content with increasing molecular weight of DOC as the NIC analysis.

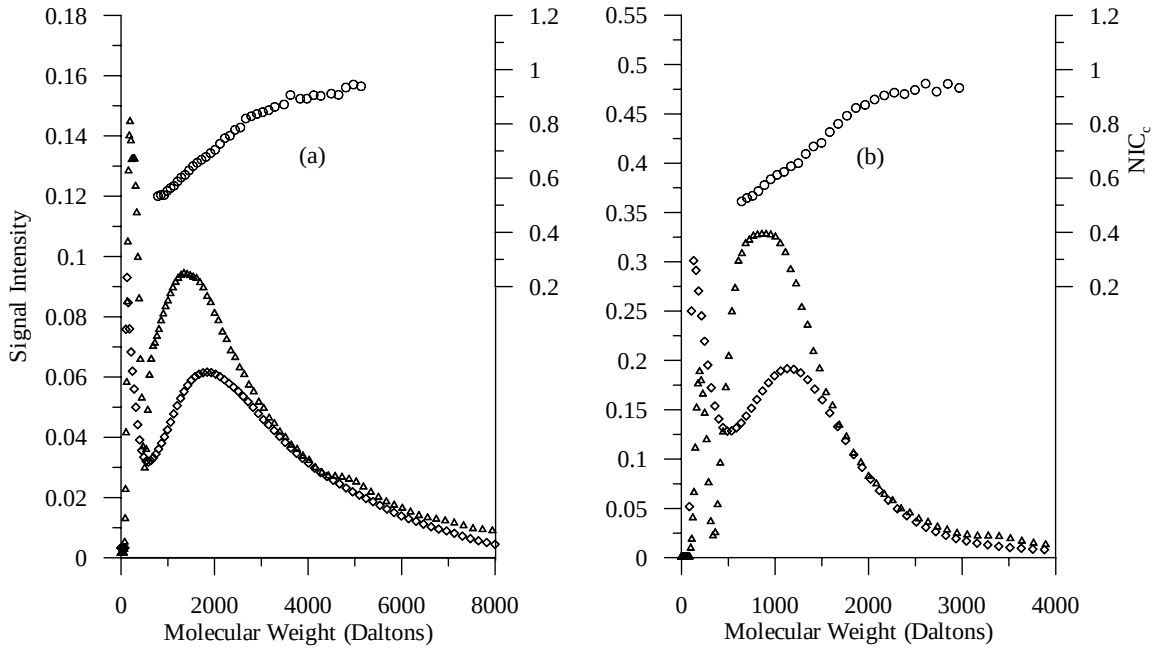

Figure 2-4: Continuous molecular weight specific Normalized Intensity Comparison (NIC_c) analysis on representative samples (a) SRNOM and (b) King Site 2.2 m. UV analyses are represented by open diamonds; DOC detector results by open triangles; and NIC values by open circles.

2.5 Conclusions

A method of characterizing dissolved organic carbon (DOC) by AsFlFFF with on-line UV and DOC detection was developed and applied to standards and natural ground water and surface water samples. DOC and UV fractograms obtained with this technique were highly reproducible and can be interpreted through a simple molecular weight calibration approach. Our testing suggests DOC detection may be a more accurate method to characterize molecular weight of the DOC than UV detection; UV detection may bias molecular weights high because of the method's inability to resolve aliphatics (usually of lower molecular weight). Coupling of the two detectors provides information on the dominant structures (aliphatic vs. aromatic content) in DOC fractions. Distinct and repeatable differences observed with a normalized intensity comparison (NIC) analysis of different samples supports the ability of this method to

characterize the aromaticity of DOC. DOC aromaticity was positively correlated with molecular weight, in both a bulk and molecular weight specific analysis.

2.6 Acknowledgements

This research was funded by research grants from the Natural Sciences and Engineering Council of Canada (NSERC) and the Potash Corporation of Saskatchewan.

2.7 References

Aiken, G.R., and Malcolm, R.L., 1987, Molecular weight of aquatic humic and fulvic acids by vapor pressure osmometry: Geochimica et Cosmochimica Acta, v. 51, p. 2177-2184.

Aravena, R., Wassenaar, L., and Plummer, L.N., 1995, Estimating 14C groundwater ages in a methanogenic aquifer: Water Resources Research, v. 31, p. 2307-2317.

Assemi, S., Newcomb, G., Hepplewhite, C., and Beckett, R., 2004, Characterization of natural organic matter fractions separated by ultrafiltration using flow field-flow fractionation: Water Research, v. 38, p. 1467-1476.

Beckett, R., Jue, Z., and Giddings, C.J., 1987, Determination of molecular weight distributions of fulvic and humic acids using flow field-flow fractionation: Environmental Science & Technology, v. 21, p. 289-295.

Benedetti, M., Ranville, J.F., Ponthieu, M., and Pinheiro, J.P., 2002, Field-flow fractionation characterization and binding properties of particulate and colloidal organic matter from the Rio Amazon and Rio Negro: Organic Geochemistry, v. 33, p. 269-279.

Chen, Y., Senesi, N., and Schnitzer, M., 1977, Information provided on humic substances by E4/E6 ratios: Soil Science Society of America Journal, v. 41, p. 352-358.

Chin, Y.-P., Aiken, G., and O'Loughlin, E., 1994, Molecular weight, polydispersity, and spectroscopic properties of aquatic humic substances: Environmental Science & Technology, v. 11, p. 1853-1858.

Chiou, C.T., Malcolm, R.L., Brinton, T.I., and Kile, D.E., 1986, Water Solubility Enhancement of Some Organic Pollutants and Pesticides by Dissolved Humic and Fulvic Acids: Environmental Science & Technology, v. 20, p. 502-508.

Crum, R.H., Murphy, E.M., and Keller, C.K., 1996, A non-absorptive method for the isolation and fractionation of natural dissolved organic matter: Water Research, v. 30, p. 1304-1311.

Dycus, P.J.M., Healy, K.D., Stearman, G.K., and Wells, M.J.M., 1995, Diffusion coefficients and molecular weight distributions of humic and fulvic acids determined by field-flow fractionation: Separation Science & Technology, v. 30, p. 1435-1453.

Geckeis, H., Mahn, T.N., Bouby, M., and Kim, J.I., 2003, Aquatic colloids relevant to radionuclide migration: characterization by size fractionation and ICP-mass spectrometric detection: Colloids and Surfaces A: Physicochemical and Engineering Aspects, v. 217, p. 101-108.

Harvey, G.R., Boran, D.A., Chesal, L.A., and Tokar, J.M., 1983, The structure of marine fulvic and humic acids: Marine Chemistry, v. 12, p. 119-132.

Hassellov, M., Lyven, B., Haraldson, C., and Sirinawin, W., 1999, Determination of continuous size and trace element distribution of colloidal material in natural water by on-line coupling of flow field-flow fractionation with ICPMS: Analytical Chemistry, v. 71, p. 3497-3502.

Hendry, M.J., Ranville, J.F., Boldt-Leppin, B.E.J., and Wassenaar, L., 2003, Geochemical and transport properties of dissolved organic carbon in a clay-rich aquitard: Water Resources Research, v. 39, p. 1194-1203.

Hendry, M.J., and Wassenaar, L., 1999, Implications of the distribution of delta-D in pore waters for groundwater flow and the timing of geologic events in a thick aquitard system.: Water Resources Research, v. 35, p. 1751-1760.

—, 2000, Controls on the distribution of major ions in pore waters of a thick surficial aquitard: Water Resources Research, v. 36, p. 503-513.

Her, N., Amy, G., Foss, D., and Cho, J., 2002a, Variations of molecular weight estimation by HP-size exclusion chromatography with UVA versus online DOC detection: Environmental Science & Technology, v. 36, p. 3393-3399.

Her, N., Amy, G., Foss, D., Cho, J., Yoon, Y., and Kosenko, P., 2002b, Optimization of method for detecting and characterizing NOM by HPLC - size exclusion chromatography with UV and on-line DOC detection.: Environmental Science & Technology, v. 36, p. 1069-1076.

Huber, S.A., and Frimmel, F.H., 1994, Direct gel chromatographic characterization and quantification of marine dissolve3d organic carbon using high-sensitivity DOC detection: Environmental Science & Technology, v. 28, p. 1194-1197.

Janos, P., 2003, Seperation methods in the chemistry of humic substances: Journal of Chromatography A., v. 983, p. 1-18.

Kim, J.I., Buckau, G., Li, G.H., Duschner, H., and Psarros, N., 1990, Characterization of humic and fulvic acids from Gorleben groundwater.: Fresnius Journal of Analytical Chemistry, v. 338.

Kononova, M.M., 1966, Soil Organic Matter: Its Nature, Its Role in Soil Formation and in Soil Fertility: London, Pergamon Press, 544 p.

Lawrence, J.R., Hendry, M.J., Wassenaar, L., Wolfaard, G.M., Germida, J.J., and Greer, C.W., 2000, Distribution and biogeochemical importance of bacterial populations in a thick clay-rich aquitard system.: Microbial Ecology, v. 40, p. 273-291.

Lyven, B., Hassellov, M., Turner, D.R., Haraldson, C., and Andersson, K., 2003, Competition between iron- and carbon-based colloidal carriers for trace metals in a freshwater assessed using flow field-flow fractionation coupled to ICPMS: Geochimica et Cosmochimica Acta, v. 67, p. 3791-3802.

Malcolm, R.L., 1985, Geochemistry of Stream Fulvic and Humic Substances, *in* Aiken, G.R., McKnight, D.M., Wershaw, R.L., and MacCarthy, P., eds., Humic Substances in Soil, Sediment and Water: New York, John Wiley & Sons, Inc., p. 181-210.

McCarthy, J.F., Williams, T.M., Liang, L., Jardine, P., Jolley, L.W., Taylor, D.L., Palumbo, A.V., and Cooper, L.W., 1993, Mobility of natural organic matter in a sandy aquifer: Environmental Science and Technology, v. 27, p. 667-676.

Means, J.L., Maest, A.S., and Crear, D.S., 1987, *in* P., H., ed., The Technology of High-Level Nuclear Waste Disposal, p. 215-247.

Perminova, I.V., Frimmel, F.H., Kudryavtsev, A.V., Kulikova, N.A., Abbt-Braun, G., Hesse, S., and Petrosyan, V.S., 2003, Molecular weight characteristics of humic substances from different environments as determined by size exclusion chromatography and their statistical evolution: Environmental Science & Technology, v. 37, p. 2477-2485.

Ranville, J.F., Hendry, M.J., Reszat, T.N., Xie, Q., and Honeyman, B.D., 2007, Quantifying uranium complexation by groundwater dissolved organic carbon using asymmetrical flow field-flow fractionation: Journal of Contaminant Hydrology, v. 91, p. 233-246.

Ranville, J.F., and Macalady, D.L., 1997, *in* Sather, O., ed., Geochemical Processes, Weathering and Groundwater Recharge in Catchments, Balkema.

Schimpf, M., and Wahlund, K.-G., 1997, Asymmetrical Flow Field-Flow Fractionation as a method to study the behaviour of humic acids in solution: Journal of Microcolumn Separations, v. 9, p. 535-543.

Scott, D.T., McKnight, D.M., Blunt-Harris, E.L., Kolesar, S.F., and Lovely, D.R., 1998, Quinone Moieties Act as Electron Acceptors in the Reduction of Humic Substances by Humics-Reducing Microorganisms: Environmental Science & Technology, v. 32, p. 2984-2989.

Shaw, J., and Hendry, M.J., 1998, Groundwater flow in a thick clay till and clay bedrock sequence in Saskatchewan, Canada: Canadian Geotechnical Journal, v. 35, p. 1041-1052.

Silverstein, R.M., Bassler, G.C., and Morrill, T.C., 1991, Spectrometric Identification of Organic Compounds: New York, John Wiley and Sons, 419 p.

Stevenson, F.J., 1985, Geochemistry of Soil Humic Substances, *in* Aiken, G.R., McKnight, D.M., Wershaw, R.L., and MacCarthy, P., eds., Humic Substances in Soil, Sediment, and Water: Geochemistry, Isolation, and Characterization: New York, John Wiley & Sons, p. 13-52.

Tan, K.H., 2003, Humic Matter in Soil and the Environment: Principles and Controversies: New York, Marcel Dekker Inc., 386 p.

Thang, N.M., Geckeis, H., Kim, J.I., and Beck, H.P., 2001, Application of the flow field flow fractionation (FFFF) to the characterization of aquatic humic colloids: evaluation and optimization of the method: Colloids and Surfaces A: Physicochemical and Engineering Aspects, v. 181, p. 289-301.

Thurman, E.M., 1985a, Humic substances in groundwater, *in* Aiken, G.R., McKnight, D.M., Wershaw, R.L., and MacCarthy, P., eds., Humic substances in soil sediment and water: Geochemistry, isolation, and characterization, John Wiley and Sons, p. 87-103.

—, 1985b, Organic Geochemistry of Natural Waters: Dordrecht, Martinus Nijhoff/Dr W. Junk Publishers, 497 p.

Wahlund, K.-G., 2000, Asymmetrical Flow-Field Flow Fractionation, *in* Schimpf, M., Caldwell, K., and Giddings, C.J., eds., Field-Flow Fractionation Handbook: New York, John Wiley & Sons, p. 279-294.

Weishaar, J.L., Aiken, G.R., Bergamaschi, B.A., Fram, M.S., Fujii, R., and Mopper, K., 2003, Evaluation of specific ultraviolet absorbance as an indicator of chemical composition adn reactivity of dissolved organic carbon: Environmental Science & Technology y, v. 37, p. 4702-4708.

3.0 QUANTIFYING URANIUM COMPLEXATION BY GROUND WATER DISSOLVED ORGANIC CARBON USING ASYMMETRICAL FLOW FIELD-FLOW FRACTIONATION

3.1 Abstract

The long-term mobility of actinides in ground waters is important for siting nuclear waste facilities and managing waste-rock piles at uranium mines. Dissolved organic carbon (DOC) may influence the mobility of uranium, but few field-based studies have been undertaken to examine this in typical ground waters. In addition, few techniques are available to isolate DOC and directly quantify the metals complexed to it. Determination of U–organic matter association constants from analysis of field-collected samples compliments laboratory measurements, and these constants are needed for accurate transport calculations. The partitioning of U to DOC in a clay-rich aquitard was investigated in 10 ground water samples collected between 2 and 30 m depths at one test site. A positive correlation was observed between the DOC (4–132 mg l^{-1}) and U concentrations (20–603 μg l^{-1}). The association of U and DOC was examined directly using on-line coupling of Asymmetrical Flow Field-Flow Fractionation (AsFlFFF) with UV absorbance (UV) and inductively coupled plasma-mass spectrometer (ICPMS) detectors. This method has the advantages of utilizing very small sample volumes (20–50 μl) as well as giving molecular weight information on U–organic matter complexes. AsFlFFF-UV results showed that 47– 98% of the DOC (4–136 mg l^{-1}) was recovered in the AsFlFFF analysis, of which 25–64% occurred in the resolvable peak. This peak corresponded to a weight-average molecular weight of about 900–1400 Daltons (Da). In all cases, AsFlFFF-ICP-MS suggested that ≤2% of the U, likely present as U(VI), was complexed with the DOC. This result was in good agreement with the U speciation modeling performed on the sample taken from the 2.3 m depth, which predicted approximately 3% DOC-complexed U. This good agreement suggests that the AsFlFFF-

ICP-MS method may be very useful for determining U–organic matter association in small volumes.

3.2 Introduction

Naturally occurring dissolved organic matter (DOM) is ubiquitous in ground water and plays an important role in its geochemical and biochemical evolution (Aravena et al., 1995; Crum et al., 1996; McCarthy et al., 1993; Thurman, 1985). Dissolved Organic Matter is most frequently reported as dissolved organic carbon (DOC, 0.45 μm filtrate) and is generally comprised of aquatic humic colloids in the form of higher molecular weight humic (HA) and fulvic acids (FA) and lower molecular weight hydrophilic organic acids (Thurman, 1985). Components of DOC (e.g., aquatic FA) are known to play an important role in geochemistry of pollutants because these humic colloids can form metal complexes, enhance the solubility of non-polar organic contaminants, influence colloid stability, and participate in redox reactions (Aiken et al., 1985; Aravena et al., 1995; Chiou et al., 1986; Crum et al., 1996; Means et al., 1987; Ranville and Macalady, 1997; Scott et al., 1998; Thurman, 1985). Actinides and radionuclides can complex with mobile DOM and FA (Chopin, 1988; Christensen et al., 1996; Higgo et al., 1993; Lenhart et al., 2000; Mantoura et al., 1978) and, as a result, can undergo facilitated transport (Artinger et al., 2000; Artinger et al., 1998; McCarthy et al., 1998; Schussler et al., 2001). In the case of actinide ions, such as the uranyl ions, DOC has been shown to cause facilitated transport in column studies using natural sand and ground water rich in DOC (Artinger et al., 2002a; Kim et al., 1994). Artinger et al. (2002) also showed that the complexation of U to DOC is kinetically controlled. To date, field-based studies of U complexation with ground water DOC (Dearlove et al., 1991; Kim et al., 1992; Zeh et al., 1997), and subsequent facilitated transport, are very limited (Kaplan et al., 1994; Kim, 1994). Additionally, most work has involved soil-derived humic substances (Crancon and van der Lee, 2003), which may differ significantly in their chemical properties as compared to older DOC associated with deeper aquifers.

In this study, we quantified the association of U with natural DOC collected from a vertical porewater profile through a thick, clay-rich aquitard. We chose to study the complexation of uranium to DOC in an aquitard system over that in an aquifer for several reasons. First, in contrast to aquifers, the transport of inorganic solutes in aquitards is dominated by molecular diffusion over advection (Desaulniers et al., 1981; Hendry and Wassenaar, 1999). The transport of DOC in aquitards is also dominated by molecular diffusion (Hendry et al., 2003; Hendry and Wassenaar, 2004). This makes determination of molecular weight/aqueous diffusion coefficient of U–organic matter complexes an important characterization. As a further consequence, in an aquitard environment, dissolved elements can remain in contact with DOC for tens of thousands of years, thus providing long contact times between the elements in the aqueous phase and the DOC and thereby minimizing any kinetic effects of complexation. This long contact time presented us with the ability to assess the long-term partitioning of elements between the "free aquo-ion" and DOC phases. Second, research has shown that aquitards frequently contain greater concentrations of DOC than aquifers (Hendry et al., 2003), thus making it easier to investigate the complexation of metals with DOC in porewaters from aquitards than aquifers. Third, thick clay-rich aquitard systems are of global interest because of their potential as repository sites for the disposal of high level radioactive wastes and heavy metals as well as their use as protective covering for regional aquifer systems (Hendry and Wassenaar, 1999). Thus, an understanding of the controls on the transport of U in aquitard systems is required.

Direct measurements of trace elements associated with DOC have commonly relied on ultrafiltration or dialysis, although both methods are subject to significant experimental artifacts (Ranville and Schmiermund, 1999). Additional information as to the molecular weight distribution of DOC and associated trace elements can be obtained from size-exclusion chromatography (SEC) and field-flow fractionation (FFF). This study was conducted by on-line coupling of Asymmetrical Flow Field-Flow Fractionation (AsFlFFF), a relatively new sub-technique of field-flow fractionation (FFF) (Wahlund, 2000), with inductively coupled plasma mass spectrometry (ICP-MS). Coupling of FFF with element specific detectors such as ICP-MS provides a method for

examining the size distributions of elements associated with colloids (Benedetti et al., 2002; Benedetti et al., 2003; Hassellov et al., 1999; Hendry et al., 2003; Ranville et al., 1999; Taylor et al., 1992). Relatively few studies of ground water DOC have used FFF-ICP-MS (Geckeis et al., 2002). FFF-ICP-MS had a number of advantages over size-exclusion chromatography (SEC) for this work. The carrier ionic strength for FFF is much lower than that required for SEC and can be similar to the sample, which may minimize the possibility of sample alteration during fractionation. Also, the higher ionic strengths needed to prevent interactions of the sample with the SEC resin are problematic for ICP-MS because of salt build-up on the cones and plasma loading. In general there are fewer chemical interactions between the sample and the FFF channel than with the SEC resin, thus making the molecular weight measurements potentially more accurate. Finally, FFF techniques give a direct measure of aqueous diffusion coefficient.

3.3 Description of the Study Site and Background Studies

This study was conducted at a site consisting of a thick (80 m), plastic, clay-rich glacial till aquitard system in western Canada (51.05°N Lat., 106.5°W Long.). The aquitard was selected for study because the geology and hydrogeology is simple and well characterized, as are the solute transport mechanisms (Hendry and Wassenaar, 1999; Shaw and Hendry, 1998), the inorganic geochemistry of the aquitard porewater (Hendry and Wassenaar, 2000; Hendry et al., 2000), and the microbiology of the aquitard (Lawrence et al., 2000). In addition, the site is instrumented with high quality piezometers (Wassenaar and Hendry, 1999). The till was deposited between 15 ka and 38 ka Before Present (BP) and unconformably overlies clay of the Snakebite Member of the Cretaceous Bearpaw Formation. The top 3 to 4 m of the till is oxidized, brown in color and contains visible fractures. The oxidation occurred since the onset of the Holocene (7 ka to 10 ka BP). Below 3 to 4 m, the till is massive, unoxidized, and dark grey in color, and defined as the aquitard. Based on detailed hydraulic and isotopic studies cited above, ground water velocity was determined to be between 0.5 and 1.0 m per 10,000 years downward through the aquitard and underlying Cretaceous clay. Thus, transport of solutes from the weathered zone through the aquitard is dominated by

molecular diffusion. All research at the site suggested that no significant biological or geochemical processes are occurring in the aquitard that could otherwise complicate the interpretation of DOC data. In an earlier paper, Hendry et al. (2003) investigated the geochemical and transport characteristics of DOC at this site over a five-year period by studying water samples collected from 14 piezometers installed between 1.2 and 43 m below ground (BG). DOC measurements yielded a well-developed vertical depth profile with the greatest concentrations in the unoxidized zone and a gradual decrease with depth to uniform background concentrations at depths greater than 15 m (Figure 3-1) (Hendry et al., 2003). They showed that DOC diffuses through the aquitard matrix, behaving much like conservative solutes (i.e., DOC exhibited no measurable sorption onto the aquitard matrix nor straining by the porous media). In a subsequent paper on the DOC at this site, Hendry and Wassenaar (2004) determined that about 30% of the DOC was FA (Hendry and Wassenaar, 2004).

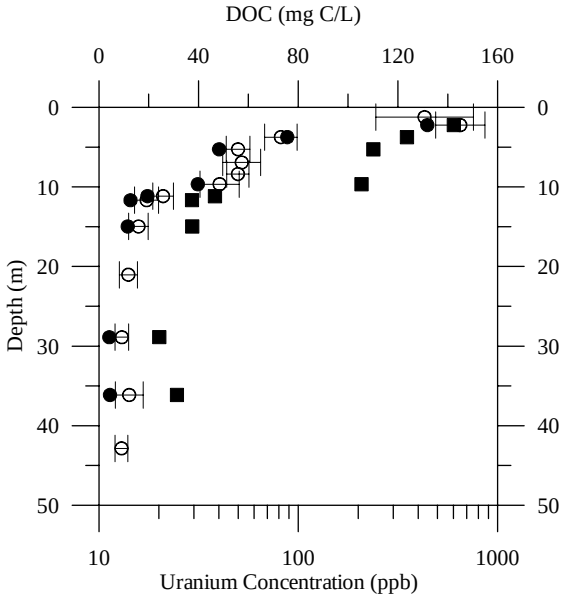

Figure 3-1: Vertical depth profiles of DOC and U concentrations. The open circles and horizontal bar represents the mean DOC and standard deviation of between 6 and 8 samples collected over a 5-year period (Hendry et al., 2003). The solid circles and solid squares represent DOC and U concentrations of water samples collected from the piezometers in June 2002.

They also used numerical simulations of the downward migration of ^{14}C–FA from the soil zone to show that the migration of DOC and FA in the aquitard was conservative and that the FA was stable over long periods of time. They further showed that the DOC in the aquitard was derived from two end members: soil organic material that formed since the onset of the Holocene (7 ka to 10 ka BP) and DOM originally deposited with the till about 15 ka BP. The Holocene derived DOC end member is reflected in high concentrations of DOC present at the 1.2 and 2.3 m depths whereas the older DOC is present below 15 m depth and has a much lower concentration (Figure 3-1). The well-defined decrease in DOC concentrations between 2.3 and 15 m depths was the result of diffusive mixing between the two end members.

3.4 Materials and Methods

3.4.1 Ground water Instrumentation, Sample Collection, and DOC Analyses

Porewater samples were collected from 8 piezometers installed in the oxidized (n=2) and unoxidized (n=6) till to a depth of 30 m (Table 3-1). These piezometers were selected for study to provide DOC samples that covered the range in DOC concentrations observed in the DOC-depth profile presented in Figure 3-1. All piezometers sampled were installed in 1995 taking great care to avoid atmospheric, soil, and microbial contamination. Construction details are provided in Wassenaar and Hendry (1999). Water samples for DOC analyses were collected from all piezometers (2.3, 4.5, 6.0, 9.1, 11.9, 12.4, 15.5, and 30.4 m depths) on June 5, 2002 and from the two piezometers installed in the oxidized till zone (2.3 and 4.5 m depths) on August 29, 2002.

All water samples were collected by slowly lowering a dedicated, sterilized, PVC bailer system to a depth of 1 m below the water column in each piezometer. Once the samples were brought to ground surface, they were field filtered using 0.45 μm membrane filters and stored in low-density polyethylene (LDPE) bottles in the dark at 5 °C until analyzed. The samples were analyzed for DOC concentration within 2 weeks of collection using a Shimadzu TOC-5050A. The standard deviation of the analyses performed with the TOC-5050A was within 1 % of the full range of measurement.

Table 3-1: Mean values (n=9) of chemical analyses (mmol l^{-1}) for porewater samples collected between January, 1996 and October, 1998 (Hendry and Wassenaar, 2000).

Depth (m)	Ca	Mg	Na	K	Cl	SO_4	Alk	pH	T	I
oxidized till										
2.3	11.0	289.8	429.7	1.6	1.8	534.1	747	7.86	6.4	0.983
4.5	9.8	157.1	272.8	1.2	1.0	303.7	780	7.62	4.7	0.653
unoxidized till										
6.0	9.8	100.0	195.6	1.1	1.4	202.1	752	8.10	4.6	0.473
9.1	9.9	30.4	100.6	0.7	3.7	86.1	760	7.38	5.4	0.228
11.9	10.5	16.2	68.8	0.5	4.5	52.8	685	7.42	5.4	0.151
12.4	10.9	9.5	42.9	0.5	5.1	33.5	612	7.44	5.6	0.103
15.5	11.7	9.1	32.5	0.4	3.0	30.6	568	7.04	5.6	0.092
30.4	12.2	8.2	9.1	0.4	1.1	21.3	389	7.23	5.6	0.064

3.4.2 Separation and Characterization of the DOC

Molecular weight (M_w) of the DOC in all porewater samples was determined using AsFlFFF, an elution technique consisting of an arrangement of pumps, AsFlFFF channel (PostNova Inc, Salt Lake City, UT), and UV–VIS detector (PostNova Inc, Salt Lake City, UT). The UV absorbance was measured at 254 nm with a one second data collection rate and from these data; fractograms (detector response vs. time) were produced. The theory and environmental applications of AsFlFFF are described in detail elsewhere (Beckett and Schimpf, 2000; Giddings, 2000). The results of a previous application of symmetrical-flow FFF technology to DOC samples from this site are presented in Hendry et al. (2003). Tests were conducted to optimize the AsFlFFF fractograms by modifying the laminar flow rate, cross-flow rate, and degassed carrier solution composition (data not presented). A 1000 Dalton (Da) regenerated cellulose

membrane (Millipore Corp) and a 100 μL sample injection loop were used. The optimum AsFlFFF separation conditions were determined to be channel flow = 0.9 mL min^{-1}; cross-field flow = 4.8 mL min^{-1}; injection flow rate = 0.1 mL min^{-1}; and carrier composition 0.001 *M* NaCl + 0.003 *M* NaN_3. Duplicate AsFlFFF analyses were performed on the samples and the fractograms averaged.

The M_w of samples was determined by calibration using polystyrene sulphonate standards (PSS) (American Polymer Standards) with M_ws of 840, 1430, 4800, and 6500 Da. PSS standards have been shown to accurately represent NOM in FFF analysis (Beckett et al., 1987). The resulting calibration plot of log retention time (*tr*) vs. log M_w yielded a slope and intercept of 0.356 and −1.212 (r^2 = 1.00). Number-average (M_n) and weight-average (M_w) molecular weights of the samples were determined from the fractograms (Giddings, 2000). M_n and M_w are described by,

$$M_n = \frac{\sum_i w_i}{\sum_i \frac{w_i}{M_i}} \qquad [3\text{-}1]$$

$$M_w = \frac{\sum_i w_i M_i}{\sum_i w_i} \qquad [3\text{-}2]$$

where w_i is the weight of *i*th component and M_i is the molar mass of the *i*th component. The UV response at any point of the fractogram is proportional to w_i.

The UV fractograms for the duplicate samples were used to quantify the percent recovery of DOC. The fractograms consisted of two regions: the void peak and the DOC peak. The void peak may contain some unresolved low molecular weight ligands. Based on the calibration standards, the cutoff between the two regions was determined to be 300 Da. This cutoff was the same as that determined by Beckett et al. (1987) using IHSS standards. The relationship between UV response and DOC was determined by pumping each sample directly through the UV detector, and recording the UV response. By dividing the UV response by the sample DOC, a factor was obtained that allowed

conversion of the UV fractograms to DOC fractograms. The amount of carbon in the void peak and DOC peak was determined by integrating the DOC fractograms, and the percent recovery determined by comparison to the total sample DOC.

3.5 AsFlFFF-ICP-MS analysis

3.5.1 ICP-MS calibration

A Micromass Platform ICP-MS (Micromass Ltd., Manchester, UK), equipped with a Hexapole collision cell, was used for all analyses. The ICP-MS had a low-flow Meinhard concentric nebulizer (Glass Expansion, Hawthorn, Australia) and a water-cooled (4 °C) Scott type double pass spray chamber. The operating parameters for the instrument are summarized in Table 3-2.

The outlet of the AsFlFFF, following the UV detector, was directly connected to the nebulizer of the ICP-MS. Flow into the ICP-MS was provided entirely by the AsFlFFF pump. Element calibration was achieved by injecting a 10 ppb multi-element standard through the AsFlFFF with the field off and measuring the elemental intensity on the ICP-MS. Peak area was used for intensity integration. The AsFlFFF separation runs were then initiated and the samples fractionated. Uranium fractograms were determined using the ion intensity collected by the ICPMS as a series of consecutive analyses, every 3 seconds. A typical analytical procedure consisted of a mobile phase (0.001 *M* NaCl + 0.003 *M* NaN_3) blank, a calibration standard, 4–6 samples, and a calibration standard. All samples and calibration standards were run in duplicate.

After a period of time sufficient to ensure all DOC was eluted from the channel (typically 2 minutes; data not presented), the field was turned off but ICP-MS data acquisition continued. This allowed larger colloids to elute from the channel and be detected by the ICP-MS (data not shown).

Table 3-2: ICP-MS operating parameters.

RF Power	1350 W
Cool gas	14 L min^{-1}
Intermediate gas	0.85 L min^{-1}
Nebulizer gas	0.80 L min^{-1}
Sampler cone	Ni, 1.0 mm
Skimmer cone	Ni, 0.8 mm
He gas	5.0 mL min^{-1}
H_2 gas	3.0 mL min^{-1}
Extraction lens	-400 V
Exit lens	400 V
Dwell time	200 ms
Acquisition mode	Peak hopping
Point/Peak	1
Total time	15 min

3.5.2 ICP-MS analyses of porewater samples

Filtered and refrigerated samples were run on the ICP-MS for total metal concentrations. All samples (and calibration standards) were run in duplicate for U.

3.5.3 Quantification of U complexed on the DOC

As was the case for the DOC, the U fractograms consisted of two regions: the void peak and the DOC peak. The void peak contained some proportion of the U in both the dissolved state and associated with unresolved, low molecular weight ligands (i.e., <300 Da). The U associated with the DOC was observed to form a distinct response peak that was resolved from the void peak and coincided with the UV response. The

amount of U in both the void peak and the DOC peak was computed by integrating the U counts and comparing to the counts obtained for the 10 ppb standard. To compute the fraction of U associated with the DOC, the concentration associated with the DOC peak was compared with that of the original water sample. The overall fraction of U recovered from the AsFlFFF was also determined by integrating the entire U fractogram.

Table 3-3: Representative reactions, binding site density (T_{HLi}), and strength (log *K*, extrapolated to zero ionic strength) for Suwannee River Humic Acid (Lenhart and Honeyman, 1999).

Reaction	T_{HLi} (mml g^{-1})	log *K* (*I* = 0)
$HL_1 = L_1^- + H^+$	0.900	-2
$HL_2 = L_2^- + H^+$	1.26	-4
$HL_3 = L_3^- + H^+$	1.16	-6
$HL_4 = L_4^- + H^+$	0.552	-8
$HL_5 = L_5^- + H^+$	1.42	-10
$UO_2^{2+} + HL_2^- = UO_2L_2^+ + H^+$		2.39
$Li^- + Na^+ = NaL_i$		1.52

3.5.4 Simulation of uranyl binding to DOC

Simulation of uranyl binding to the DOC from a sample collected from the oxidized till was based on the stability constants derived by Lenhart and Honeyman (1999) for Suwannee River Humic Acid (nominal M_w = 1200). In the modeling described below, the chemical behavior of NOM is described using a discrete ligand approach advocated by several researchers (Fish et al., 1986; Tipping and Hurley, 1992) and as implemented by Westall et al. (1995). In our model, NOM is represented as 'an assembly' of monoprotic acids with assumed p*K* values and without explicit correction for electrostatic effects. Table 3-3 presents the reactions implemented in our model. The protolysis reactions were derived through inverse modeling of titration data using FITEQL version 4.0 (Herbelin and Westall, 1996). The 5 ligands are established from titration data to fit the protonation reactions.

The uranium binding data are then optimized to determine the ligand that best describes the data. In this case HL_2^- is the only ligand needed to explain the data. The reaction between sodium and the ligand L_i is used to account for ionic strength effects during the humic acid titrations. In addition, the source for uranyl solution-phase reactions was Grenthe (1992); Sandino and Bruno (1992); Silva, (1992). Simulation of the ground water data were conducted using the water chemistry data from Tables 3-1 and 3-4. The distribution of the DOC 'ligands' was set to the distribution shown in Table 3-3, with $T_{HLi} = 5.29 \times 10^{-3}$ mol g^{-1}. Alkalinity data were input as C_T (M).

Table 3-4: DOC and uranium analyses of porewater samples used in the AsFlFFF-ICP-MS experiments.

Depth (m)	DOC (mg l^{-1})	U (ppb)
Oxidized till		
2.3	132	603
2.3[a]	136	463
4.5	76	351
4.5[a]	77	430
Unoxidized till		
6.0	48	238
9.1	40	208
11.9	19	38
12.4	13	29
15.5	12	29
30.4	4	20

[a] All samples were collected as part of the June 2002 sampling campaign with the exception of those noted by [a]. These samples were collected in August 2002.

3.6 Results and Discussion

3.6.1 Concentrations and Molecular Weight of DOC

The DOC measurements for the repeated 2.3 and 4.5 m depths (June and August 2002) exhibited little variability (Table 3-4) and suggested a lack of temporal variability

in the DOC data. This was supported by the good correlation between the DOC data collected in this study and the well-developed vertical depth profile of DOC obtained by Hendry et al. (2003) over a 5-year period. These data showed that the highest DOC concentrations occurred in the oxidized zone, and gradually decreased with depth to uniform background values at depth >15 m (Figure 3-1).

The UV absorbance fractograms for all porewaters were well-defined as exemplified by the data for the 2.3, 4.5, and 11.9 m piezometers shown in Figure 3-2. Analysis of duplicates resulted in fractograms having nearly identical appearance. The differentiation between the void volumes and the DOC peaks at 300 Da (i.e., the minima) is clearly evident in these plots. The decrease in UV absorbance with increased depth was attributed to a decrease in DOC concentrations with increasing depth and a decrease in specific UV absorbance of the DOC (SUVA) with increasing depth. The latter point was noted by Hendry et al. (2003).

The M_w and M_n of the DOC were uniform with depth, ranging from 1250–1480 and 830–980 Da respectively (Table 3-5), and were in good agreement with the generally accepted range for FA (Benedetti et al., 2003). These results are approximately 25 % greater than the M_w values previously reported for the site by Hendry et al. (2003) who report M_n and M_w values ranging from 710–1150 and 510–740 Da. The differences between the two sets of data were attributed to different analytical methods (symmetrical flow FFF in Hendry et al. (2003) vs. AsFlFFF in this study). The uniformity of the molecular weights with depth was also reflected in the timing and Gaussian shape of the UV absorbance fractograms for representative DOC samples in Figure 3-2. The relatively low M_w (<1000 Da) and strong UV signal in the resolvable peak suggested that this DOC was more likely to be primarily FA as compared to HA or non-humic substances, the latter generally having low specific UV absorbance. This was supported by results of Hendry and Wassenaar (2004) who determined that about 30 % of the DOC was FA in samples collected from this site (Hendry and Wassenaar, 2004).

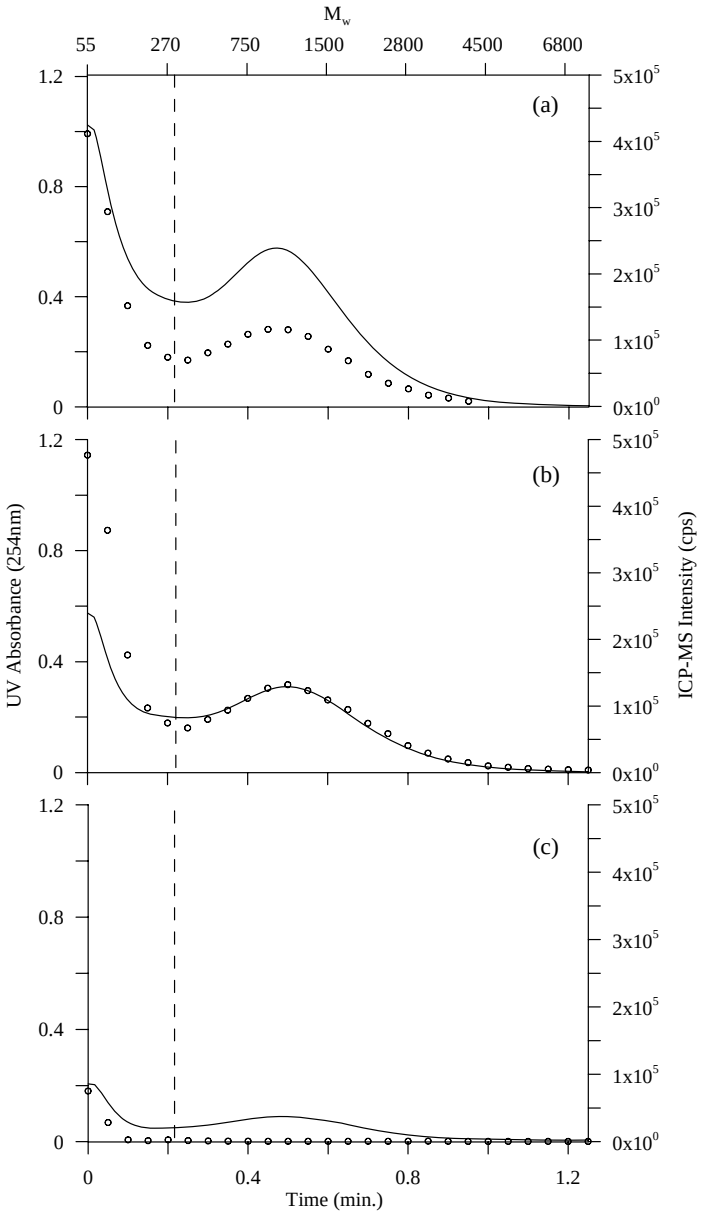

Figure 3-2: Representative fractograms for UV absorbance (solid line) and uranium counts (symbol) for piezometers installed at (a) 2.3, (b) 4.5, and (c) 11.9 m depths below ground surface. Time zero was assigned to the maximum concentration in the void volume. The vertical line represents 300 Da cutoff between the resolvable and unresolvable peaks.

Table 3-5: Characteristics of the DOC and U from the fractograms.

Depth (m)	M_n (Da)	M_w (Da)	DOC Recov. (%)	U Recov. (%)	μg U g^{-1} DOC	K_d (ml g^{-1} C)
Oxidized till						
2.3	840	1270	44[a] (75)[b]	0.51 (0.96)	50[c] (54)[d]	83[c] (90)[d]
2.3[e]	910	1430	46 (78)	1.10 (2.14)	84 (96)	181 (207)
4.5	900	1420	48 (80)	0.52 (0.95)	46 (49)	131 (140)
4.5[e]	940	1480	50 (86)	0.63 (1.15)	64 (67)	149 (156)
Unoxidized till						
6.0	950	1440	40 (59)	0.38 (0.70)	48 (59)	202 (248)
9.1	900	1450	64 (94)	0.07 (0.15)	7.3 (10.9)	35 (52)
11.9	910	1470	64 (98)	b.d.l.[f]	--	--
12.4	920	1300	31 (50)	b.d.l.	--	--
15.5	900	1350	42 (66)	b.d.l.	--	--
30.4	980	1370	25 (47)	b.d.l.	--	--

[a] Percentage under resolvable UV peak (i.e., >300 Da)
[b] Percentage under total UV peak (i.e., resolvable + void peak)
[c] Based on percentages under resolvable UV peak
[d] Based on percentages under total UV peak
[e] Sample collected on August 29, 2002. All other samples collected on June 05, 2002.
[f] b.d.l. = below detection limit. The detection limit for influent samples was determined to be 40 ppb.

The percentage of injected DOC recovered with the AsFlFFF system was determined in two ways. First, the percent recoveries were calculated for only the resolvable DOC peak (i.e., >300 Da; Figure 3-2). Because the void peak may contain some unresolved low molecular weight organic ligands, the second method used to determine the percent recovery was to integrate the UV signal under both the void and the DOC peak. The variation in percent areas under the curves for the duplicate runs was generally <2 %. The percent recoveries ranged from 25–64 % (mean = 45 %) and 47–98 % (mean = 73 %) for the DOC and DOC + void peak (Table 3-4). The low recovery of DOC under the DOC peak and the presence of unresolvable (<300 Da) DOC suggested that some DOC may have been lost through the 1 kDa membrane.

3.6.2. Concentrations of Uranium in Porewaters

Concentrations of U for ground waters are presented in Table 3-3. The U data for the samples for the 2.3 and 4.5 m depths from the June sampling period were 130 and 82 % of those for August. No apparent seasonal trend was evident from these limited data. The observed variability of U in this fractured and oxidized zone was anticipated because the major ion chemistry, deuterium, and DOC concentrations in this zone exhibited seasonal variability (Hendry et al., 2003; Hendry and Wassenaar, 1999, 2000). In contrast to the variability noted in the oxidized zone, the same parameters exhibited a lack of variability in the underlying unoxidized zone. The lack of variability in this zone reflected the very low hydraulic conductivity of this medium and was consistent with the DOC data. Cross plotting the measured pH data (Table 3-1) with the measured and calculated Eh data (−80 to +290 mV) (Yan et al., 2000) for the porewaters showed that the dominant species of U in the porewaters is likely to be U(VI). The U concentrations of the porewater varied with depth by more than one order of magnitude (Table 3-3 and Figure 3-1). The greatest concentrations were measured in the oxidized zone (2.3 and 4.5 m depths) (351–603 ppb) and decreased slightly to the 10.4 m depth (208 ppb). Below this depth the U concentrations were much lower and ranged from 20–38 ppb. A very strong linear correlation between the DOC and U data ($r^2 = 0.99$) suggested similar end members for these parameters. As noted above, the two end members for DOC were identified as soil organic material formed since the onset of the Holocene (7–10 ka BP) and organic matter originally deposited with the till (about 15 ka BP). With the exception of Ca, the distributions of soluble salts through the profile (Table 3-1) were positively correlated with the DOC. No depth trend was evident in the Ca data. The elevated concentrations of dissolved salts at shallow depths in the profile were the result of chemical weathering in the oxidized zone after glaciation (Hendry et al., 1986; Hendry and Wassenaar, 2000).

3.6.3. Uranium Complexed with the DOC

The U ion count fractograms for porewaters collected to a depth of 10.4 m exhibited a positive correlation to the UV absorbance intensity. This is clearly

exemplified by the data for the 2.3, 4.5, and 11.9 m data (Figure 3-2). Although UV fractograms were obtained for samples from depths ≥ 11.9 m, no U fractograms were measurable. The percentage of U associated with the DOC peak (Table 3-5) ranged from 0.07–1.10 % of the total U. From these results, the detection limit of the AsFlFFF-ICP-MS for DOC-associated U in these samples was determined to be about 50 ppb total U or 0.05 ppb DOC-associated U. Some, as yet unknown, percentage of U and DOC may have been lost by either adsorption to or passage through the membrane. Although in the case of the DOC, the M_w values were larger than the membrane size and thus the DOC should not be lost in the cross flow. Additionally, charged molecules such as humic substances are retained in the flow FFF channel even when their molecular weights are smaller than the stated pore-size cutoff (Beckett and Schimpf, 2000).

The low recoveries of U from the AsFlFFF suggested that the U present in the <300 Da M_w was present either as aquo-ion, inorganic complexes (e.g. $UO_2CO_3^-$, $UO_2(CO_3)_2^{2-}$), or associated with very low molecular weight organic ligands. The much lower percent recovery of U compared to DOC supported the presence of U as an aquo-ion and inorganic complexes. The concentration of μg U g^{-1} DOC (Table 3-5) was consistent with these results. The minor amount of DOC-associated U is in agreement with the results of geochemical modeling performed assuming the DOC consisted entirely of HA. With a DOC concentration of 135 mg l^{-1} and U concentration of 2×10^{-6} *M*, forward FITEQL simulations of the oxidized till for the depth of 2.3 m yielded 3 % of the total U(VI) associated with the DOC. The predicted K_d value is equal to 234 ml g^{-1} and the simulated ratio of U(VI) to DOC is 137 μg U g^{-1} DOC. These results are in very good but not perfect agreement with those determined by AsFlFFF-ICP-MS (Table 3-5). The lower measured amount of DOC-associated U (approximately a factor of 2), could be explained by several possibilities. First the model employed constants derived for HA whereas the low measured SUVA (Hendry et al., 2003) and M_w values suggest the material is not predominantly HA. The lower M_w and SUVA may suggest the DOC has a weaker affinity for metals such as U. Alternatively, if the DOC lost in the AsFlFFF separation contained bound U, this could explain the lower U–DOC concentration. Regardless of these possibilities the agreement to within better than a factor of 2 shows

that the AsFlFFF-ICP-MS method shows great promise as a tool of measuring DOC-associated U in environmental samples.

Work by Hummel et al. (2000) further demonstrated the importance of carbonate in limiting predicted U–humate interactions and also suggested that competition with other major cations for humic binding sites needs to be considered. Zeh et al. (1997) have also demonstrated for Gorleben ground waters, that elevated partial pressures of CO_2, as occur in the aquitard system under study, significantly limit the formation of U–DOC complexes. In contrast, for waters having lower pH (<6) and carbonate concentrations, such as soil porewaters, DOC complexation of U is more significant (Crancon and van der Lee, 2003; Giesy et al., 1986; Jackson et al., 2005) with the authors reporting values from 10–30 % complexed U. In column experiments using quartz sand and U-spiked Gorleben ground waters, Artinger et al. (2002b) determined that <7.6 % of the U was transported by humic colloids at near-neutral pH. Our lower result (<2 %) for DOC-associated U, obtained from field-collected samples, may be explained in part by the much more hydrophilic nature of the DOC in the current study as compared to that used by Artinger et al.(2002b). In a previous study, Hendry and Wassenaar (2004) determined that roughly 30 % of the DOC was present as FA. In contrast, the Gorleben ground water DOC was derived from brown-coal deposits and consisted of roughly 90 % FA+HA (Artinger et al., 1998) having potentially larger complexation capacity.

3.7 Conclusions

It could be concluded from our results, and the cited research, that facilitated transport of U by humic colloids, is unimportant for aquifers with pH greater than about 7 if substantial dissolved carbonate is present. The present work cannot eliminate the possibility of U transport by low MW ligands that would be lost through the membrane. If we assume that the 10–50% loss of DOC through the membrane complexed similar concentrations of U to that of the FA, this would suggest at most an additional 2% of the total U could be associated with DOC. Dissociation of U–ligand complexes is possible during the AsFlFFF analysis but the similarity of the measured amount of complexed

uranium to the model-predicted result suggest this is not significant. The work clearly demonstrates the utility of using AsFlFFF-ICP-MS to determine *in-situ* association constants (K_d) for U–DOC complexes. It also represents the first attempt to compare U speciation modeling to laboratory chromatographic measurements of DOC complexation of U in porewater samples. The AsFlFFF-ICP-MS technique is sufficiently sensitive to allow measurement of U–DOC complexation at natural DOC and U concentrations. This approach is particularly useful if sample volumes are limited as might be the case for porewater studies.

3.8 Acknowledgements

This research was funded by a research grant from the Natural Sciences and Engineering Council of Canada (NSERC) to M.J. Hendry and a USEPA research grant to J.F. Ranville.

3.9 References

Aiken, G.R., McKnight, D.M., Wershaw, R.L., and McCarthy, P., 1985, An Introduction to Humic Substances in Soil, Sediment, and Water, *in* MacCarthy, P., ed., Humic Substances in Soil, Sediment, and Water: Geochemistry, Isolation, and Characterization: New York, John Wiley & Sons, Inc., p. 1-9.

Aravena, R., Wassenaar, L.I., and Plummer, L.N., 1995, Estimating C-14 Groundwater Ages in a Methanogenic Aquifer: Water Resources Research, v. 31, p. 2307-2317.

Artinger, R., Buckau, G., Geyer, S., Fritz, P., Wolf, M., and Kim, J.I., 2000, Characterization of groundwater humic substances: influence of sedimentary organic carbon: Applied Geochemistry, v. 15, p. 97-116.

Artinger, R., Kienzler, B., Schussler, W., and Kim, J.I., 1998, Effects of humic substances on the Am-241 migration in a sandy aquifer: column experiments with Gorleben groundwater/sediment systems: Journal of Contaminant Hydrology, v. 35, p. 261-275.

Artinger, R., Rabung, T., Kim, J.I., Sachs, S., Schmeide, K., Heise, K.H., Bernhard, G., and Nitsche, H., 2002a, Humic colloid-borne migration of uranium in sand columns: Journal of Contaminant Hydrology, v. 58, p. 1-12.

Artinger, R., Schuessler, W., Scherbaum, F., Schild, D., and Kim, J.I., 2002b, Am-241 migration in a sandy aquifer studied by long-term column experiments: Environmental Science & Technology, v. 36, p. 4818-4823.

Beckett, R., Jue, Z., and Giddings, J.C., 1987, Determination of Molecular-Weight Distributions of Fulvic and Humic Acids Using Flow Field-Flow Fractionation: Environmental Science & Technology, v. 21, p. 289-295.

Beckett, R., and Schimpf, M.E., 2000, Characterization of Humic Substances by Flow FFF, *in* Giddings, C.J., ed., Field-Flow Fractionation Handbook: New York, John Wiley & Sons, p. 497-505.

Benedetti, M., Ranville, J.F., Ponthieu, M., and Pinheiro, J.P., 2002, Field-flow fractionation characterization and binding properties of particulate and colloidal organic matter from the Rio Amazon and Rio Negro: Organic Geochemistry, v. 33, p. 269-279.

Benedetti, M.F., Ranville, J.F., Allard, T., Bednar, A.J., and Menguy, N., 2003, The iron status in colloidal matter from the Rio Negro, Brasil: Colloids and Surfaces A: Physicochemical and Engineering Aspects, v. 217, p. 1-9.

Chiou, C.T., Malcolm, R.L., Brinton, T.I., and Kile, D.E., 1986, Water Solubility Enhancement of Some Organic Pollutants and Pesticides by Dissolved Humic and Fulvic-Acids: Environmental Science & Technology, v. 20, p. 502-508.

Chopin, G.R., 1988, Humics and Radionuclide Migration: Radiochimica Acta, v. 44-5, p. 23-28.

Christensen, J.B., Jensen, D.L., and Christensen, T.H., 1996, Effect of dissolved organic carbon on the mobility of cadmium, nickel and zinc in leachate polluted groundwater: Water Research, v. 30, p. 3037-3049.

Crancon, P., and van der Lee, J., 2003, Speciation and mobility of uranium(VI) in humic-containing soils: Radiochimica Acta, v. 91, p. 673-679.

Crum, R.H., Murphy, E.M., and Keller, C.K., 1996, A non-adsorptive method for the isolation and fractionation of natural dissolved organic carbon: Water Research, v. 30, p. 1304-1311.

Dearlove, J.P.L., Longworth, G., Ivanovich, M., Kim, J.I., Delakowitz, B., and Zeh, P., 1991, A Study of Groundwater-Colloids and Their Geochemical Interactions with Natural Radionuclides in Gorleben Aquifer Systems: Radiochimica Acta, v. 52-3, p. 83-89.

Desaulniers, D.E., Cherry, J.A., and Fritz, P., 1981, Origin, Age and Movement of Pore Water in Argillaceous Quaternary Deposits at 4 Sites in Southwestern Ontario: Journal of Hydrology, v. 50, p. 231-257.

Fish, W., Dzombak, D.A., and Morel, F.M.M., 1986, Metal-Humate Interactions. 2. Application and comparison of models: Environmental Science & Technology, v. 20, p. 676-683.

Geckeis, H., Rabung, T.H., Ngo Mahn, T., Kim, J.I., and Beck, H.P., 2002, Humic colloid-borne natural polyvalent metal ions: Dissociation experiment: Environmental Science & Technology, v. 36, p. 2946-2952.

Giddings, C.J., 2000, The field flow fractionation family, underlying principles, *in* Schimpf, M.E., Caldwell, K., and Giddings, C.J., eds., Field-Flow Fractionation Handbook: New York, Wiley Interscience, p. 3-30.

Giesy, J.P., Geiger, R.A., Kevern, N.R., and Alberts, J.J., 1986, Uo-2(2+)-Humate Interactions in Soft, Acid, Humate-Rich Waters: Journal of Environmental Radioactivity, v. 4, p. 39-64.

Grenthe, I., 1992, Chemical Thermodynamics of Uranium: Amsterdam, North-Holland.

Hassellov, M., Lyven, B., and Beckett, R., 1999, Sedimentation field-flow fractionation coupled online to inductively coupled plasma mass spectrometry-New possibilities for studies of trace metal adsorption onto natural colloids: Environmental Science & Technology, v. 33, p. 4528-4531.

Hendry, M.J., Cherry, J.A., and Wallick, E.I., 1986, Origin and Distribution of Sulfate in a Fractured Till in Southern Alberta, Canada: Water Resources Research, v. 22, p. 45-61.

Hendry, M.J., Ranville, J.R., Boldt-Leppin, B.E.J., and Wassenaar, L.I., 2003, Geochemical and transport properties of dissolved organic carbon in a clay-rich aquitard: Water Resources Research, v. 39, p. 1194-1203.

Hendry, M.J., and Wassenaar, L.I., 1999, Implications of the distribution of delta-D in pore waters for groundwater flow and the timing of geologic events in a thick aquitard system.: Water Resources Research, v. 35, p. 1751-1760.

—, 2000, Controls on the distribution of major ions in pore waters of a thick surficial aquitard: Water Resources Research, v. 36, p. 503-513.

—, 2004, Transport and geochemical controls on the distribution of solutes and stable isotopes in a thick clay-rich till aquitard, Canada: Isotopes in Environmental and Health Studies, v. 41, p. 3.

Hendry, M.J., Wassenaar, L.I., and Kotzer, T., 2000, Chloride and chlorine isotopes (Cl-36 and delta Cl-37) as tracers of solute migration in a thick, clay-rich aquitard system: Water Resources Research, v. 36, p. 285-296.

Herbelin, A.L., and Westall, J.C., 1996, FITEQL A computer program for determination of chemical equilibrium constants from experimental data, Oregon State University.

Higgo, J.J.W., Williams, G.M., Harrison, I., Warwick, P., Gardiner, M.P., and Longworth, G., 1993, Colloid transport in a glacial sand aquifer. Laboratory and field results: Colloids and Surfaces A: Physicochemical and Engineering Aspects, v. 73, p. 179-200.

Hummel, W., Glaus, M.A., and Van Loon, L.R., 2000, Trace metal-humate interactions, II. The 'conservative roof' model and it's application.: Applied Geochemistry, v. 15, p. 975-1001.

Jackson, B.P., Ranville, J.F., Bertsch, P.M., and Sowder, A.G., 2005, Characterization of colloidal and humic-bound Ni and U in the "dissolved" fraction of contaminated sediment extracts: Environmental Science & Technology, v. 39, p. 2478-2485.

Kaplan, D.I., Bertsch, P.M., Adriano, D.C., and Orlandini, K.A., 1994, Actinide Association with Groundwater Colloids in a Coastal-Plain Aquifer: Radiochimica Acta, v. 66-7, p. 181-187.

Kim, J.I., 1994, Actinide Colloids in Natural Aquifer Systems: Mrs Bulletin, v. 19, p. 47-53.

Kim, J.I., Delakowitz, B., Zeh, P., Klotz, D., and Lazik, D., 1994, A Column Experiment for the Study of Colloidal Radionuclide Migration in Gorleben Aquifer Systems: Radiochimica Acta, v. 66-7, p. 165-171.

Kim, J.I., Zeh, P., and Delakowitz, B., 1992, Chemical Interactions of Actinide Ions with Groundwater Colloids in Gorleben Aquifer Systems: Radiochimica Acta, v. 58-9, p. 147-154.

Lawrence, J.R., Hendry, M.J., Wassenaar, L.I., Germida, J.J., Wolfaardt, G.M., Fortin, N., and Greer, C.W., 2000, Distribution and biogeochemical importance of bacterial populations in a thick clay-rich aquitard system: Microbial Ecology, v. 40, p. 273-291.

Lenhart, J.J., Cabaniss, S.E., MacCarthy, P., and Honeyman, B.D., 2000, Uranium(VI) complexation with citric, humic and fulvic acids: Radiochimica Acta, v. 88, p. 345-353.

Lenhart, J.J., and Honeyman, B.D., 1999, Uranium(VI) sorption to hematite in the presence of humic acid: Geochimica Et Cosmochimica Acta, v. 63, p. 2891-2901.

Mantoura, R.F.C., Dickson, A., and Riley, J.P., 1978, Complexation of Metals with Humic Materials in Natural-Waters: Estuarine and Coastal Marine Science, v. 6, p. 387-408.

McCarthy, J.F., Czerwinski, K.R., Sanford, W.E., Jardine, P., and Marsh, J.D., 1998, Mobilization of transuranic radionuclides from disposal trenches by natural organic matter: Journal of Contaminant Hydrology, v. 30, p. 49-77.

McCarthy, J.F., Williams, T.M., Liang, L., Jardine, P., Jolley, L.W., Taylor, D.L., Palumbo, A.V., and Cooper, L.W., 1993, Mobility of natural organic matter in a sandy aquifer: Environmental Science & Technology, v. 27, p. 667-676.

Means, J.L., Maest, A.S., and Crear, D.S., 1987, *in* P., H., ed., The Technology of High-Level Nuclear Waste Disposal, p. 215-247.

Ranville, J.F., Chittleborough, D.J., Shanks, F., Morrison, R.J.S., Harris, T., Doss, F., and Beckett, R., 1999, Development of sedimentation field-flow fractionation-inductively coupled plasma mass-spectrometry for the characterization of environmental colloids: Analytica Chimica Acta, v. 381, p. 315-329.

Ranville, J.F., and Macalady, D.L., 1997, *in* Sather, O., ed., Geochemical Processes, Weathering and Groundwater Recharge in Catchments, Balkema.

Ranville, J.F., and Schmiermund, R.L., 1999, General aspects of aquatic colloids in environmental geology, *in* Logsdon, M.J., ed., The environmental geochemistry of mineral deposits Part A: Processes, techniques, and health issues., Volume 6A: Reviews in Economic Geology: Chelsea, Society of Economic Geologists, Inc., p. 183-199.

Sandino, A., and Bruno, J., 1992, The Solubility of (Uo2)3(Po4)2.4H2O(S) and the Formation of U(Vi) Phosphate Complexes - Their Influence in Uranium Speciation in Natural-Waters: Geochimica Et Cosmochimica Acta, v. 56, p. 4135-4145.

Schussler, W., Artinger, R., Kim, J.I., Bryan, N.D., and Griffin, D., 2001, Numerical modeling of humic colloid borne Americium(III) migration in column experiments using the transport/speciation code K1D and the KICAM model: Journal of Contaminant Hydrology, v. 47, p. 311-322.

Scott, D.T., McKnight, D.M., Blunt-Harris, E.L., Kolesar, S.F., and Lovely, D.R., 1998, Quinone Moieties Act as Electron Acceptors in the Reduction of Humic Substances by Humics-Reducing Microorganisms: Environmental Science & Technology, v. 32, p. 2984-2989.

Shaw, J., and Hendry, M.J., 1998, Groundwater flow in a thick clay till and clay bedrock sequence in Saskatchewan, Canada: Canadian Geotechnical Journal, v. 35, p. 1041-1052.

Silva, R.J., 1992, Mechanisms for the retardation of uranium (VI) migration: Mater. Res. Cos. Symp. Proc., v. 257, p. 323-330.

Taylor, H.E., Garbarino, J.R., Murphy, D.M., and Beckett, R., 1992, Inductively Coupled Plasma Mass-Spectrometry as an Element-Specific Detector for Field-Flow Fractionation Particle Separation: Analytical Chemistry, v. 64, p. 2036-2041.

Thurman, E.M., 1985, Organic Geochemistry of Natural Waters: Dordrecht, Martinus Nijhoff/Dr W. Junk Publishers, 497 p.

Tipping, E., and Hurley, M.A., 1992, A unifying model of cation binding by humic substances: Geochimica Et Cosmochimica Acta, p. 3627-3641.

Wahlund, K.-G., 2000, Asymmetrical Flow-Field Flow Fractionation, *in* Giddings, C.J., ed., Field-Flow Fractionation Handbook: New York, John Wiley & Sons, p. 279-294.

Wassenaar, L.I., and Hendry, M.J., 1999, Improved piezometer construction and sampling techniques to determine pore water chemistry in aquitards: Ground Water, v. 37, p. 564-571.

Westall, J.C., Jones, J.D., Turner, G.D., and Zachara, J.M., 1995, Models for Association of Metal-Ions with Heterogeneous Environmental Sorbents. 1. Complexation of Co(II) by Leonardite Humic-Acid as a Function of pH and $NaClO_4$ Concentration: Environmental Science & Technology, v. 29, p. 951-959.

Yan, X.P., Kerrich, R., and Hendry, M.J., 2000, Distribution of arsenic(III), arsenic(V) and total inorganic arsenic in porewaters from a thick till and clay-rich aquitard sequence, Saskatchewan, Canada: Geochimica Et Cosmochimica Acta, v. 64, p. 2637-2648.

Zeh, P., Czerwinski, K.R., and Kim, J.I., 1997, Speciation of uranium in Gorleben groundwaters: Radiochimica Acta, v. 76, p. 37-44.

4.0 COMPLEXATION OF AQUEOUS ELEMENTS BY DOC IN A CLAY AQUITARD

4.1 Abstract

The extent of partitioning of several elements (Cu, Mn, Mo, Ni, Sr, U and Zn) on DOC was investigated in pore water samples collected from a clay-rich aquitard. High DOC concentrations in the aquitard, ranging from 21-143 mg l^{-1}, and natural aqueous metal concentrations higher than in most ground water environments facilitated complexation studies at this site. Analyses were conducted using on-line coupling of Asymmetrical Flow Field-Flow Fractionation (AsFlFFF) with UV, TOC and ICP-MS detectors. Of the elements investigated, only U and Zn were complexed with all DOC samples, ranging from 2.2-60 μg U g^{-1} DOC (0.4-3% of the total U in the pore waters) and 0.04-.0.5 μg Zn g^{-1} DOC (0.1-0.9% of the total Zn in the pore waters), respectively. Laboratory experiments conducted over a range in pH (1.3-9.7) and geochemical modeling supported the measured complexation of U and Zn on the DOC. The *in situ* association constant, K_d, for U decreased with depth from 76 ml g^{-1}C for pore water samples at 2.2 m below ground (B.G.) to 24 ml g^{-1}C at 9.7 m B.G.. The decrease was attributed to a decrease in aromaticity of the DOC with depth. Zn K_d values constants ranged from 2-12 ml g^{-1}C and exhibited no trend with depth. Results of the current study suggest minor masses of U and Zn (≤4% of total) complex with this DOC under *in situ* pH conditions. Our data suggest that competitive complexation by other ligands may limit the importance of DOC facilitated transport of the elements studied in waters of similar chemical composition.

4.2 Introduction

Naturally occurring dissolved organic matter is ubiquitous in ground water (Thurman, 1985b). Dissolved organic matter is usually reported as dissolved organic

carbon (DOC, 0.45 μm filtrate) and is generally comprised of aquatic humic colloids in the form of higher molecular weight humic (HA) and fulvic acids (FA) and lower molecular weight hydrophilic organic acids (Thurman, 1985a). Because elements can complex with DOC (Choppin, 1988; Christensen et al., 1996; Lenhart et al., 2000; Mantoura et al., 1978), they can undergo facilitated transport in ground waters (Artinger et al., 2000; Artinger et al., 1998; Schussler et al., 2001). In particular, heavy metal speciation and mobility can be significantly altered by different forms of DOC due to formation of aqueous metal complexes (Geckeis et al., 2002; Porasso et al., 2002).

Laboratory-based studies show actinides and rare earth elements complex to DOC depending upon solution pH and ionic strength (Czerwinski et al., 1996; Schafer et al., 2003; Tang and Johannesson, 2003). Christensen and Christensen (1999) assessed the complexation of Cd, Ni, and Zn to DOC using resin exchange methods and compared the results to computer speciation modeling. Similarly, Cheng et al. (2005) studied Zn binding to DOC using anodic stripping voltammetry and compared the results to speciation modeling. Both studies show elemental complexation to DOC occurs but the extent of complexation varies. Size-exclusion chromatography (SEC) coupled with ICP-MS shows Al, Fe, Ni, and Pb complexation occurs with natural organic matter from bog lake water (Schmitt et al., 2001). Actinide ions, such as the uranyl ion, form complexes with DOC, which facilitate transport of the elements in column studies using natural sand and ground water rich in DOC (Artinger et al., 2002; Kim et al., 1994).

In contrast to lab based studies, few field-based studies of U complexation with DOC and subsequent facilitated transport have been conducted (Kaplan et al., 1994; Kim, 1994; Ranville et al., 2007; Zeh et al., 1997). The available studies show metal complexation to DOC occurs, but the degree of complexation is dependant upon environmental conditions. Further, most work on complexation to date has involved soil-derived humic substances, whose properties may differ significantly from DOC associated with older ground waters (Ranville et al., 2007).

The objectives of this study were to quantify the mass of element complexation with DOC in ground waters. Samples were selected from an aquitard instead of samples from an aquifer for three reasons. First, aquitards frequently contain greater concentrations of DOC (2-160 mg l^{-1}; Hendry and Wassenaar (2004) compared to aquifers (0.2-15 mg l^{-1}; Thurman (1985b), thus making investigation of element-DOC complexation easier (Hendry et al., 2003). Second, the transport of inorganic solutes and DOC in aquitards is dominated by long-term molecular diffusion (Hendry et al., 2003; Hendry and Wassenaar, 1999, 2004, 2005) and contact between the aqueous phase trace elements and the DOC can occur for several thousands of years (Hendry and Wassenaar, 2005), thus minimizing kinetic effects associated with element-DOC complexation and allowing determination of the long-term partitioning of elements. Third, the study of facilitated transport of metals and actinides in aquitards is of specific interest because of their potential as repository sites for high-level radioactive waste (Claret et al., 2005; Lebon and Mouroux, 1999).

Detectable elements were quantified in pore water samples collected through the upper 12 m of a thick (80 m), low permeability clay-rich till aquitard. The elements associated with the DOC and the aqueous phase were determined by on-line coupling of Field-Flow Fractionation (FFF) (Wahlund, 2000) with inductively coupled plasma-mass spectrometry (ICP-MS) (Benedetti et al., 2002; Geckeis et al., 2003; Hassellov et al., 1999; Ranville and Schmiermund, 1999; Van den Kammer et al., 2003). Although relatively few studies of ground water DOC have used FFF-ICP-MS (Geckeis et al., 2003; Ranville et al., 2007), it has a number of advantages over SEC. In general fewer chemical interactions take place between the sample and the FFF channel. Further, the ionic strength of the carrier solution for FFF is much lower than required for SEC and can be similar to the ionic strength of the sample, which may minimize the possibility of sample alteration during fractionation.

This study builds on work conducted by Ranville et al. (2007) who quantified U complexation with DOC using AsFlFFF-ICP-MS at the same study site. However, the current study differs from that of Ranville et al. (2007) in several ways. It addresses the complexation of a wider range of elements to DOC and does so across a more detailed

pore water – depth profile. In addition, the current study also examines the effects of pH on U complexation to DOC and the kinetics of the complexation/dissociation of U and Zn to DOC. Further, in addition to the on-line UV detection method used by Ranville et al. (2007), this study applies on-line TOC analysis. The current study also determines K_d values for U and Zn on the DOC with depth at the research site and provides a potential explanation for these values. Lastly, the current study provides a comparison between the binding of U and Zn in a natural ground water system to that in an ideal system containing only fulvic acid and elements (with no competitive complexation present). These results may explain why lab based studies commonly document considerable metal complexation with DOC, wheras under field conditions this may not be the case.

4.3 Site Description

Porewater samples were collected from the King aquitard research site in southern Saskatchewan (51.05 N Lat., 106.5 W Long). This site was selected for study because the hydrogeology (Hendry and Wassenaar, 2004; Shaw and Hendry, 1998) and hydrochemistry (Hendry and Wassenaar, 2000; Johannesson and Hendry, 2000; Yan et al., 2000) are well defined. In addition, the characteristics, source areas, ages, and mode of migration of DOC are documented (Hendry et al., 2003; Hendry and Wassenaar, 2005; Reszat and Hendry, 2005), as is an initial assessment of U-DOC complexation (Ranville et al., 2007).

The King site is a thick aquitard sequence, consisting of 80 m of a homogeneous clay-rich Pleistocene glacial till (20 ka – 30 ka BP) overlying 76 m of massive clay from the Cretaceous Snakebite member of the Bearpaw Formation (71 ka – 72 ka). The upper 3 m of the till is fractured, weathered and brown. Ground water flow in this zone is dynamic and exhibits seasonal fluctuations. At depths >3-4 m, the till appears massive, unoxidized, dark grey, and non-fractured. The average downward ground water velocity through this zone is sluggish, ranging between 0.5 and 0.8 m per 10 ka (Hendry and Wassenaar, 1999, 2005; Shaw and Hendry, 1998). The low ground water velocity at this site results in solute transport being dominated by diffusive processes (Hendry and Wassenaar, 1999, 2005).

DOC concentrations at the King site range from 145 mg l^{-1} in the upper weathered zone to a minimum of around 10 mg l^{-1} at 30 m below ground (B.G.) (Hendry et al., 2003; Hendry and Wassenaar, 2005). Radiocarbon and $\delta^{13}C$ measurements on DOC and numerical simulations of DOC transport show two end members in the diffusive mixing profile: soil derived organic carbon formed since the Holocene (about 10 ka BP) and DOC from connate pore water (about 15 ka BP) (Hendry and Wassenaar, 2005). The chemical structure of DOC in the till is comprised almost entirely of aliphatic carbon bonds, suggesting predominantly fulvic type acids (Reszat and Hendry, 2005). DOC at this site has a Weight Averaged Molecular Weight (M_w) of 1100 to 1390 daltons, a Number Averaged Molecular Weight (M_n) of 890 to 1120 daltons, and Polydispersity (M_w/M_n) of 1.22-1.33 (Reszat and Hendry, 2005). Ranville et al. (2007) observed <2% of total aqueous U at the site was associated with DOC and supported their findings with geochemical modeling .

4.4 Materials and Methods

4.4.1 Pore water Sampling and Analyses

Pore water samples for DOC analyses were collected from 8 piezometers installed in the upper oxidized (1.2 and 2.2 m B.G.) and lower unoxidized till (3.7, 5.3, 6.9, 8.4, 9.7, and 11.2 m B.G.) on November 4, 2004. All samples were collected by slowly lowering a dedicated, sterilized, PVC bailer system to a depth of 1 m below the water column in each piezometer. Once the samples were brought to ground surface, they were field filtered using 0.45 μm membrane filters and stored in low-density polyethylene (LDPE) bottles in the dark at 5 ºC until analysis. A portion of the sample was split in the field and acidified with ultra-pure nitric acid for metal analysis. All chemical analyses were performed within two weeks of sampling. Separation experiments (described below) were performed two months after sampling. More details on sampling techniques used in this aquitard are provided in (Hendry and Wassenaar, 2000) and (Johannesson and Hendry, 2000).

All samples were analyzed for DOC concentration using a Shimadzu TOC-5050A. The major ion chemistry of pore water samples (SO_4, Ca, Mg, and Na) was determined using ion chromatography. Alkalinity (reported as HCO_3) was determined using a Radiometer Analytical Titration system. Total element analyses (Cu, Mn, Mo, Ni, Sr, U and Zn) were performed by Inductively Coupled Plasma – Atomic Emission Spectroscopy at SRC Analytical Laboratories, Saskatoon, Canada. Eh, pH and temperature were determined in the field during sampling using an Orion field portable meter (Thermo Electron). Lower limits of detection (LLD), where available, are provided in Table 4-2.

4.4.2 Standards

In addition to the natural pore water samples, a 500 ppb uranyl nitrate solution was prepared with 70 mg l^{-1} Suwannee River Fulvic Acid Standard (SRFA; International Humic Substances Society - 2S101F) in 0.1 *M* Na_2SO_4. The pH was adjusted to 7.5 with NaOH. This solution (DOC + U solutions) was allowed to equilibrate for 1 month prior to separation experiments. This time period was considered adequate to attain near equilibrium conditions (see discussion on kinetics, below). DOC (TOC 5050) and U (ICP-MS) concentrations in the standard were confirmed within one week of preparation.

4.4.3 Characterizing the DOC.

DOC was separated from the aqueous phase of each pore water sample using an Asymmetrical Flow Field-Flow Fractionation (AsFlFFF) system (model HRFFF 10.000) from Postnova Analytics (FFFractionation, Salt Lake City, Utah). The PC controlled instrumentation consisted of an arrangement of pumps, an AsFlFFF channel, and a vacuum degasser. The AsFlFFF system primarily separates colloids by molecular weight. Colloids, in this case DOC, are detected as they elute from the system after fractionation. The resulting plots of detector intensity vs. time, termed fractograms, consist of two regions: the void peak, which may contain some undifferentiated low molecular weight ligands, and the colloidal peak(s). The theory and application of AsFlFFF are presented elsewhere (Wahlund, 2000).

Characterization and identification of DOC was done with UV (254 nm) and DOC analysis as described in Reszat and Hendry (2005). Molecular weight of the DOC was determined from system calibration with sodium poly(styrene sulphonate) standards (American Polymer Standards Corp.) (M_w = 910, 1430, 4800, 6500 and 15450 Daltons). All fractograms were measured in duplicate and the results averaged. The lower limit of detection (LLD) of the TOC and UV analyzers with online measurements depends on detector setting, as well as separation efficiency of the AsFlFFF. For the instrument settings used in this experiment, the approximate LLD for DOC with UV analysis was 5 mg l^{-1} total DOC, and for the TOC analyzer was 0.5 mg l^{-1} total DOC. The AsFlFFF conditions consisted of a laminar in flow of 5.0 mL min^{-1}, a laminar out flow of 1.5 ml min^{-1}, a cross flow of 70%, and an injection volume of 100 μl.

The relative amount of aromatic carbon was determined on all DOC samples using a technique termed Normalized Intensity Comparison (NIC) developed by Reszat and Hendry (2005). Because UV detection (254 nm) resolves the aromatic carbon in a fraction of DOC, and TOC detection can resolve all carbon moieties, aromaticity was determined from the difference in normalized area calculations from a UV detector to that from the TOC detector in different DOC fractions. As a result, differences between NIC measurements provide an indication of the relative amounts of aliphatic carbon present in these samples.

The amount of recovered DOC after fractionation was determined for all pore water and DOC standard samples used in complexation experiments using a fraction collector (ISCO Foxy Jr.). In these tests, the void and the DOC peaks were recovered and the DOC concentration in the fractions determined using a Shimadzu TOC 5050. The fractionated peaks were recovered in consecutive runs ($n \approx 10$) until enough volume was collected in each fraction (approximately 10 ml) to allow the DOC concentration of the fractions to be measured. The total amount of DOC injected into the AsFlFFF channel (from the injection loop size and the DOC concentration in the sample) and the recovered peak concentrations were used to calculate the amount of recovered DOC.

4.4.4 Defining Element-DOC Complexation

To define element complexation with DOC the effluent stream from the AsFIFFF channel was first routed to the UV detector (Postnova Analytics, 254 nm) where the DOC-element complex was separated and the DOC peak quantified. After the AsFlFFF effluent passed through the UV detector, it was routed directly into the nebulizer of the ICP-MS where elements associated with the DOC were quantified. In these separations, the UV detector was used because, unlike the TOC detector, it is non-consumptive with respect to DOC. A Micromass Platform ICP-MS (Micromass Ltd., Manchester, UK), equipped with a Hexapole collision cell, was used for all analyses.

Element calibration was achieved by injecting 1, 10 and 100 ppb multi-element standard through the AsFlFFF with cross-flow field off and measuring the element intensity with the ICP-MS. Peak areas were used for intensity integration and the creation of a calibration curve for element concentrations in each sample. A typical analytical procedure consisted of a mobile phase (0.005 *M* Na_2SO_4 + 0.003 *M* NaN_3) blank, the calibration standards, a sample, and the calibration standards again. Calibration curves were constructed for each sample from an average of the standards run before and after the samples. All samples and calibration standards were run in duplicate and results averaged.

The fraction of element associated with the DOC was calculated by dividing the concentration associated with the DOC peak by that of the total element concentration in the filtered water sample. Importantly, the majority of elemental mass in the aqueous state (aquo-ions) are pulled through the membrane and ceramic frit into the waste stream by the cross-flow pump and are not eluted to the detection systems. As a result, the elemental responses noted with ICP-MS are attributable to colloidal material.

4.4.5 pH Control on DOC-Element Complexation

Kinetic tests were performed to determine how DOC-element complexes respond to a change in pH over time. Tests were conducted by monitoring the changes in U and Zn (chosen based on results of element-DOC complexation, discussed below)

complexed to the DOC by altering the pH of two pore water samples (2.2 and 5.3 m B.G.) and monitoring the change in concentrations on the DOC with time using the coupled UV-ICP-MS technique. First, concentrations of U and Zn on pore water DOC were determined at the *in-situ* pH. At time zero, the samples (50 ml) were acidified to pH 2.5 using concentrated sulphuric acid, and U and Zn concentrations on the DOC were measured with time (t = 0, 4, 16, 50, 100, 180, and 970 min).

Subsequent to these kinetic tests, a pH titration was performed on the pore water sample (50 ml) from 2.2 m B.G. and the SRFA-U solution to determine the impact of competing ligands on the speciation of U and Zn over a range in pH, as well as examining the complexation capability of the DOC functional groups over a range in pH. The analysis of the pore water sample containing ligands such as carbonate and sulphate was compared to a sample containing only DOC and U (SRFA-U solution). In these tests, the pH was incrementally changed with concentrated H_2SO_4 (18 *M*; for pH <7.5) and NaOH (19.4 *M*; for pH >7.5). The solutions with altered pH were allowed to equilibrate for 2 h (based on results of the kinetic tests) before determining the elemental concentrations on DOC using UV- ICP-MS. Sulphuric acid and sodium hydroxide were used because the pore water samples are Na- and SO_4-type waters (Hendry and Wassenaar, 2000). The total mass of U and Zn on the DOC at each pH was calculated using the method previously described.

A linear *in-situ* association constant (K_d) was calculated for the U and Zn complexed with DOC for each pore water sample analyzed using

$$K_d = C^* / C \qquad [1]$$

where C^* is the mass of element complexed per unit weight of DOC, and C is the concentration of the element in solution in equilibrium with mass of DOC.

4.4.6 Geochemical Modeling

Geochemical modeling of U and Zn binding to the DOC in the pore water samples and SRFA-U solutions (including pH titrations) was performed using Visual

MINTEQ version 2.32 (Gustafsson, 2005). The objectives of modeling were to verify that the experimental results were consistent with previously measured values and current knowledge of DOC-metal complexation. Modeling also provided insight into metal partitioning aside from the DOC-metal complexes which were measured in the experiments. Modeling used the Non-Ideal Competitive Adsorption (NICA-Donnan) model properties for a generic fulvic acid (FA).

The NICA-Donnan model was created by combining the NICA isotherm with a Donnan model to describe counter ion accumulation (Benedetti et al., 1996; Christensen et al., 1998; Milne et al., 2001; Milne et al., 2003). Visual MINTEQ contains site specific sites which are type 1 (carboxylic – FA1) and type 2 (phenolic and other – FA2). The parameters used in the models were for a generic FA. Log K values from the MINTEQ database were used (Table 4-1). Previous work at this site shows the DOC is aliphatic relative to typical DOC (Reszat and Hendry, 2005) and therefore no humic acid was considered in the model simulations.

Table 4-1. Thermodynamic data used to simulate the binding of aqueous metal species to humic substances in the complexation modeling (data from the MINTEQ Database; (Gustafsson, 2005))

Reaction – FA1	log K	Reaction – FA2	log K
FA1- + H+ = FA1-H	2.34	FA2- + H+ = FA2-H	8.6
FA1- + Cu+2 = FA1-Cu	0.26	FA2- + Cu+2 = FA2-Cu	8.26
FA1- + Mg+2 = FA1-Mg	-2.1	FA2- + Mg+2 = FA2-Mg	-2.4
FA1- + Ni+2 = FA1-Ni	-2.07	FA2- + Ni+2 = FA2-Ni	2.03
FA1- + Sr+2 = FA1-Sr	-2.5	FA2- + Sr+2 = FA2-Sr	-4.6
FA1- + UO2-2 = FA1-UO2	0.78	FA2- + UO2-2 = FA2-UO2	9.06
FA1- + Zn+2 = FA1-Zn	-3.84	FA2- + Zn+2 = FA2-Zn	-0.73

The simulations contained the elements which were chemically analyzed and had FA binding parameters included in the Visual MINTEQ model in order to account for competitive complexation of metals by FA. Discussion of metal binding, however, is limited to U and Zn, to which a direct comparison of results could be made.

Table 4-2. Selected pore water chemistry data (<0.45 μm) from the King research site.

	Units	LLD[b]	1.2 m	2.2 m	3.7 m	5.3 m	6.9 m	8.4 m	9.7 m	11.2 m
Ionic strength	mol l^{-1}	n/a[c]	0.84	1.00	0.65	0.49	0.40	0.29	0.26	0.15
Eh	volts	n/a	0.17	0.09	0.05	-0.04	-0.03	-0.16	-0.17	-0.17
pH	units	0.07	8.0	8.1	8.3	8.1	7.9	7.9	7.9	7.9
HCO_3	mg l^{-1}	1	681	742	852	946	972	924	965	889
Ca	mg l^{-1}	2	400	410	370	400	420	410	400	380
Mg	mg l^{-1}	2	82	88	56	52	48	37	34	23
Na	mg l^{-1}	2	8900	10400	6600	4600	3630	2850	2690	1580
SO_4	mg l^{-1}	4	41200	49500	27700	21000	15400	10900	9300	4900
Cu	μg l^{-1}	1.18	69	150	43	11	12	17	16	21
Mn	μg l^{-1}	1.19	7	142	470	1900	1400	1110	1290	950
Mo	μg l^{-1}	0.63	240	250	270	91	100	88	140	16
Ni	μg l^{-1}	7.01	38	36	73	41	300	210	190	53
Sr	μg l^{-1}	0.14	7490	10100	8200	12400	11700	8450	7430	4310
U	μg l^{-1}	0.06	556	789	582	491	349	302	224	53
Zn	μg l^{-1}	0.21	45	50	70	30	40	18	21	53
DOC	mg l^{-1}	n/a	98.7	142.7	71.3	51.4	50.7	47.6	40.1	20.9
M_w DOC[d]	Da	n/a	1200	1140	1160	1270	1390	1200	1240	1290
M_n DOC[d]	Da	n/a	920	890	900	960	1120	980	1020	1030
M_w/M_n[d]		n/a	1.30	1.28	1.29	1.33	1.24	1.23	1.22	1.25

[a] from Hendry and Wassenaar (2000).
[b] LLD = lower limit of detection
[d] determined from TOC fractogram data.

4.5 Results and Discussion

4.5.1 Distribution of DOC

Total DOC concentrations in the pore water samples range from 142 mgC l^{-1} near the surface to 21 mg l^{-1} at 11.2 m B.G. (Table 4-2). These data compare well with previous measurements of DOC (10 years of measurements; n=12) (Hendry and Wassenaar, 2005). Standard deviations for the 10 yr data set are presented in Figure 4-1. The UV and TOC fractograms are well defined as represented by the fractograms for 1.2 and 8.4 m B.G. (Figure 4-2). In both cases the fractograms consist of two clearly defined regions: the void peak and DOC peak. The void peak (0-500 Da) consists of undifferentiated low molecular weight material, which the AsFlFFF system is unable to separate. The differentiated peak above 500 Da constitutes the fractionated DOC. The presence of organic matter in this peak was verified using the TOC detection system, which identifies only organic carbon. The concentration of DOC in the pore waters decreases with depth (Table 4-2), shown by the decrease in intensity of the UV and TOC signals between the 1.2 and 8.4 m samples. The M_w of the differentiated DOC peak ranges from 1098-1205 Da and 1380-1520 Da using the TOC and UV fractograms data, respectively. In both cases M_w is uniform with depth. We present the M_w data from the TOC analysis as being most representative of the DOC in Table 4-2 and Figure 4-2 because Reszat and Hendry (2005) show M_w data from TOC analysis are more representative of the DOC than M_w data from the UV data. The M_w and UV of the DOC suggest DOC is dominated by FA, in keeping with the observations of Ranville et al. (2007). The calculated M_w values are in agreement with other measurements of FA, taking into consideration differences in analytical technique (Perminova et al., 2003).

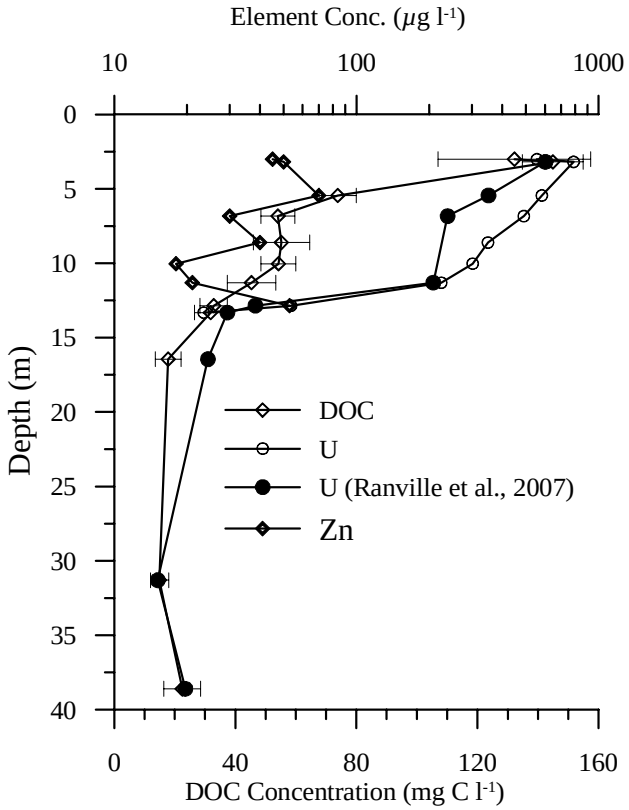

Figure 4-1. Pore water DOC, U and Zn concentrations vs. depth at the King site. DOC concentrations from this study are presented as data points, with the standard deviation from 10 years of measurements (n=12) presented as error bars (Hendry et al., 2003). U concentrations from Ranville et al. (2007) are shown for comparison.

A plot of NIC vs. depth for the pore water DOC is presented in Figure 4-3a. Additional NIC data from other piezometers and a surface water sample from the site (Reszat and Hendry 2005) are also presented in Figure 4-3a. These data sets show that the NIC decreases with depth from 0.58 at 1.2 m to 0.46 at 11.2 m. As discussed by Reszat and Hendry (2005), these data reflect a decrease in aromaticity of DOC with depth. The mass of DOC recovered from the FFF experiments range between 20-28% (Table 4-3). Because the 1000 Da membrane used in the FFF is close to the mean molecular weight of the DOC (Table 4-2), the low recoveries may be attributed in part to the loss of some low M_w DOC though the membrane of the channel during fractionation. In addition, low recoveries may be exacerbated by the presence of some low M_w DOC in the void peak.

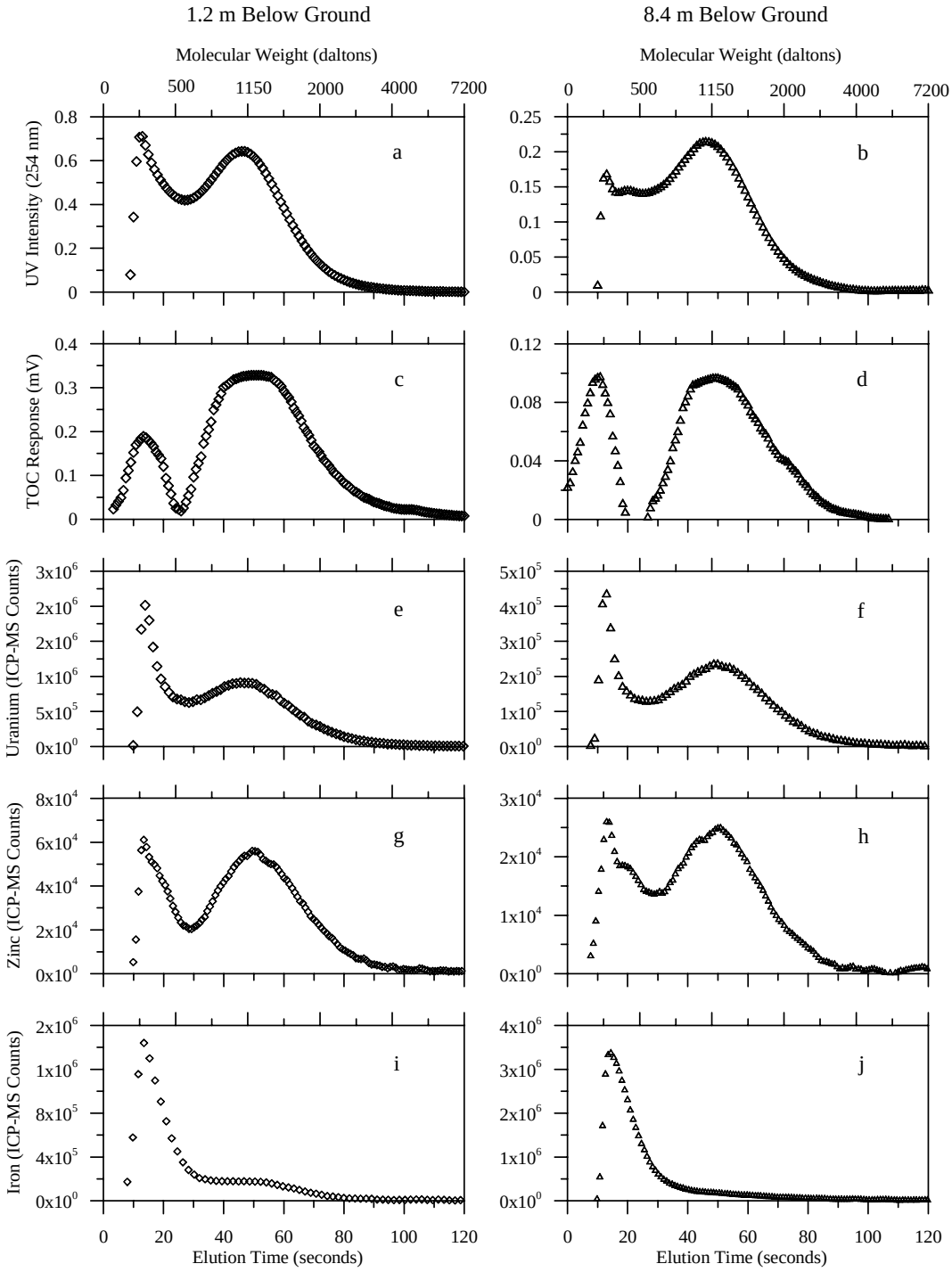

Figure 4-2. Selected fractograms for UV, TOC, U, Zn and Fe from pore water samples. (a), (c), (e), (g) and (i) are data collected from the piezometer installed at 1.2 m B.G. (open diamonds), and (b), (d), (f), (h) and (j) are data collected from the piezometer installed 8.4 m B.G. (open triangles). Note the difference in the scale of the y-axes between the 1.2 and 8.4 m B.G. samples.

Table 4-3. Measured, calculated and modeled complexation of U and Zn on pore water DOC.

	Units	1.2 m	2.2 m	3.7 m	5.3 m	6.9 m	8.4 m	9.7 m	11.2 m
DOC Recovery	%	22	20	25	28	25	24	24	24
Measured U on DOC	μg U g^{-1}DOC	37	60	39	30	20	13	4.9	2.2
Measured U on DOC	%	2.6	3.2	1.9	1.3	1.1	1.0	0.47	0.43
Modeled U on DOC	%	3.7	3.8	1.3	0.88	0.95	1.0	0.99	0.78
K_d (U-DOC)	mL g^{-1}DOC	65	76	66	62	54	45	24	32
Meaured Zn on DOC	μg Zn g^{-1}DOC	0.50	0.46	0.43	0.31	0.28	0.21	0.038	b.d.l[a].
Measured Zn on DOC	%	0.90	0.75	0.68	0.57	0.45	0.51	0.10	b.d.l.
Modeled Zn on DOC	%	0.39	0.53	0.50	0.47	0.51	0.63	0.64	0.42
K_d (Zn-DOC)	ml g^{-1}DOC	11	9	6	10	7	12	2	b.d.l.

[a] b.d.l. = below detection limit

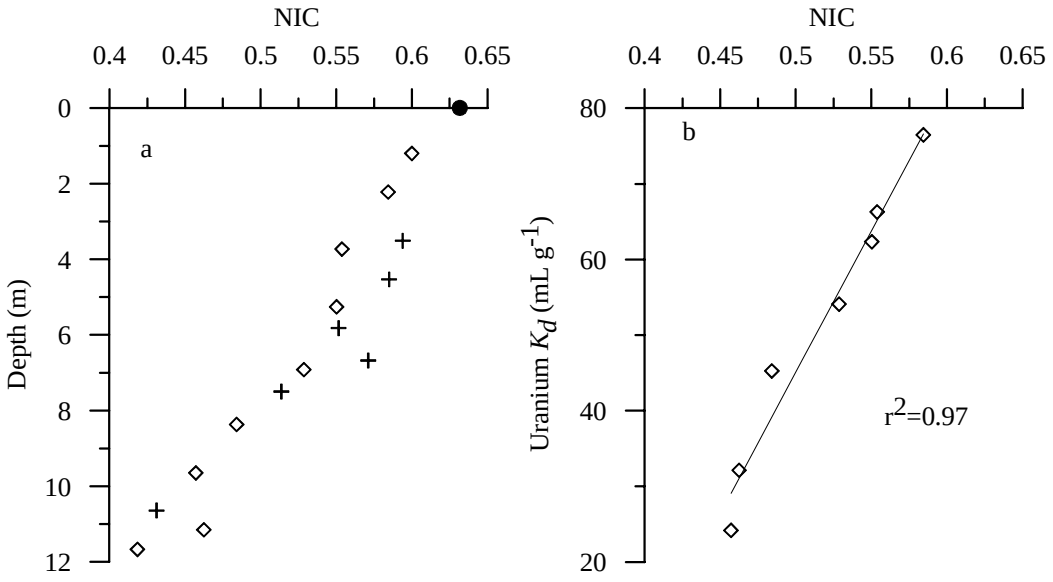

Figure 4-3. (a) Normalized Intensity Comparison (NIC) vs. depth below ground and (b) NIC vs. U K_d values. The open diamonds represent pore water samples for this experiment, the solid circle represents a sample of spring melt water collected at this site (Reszat and Hendry, 2005), and the crosses represent the NIC values for pore water samples determined by Reszat and Hendry (2005).

If the DOC present in the void peak is included in mass of recoverable DOC estimates, recoveries increase to about 45%. These overall low recoveries suggest some DOC may have been lost through the membrane. Ranville et al. (2007) obtained total DOC recoveries (DOC peak + void) of 47-98%, of which 25-64% were in the resolvable DOC peak. The greater recoveries of Ranville et al. (2007) may be attributed to differences in the separation conditions in the two experiments. The separation conditions used in the current study optimized conditions for the recovery of DOC in a Na_2SO_4 carrier solution, as well as for identification of DOC with the TOC analysis.

4.5.2 Pore Water Chemistry

The concentrations of the major ions (i.e., SO_4, Na, Mg and alkalinity as HCO_3) and other aqueous elements (Cu, Mn, Mo, Ni, Sr, U and Zn) in the pore water samples (<0.45 µm) are presented in Table 4-2. The major ion data are in keeping with earlier chemistry data from this site reported by Hendry and Wassenaar (2000) suggesting the pore water chemistry is stable with time as would be expected in a diffusion dominated

environment. The waters at this site are a Na-SO_4-type water with elevated carbonate concentrations. The Eh of the pore waters decrease from 0.17 V at 2.2 m to -0.17 V at 11.2 m B.G. (Hendry and Wassenaar, 2000). The pH ranges from 7.9 to 8.3 (Table 4-2). Concentrations of some aqueous constituents (Na, SO_4, Cu, Mg, Sr, and U) are highest in the oxidized zone and decrease with depth through the unoxidized zone. Unlike these constituents, the concentrations of HCO_3, Mn, Mo, Ni, and Zn exhibit no trend with depth. To exhibit the two depth trends U and Zn data are plotted vs. depth in Figure 4-1. The U concentrations range from 789 μg l^{-1} at 2.2 m and decrease to 53 μg l^{-1} at 11.2 m. The Zn concentrations range from 70 μg l^{-1} (3.7 m B.G.) to 18 μg l^{-1} (8.4 m B.G.). In the case of U, the measured values are in keeping with existing data for this site collected in June and August 2002 and reported by Ranville et al. (2007) (Figure 4-1). The distribution of these data reflect the presence of two end-members: elevated solute concentrations in the oxidized zone attributed to geochemical weathering that occurred since the start of the Holocene (and subsequent diffusion downward) and connate Pleistocene-age water between 20 and 45 m B.G. (Hendry and Wassenaar, 2000).

4.5.3 Distribution of Elements Complexed with DOC

Fractionated DOC was scanned with ICP-MS for several possible complexed elements (Cu, Fe, Mn, Mo, Ni, Sr, U and Zn). Other trace elements and metals were deemed too low in concentration within the pore water to be identified by the methods used in this study. Only Fe, Zn and U are observed to be associated with DOC. Fractograms of the DOC peaks and associated Fe, Zn and U for the 1.2 m and 8.4 m samples are presented as representative examples in Figure 4-2. From this figure, some of the U and Zn is associated with the void peaks (<500 Da). The majority, however, is associated with the resolvable DOC (peak maxima at 1150 Da). Scanning for Fe complexed to DOC (>500 Da) indicated Fe is slightly above baseline for the 1.2 m pore water sample, but not higher than baseline ICP-MS response in all deeper samples.

The inability to resolve element concentrations above baseline values for Cu, Fe, Mn, Mo, Ni, and Sr with the ICP-MS does not necessarily mean these elements are not complexed with DOC. A high baseline could mask the element concentrations that are

complexed. Although ultra-pure reagents were used in all experiments and the flowlines in the AsFlFFF system consist mainly of PEEK tubing, sources of contamination may still exist in the system. For example, pump pistons, bodies, and the AsFlFFF channel body were constructed of stainless steel, all of which could contribute to a high element baseline within the carrier solution. A possible remedy for high baselines could be to construct a channel and replace pump parts with inert materials. Because well defined element-DOC relationships were only measured for U and Zn, further discussion focuses on these two elements.

The masses of U and Zn associated with the DOC peak were determined by integrating the element counts under the fractograms and comparing these values to the counts obtained for standard calibration curves. From these values, we determined the DOC recovery was determined as was the mass of U and Zn complexed to DOC, and the percentage of the elements that were in solution (<0.45 μm filtrate) complexed with DOC (Table 4-3). The concentrations of U and Zn complexed with the DOC ranges from 2.2-60 μg U g^{-1} DOC and 0.038-0.5 μg Zn g^{-1} DOC with the greatest concentrations in the shallower pore water samples. Between 0.43 and 3.2% of the total aqueous U and 0.1 and 0.9% of the total aqueous Zn in the pore water samples are associated with DOC. Ranville et al. (2007) show <2% of U is complexed with the DOC at this site, which compares well with our values. Undifferentiated masses of U and Zn are also associated with the <500 Da fraction of the DOC (void peak). Although some organic matter exists in the void peak (as can be seen in Figure 4-2c and d), quantifying how much of the elemental mass is attributable to organic matter, and how much is attributable to other unresolved low molecular weight ligands, is not possible. Thus, further discussion only addresses the elemental mass associated with the DOC peak (>500 Da).

We assumed a linear isotherm adequately describes the DOC-element complexation because both the complexation of U and Zn to the DOC is reversible and the concentrations of these elements in the pore waters are low. Evidence to support the reversibility of complexation is provided in a following section. Further, as the elements are in contact with the DOC for very long time periods (hundreds to thousands of years),

equilibrium conditions were assumed to exist between the elements and the DOC. In addition, the K_d approach to complexation was used in other organic-element studies (Geckeis et al., 2003; Ranville et al., 2007; Vesely et al., 2001).

The calculated K_d values for U decrease with depth from 76 ml g^{-1}C for a shallow sample (2.2 m) to 24 ml g^{-1}C at 9.7 m B.G. (Table 4-3). This decrease in K_d with depth is attributed to changes in the properties of the DOC with depth as reflected by the decrease in the aromaticity of the DOC with depth (Figure 4-3a). This relationship is further evidenced by the cross plot of K_d and NIC (Figure 4-3b; $r^2 = 0.97$) that suggests the aromaticity of the samples (as represented by the NIC) may control the degree of complexation. The amount of complexation by DOC from greater depths may be reduced because the lower aromaticity of these DOC should result in fewer reactive surface sites on the DOC available for complexation (Her et al., 2002). The K_d values reported by Ranville et al. (2007) for U ranged from 35-181 ml g^{-1}C, and show no trend with depth. Their values were slightly higher, but comparable to the K_d values measured here. The calculated K_d values for Zn are lower than those for U, ranging from 2-12 ml g^{-1}C (Table 4-3). These values do not exhibit any trend with depth and appear to be independent of aromaticity.

4.5.4 U- and Zn-DOC complexation

Kinetic testing was conducted to determine the rate at which U and Zn complex/dissociate from the DOC as a result of changes in pH. In both cases the U and Zn complexation with DOC rapidly responds to a reduction in pH from 8.1 to 2.5, attaining steady state complexation after about 60 min. The measured U and Zn data for the 5.3 m sample during the test period is presented in Figure 4-4 as representative. Rao et al. (1994) show the kinetics of U(VI) and Eu(III) binding to humic acid is rapid (after a few minutes contact time), which supports our findings of rapid equilibration.

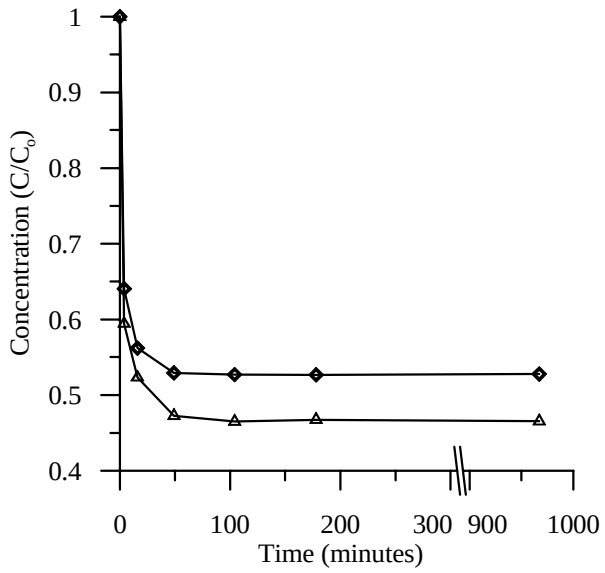

Figure 4-4. Dimensionless concentrations of U(VI) (open diamonds) and Zn(II) (open triangles) dissociation from DOC in pore water sample from 5.3 m B.G. vs. time resulting from an instantaneous decrease in pH from 8.1 to 2.5 at time zero. Note break in axis from 300 to 900 min.

Based on the results of these experiments, an equilibration time of 120 min was considered sufficient to assess the complexation/dissociation of U and Zn on DOC from pH 1.3-9.7. In this experiment, the maximum complexation of U to DOC is observed at pH of about 5 (6% of total U; Figure 4-5a). At higher and lower pH values, U is observed to dissociate (yielding 1% of total U complexed). This trend is similar to that of Zeh et al. (1997) who show maximum complexation of U to DOC between pH 4-6 and dissociation at higher and lower pH values. A similar trend with pH as that presented for U is observed for Zn complexation with DOC. The maximum amount of complexation is at pH 5-5.5 (3% of total Zn; Figure 4-5b). The decrease in U and Zn complexation at low pH can be explained by increased proton competition for binding sites, which leads to reduced element binding (Cheng et al., 2005).

The pore water samples in Figure 4-5 show a 'baseline' mass of U and Zn that does not dissociate from the DOC at either low or high pH. These non-dissociating masses of ~20 and 0.12 μg g^{-1} DOC for U and Zn, respectively, are attributed to the presence of strongly bound complexes, perhaps present in the matrix of the DOC structure.

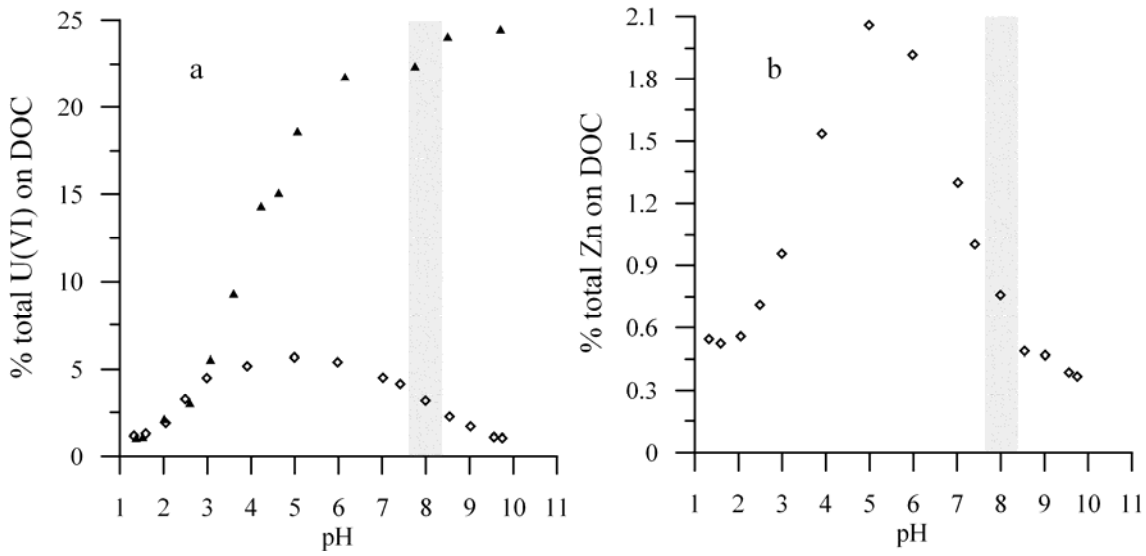

Figure 4-5. Percentages of total available (a) U and (b) Zn complexed with DOC vs. pH for the pore water sample from 2.2 m B.G. (open diamonds) and SRFA (solid triangles). The shaded areas represent the range of pH in the pore waters (Table 4-2).

These results are in keeping with that of Haitzer, Aiken, and Ryan (2002) on dissolved organic matter in surface water. Their study suggests that reactive thiol groups are responsible for strong binding of mercury to DOM. In addition, Lenheer et al. (1998) suggests organic matter contains polydentate binding sites, and both inner and outer sphere metal complexes to DOM could be present. The presence of strongly binding or presence of multiple binding sites supports our findings of non-dissociating or slowly dissociating elements. These experiments show the majority of the element mass bound to DOC readily complexes/dissociates when subjected to a change in pH. Zeh et al. (1997) also show the ability of the U(VI) to rapidly complexes/dissociates with humic acids. Although we demonstrate the kinetics of complexation/dissociation from DOC can be considered rapid, Geckies et al. (2003) present data indicating that at a fixed pH, complexation increases considerably with increased contact time between organic matter and spiked elements. However, whether or not pH will have the same effect on complexation kinetics is not clear, but some mass of an element may be present in stable complexes with DOC (Schmitt et al., 2001).

The masses of U complexed to the SRFA standard were measured over pH 1.3-9.7 to provide a comparison to the pore water DOC (Figure 4-5a). The SRFA standard displays increasing complexation with increasing pH throughout the range in pH tested. It does not exhibit the decrease in U complexed at pH >5 observed for the pore water sample. Further, the mass of U complexed is greater than that for the natural DOC (20% vs. 3% of total U at pH 8; Figure 4-5a). The standard was comprised of only Na, SO_4 (0.1 *M* Na_2SO_4), DOC, and U. In addition a minor amount of carbonate from atmospheric CO_2, was also present in the standard solution. As a result, this system contained no competing ligands in high enough concentrations to limit U-DOC interactions (Hummel et al., 2000). As a result, minimal competition existed for U in this system at higher pH, or for binding sites on DOC in the SRFA solution. In the pore water samples, competition for complexation sites plays a role in determining the amount of complexation. This is supported by experiments conducted in surface waters, which show greater binding affinity for Zn on DOC when no competitive cations exist in solution (Cheng et al., 2005). U-SO_4 species possibly exist at lower pH values (pH <3), but at higher pH these should not compete with U complexation to DOC. In addition, SRFA is expected to have a greater affinity for complexation and greater K_d values because the number of carboxylic functional groups and aromaticity is greater than in the pore water DOC examined (Reszat and Hendry, 2005). The presence of competing ligands in natural water samples reduces the amount of complexation by DOC. As we demonstrate here, assessing the importance of DOC-element interactions with *in situ* or field-based experiments is critical.

4.5.5 Geochemical Modeling

Modeling results for U in the pore water support the experimental complexation values (Figure 4-5 vs. Figure 4-6a). Measured and modeled U-FA species are dominant within similar pH ranges (pH 3-6). Model results show U is primarily in the form of the free ion UO_2^{+2} between pH 1.5 to 2.5. Furthermore, DOC is the primary U ligand between pH 2.5-6.5. At higher pHs, U is dominated by $Ca_2UO_2(CO_3)_3(aq)$ and $UO_2(CO_3)_3^{-4}$. These results are in good agreement with the measured masses of

complexed U under *in situ* pH conditions (Table 4-3). For all pore waters examined, the modeled data are highly representative of the measured data (r^2 = 0.82). Models of U(VI)-binding to humic substances in Gorleben ground waters predict < 1% of U is complexed with humic substances (Zeh et al., 1997), which is in keeping with our results. As was the case for U, good agreement between the measured and modeled data is also obtained for Zn complexation to FA. Modeling shows FA plays a minor role in Zn speciation (Figure 4-6b).

Between pH 1.5-8.5, Zn species are primarily $Zn(SO_4)_2^{-2}$, $ZnSO_4$(aq) and the free 'aquo ion' Zn^{+2}. $ZnCO_3$(aq) complexes consist of up to 10% of the Zn species between pH 7.5-10. At higher pH, $Zn(OH)_2$(aq) and $Zn(OH)_3^-$ are the dominant species in solution (Figure 4-6b). Modeling yields a maximum of 1.5% of total Zn complexed with FA at pH 9. In the 1.2 m pore water sample, 0.9% of the total Zn is measured as being complexed with FA, whereas the model yields 0.4% of total Zn (Table 4-3).

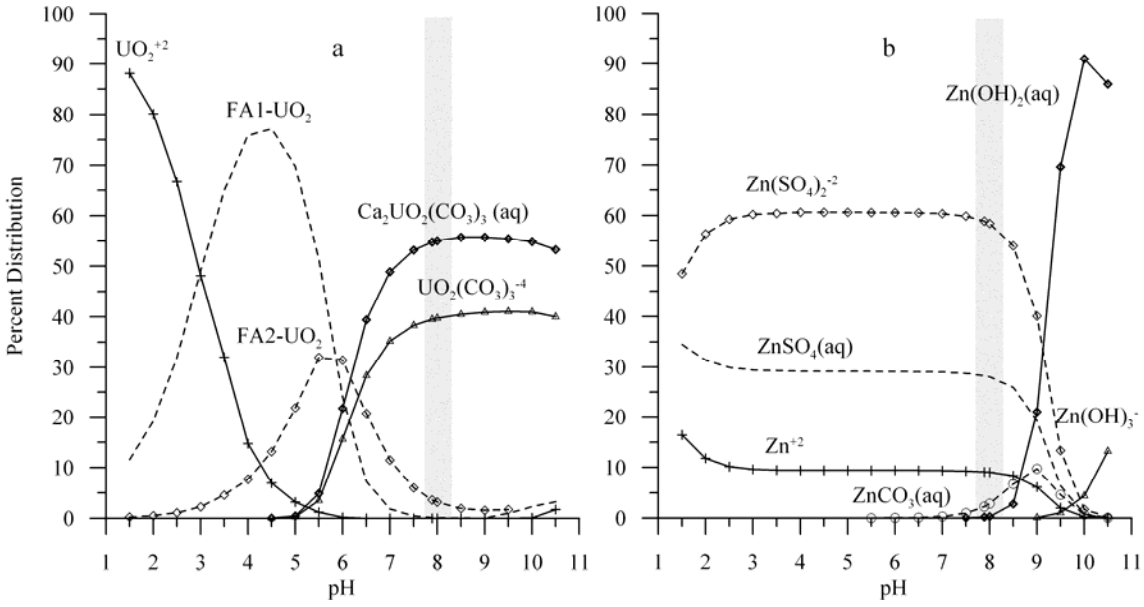

Figure 4-6. Distribution of dominant aqueous phase species for (a) U and (b) Zn in the 2.2 m porewater sample calculated using the NICA-Donnan model (Gustafsson, 2005) vs. pH. The shaded bars represent the range of pH in the pore waters (Table 4-2).

The measured Zn-FA complexation curve (Figure 4-5b) shows a maximum complexation of Zn at pH 5 (suggesting the majority of complexation is with carboxylic

sites on FA). Modeling results yield very little Zn complexation at pH 5, with the maximum complexation of Zn occurring at pH 9 (1.5% of total Zn). In spite of this discrepancy, Zn complexation with DOC within this aquitard can be considered negligible, as was the case with U. This has not been demonstrated in other Zn-DOC complexation experiments, typically on lab-based samples, which show Zn-DOC complexation is a factor to consider when examining speciation of this metal (Cheng et al., 2005; Christensen et al., 1999). The NICA-Donnan model predicts only 23% of the available carboxylic sites are occupied by cations at the pH of the pore waters (between 7.5 and 8.5). For the available phenolic (FA2) sites under these conditions, only about 7% are occupied. Aqueous element concentrations in the aquitard are not high, and the Visual MINTEQ modeling demonstrates competition from carbonate and sulphate species within the aquitard at ground water pH conditions prevents large amounts of complexation by FA from occurring.

4.6 Conclusions and Implications

Element speciation experiments to account for complexation with DOC are few, and the majority of those in literature do not account for complexation in *in-situ* ground water conditions. In this study, a coupled AsFlFFF-UV-TOC-ICP-MS technique yielded valuable knowledge of DOC-element complexation (Zn and U) in a natural aquitard environment. The experiments were conducted under conditions that approach field conditions with only minor alterations (filtration and pH adjustment). Modeling results suggest only 23% of carboxylic and 7% of phenolic sites on DOC are occupied by all elements studied at ground water pH conditions (pH 7.9 to 8.3). Uranium K_d values were linearly related to NIC (aromaticity) in the DOC samples, suggesting slight changes in DOC properties have an appreciable effect on their complexation capacity. AsFlFFF-ICP-MS analyses and geochemical modeling suggest less than 4% of total aqueous U and Zn are associated to DOC in these ground waters indicating facilitated transport in this system will be limited. Further, our data suggest DOC facilitated transport of these elements may be of limited importance in ground waters with similar (typical) chemistries. Elevated background concentrations of Fe, Mn, Ni, Cu, Sr, and Mo in the effluent from the AsFlFFF system may have masked any complexation of these

elements with DOC in the ICP-MS detector, making it impossible to quantify their complexation. This issue should be resolved in further studies.

4.7 Acknowledgements.

This research was funded by research grants from the Natural Sciences and Engineering Council of Canada (NSERC) through the Industrial Research Chair Program and the Potash Corporation of Saskatchewan. Thanks to Dr. Jianzhong Fan for technical assistance with ICP-MS instrumentation. The constructive comments provided by Dr. Karen Johannesson and two anonymous reviewers were very helpful in improving this manuscript.

4.8 References

Artinger, R., Buckau, G., Geyer, S., Fritz, P., Wolf, M., and Kim, J.I., 2000, Characterization of groundwater humic substances: influence of sedimentary organic carbon: Applied Geochemistry, v. 15, p. 97-116.

Artinger, R., Kienzler, B., Schussler, W., and Kim, J.I., 1998, Effects of humic substances on the Am-241 migration in a sandy aquifer: column experiments with Gorleben groundwater/sediment systems: Journal of Contaminant Hydrology, v. 35, p. 261-275.

Artinger, R., Schuessler, W., Scherbaum, F., Schild, D., and Kim, J.I., 2002, Am-241 migration in a sandy aquifer studied by long-term column experiments: Environmental Science & Technology, v. 36, p. 4818-4823.

Benedetti, M.F., Ranville, J.F., and Pinheiro, J.P., 2002, Characterization and binding properties of colloidal organic matter from the Rio Amazon and Rio Negro.: Abstracts of Papers of the American Chemical Society, v. 223, p. U604-U604.

Benedetti, M.F., vanRiemsdik, W.H., and Koopal, L.K., 1996, Humic substances considered as a heterogeneous donnan gel phase: Environmental Science & Technology, v. 30, p. 1805-1813.

Cheng, T., De Schamphelaere, K., Lofts, S., Janssen, C., and Allen, H.E., 2005, Measurement and computation of zinc binding to natural dissolved organic matter in European surface waters: Analytica Chimica Acta, v. 542, p. 230-239.

Choppin, G.R., 1988, Humics and Radionuclide Migration: Radiochimica Acta, v. 44-5, p. 23-28.

Christensen, J.B., Botma, J.J., and Christensen, T.H., 1999, Complexation of Cu and Pb by DOC in polluted groundwater: A comparison of experimental data and predictions by computer speciation models (WHAM and MINTEQA2): Water Research, v. 33, p. 3231-3238.

Christensen, J.B., and Christensen, T.H., 1999, Complexation of Cd, Ni,and Zn by DOC in polluted groundwater: A comparison of approaches using resin exchange, aquifer material sorption, and computer speciation models (WHAM and MINTEQA2): Environmental Science & Technology, v. 33, p. 3857-3863.

Christensen, J.B., Jensen, D.L., and Christensen, T.H., 1996, Effect of dissolved organic carbon on the mobility of cadmium, nickel and zinc in leachate polluted groundwater: Water Research, v. 30, p. 3037-3049.

Christensen, J.B., Tipping, E., Kinniburgh, D.G., Gron, C., and Christensen, T.H., 1998, Proton binding by groundwater fulvic acids of different age, origins, and structure modeled with the Model V and NICA-Donnan model: Environmental Science & Technology, v. 32, p. 3346-3355.

Claret, F., Schafer, T., Rabung, T., Wolf, M., Bauer, A., and Buckau, G., 2005, Differences in properties and Cm(III) complexation behavior of isolated humic and fulvic acid derived from Opalinus clay and Callovo-Oxfordian argillite: Applied Geochemistry, v. 20, p. 1158-1168.

Czerwinski, K.R., Kim, J.I., Rhee, D.S., and Buckau, G., 1996, Complexation of trivalent actinide ions (Am3+, Cm3+) with humic acid: The effect of ionic strength: Radiochimica Acta, v. 72, p. 179-187.

Geckeis, H., Ngo Mahn, T., Bouby, M., and Kim, J.I., 2003, Aquatic colloids relevant to radionuclide migration: characterization by size fractionation and ICP-mass spectrometric detection: Colloids and Surfaces A: Physicochemical and Engineering Aspects, v. 217, p. 101-108.

Geckeis, H., Rabung, T.H., Ngo Mahn, T., Kim, J.I., and Beck, H.P., 2002, Humic colloid-borne natural polyvalent metal ions: Dissociation experiment: Environmental Science & Technology, v. 36, p. 2946-2952.

Gustafsson, J.P., 2005, Visual Minteq ver. 2.32: Stockholm, Sweden.

Hassellov, M., Lyven, B., Haraldson, C., and Sirinawin, W., 1999, Determination of continuous size and trace element distribution of colloidal material in natural water by on-line coupling of flow field-flow fractionation with ICPMS: Analytical Chemistry, v. 71, p. 3497-3502.

Hendry, M.J., Ranville, J.R., Boldt-Leppin, B.E.J., and Wassenaar, L.I., 2003, Geochemical and transport properties of dissolved organic carbon in a clay-rich aquitard: Water Resources Research, v. 39, p. 1194-1203.

Hendry, M.J., and Wassenaar, L.I., 1999, Implications of the distribution of delta-D in pore waters for groundwater flow and the timing of geologic events in a thick aquitard system.: Water Resources Research, v. 35, p. 1751-1760.

—, 2000, Controls on the distribution of major ions in pore waters of a thick surficial aquitard: Water Resources Research, v. 36, p. 503-513.

—, 2004, Transport and geochemical controls on the distribution of solutes and stable isotopes in a thick clay-rich till aquitard, Canada: Isotopes in Environmental and Health Studies, v. 41, p. 3.

—, 2005, Origin and migration of dissolved organic carbon fractions in a clay-rich aquitard: C-14 and delta C-13 evidence: Water Resources Research, v. 41, p. -.

Her, N., Amy, G., Foss, D., and Cho, J., 2002, Variations of molecular weight estimation by HP-size exclusion chromatography with UVA versus online DOC detection: Environmental Science & Technology, v. 36, p. 3393-3399.

Hummel, W., Glaus, M.A., and Van Loon, L.R., 2000, Trace metal-humate interactions, II. The 'conservative roof' model and it's application.: Applied Geochemistry, v. 15, p. 975-1001.

Johannesson, K.H., and Hendry, M.J., 2000, Rare earth element geochemistry of groundwaters from a thick till and clay-rich aquitard sequence, Saskatchewan, Canada: Geochimica Et Cosmochimica Acta, v. 64, p. 1493-1509.

Kaplan, D.I., Bertsch, P.M., Adriano, D.C., and Orlandini, K.A., 1994, Actinide Association with Groundwater Colloids in a Coastal-Plain Aquifer: Radiochimica Acta, v. 66-7, p. 181-187.

Kim, J.I., 1994, Actinide Colloids in Natural Aquifer Systems: Mrs Bulletin, v. 19, p. 47-53.

Kim, J.I., Delakowitz, B., Zeh, P., Klotz, D., and Lazik, D., 1994, A Column Experiment for the Study of Colloidal Radionuclide Migration in Gorleben Aquifer Systems: Radiochimica Acta, v. 66-7, p. 165-171.

Lebon, P., and Mouroux, B., 1999, Knowledge of the three French underground laboratory sites: Engineering Geology, v. 52, p. 251-256.

Lenhart, J.J., Cabaniss, S.E., MacCarthy, P., and Honeyman, B.D., 2000, Uranium(VI) complexation with citric, humic and fulvic acids: Radiochimica Acta, v. 88, p. 345-353.

Mantoura, R.F.C., Dickson, A., and Riley, J.P., 1978, Complexation of Metals with Humic Materials in Natural-Waters: Estuarine and Coastal Marine Science, v. 6, p. 387-408.

Milne, C.J., Kinniburgh, D.G., and Tipping, E., 2001, Generic NICA-Donnan Model parameters for proton binding by humic substances: Environmental Science & Technology, v. 35, p. 2049-2059.

Milne, C.J., Kinniburgh, D.G., van Riemsdijk, W.H., and Tipping, E., 2003, Generic NICA-Donnan Model parameters for metal-ion binding by humic substances: Environmental Science & Technology, v. 37, p. 958-971.

Perminova, I.V., Frimmel, F.H., Kudryavtsev, A.V., Kulikova, N.A., Abbt-Braun, G., Hesse, S., and Petrosyan, V.S., 2003, Molecular weight characteristics of humic substances from different environments as determined by size exclusion chromatography and their statistical evolution: Environmental Science & Technology, v. 37, p. 2477-2485.

Porasso, R.D., Benegas, J.C., van den Hoop, M.A.G.T., and Paoletti, S., 2002, Analysis of trace metal humic acid interations using counterion condensation theory: Environmental Science & Technology, v. 36.

Ranville, J.F., Hendry, M.J., Reszat, T.N., Xie, Q., and Honeyman, B.D., 2007, Quantifying uranium complexation by groundwater dissolved organic carbon using asymmetrical flow field-flow fractionation: Journal of Contaminant Hydrology, v. 91, p. 233-246.

Ranville, J.F., and Schmiermund, R.L., 1999, General aspects of aquatic colloids in environmental geology, *in* Logsdon, M.J., ed., The environmental geochemistry of mineral deposits Part A: Processes, techniques, and health issues., Volume 6A: Reviews in Economic Geology: Chelsea, Society of Economic Geologists, Inc., p. 183-199.

Rao, L., Choppin, G.R., and Clark, S.B., 1994, A study of metal humate interactions using cation exchange: Radiochimica Acta, v. 66/67, p. 141-147.

Reszat, T.N., and Hendry, M.J., 2005, Characterizing Dissolved Organic Carbon Using Asymmetrical Flow Field-Flow Fractionation with On-Line UV and DOC Detection: Analytical Chemistry, v. 77, p. 4194-4200.

Schafer, T., Artinger, R., Dardenne, K., Bauer, A., Schuessler, W., and Kim, J.I., 2003, Colloid-borne americium migration in gorleben groundwater: Significance of iron secondary phase transformation: Ranville, J.F., Hendry, M.J., Reszat, T.N., Xie, Q., and Honeyman, B.D.,, v. 37, p. 1528-1534.

Schmitt, D., Muller, M.B., and Frimmel, F.H., 2001, Metal distribution in different size fractions of natural organic matter: Acta Hydrochimica Et Hydrobiologica, v. 28, p. 400-410.

Schussler, W., Artinger, R., Kim, J.I., Bryan, N.D., and Griffin, D., 2001, Numerical modeling of humic colloid borne Americium(III) migration in column

experiments using the transport/speciation code K1D and the KICAM model: Journal of Contaminant Hydrology, v. 47, p. 311-322.

Shaw, J., and Hendry, M.J., 1998, Groundwater flow in a thick clay till and clay bedrock sequence in Saskatchewan, Canada: Canadian Geotechnical Journal, v. 35, p. 1041-1052.

Tang, J., and Johannesson, K.H., 2003, Speciation of rare earth elements in natural terrestrial waters: Assessing the role of dissolved organic matter from the modeling approach: Geochimica Et Cosmochimica Acta, v. 67, p. 2321-2339.

Thurman, E.M., 1985a, Humic substances in groundwater, *in* MacCarthy, P., ed., Humic substances in soil sediment and water: Geochemistry, isolation, and characterization, John Wiley and Sons, p. 87-103.

—, 1985b, Organic Geochemistry of Natural Waters: Dordrecht, Martinus Nijhoff/Dr W. Junk Publishers, 497 p.

Van den Kammer, F., Baborowski, M., Tadjiki, S., and V. Tumpling Jr., W., 2003, Colloidal particles in sediment pore waters: particle size distrubution and associated element size distrubutions in anoxic and re-oxidized samples, obtained by FFF-ICP-MS coupling: Acta Hydrochimica Et Hydrobiologica, v. 4-5, p. 400-410.

Vesely, J., Majer, V., Kucera, J., and Havranek, V., 2001, Solid-water partitioning of elements in Czech freshwaters: Applied Geochemistry, v. 16, p. 437-450.

Wahlund, K.-G., 2000, Asymmetrical Flow-Field Flow Fractionation, *in* Giddings, C.J., ed., Field-Flow Fractionation Handbook: New York, John Wiley & Sons, p. 279-294.

Yan, X.-P., Kerrich, R., and Hendry, M.J., 2000, Trace element geochemistry of a thick till and clay-rich aquitard sequence, Saskatchewan, Canada.: Chemical Geology, v. 164, p. 93-120.

Zeh, P., Czerwinski, K.R., and Kim, J.I., 1997, Speciation of uranium in Gorleben groundwaters: Radiochimica Acta, v. 76, p. 37-44.

5.0 CONTROLS ON COLLOID TRANSPORT IN NON-FRACTURED LOW PERMEABILITY GEOLOGIC MATERIALS

5.1 Abstract

The migration of colloids in low permeability geologic materials has been examined for the first time. Movement of colloids in these environments is found to be controlled by pore throat constrictions in the range of 2 – 2.2 nm, determined from the cut-off diameter of colloids that were able to diffuse in this material. The diameter of colloid examined ranged from 1.45 nm to 6.05 nm, and transport was limited to the smallest colloids, with a mean diameter ranging from 1.45 -1.80 nm. The aqueous diffusion coefficient for the colloids ranged from 2.62×10^{-10} to 6.31×10^{-10} m^2 s^{-1} and the effective diffusion coefficient from 1.5×10^{-10} to 6.5×10^{-11} m^2 s^{-1}. The experimentally determined aqueous and effective diffusion coefficients enabled a calculation of a tortuosity factor for colloids ranging from 0.31 to 0.57, decreasing with increasing colloid diameter. The effective porosity calculated for the colloids ranged from 0.26 to 0.30, in good agreement with a total porosity of 0.31, with values decreasing with increasing colloid diameter. Colloids smaller than 2 nm are observed to diffuse through the till, whereas larger materials are excluded from movement due to straining mechanisms. Results from other aquitards suggest the diameter of dissolved organic carbon can be used as a proxy to determine control on colloidal transport in other low permeability units.

5.2 Introduction

Because colloids are generally accepted to have the ability to enhance the movement of contaminants through geologic media, an understanding of the controls on mobility of colloids is important. This is a challenge as colloidal particles vary in concentration, composition, structure, and size. Furthermore, in the natural subsurface they may be introduced or endemic in origin. A variety of inorganic, organic and

microbial constituents fall under the definition of colloidal material, including bio-colloids (viruses, bacteria, and protozoa), silicates, clays, Fe-, Mn- and Al-oxides, mineral precipitates, the macromolecular portion of dissolved organic carbon (DOC) and various other suspended particles(Ryan and Elimelich, 1996). A major control on colloid transport is the size of both the colloid and the pores or fractures within which it is contained. For comparison, viruses are in the range of 20 – 250 nm, bacteria from 200 – 5000 nm, protozoa from 10,000 – 100,000 nm, inorganic minerals from 50 to 50,000 nm, and DOC from 1 to 10 nm (Matthess and Peckdeger, 1985; Thurman, 1985). The movement of larger colloids in the 50-1000 nm size range has been of considerable recent interest, including a special section in *Water Resources Research* (Saiers and Ryan, 2006). Virus movement (26 –62 nm in diameter) through fractured clay till has been attributed to fracture flow (McKay et al., 1993). Bacterial transport through fractures and coarse grained porous media is well understood (Foppen et al., 2005; Harvey et al., 1989; Harvey et al., 1993). Lab column studies of clay and Fe-oxide movement in fractured saprolite (<200 nm diameter) (Kretzschmar et al., 1994; Kretzschmar et al., 1995), field and lab based tracer experiments of colloids in fractured shale saprolites (Cumbie and McKay, 1999; McCarthy et al., 2002; McKay et al., 2000), and controls on movement of various colloids through non-fractured coarse grained porous media are well documented (Bradford et al., 2004; Bradford et al., 2003; Bradford et al., 2002; Moridis et al., 2003). A common tracer used in transport studies is manufactured plastic colloids with a narrow size distribution range. Studies include the movement of 450 – 3200 nm latex colloids in saturated soil columns (Bradford et al., 2002), 110 – 120 nm polystyrene latex particles in columns (Grolimund et al., 1998), and various latex microspheres (50 – 4200 nm) in a fractured saprolite (Cumbie and McKay, 1999; McCarthy et al., 2002; McKay et al., 2000).

A review of existing literature reveals the absence of studies of colloid transport mechanisms in the micro-colloidal (1-50 nm) size range within low permeability media. Knowledge of contaminant transport through fine grained material is critical from a waste disposal point of view because low permeability geologic media have been extensively used as barrier materials. These media can be engineered barriers such as

liners and grout curtains or be present as naturally occurring formations. Transport mechanisms of dissolved contaminants through fine-grained materials are well understood (Gillham et al., 1984; Helmke et al., 2005; Hendry and Wassenaar, 2004a; Jorgensen et al., 2004; Perkins and Johnston, 1963; Shackelford, 1991; van der Kamp et al., 1996; Van Loon et al., 2005; Wersin et al., 2004). Dissolved contaminant flux and mechanisms such as retardation that affect their movement through fine grained media are well documented. Matrix diffusion of colloids from fractures considerably slows the movement of contaminants, as well as decreasing the concentration of these contaminants in the fractures (Cumbie and McKay, 1999; Jorgensen et al., 2004). The link between the fracture flow and matrix diffusion is recognized as important, however aside from empirical observations no effort has been made to identify the controls on colloid movement in low permeability materials.

Bacterial transport within fine grained units has been studied due to the existence of bacteria in non-fractured clays and tills. The presence of these bacteria in old formations might imply these colloids are mobile in low permeability units. However, the populations within these clays and tills were likely emplaced at the time of deposition as transport through the units was improbable (BoivinJahns et al., 1996; Lawrence et al., 2000). BoivinJahns, et al.(1996) suggests bacteria require interconnected pores >200 nm for sustained activity.

We focus here on the transport of colloids in the macromolecular (1 to 10 nm) range. A number of transport mechanisms may influence the mobility of colloids at this scale, including diffusion, attachment (sorption), and ion exclusion. Transport of larger dissolved material in low permeability units is controlled to a large degree by the pore throat diameters, and thus physical straining (filtration) and straining due to electrostatic repulsion is expected to be a critical parameter in the control of the movement of colloids within diffusion dominated systems. Straining is commonly determined in sediments by establishing the ratio of the mean pore throat diameter of the grains and the mean size of the colloid.

Pore diameters for determining particle straining have been estimated by a number of methods that assume the sediment has uniform grain size distribution. This is a purely geometric calculation based on averages and assumes colloidal particles are spherical (Bradford et al., 2003; Bradford et al., 2002; Matthess and Peckdeger, 1985). Actual measurement of pore diameters in fine-grained media is difficult; however, these can be determined to a certain degree with Hg-injection porosimetry and micro imaging systems such as computer assisted X-Ray tomography and scanning electron microscopy. These systems estimate the actual pore throat diameters and range in pore sizes within a system; however, they cannot determine the interactions between the porous media and colloidal material. A pore diameter for shale measured by mercury injection was 10 to 30 nm (Fredrickson et al., 1997). In a clay-rich till the median diameter of pores was determined to be 170 nm, with smallest measured pores around 10 nm (Quigley et al., 1987). The largest pore size in Boom clay is reported at 100–200 nm with a median pore size between 10 and 20 nm (BoivinJahns et al., 1996).

Physical pore diameter methods such as porosimetry cannot be directly related to colloid movement because the pore throat diameter distribution of interconnected pores in sediments is random. In addition, the pore throat diameters or the constrictions between larger pores, which are critical for colloidal movement, are a few orders of magnitude smaller than the pore radii (Foppen et al., 2005). Accurate measurement of pore constrictions in clay or glacial till materials is improbable, as they are below the practical resolution of mercury porosimetry and electron microscopy. Direct physical size measurements cannot be used to determine if colloids will pass through pore throats. The exclusion of colloids may occur if electrostatic repulsion exists between the colloids and the porous media. This would serve to limit the size of pores available to transport. Anion exclusion has been reported to restrict the number of active pore networks available for transport (Gvirtzman and Gorelick, 1991).

This paper describes a series of laboratory experiments that examine the diffusive transport of colloidal material in non-fractured clay-rich glacial till using double reservoir diffusion cells. The specific objectives of this study were to quantify the controls on colloid transport within non-fractured, fine-grained geologic media and

to directly determine the effective pore throat cut-off for colloidal material. To that aim, the diffusion of natural groundwater DOC, Suwannee River Humic Acid (SRHA), Suwannee River Fulvic Acid (SRFA) and a range of poly(styrene sulphonate) polymers were examined through clay-rich glacial till.

5.3 Theoretical Transport Description

One dimensional diffusive flux of solutes or colloids, i, through a porous medium can be described by an equation similar to Fick's first law of diffusion through free water:

$$J_D^i = -D_e^i n_e^i \frac{\partial C^i}{\partial x} \qquad [5\text{-}1]$$

where D_e^i is the effective diffusion coefficient, n_e^i is the effective porosity, and $\partial C^i / \partial x$ is the concentration gradient of i.

The diffusion process of i in a porous medium is different than in free water since the diffusion is affected by the length of the diffusion path, or tortuosity (τ^i), for each constituent. Thus the D_e^i in a porous media is less than the aqueous diffusion coefficient (D_o^i). Effective porosity in our system can be determined independently; therefore we define the effective diffusion coefficient as,

$$D_e^i = \tau^i D_o^i \qquad [5\text{-}2]$$

Tortuosity can be expressed by the application of the Hagen-Poiseuille equation,

$$\tau^i = \left(\frac{l}{l_e} \right)^2 \qquad [5\text{-}3]$$

where l is the straight line distance between two points, and l_e is the actual distance of transport through the porous media. In this experiment, both the effective and free water diffusion coefficients were determined experimentally, so no assumption or derivation of the tortuosity was required.

The one-dimensional diffusion equation for a porous medium, according to Fick's second law (Bear, 1972), is:

$$\frac{\partial C}{\partial t} = \frac{D_e^i}{R_d^i}\frac{\partial^2 C}{\partial x^2} \qquad [5\text{-}4]$$

where C is the concentration of solutes or colloids in solution, t is the time, x is the distance, and R_d^i is the retardation factor.

5.4 Materials and Methods

5.4.1 Site Description

Porewaters and solid samples were collected from an aquitard research site, the King site, located in Saskatchewan, Canada (51.05 N Lat., 106.5 W Long). This site was selected for study because its hydrogeology and hydrochemistry is well characterized (Hendry and Wassenaar, 1999, 2000a; Shaw and Hendry, 1998b).

The King aquitard site consists of the laterally extensive, plastic, thick (80 m), clay-rich Battleford till (39% sand, 26% silt, and 35% clay), deposited between 12-18 ka. The clay fraction of the till is dominated by smectite (50-60%) with lesser amounts of illite (5-15%) (Hendry and Wassenaar, 2000b). The till disconformably overlies 77 m of a Cretaceous clay aquitard (5% sand, 38% silt, and 57% clay) deposited between 71 and 72 ma (Shaw and Hendry, 1998b). The upper 3-4 m of the till is oxidized and visibly fractured whereas the underlying till and clay are massive, unoxidized and appear non-fractured. Groundwater velocity through the non-fractured till and clay is between 0.75 and 1.0 m/10ka (Hendry and Wassenaar, 1999; Shaw and Hendry, 1998a).

In addition to being well characterized with respect to hydrogeology and hydrochemistry, the characteristics and migration of DOC in the till aquitard are known (Hendry et al., 2003a; Hendry and Wassenaar, 2000a; Hendry and Wassenaar, 2004b). The DOC concentrations in the till decrease from about 150 mg l^{-1} near the water table (2.2 m below ground surface (BG)) to 10 mg l^{-1} at 23 m BG. The trend of decreasing DOC concentration with increasing depth combined with ^{14}C and $\delta^{13}C$ analyses indicate

this DOC profile can be attributed to diffusive mixing of soil organic carbon from the surface and older DOC (15 ka) at depth (Hendry and Wassenaar, 2005). The older DOC was deposited at the time of till deposition whereas the near surface DOC has formed since the Holocene (Hendry and Wassenaar, 2005). DOC diffuses through the till aquitard with minimal interactions with the till matrix (i.e., K_d of 1.1 x 10^{-3} ml g^{-1}; (Hendry et al., 2003a)). The DOC also exhibits a decrease in aromaticity and functional group concentration with age and depth at the site (Reszat and Hendry, 2005). DOC from the till at the King site (all depths) has a weight averaged molecular weight (M_w) of 1200 daltons (Da) (Reszat and Hendry, 2005).

5.4.2 Solids and Pore Water Sampling and Analysis

A 1.5 m long x 76 mm OD Shelby tube was collected from the till aquitard at a depth of 11.8 to 13.3 m BG in August 2001. Once the Shelby tube was removed from the borehole, the tube was waxed at the ends then stored at 15^{o}C and 80% relative humidity until laboratory testing. Details of core sampling are presented in (Hendry et al., 2003a).

Pore water samples were collected from six piezometers completed in the till (2.2, 3.7, 6.9, 9.7 and 11.7 m BG) in October 2002. These piezometers were selected to represent a range in natural DOC concentrations (19 – 145 mg l^{-1}) (Hendry et al., 2003a) for use in batch testing. The pore water sample from 11.7 m BG was assumed to reflect the chemistry, including DOC, of pore water in equilibrium with the core from the Shelby tube and, as a result, was also used to represent the pore water chemistry in core samples tested in the diffusion cells. The pore water sample collected from the piezometer installed at 2.2 m, which contains elevated DOC concentrations (145 mg l^{-1}) (Hendry et al., 2003a), was also used as a source of a natural colloidal tracer (i.e., DOC) in diffusion cell testing. The six piezometers sampled were constructed in 1995 (Wassenaar and Hendry, 1999).

Based on detailed spatial and depth distribution of pore water chemistry data from this site (Hendry and Wassenaar, 2000b; Reszat and Hendry, 2007), these pore waters were classified as sodium-sulphate type waters and had ionic strengths ranging

from 0.9 at 2.2 m BG to 0.1 at 11.7 m BG (Hendry and Wassenaar, 2000b). Porewater DOC for all samples was measured with a Shimadzu TOC-5050A as per previous studies at the site (Hendry et al., 2003a). In addition, dissolved major ions were analyzed by ion chromatography on pore water samples collected from piezometers (data not presented).

5.4.3 Colloid Tracers

Eight colloid tracers covering a range in M_ws from 910 to 15400 Da were used in batch and diffusion cell experiments. Five of the tracers were synthetic colloids, specifically PSS 910 polymer (Polymer Standards Service), PSS 1430, PSS 4800, PSS 6500, and PSS 15450 (American Polymer Standards Corp.). The PSS polymers are anionic and have narrow ranges in M_w (with different diameters). Composed of repeating units of $[\text{-}CH_2CH(C_6H_4SO_3Na)\text{-}]_n$, they form colloidal material freely in aqueous solution and have a manufacturers reported density of 1.910 g cm^3. In addition to these synthetic colloids, batch and diffusion cell experiments were conducted using natural DOC from the King site, with a weight averaged molecular weight (M_w) of 1200 Da (Reszat and Hendry, 2005), and two Suwannee River (SW) humic standards (International Humic Substances Society) – Humic Acid (HA, 1S101H) and Fulvic Acid (FA, 2S101F) – with M_w of 3200 and 1700 Da, respectively.

Characterization of the concentration, M_w and hydrodynamic diameter (D_H) of the colloids (DOC and polymers) collected from the diffusion cells and batch experiments was performed using an Asymmetrical Flow Field-Flow Fractionation (AsFlFFF) system (model HRFFF 10.000) from Postnova Analytics (FFFractionation, Salt Lake City, Utah). The AsFlFFF allowed individual colloids to be identified as separate peaks. The integration of each peak (area) was linearly related to its concentration, with an r^2 value of not less than 0.99 (data not presented). This approach allowed us to differentiate natural DOC contained within pore water samples from the other colloids, as well as measure changes in all colloidal concentrations in the batch and diffusion cell experiments. The PC controlled AsFlFFF system consisted of an arrangement of pumps, an AsFlFFF channel, and a vacuum degasser (to remove air

bubbles from the carrier solution that may interfere with separation efficiency in the AsFlFFF channel). The AsFlFFF system primarily separates colloids by differences in aqueous diffusion coefficients (D_o^i). Particles are detected by a UV detector (254 nm) as they elute from the system after fractionation. The resulting plots of detector intensity vs. time, called fractograms, consist of two regions: the void peak, which may contain some undifferentiated low molecular weight (MW) ligands, and the colloidal peak(s). UV measurements were made at 1 s intervals with data acquisition software provided by Postnova Analytics (NovaFFF version 3.14). To ensure colloidal material of interest was not lost through the membrane into the cross flow during analysis, the AsFlFFF channel was fitted with regenerated cellulose acetate membranes (Millipore Corp.) with a nominal MW cut-off of 1000 Da. A Rheodyne 100 μl manual sample injection loop was used to inject filtered (<0.45 μm) water samples into the AsFlFFF.

Hydrodynamic diameters of the polymers and DOC were determined from AsFlFFF theory and the elution time of each component. The elution time of any particle separated by AsFlFFF is dependant on the experimental setup and flow rates within the channel, which affect the retention time of the colloid. The retention of a component within the channel is expressed by:

$$R = \frac{t^O}{t_r} \qquad [5\text{-}5]$$

where R is the retention ratio, t_r is the retention time, and t^0 is the void time. The void time of the channel is calculated from the expression,

$$t^0 = \frac{V^0}{V_c} \ln\left(1 + \frac{V_c}{V_{out}}\left[1 - \frac{\omega\left(b_0 z' - \frac{b_0 - b_L}{2L} z'^2 - y\right)}{V^0}\right]\right) \qquad [5\text{-}6]$$

where V_{out} is the channel outlet flow rate, z' is the distance from the inlet to the focusing point, L is the channel length, b_0 and b_L are the channel breadths at the inlet and outlet, respectively, and y is the area cut off by the tapered inlet end. To calculate the void time,

the flow parameters of the channel are measured volumetrically, and the channel thickness is measured from a standard of known diffusion coefficient. In this case we used ferritin (M_w = 440000). With the diffusion coefficient for ferritin, the channel thickness is calculated using,

$$\omega = \sqrt{\frac{D6t_r}{\ln\left(1+\frac{V_C}{V_{out}}\left[1-\frac{\left(b_o z' - \frac{(b_o - b_L)}{2L} z'^2 - y\right)}{A}\right]\right)}} \qquad [5\text{-}7]$$

From the retention ratio the retention parameter, λ, is determined using,

$$R = 6\lambda\left[\coth\left(\frac{1}{2\lambda}\right) - 2\lambda\right] \qquad [5\text{-}8]$$

The D_H of the fractionated particles is then calculated using,

$$D_H = \frac{kTV^0}{3\pi\eta V_C \omega^2}\frac{1}{\lambda} \qquad [5\text{-}9]$$

and D_o^i is calculated using,

$$D_o^i = \frac{kT}{3\pi\eta D_H} \qquad [5\text{-}10]$$

The calculation of colloid D_H assumes spherical particles. Although a valid assumption for the poly(styrene) suphonates, this remains to be tested for the DOC colloids. A full description of AsFlFFF theory and application, as well as derivations of the equations above are presented elsewhere (Litzen and Wahlund, 1991; Wahlund, 2000; Wahlund and Giddings, 1987).

5.4.4 Batch Sorption Testing.

The degree of sorption of colloidal material onto the till was determined using batch sorption tests. Subsamples of core from 11.5 – 12.0 m BG were oven dried at 80°C and this material was used in batch tests using a 1:4 soil to water ratio (3 g soil to 12 g solution). The extent of sorption of colloidal material (PSS 910, PSS 1430, PSS 4800, PSS 6500, PSS 15450, SRHA, SRFA) was examined by creating solutions of 11.7 m BG pore water (in equilibrium with core material) with a range in colloid concentrations (5 – 300 mg l^{-1}). To determine sorption of the naturally occurring DOC to the till, pore waters from 2.2, 3.7, 6.9, 9.7 and 11.7 m BG (with a range in DOC concentrations from 30 to 145 mg l^{-1}; refer to Results and Discussion Section) were mixed at 1:4 soil water ratio with the solids collected from 11.5 – 12 m BG. The soil-water mixtures were agitated on a wrist action shaker for 48 h. After the soil settled in the mixtures (about 1 h), the supernatant was collected and filtered through 0.45 μm filters. This approach was used to minimize the potential for the settlement of colloids during centrifugation. Colloid concentrations remaining in solution were measured using area units from AsFlFFF runs. Each sample was run in triplicate and results averaged. The areas determined from the AsFlFFF were then recalculated as concentrations, and plotted as C vs. S, where C is the concentration of colloid in solution in equilibrium with the mass of colloid sorbed onto the clay (mg l^{-1}), and S is the mass of colloid sorbed per dry unit weight of solid (mg kg^{-1}). The resulting plot was used to determine the distribution coefficient K_d^i (ml g^{-1}) using,

$$S = K_d^i C \qquad [5\text{-}11]$$

Since the sorption plots were linear (data presented below), we used a linear sorption isotherm to determine the retardation factor (R_d^i), specifically,

$$R_d^i = 1 + \frac{\rho_{bulk}}{n_e^i} K_d^i \qquad [5\text{-}12]$$

where ρ_{bulk} is the bulk density of the porous media (g cm^{-3}), K_d^i is solid-solution distribution ratio, with units of ($mass^i/mass_{bulk}$)($volume_{solution}/mass^i$) (ml g^{-1}), and n_e^i is the effective porosity of the tills with respect to each colloid. A ρ_{bulk} of 2.17 g ml^{-1} was used in these calculations (Shaw and Hendry, 1998b) and the n_e^i was determined from 1D diffusion modeling of the diffusion cell test results (described below).

5.4.5 Diffusion Cell Testing.

Double reservoir diffusion tests were conducted to determine D_e^i and n_e^i, and to provide an additional estimate of the R_d^i of the colloidal particles,. The diffusion cells were constructed from stainless steel and consisted of two sections. One section consisted of a fluid reservoir (Reservoir A) and the core sample holder. The other section consisted of a second fluid reservoir (Reservoir B) (Figure 5-1). The core samples were sub-cored from the Shelby tube and inserted into the sample holder of the diffusion cell. The cores in the cells were 30 mm in length and were saturated with pore water collected from 11.9 m BG for one week prior to assembly of the cells. This equilibration period ensured an adequate seal existed between the core and the sides of the sample holder. The range in solutions and colloids used in the diffusion cell testing are presented in Table 5-1. Glass beads (5 mm diameter) were placed into both fluid reservoirs to enable a specific volume of solution to be placed in each reservoir with no head space. Once assembled, and to minimize advective transport, the diffusion cells were placed on their sides for the duration of the testing. The cells were rotated 180° daily to minimize the effects of sedimentation.

Two suites of diffusion cell experiments were conducted. The first suite (Cells 1 through 3; Table 5-1) allowed natural DOC to diffuse from Reservoir B to Reservoir A (high to low concentrations). These tests were conducted for 540 days. In this suite of tests, polymer spikes were introduced into Reservoir A and allowed to diffuse to Reservoir B. Complete separation of the natural background DOC peak from the polymers spiked in these reservoirs and subsequent integration of each peak area was possible in these samples (Table 5-1 and Figure 5-2). Natural pore water DOC was

monitored in the A and B reservoirs of all three cells, thus providing triplicate sets of analyses. These triplicate tests proved useful for assessing the accuracy of individual diffusion cell tests and to determine any difference(s) in diffusion rates between sub-cores tested.

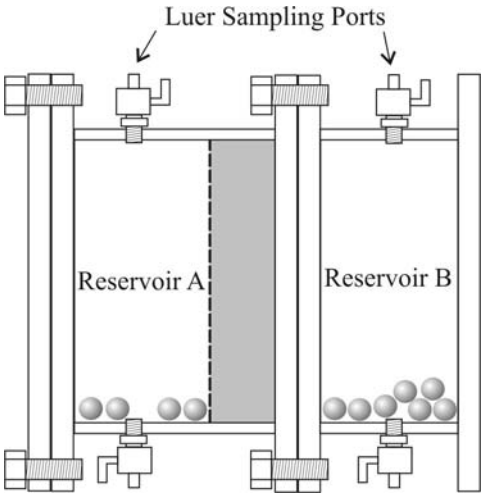

Figure 5-1. Schematic of the stainless steel diffusion cells (not to scale). Spheres shown in the reservoirs are glass beads, which were used to fill each reservoir with the correct volume solution and avoid the presence of head space.

The second suite of diffusion cell tests (Cells 4 through 7; Table 5-1) was conducted using polymer and humic standard spikes similar in MW to the natural DOC. These tests were run for 255 days. In these cells, the background concentrations of DOC were held constant in both reservoirs and in the core. The spikes were introduced into Reservoir A and concentrations monitored in both reservoirs with time. The background fractogram area consisting of DOC was subtracted from the introduced colloidal concentrations.

Table 5-1. Concentrations, M_w, and diameters of colloids in Reservoir A and B in diffusion cells 1 – 7.

Cell	Reservoir A				Core				Reservoir B				Duration
	Colloid(s)	Conc. (mg l^{-1})	M_w (Da)	Size (nm)	Colloid	Conc. (mg l^{-1})	M_w (Da)	Size (nm)	Colloid	Conc. (mg l^{-1})	M_w (Da)	Size (nm)	(days)
1	11.7 m G/W	30[1]	1200	1.70	11.7 m G/W	30[1]	1200	1.70	2.2 m G/W	145[1]	1200	1.70	540
	PSS 4800	100[2]	4800	3.05									
2	11.7 m G/W	30[1]	1200	1.70	11.7 m G/W	30[1]	1200	1.70	2.2 m G/W	145[1]	1200	1.70	540
	PSS 6500	100[2]	6500	3.80									
3	11.7 m G/W	30[1]	1200	1.70	11.7 m G/W	30[1]	1200	1.70	2.2 m G/W	145[1]	1200	1.70	540
	PSS 15450	100[2]	15450	6.05									
4	11.7 m G/W	30[1]	1200	1.70	11.7 m G/W	30[1]	1200	1.70	11.7 m G/W	30[1]	1200	1.70	255
	PSS 910	250[2]	910	1.45									
5	11.7 m G/W	30[1]	1200	1.70	11.7 m G/W	30[1]	1200	1.70	11.7 m G/W	30[1]	1200	1.70	255
	PSS 1430	250[2]	1430	1.75									
6	11.7 m G/W	30[1]	1200	1.70	11.7 m G/W	30[1]	1200	1.70	11.7 m G/W	30[1]	1200	1.70	255
	SRHA	250[2]	3200	2.70									
7	11.7 m G/W	30[1]	1200	1.70	11.7 m G/W	30[1]	1200	1.70	11.7 m G/W	30[1]	1200	1.70	255
	SRFA	250[2]	1700	2.15									

[1] Concentration refers to natural background DOC contained in groundwater samples.
[2] Concentration refers to spiked amount added to background groundwater.

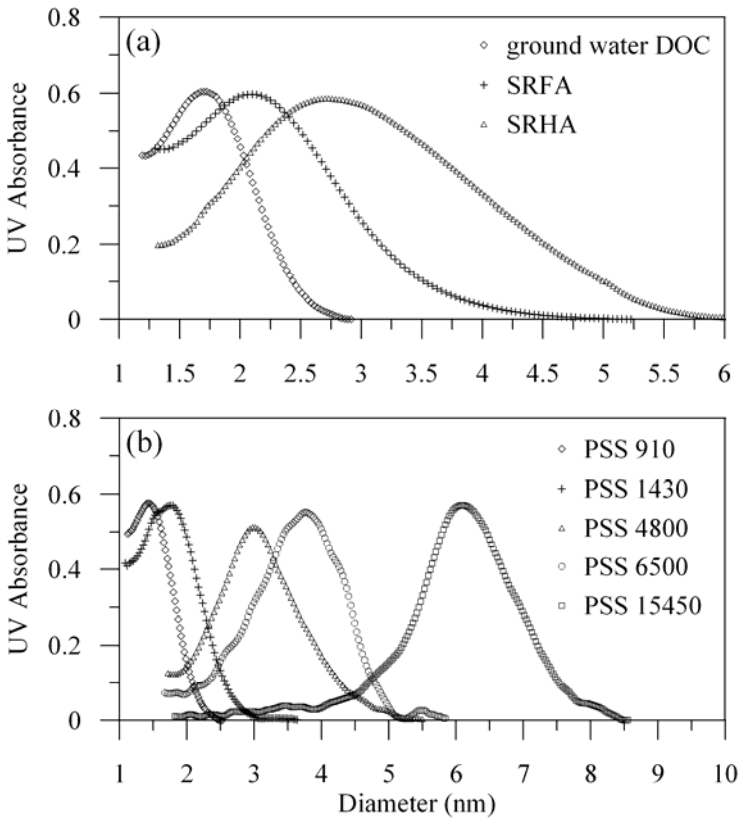

Figure 5-2. AsFlFFF fractograms of all colloids used in this study. (a) Size distributions of organic matter. (b) Size distributions of poly(styrene) sulphonate polymers. Note difference in x-axis scale between graphs.

5.4.6 Estimates of Diffusion Parameters

The one-dimensional numerical model *POLLUTE*v6 (Rowe et al., 1997) was used to solve equations [1] and [4] and, thus obtain a best-fit for the colloids in both reservoirs of the diffusion cells. Three layers were defined in the model: fluid reservoirs A and B bounding a porous medium (Figure 5-1). Porous medium properties used in the numerical model included dry density, $n_e^i D_e^i$, and K_d^i. Dry density of the till was determined to be 1.87 g ml^{-1} (Shaw and Hendry, 1998b).An initial concentration profile was applied to the model based on the initial concentrations of solutions in each reservoir of the diffusion cells (Table 5-1). Concentration of colloidal material in the core was defined as the same as in Reservoir B. The top and bottom cell boundaries were defined as zero flux. Darcy velocity was set to zero, and the model was executed as a concentration change with depth over time (550 days; 18 time increments).

Concentration profiles vs. time in the reservoirs were entered in Microsoft EXCEL using a Visual Basic Macro. These results were compared to the concentration profiles measured in the reservoirs. Parameters (i.e., D_e^i, n_e^i and K_d^i) were varied in the model to optimize the fit between the calculated and measured colloidal data,. Initially a visual best fit between calculated and measured data was used; a statistical approach was then applied to all visually fit data. A least squares fit between experimental and modeled data point was applied to generate a coefficient of determination (r^2) at each sampling time.

5.5 Results and Discussion

5.5.1 Colloid Properties

The DOC concentrations measured for this study (145, 77, 47, 42, and 30 mg l^{-1} at 2.2, 3.7, 6.9, 9.7, and 11.7 m BG, respectively) were in good agreement with previous reports from this site. AsFlFFF fractograms of the eight colloids investigated in this study are presented in Figure 5-2. The D_H and D_o^i values calculated for the individual colloids, reported as peak maxima, are presented in Table 5-2. As M_w increased from 910 to 15450 Da, the D_H values increased from 1.5 to 6.1 nm. The D_o^i values were greatest for the smallest colloid (2.6×10^{-10} m^2 s^{-1} for the 1.45 nm polymer) and decreased with increasing MW (to a minimum value of 6.3×10^{-11} m^2 s^{-1} for the 6.05 nm polymer). These trends are expected, and calculated D_o^i values for the groundwater DOC, SRFA, and SRHA (1.41×10^{-10} m^2 s^{-1} for SRHA up to 2.24×10^{-10} m^2 s^{-1} for ground water) agree well with literature values (1.24×10^{-10} to 4.10×10^{-10} m^2 s^{-1} for a variety of natural and standard humic and fulvic acids (Beckett et al., 1987; Dycus et al., 1995)).

Table 5-2. Calculated and modeled transport parameters of colloids.

M_w Da	D_H nm	Colloid Type	B.T. Days	D_o^i $m^2\ s^{-1}$	D_e^i $m^2\ s^{-1}$	τ^i	n_e^i	K_d^i ml g^{-1}	R_d^i	K_d^i ml g^{-1}	R_d^i
910	1.45	polymer	16	2.62×10^{-10}	1.5×10^{-10}	0.57	0.30	0.12 [2]	1.9	0.10 [3]	1.7 [3]
1200	1.70	DOC	31	2.24×10^{-10}	9.5×10^{-11}	0.42	0.28	0.39	4.0	0.30	3.3
1430	1.75	polymer	34	2.18×10^{-10}	7.0×10^{-11}	0.32	0.27	0.15	2.2	0.20	2.6
1500	1.80	fulvic acid	37 [1]	2.12×10^{-10}	6.5×10^{-11}	0.31	0.26	2.9	24.3	0.80 [1]	7.7 [1]
1700	2.15	fulvic acid	> 255	1.78×10^{-10}				2.9	24.3 [4]		
3200	2.70	humic acid	> 255	1.41×10^{-10}				3.4	28.3 [4]		
4800	3.05	polymer	> 540	1.25×10^{-10}				0.88	8.1 [4]		
6500	3.80	polymer	> 540	1.00×10^{-10}				1.3	11.5 [4]		
15450	6.05	polymer	> 540	6.31×10^{-11}				1.5	13.1 [4]		

[1]calculated/observed from 1.80 nm fraction of SRFA
[2]measured data.
[3]modeled data.
D_H is calculated hydrodynamic diameter
B.T. is breakthrough time

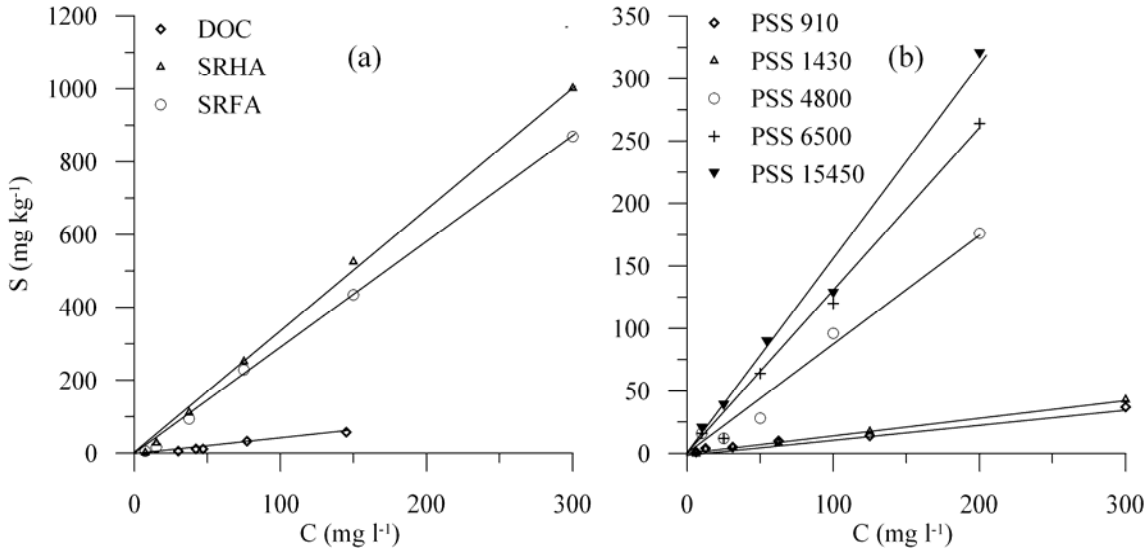

Figure 5-3. Sorption coefficient fits for all colloids examined.

5.5.2 Batch Testing

Plots of C vs. S for the colloids after batch testing (Figure 5-3) yielded well defined linear sorption isotherms (r^2 ranging from 0.95 to 0.99) over the concentration ranges tested. K_d^i and R_d^i values determined from batch sorption tests (Table 5-2) ranged from 0.12 to 3.4 and 1.9 to 28.3, respectively. The organic matter shows an increased amount of sorption with diameter: 0.39 ml g^{-1} for groundwater DOC to 3.4 ml g^{-1} for SRHA. Increased sorption with increasing diameter or molecular weight is expected and results are consistent with those in (Reszat and Hendry, 2005) who showed an increase in aromaticity and reactivity of organic matter with an increase in diameter. The K_d^i and R_d^i results for DOC are greater than those determined by (Hendry et al., 2003a) (1.1 x 10^{-3} ml g^{-1} and 1.0, respectively), who used the same till and porewaters. The discrepancies may be attributed to differences in experimental set up and batch testing methods used. In (Hendry et al., 2003a), sorption was estimated using a diffusive sorption experiment, whereby clay was allowed to equilibrate with the soil without agitation (Headley et al., 2001). These tests suggest sorption reactions between DOC and the matrix material are negligible and need not be considered in diffusion modeling. Whether this type of sorption testing is analogous to natural conditions has not been proven.

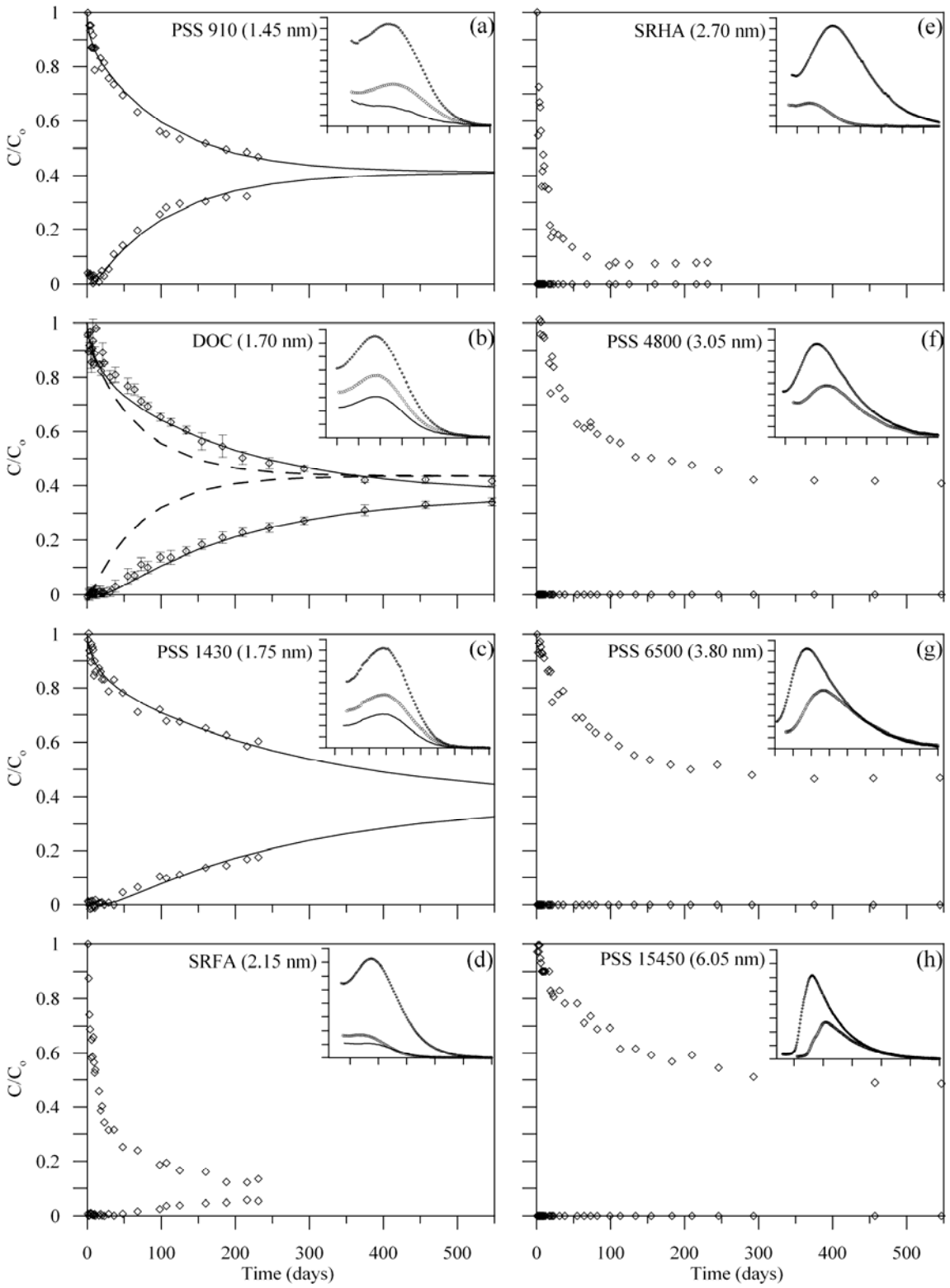
PSS 910 (1.45 nm)
(a)
SRHA (2.70 nm)
(e)
DOC (1.70 nm)
(b)
PSS 4800 (3.05 nm)
(f)
PSS 1430 (1.75 nm)
(c)
PSS 6500 (3.80 nm)
(g)
SRFA (2.15 nm)
(d)
PSS 15450 (6.05 nm)
(h)
C/C$_o$
Time (days)
0
100
200
300
400
500
0.2
0.4
0.6
0.8
1

Figure 5-4. Experimental (open diamonds) and modeled (solid line) diffusion traces of colloids. The groundwater DOC experimental data shows an average of 3 diffusion cells and the standard deviation of these measurements, and the modeled diffusion trace of a conservative chloride tracer (dashed lines). The inset graphs compare the initial size distribution of the colloid in the source reservoir (t = 0 days; upper trace), the final size distribution in the source reservoir (t = 255 or 540 days; middle trace), and the size distribution in the collection reservoir (t = 255 or 540 days; lower trace).

Groundwater DOC would be expected to have minimal sorption to the till matrix, as they have been in contact for thousands of years (Hendry and Wassenaar, 2005). However, the higher amount of sorption found in this experiment may be partially due to a more reactive DOC from shallower piezometers being utilized in the batch tests. DOC in the shallower piezometers is younger and as a result is more aromatic and contains more functional groups than DOC found at 12 m depth (Reszat and Hendry, 2005). This may lead to a higher amount of sorption than would be expected at equilibrium 12 m conditions. The sorption values reported here are considered representative as they were determined with conditions actually present in the diffusion cells (2.2 m depth DOC sorbing to 11.7 m depth core). The amount of sorption of the sodium poly(styrene) polymers ranged from 0.12 – 1.5 ml g^{-1} and also showed an increase with molecular weight.

5.5.3 Diffusion Cell Testing.

Figure 5-4 shows the experimental and modeled diffusion cell results, plotted as normalized (C/C_0) concentrations for all compounds in each cell. Each diffusion cell has two traces, the upper showing an initial high concentration which decreases over time in the source reservoir, and the lower showing an initial concentration of zero, increasing with time after some time lag, or breakthrough time, in the collection reservoir. The breakthrough time is the transport time of the colloid through the clay core, which has an initial colloid concentration of zero. The breakthrough time increased with increasing colloid diameter, from 16 days for the 1.45 nm colloid to 37 days for the 1.80 nm colloid. The diffusion traces show the 1.45 and 1.75 nm polymers, the 1.70 nm groundwater DOC, as well as a fraction (1.80 nm) of the SRFA diffused through the till.

A larger fraction of SRFA, the 2.70 nm SRHA, and the larger polymers (3.05, 3.80 and 6.05 nm) decreased in concentration in the source reservoir, but no mass was observed in the collection reservoir.

Three separate diffusion profiles can be identified from Figure 5-4. Profile 1 shows a well defined source and collection reservoir, increasing and decreasing respectively, and includes PSS 910 (5-4a), groundwater DOC (5-4b), and PSS 1430 (5-4c). The groundwater DOC diffusion results are an average of measurements in three diffusion cells. Groundwater DOC follows the same trend in all cells, which shows these diffusion cells have good repeatability, and profiles are similar to a previous study (Hendry et al., 2003b). The inset graphs in these three diffusion profiles show the mean diameter of the colloid does not change in the collection reservoir with time, so preferential diffusion or sorption to the clay core is not occurring. The mean diameter of these colloids is similar in the source reservoir, which suggests the full distribution of this colloid is mobile.

Diffusion profile 2 exhibits a large decrease in colloid mass in the source reservoir, and either a small or no increase in colloid mass in the collection reservoir. In these profiles the colloid mass in the source reservoir became low (85-90% depletion of mass) with respect to the previous profiles (50-60% depletion of mass). Profile 2 is illustrated in the SRFA (5-4d) and SRHA (5-4e) diffusion traces. SRFA diffuses through the clay and appears in the collection reservoir but SRHA does not. The inset graphs in Figure 5-4 for both SRFA and SRHA shows a marked decrease in the mean diameter of colloids which remain in the source reservoir over time. This can be attributed to either an increased amount of adsorption of the larger fraction of the colloid, or a higher diffusion rate of the larger fraction of the colloid, which is improbable. The SRFA diffusion trace shows the size fraction transported in the source reservoir also exhibits a substantial decrease in mean diameter over the original size distribution, suggesting sorption to the till matrix is the probable primary mechanism for an observed decrease in colloid diameter.

Diffusion profile 3, illustrated by the traces of the 3.05 nm (5-4f), 3.80 nm (5-4g), and 6.05 nm (5-4f) colloids, exhibits a moderate decrease in colloid mass in the source reservoir (50-60%), and no corresponding increase in the collection reservoir. The inset graphs in Figure 5-4 for these colloids show an increase in the mean colloid diameter remaining in the source reservoir with time, suggesting the smaller diameter fraction of these colloids preferentially diffuses into the till, the diffusion rate of the smaller fraction is higher, or a combination of both.

5.5.4 Diffusion Test Results

Best fit modeling results from *POLLUTE* are shown as solid lines in Figure 5-4. Root mean squared test were applied to the modeled data to best match the experimental data. r^2 values of 0.995, 0.996 and 0.998 were obtained for the 1.45 nm polymer, the groundwater DOC, and for the 1.70 nm colloids, respectively. Only the collection reservoir model was matched to experimental data, as will be explained below, resulting in an r^2 of 0.90. Figure 5-4c shows the results of modeling the conservative tracer chloride. Transport parameters of Cl diffusion through the till are from (Hendry et al., 2000), using a radial diffusion cell. Note the equilibrium concentration of Cl is higher than DOC because no adsorption of this tracer to the aquitard matrix occurs. The reported D_e^i and n_e^i for each colloid determined from the best fit models are shown in Table 5-2.

5.5.5 Straining

Straining should theoretically block colloid movement through a porous media, where the physical (and electrostatic) pore throat diameters are smaller than the diffusing colloids. The effects of straining can be seen in the size distributions of SRFA that are able to diffuse through the core sample. For SRFA (Fraction 'B'), a mean diameter of 2.15 nm placed in the source reservoir of the diffusion cell was reduced to 1.80 nm in the collection reservoir. Figure 5-5 is similar to the inset graph in Figure 5-4d, however colloid concentrations are normalized to the void peak in each sample. From these results, the diameter of the larger fraction of SRFA was determined to be

greater than the effective pore throat diameter for anionic colloids in the till material. The SRHA and larger colloids are entirely blocked from movement, as demonstrated by no mass in the collection reservoir.

Some movement of colloids occurs into the larger pore throats in the upper portion of the till. However, these colloids are eventually excluded from movement and entrained in the upper layer of till material. The timeframe of the experiments (540 days) was assumed to be sufficient for the larger colloidal material to diffuse through the till, even accounting for an increase in the effective porosity and lower effective diffusion coefficients.

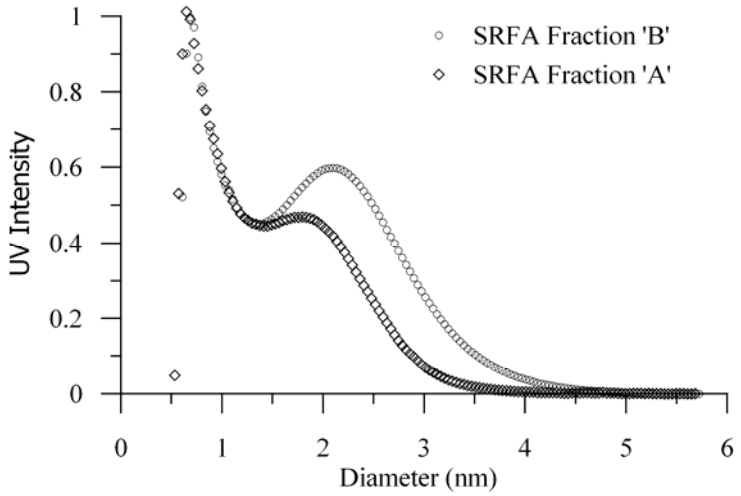

Figure 5-5. Size distribution of SRFA initially in the source reservoir (Fraction‘A’) and in the collection reservoir (Fraction ‘B’).

5.5.6 Porosity

Measured total porosity (n_t) for the till is 0.31 ± 0.01 (n = 10) (Shaw and Hendry, 1998b). Mercury intrusion porosimetry data revealed a total connected porosity of 0.30 for 12 m BG at the research site (Hendry et al., 2003b). Effective porosity values were modeled results, from best fit curves to the measured data. Effective porosities calculated for the colloids were in keeping with the porosimetry value. The smallest colloid, 1.43 nm, has an effective porosity of 0.30, which suggests this diameter colloid could access the majority or all, of the connected porosity. A decrease in the effective

porosity for the colloids was observed as the mean diameter increased (Table 5-2). The ratio of total porosity to measured porosity for all colloidal material ranged from 0.97 to 0.87. Reported differences between n_e^i and n_t values are shown in (Pearson, 1999) with significantly different ratios, ranging from 1 to 0.23 for a variety of materials. Some conservative solutes have an effective porosity similar to the actual porosity whereas others have an effective porosity that is much smaller.

An examination of porosimetry data from Hendry et al. (2003) shows a median measured pore diameter of 150 nm with 95 % of the pores below 2400 nm in diameter. The minimum measured pore diameter is 8 nm, with 12 % of total porosity below this value. This is in keeping with pore throat diameters reported for fine grained shale and mudstone of 10 to 30 nm, with all pores less than 200 nm (Fredrickson et al., 1997). At least 88 % of the pores are larger than the diameter of the colloidal material examined in this study (1.45 – 6.05 nm), which suggests the larger pore throats do not control movement of colloidal material, but rather the pore throat constrictions control colloid transport.

5.5.7 Modeled K_d^i

Modeled K_d^i values for diffusion profile 1 samples were similar to the calculated values with only slight deviations. The resultant retardation parameters (R_d^i) were calculated from the modeled K_d^i values and the n_e^i calculated above, and are presented in Table 5-2. The measured K_d^i for SRFA is considerably higher than the modeled value due to preferential sorption of the less mobile larger diameter fraction of this colloid.

5.5.8 Diffusion Coefficients

Modeled effective diffusion coefficients ranged from 1.5×10^{-10} m^2 s^{-1} for the 1.45 nm polymer to 6.5×10^{-11} m^2 s^{-1} for the 1.80 nm fraction of fulvic acid. D_e^i values could only be determined from colloidal material that was able to pass through the till. The D_e^i of groundwater DOC modeled in this study compared well with previous results

obtained from this research site. A D_e^i of 9.5×10^{-11} m^2 s^{-1} for groundwater DOC was the average of three diffusion cells (Table 5-1). Previous studies report a D_e^i of 9×10^{-11} m^2 s^{-1} (Hendry et al., 2003a). Slight differences were attributed to the addition of sorption in this study, as discussed previously.

Due to the fractionation of SRFA in the diffusion cells from straining and preferential sorption of the larger fraction, D_e^i was calculated differently than the other colloids. Model fits were only concerned with achieving a match for the collection reservoir. The n_e^i of the mobile SRFA was estimated to be 0.26 (Table 5-2), and parameters D_e^i and K_d^i were altered in the model. Too many uncertainties existed to model all three unknown parameters to only a breakthrough time and collection reservoir profile. The modeled K_d^i was considerable lower than the measured value because the larger mass fraction has a higher sorption to the till than the modeled mobile fraction.

5.5.9 Tortuosity

Tortuosity values were calculated with Equation [2], using the experimentally derived free water diffusion coefficients and best fit effective diffusion coefficients. Tortuosity values ranged from 0.57 to 0.31, decreasing with increasing colloidal diameter (Table 5-2). Equation [3] suggests the smaller colloids follow a more direct route though the matrix. Their l_e, or travel distance, is closer to the straight line travel distance, l. The results seem counterintuitive if the effective porosity decreases with an increase in colloid diameter. The effective porosity increase suggests the smaller colloids can access more of the total porosity than the larger colloids, and therefore an increased travel distance for the smaller colloids would be expected. Previous studies of dissolved constituents are not consistent with what was measured, however tortuosity has never been calculated for colloidal material in either diffusion or advection dominated systems. Our tortuosity values are in the ranges suggested in previous studies. (Bear, 1972) cites values of 0.8 to 0.4 from the literature, while others report a

range from 0.01 to 0.4 for non-reactive solutes in saturated porous media (Helmke et al., 2005; Perkins and Johnston, 1963).

5.5.10 Effective Pore Throat Diameter

The effective pore throat cut-off (smallest pore throats) was determined from the diameter of the colloidal material that could move through the till. The 1.45 and 1.75 nm polymer, the 1.70 nm DOC, as well as the smaller 1.80 nm fraction of SRFA were able to migrate through the till. Straining was observed for the SRFA greater than 1.80 nm, SRHA, and the polymers 3.05 nm and greater. Taking the range in diameters for each colloid into consideration, we can determine the effective pore throat diameter within the till is 2.0 to 2.2 nm for anionic colloidal material. Ion exclusion is produced by electrostatic repulsion of ions away from particle surfaces of like charge. For these materials, exclusion of anionic colloids would result in a decrease of the effective pore throat diameters (Gvirtzman and Gorelick, 1991; Smith et al., 2004). The Debye length within the pore constrictions is dependant on pH and ionic strength of the solution and would greatly reduce the effective pore diameter as is observed here (Bowen et al., 2002; Odiachi and Prieve, 1999). Cationic or neutral colloids somewhat greater than 2 nm may be able to move through these materials.

5.6 Diffusion Profiles

5.6.1 Diffusion Profile 1

Diffusion profile 1 includes the PSS 910, DOC and PSS 1430 colloids, and is similar to the diffusion profiles of a conservative tracer (Figure 5-4c), with the addition of some sorption to the till. The K_d^i in these samples is low. D_e^i and n_e^i values decrease with increasing colloidal diameter, as expected.

5.6.2 Diffusion Profile 2

Diffusion profile 2 is demonstrated by SRFA and SRHA. These samples show a high amount of adsorption, with the larger diameter being preferentially sorbed to the

till. These profiles are a combination of the diffusion profile 1 and 3. The D_e^i and n_e^i continue to decrease with increasing diameter (as in profile 1). Modeling the diffusion of these colloids cannot be done without understanding the processes affecting diffusion profile 3.

5.6.3 Diffusion Profile 3

Diffusion profile 3 is shown by PSS 4800, PSS 6500, and PSS 15450. Consideration of the diameter of these colloids (and their breakthrough times) indicates the experimental time was sufficient to allow breakthrough. The lack of colloidal matter in the collection reservoir suggests the effective pore throat diameter is too large to allow these colloids to move through the till. Colloid filtration in a diffusion dominated system has not been modeled in the literature, and several problems arise when filtration theory is applied to these samples.

The mass of colloid in the source reservoir is highly depleted (Figure 5-4f, g, h). The colloids show a moderate amount of sorption to the till, but less than the organic samples. A mass balance of sorption processes to the till matrix cannot account for 50 to 60% loss of colloid mass from the source reservoir. From the batch test K_d^i results, a maximum of 20% depletion of mass can be expected. Assuming the colloids are diffusing into the till and being trapped in the pore spaces still cannot account for the mass depletion from the source reservoir. With a 2.5 cm thick core and a maximum porosity of 0.3, the calculated amount of available porosity in the till is only 23% of the volume of the source reservoir.

Following the trend of the rest of the samples, the n_e^i and D_e^i for the larger colloids should continue to decrease. The calculated D_o^i of these samples and those determined for SRHA decrease systematically with increasing diameter, which is expected.

Sedimentation or coagulation of the PSS polymers may be occurring in the larger pores voids of the till. Sedimentation from chemical differences in the pore voids

of the till is unlikely because the pore water in the till is in equilibrium with the fluid reservoirs, and the density of the PSS particles is neutral and they readily dissolve. In several previous experiments, excessive agitation of high concentrations of larger PSS polymers resulted in coagulation/ entanglement, which may cause entrapment or sedimentation. To model the effects of sedimentation, an increase in the K_d^i parameter in the model simulates the removal of colloid mass from solution.

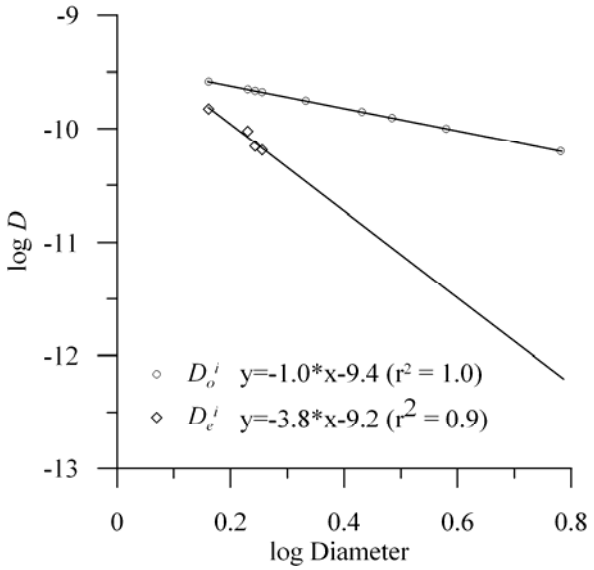

Figure 5-6. Free water and effective diffusion coefficients against colloid diameter.

To simulate the effect of sedimentation on the diffusion profile 3 colloids, an appropriate D_e^i value was estimated. Figure 5-6 shows the systematic increase of D_o^i with colloid diameter. This is expected as D_o^i and particle diameters are calculated from one another (Equation 10). Plotting the four estimated D_e^i values against colloid diameter for the few data points available shows a similar trend. Notably, this is strictly an estimation, and directly estimating the D_e^i from diameter data in this manner may not be possible. As seen in other experiments, the matrix diffusion coefficient may not increase linearly with colloidal size (Oswald and Ibaraki, 2001). For these models, n_e^i was kept constant at 0.26, and the K_d^i and D_e^i were varied. Best fit models were

obtained from: D_e^i = 2x10^{-11} m^2 s^{-1} and K_d^i = 5 for PSS 4800, D_e^i = 1x10^{-11} m^2 s^{-1} and K_d^i = 6.5 for PSS 6500, and D_e^i = 6.5x10^{-12} m^2 s^{-1} and K_d^i = 8.5 for PSS 15450 (Figure 5-7).

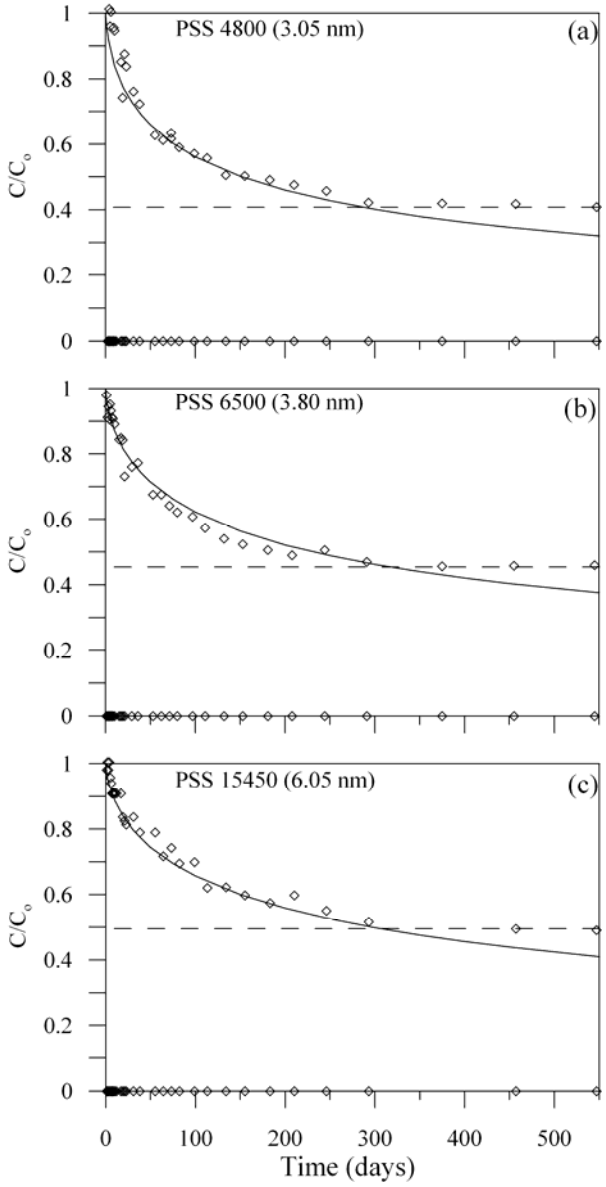

Figure 5-7. Modeling results considering sedimentation of larger colloidal matter within pore throat of clay rich glacial-till core. Shown are experimental (open diamond), modeled (solid line) and equilibrium concentrations of colloid.

The experimental data in Figure 5-7a, b, and c show the colloid mass in the source reservoir coming to equilibrium at about 250 to 300 days, with no subsequent decrease. Increasing K_d^i to approximate sedimentation simulates the diffusion profile well until 300 days, at which point the modeled values continue to decrease but the experimental ones come to equilibrium. The equilibrium concentration increases with diameter, with equilibrium at $C/C_0 = 0.40$ for PSS 4800, 0.45 for PSS 6500, and 0.50 for PSS 15450. In addition, the three largest colloids reach equilibrium concentration much faster than the smaller colloids (Figure 5-4). Faster diffusion of the larger colloids is not likely; however if these polymers are only diffusing part way into the clay before becoming entrained, a faster equilibration time than the smaller colloids may be observed due to a shorter transport distance. This and the model support the theory that the larger colloids may become trapped through some mechanism in the upper portion of the till.

A possible explanation for the equilibrium concentration in the till is the phenomenon of pore plugging or layer cake formation. Straining efficiency of a soil may increase with time as the colloidal material accumulates, resulting in the blocking of pore throats and essentially constricting movement through these materials (Gerba et al., 1991). If the smaller pores are being plugged in the till by the larger colloids, simulating diffusion with some sedimentation (those particles that are removed from the aqueous state by plugging pores) could match the observed profiles. When the pores are plugged, the system would reach equilibrium. Surface cake formation and pore plugging has been observed in advective systems; however, whether or not this occurs in a diffusion system has yet to be determined. In a diffusive system, no driving force exists to plug the pore throats. The colloids would hypothetically remain in the larger voids and not be forced into the smaller pore throats by water movement, and are too large to move through the pore throat constrictions.

The larger colloids showing the anomalous diffusion profiles are in diffusion cells with counter diffusing DOC (Table 5-1). If the pore throats were being plugged with larger colloids after some time period, and the filter efficiency of the clay was

improving, the diffusive profile of DOC could have been affected, but this could not be observed. After 300 days, DOC concentrations in the collection reservoir (the source reservoir for the larger polymers) were still decreasing. Modeling results would have shown a difference in diffusion coefficient for DOC, but those measured here compare well with previous measurements ($9.5x10^{-11}$ vs. $9.0x10^{-11}$ m^2 s^{-1}) (Hendry et al., 2003a).

What is lacking for a more comprehensive understanding of colloid straining in these experiments is the actual colloid distribution in the core sample. The colloid mass is distributed within the 2.5 cm core sample, and clearly the larger colloids are restricted from movement, but the location of the colloids in the core is not known. The clay cores were sectioned after the experiments were complete, and several attempts were made to extract the colloids from the clay. The very low hydraulic conductivity made squeezing or centrifuging water from the core impossible. Addition of water to the core sections to create a slurry for extraction was also unsuccessful; this resulted in the excessive dilution of the colloids, and they could not be identified through AsFlFFF methods. Other methods to visualize the location of the colloids in the core were also unsuccessful. The colloids are a maximum of 6 nm in diameter, which is below the practical resolution of SEM and TEM. These methods are also destructive to the sample and colloids, so could not be attempted. Further experiments could be conducted with readily available fluorescent latex micro-spheres, which would allow determination of penetration depth and distribution of the larger colloids. However, the use of fluorescent colloids would still not allow any visualization of the straining mechanisms.

A quantitative description of colloid straining in natural porous media is difficult because large pore size distribution, complex pore geometry, tortuous flow paths and surface heterogeneity exists in these media. Also, natural geologic materials are not homogeneous, and pore walls may be coated with mineral precipitates or contain adsorbed organic matter, all of which will affect theoretical straining mechanisms. Straining was observed in these experiments, and a determination of the cutoff diameter of colloids with respect to migration could be determined, but actual application of straining theory to natural systems was not possible.

5.7 Implications for Contaminant Transport

The effective pore throat diameter determined for this clay-rich glacial till is the same the maximum diameter of DOC in the groundwater in the glacial till. Calculated groundwater DOC ranges from 1.65 – 1.75 nm (M_w 1140 to 1390 Da), with a maximum diameter of about 2 nm (M_w 1800 Da). Surficial snowmelt and recharge water from the King Site collected in spring contains DOC with a mean diameter of 2 – 2.2 nm (M_w 1800 – 2100 Da), however the larger DOC is not found at depth in the till. Previous studies show DOC follows a diffusive mixing profile in this aquitard, with recent soil organic carbon at surface mixing with older DOC at depth (Hendry and Wassenaar, 2005). DOC M_w in the groundwaters is consistent from the near surface to 80 m depth. If the till is being recharged with organic matter from the surface, the DOC, at least in the near surface, should have similar properties to that contained in the surficial DOC; however, the M_w of surface water DOC is much larger. This suggests straining affects the larger DOC, allowing only the smaller DOC to migrate through the system due to an effective pore throat diameter of 2 nm. Determining the diameter of potentially mobile colloids (DOC) within low permeability formations could serve as a proxy to estimate an effective pore throat diameter and allow assumptions to be made about other colloid and contaminant mobility in these environments.

DOC in groundwaters from the Warman site, another clay-rich glacial till, has a mean diameter of 1.7 nm (M_w 1170 Da), with no change observed with depth (Reszat and Hendry, 2007). DOC in a clay aquitard in the Chalco basin of Mexico City ranges from 1.5 to 1.7 nm (M_w 990 – 1240 Da), with a decrease in M_w observed with depth (Reszat and Hendry, 2007). This lacustrine clay has been shown to be consolidating from the bottom up due to extensive groundwater withdrawal from the underlying aquifer, resulting in an increased downward hydraulic gradient that increases with depth (Ortega-Guerrero et al., 1993). Consolidation of sediments will decrease the porosity of the formation, and due to tighter grain packing will decrease the effective pore throat diameter of the material. The decrease in diameter of DOC observed with depth in this clay could be explained by a decrease in the effective pore throat diameters with depth. DOC in the Boom Clay in Belgium, another low permeability unit, has a reported mean

diameter of 1.8 nm (M_w 1800 Da) (Thang et al., 2001), similar to what is observed in the King Site, Warman Site and Chalco basin aquitards. DOC reported for coarse grained sediments and surface water is considerably larger than what has been observed in aquitards. The Gorleben Aquifer has reported diameters of 2.2 – 3.43 nm (M_w 4100 - 9400 Da) (Kim et al., 1990; Thang et al., 2001). The smaller diameter of DOC in aquitard environments is in agreement with our conclusions that DOC can be a proxy for pore throat cut off in a material and possibly the movement of other colloids.

The diffusive mixing profile with depth can be observed at both King Site and Warman Site aquitards. Figure 5-8a shows the concentration of DOC with depth at both sites, normalized to a concentration of 1. Models were run to determine the time required to set up the diffusive profile to 50 m depth. Parameters used to model DOC diffusion were from Table 5-2, with the exception of K_d^i, which was assumed to be 0, after (Hendry et al., 2003a). The DOC at each depth in the till was assumed to be in equilibrium with the till and no sorption to the till was expected, unlike the diffusion cells in this study that monitored the diffusion of DOC from a shallow piezometer with till from a deeper borehole. The best fit was obtained for a diffusive mixing profile being established at 6 ka. This is in good agreement with estimates of the prairie soil zone being developed between 7.5 to 5.0 ka (Sauchyn, 1990).

Figure 5-8b shows the results of diffusion modeling of the chloride and mobile colloids through the till for a time period of 1000 years with a constant source concentration using the properties determined from the colloids in Table 5-2. After 1000 years, 50% of the Cl has diffused 2.5 m into the till, both PSS 910 and DOC have diffused 1.6 m into the till, PSS 1430 has diffused 0.9 m into the till, and SRFA has diffused 0.52 m into the till. The maximum amount of movement for any solute in this system is approximately that of the conservative solute, Cl. Any material stored in or on the till has minimal movement through these units, provided they are fractured and homogenous.

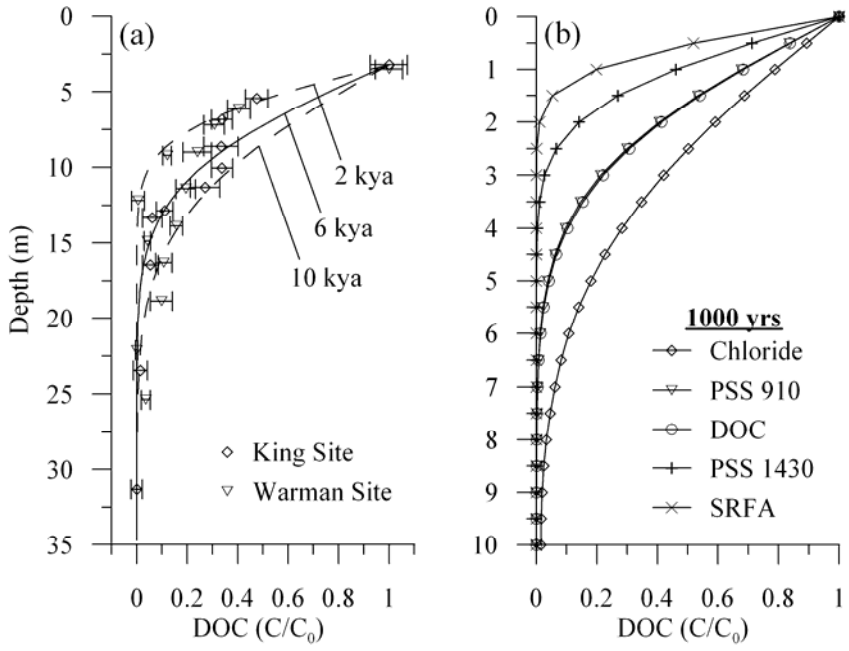

Figure 5-8. (a) DOC from both King and Warman site with depth normalized to 1. Solid lines are best fit diffusion models from Table 3 for 2, 6, and 12 thousand years to simulate observed diffusion profile at the site. (b) Depth of penetration of a conservative tracer and mobile colloids after a period of 1000 years.

Figure 5-9 shows the commonly accepted continuum of colloidal material in natural waters (Matthess and Peckdeger, 1985; Thurman, 1985). The majority of possible groundwater organic colloids such as humic acids (2 – 10 nm), viruses (20 – 250 nm), bacteria (0.2 – 5 μm), and protozoa (10 – 100 μm) are larger than the effective pore throat diameter of the till, and as such these materials are not expected to diffuse through non-fractured tills. If the tills are fractured, a considerable amount of matrix diffusion and colloid retardation within the fracture will occur for those materials that are able to diffuse into the till; however colloidal material larger than 2 nm is expected to be transported solely in fractures, with minimal retardation due to matrix diffusion.

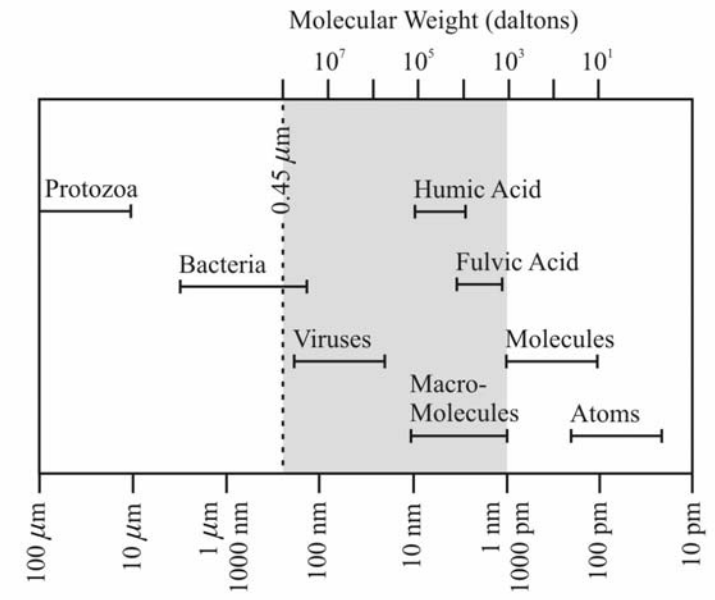

Figure 5-9. The continuum of dissolved, colloidal, and particulate matter within natural waters. Shaded area from 1 – 450 nm is the generally accepted range in colloid size. Adapted from (Matthess and Peckdeger, 1985; Thurman, 1985).

5.8 Conclusions

Colloid migration in low permeability units is controlled by particle diameter. The effective pore throat diameter of the clay material controls the diameter of colloids able to migrate through these materials. For the glacial till in Saskatchewan this was determined to be 2 – 2.2 nm. Colloids used in our experiments ranged from 1.45 to 6.05 nm. Mobility was limited to colloids with diameters of 1.45 to 1.80 nm. Movement of the larger colloids (>1.80 nm) was restricted by straining within small pore throat constrictions in the glacial till. Other aquitards tested have similarly low diameters of mobile colloids, which may indicate similar effective pore throat diameters. DOC diameter may be a proxy for the pore throat diameter, at least in low permeability groundwater environments.

Breakthrough time of the colloids increased with diameter. The D_o^i and D_e^i of the colloids decreased with increasing colloid diameter. D_o^i ranged from 2.62×10^{-10} to 6.31×10^{-11} m s^{-1} (for all colloids) and D_e^i ranged from 2.62×10^{-10} to 2.62×10^{-10} m s^{-1} (for

the mobile colloids). From both diffusion coefficients, τ^i ranged from 0.57 – 0.37, decreasing with increasing colloidal diameter. The effective porosity ranged from 0.30 for the 1.45 nm colloid, similar to conservative solutes, to 0.26 for the 1.80 nm fraction of SRFA.

Diffusion parameters of DOC estimated in these experiments were applied to the observed diffusion profile at the King Site and Warman Site aquitards in Saskatchewan, Canada. Best fit models estimate the time of soil zone formation for both sites post-glaciation at 6 thousand years before present. Models examining the movement of possible contaminants at these sites showed 50% of the conservative solute Cl migrates 2.5 m into the till after 1000 years. Colloid movement is much slower, with the 1.45 nm colloids migrating 1.6 m, and SRFA migrating only 0.5 m after 1000 years. Straining will prevent the migration of larger colloidal material such as viruses (20 – 250 nm), bacteria (0.2 – 5 μm), and protozoa (10 – 100 μm) in non-fractured low permeability groundwater environments. Smaller organic contaminants may be able to migrate through the till depending on their sorption affinity to the glacial tills, however colloid migration rates are slower than those of conservative solutes and are controlled by diffusion mechanisms. Knowledge of colloid diffusion mechanisms in the matrix of fractured low permeability geologic media will aid contaminant migration predictions in non-fractured systems and also in fractured low permeability environments. The amount of matrix diffusion from the fractures may considerably retard the migration of colloids in fractures, as for conservative solutes.

5.9 Acknowledgements

This research was funded by research grants from the Natural Sciences and Engineering Council of Canada (NSERC) through the Industrial Research Chair Program and the Potash Corporation of Saskatchewan. Thanks to Dr. M. Adrián Ortega-Guerrero from the National Autonomous University of Mexico for providing samples from the Chalco Aquitard.

5.10 References

Bear, J., 1972, The Dynamics of Fluids in Porous Media: New York, Dover Publications, Inc., 764 p.

Beckett, R., Jue, Z., and Giddings, J.C., 1987, Determination of Molecular-Weight Distributions of Fulvic and Humic Acids Using Flow Field-Flow Fractionation: Environmental Science & Technology, v. 21, p. 289-295.

BoivinJahns, V., Ruimy, R., Bianchi, A., Daumas, S., and Christen, R., 1996, Bacterial diversity in a deep-subsurface clay environment: Applied and Environmental Microbiology, v. 62, p. 3405-3412.

Bowen, W.R., Doneva, T.A., and Stoton, J.A.G., 2002, The use of atomic force microscopy to quantify membrane surface electrical properties: Colloids and Surfaces a-Physicochemical and Engineering Aspects, v. 201, p. 73-83.

Bradford, S.A., Bettahar, M., Simunek, J., and van Genuchten, M.T., 2004, Straining and attachment of colloids in physically heterogeneous porous media: Vadose Zone Journal, v. 3, p. 384-394.

Bradford, S.A., Simunek, J., Bettahar, M., Van Genuchten, M.T., and Yates, S.R., 2003, Modeling colloid attachment, straining, and exclusion in saturated porous media: Environmental Science & Technology, v. 37, p. 2242-2250.

Bradford, S.A., Yates, S.R., Bettahar, M., and Simunek, J., 2002, Physical factors affecting the transport and fate of colloids in saturated porous media: Water Resources Research, v. 38, p. -.

Cumbie, D.H., and McKay, L.D., 1999, Influence of diameter on particle transport in a fractured shale saprolite: Journal of Contaminant Hydrology, v. 37, p. 139-157.

Dycus, P.J.M., Healy, K.D., Stearman, G.K., and Wells, M.J.M., 1995, Diffusion-Coefficients and Molecular-Weight Distributions of Humic and Fulvic-Acids Determined by Flow Field-Flow Fractionation: Separation Science and Technology, v. 30, p. 1435-1453.

Foppen, J.W.A., Mporokoso, A., and Schijven, J.F., 2005, Determining straining of Escherichia coli from breakthrough curves: Journal of Contaminant Hydrology, v. 76, p. 191-210.

Fredrickson, J.K., McKinley, J.P., Bjornstad, B.N., Long, P.E., Ringelberg, D.B., White, D.C., Krumholz, L.R., Suflita, J.M., Colwell, F.S., Lehman, R.M., Phelps, T.J., and Onstott, T.C., 1997, Pore-size constraints on the activity and survival of subsurface bacteria in a late Cretaceous shale-sandstone sequence, northwestern New Mexico: Geomicrobiology Journal, v. 14, p. 183-202.

Gerba, C.P., Yates, M.V., and Yates, S.R., 1991, Quantification of factors controlling viral and bacterial transport in the subsurface, *in* Hurst, C.J., ed., Modeling the Environmental Fate of Microorganisms: Washington, DC, American Society of Microbiology, p. 77-88.

Gillham, R.W., Robin, M.J.L., Dytynyshyn, D.J., and Johnston, H.M., 1984, Diffusion of Nonreactive and Reactive Solutes through Fine-Grained Barrier Materials: Canadian Geotechnical Journal, v. 21, p. 541-550.

Grolimund, D., Elimelech, M., Borkovec, M., Barmettler, K., Kretzschmar, R., and Sticher, H., 1998, Transport of in situ mobilized colloidal particles in packed soil columns: Environmental Science & Technology, v. 32, p. 3562-3569.

Gvirtzman, H., and Gorelick, S.M., 1991, Dispersion and Advection in Unsaturated Porous-Media Enhanced by Anion Exclusion: Nature, v. 352, p. 793-795.

Harvey, R.W., George, L.H., Smith, R.L., and Leblanc, D.R., 1989, Transport of Microspheres and Indigenous Bacteria through a Sandy Aquifer - Results of Natural-Gradient and Forced-Gradient Tracer Experiments: Environmental Science & Technology, v. 23, p. 51-56.

Harvey, R.W., Kinner, N.E., Macdonald, D., Metge, D.W., and Bunn, A., 1993, Role of Physical Heterogeneity in the Interpretation of Small-Scale Laboratory and Field Observations of Bacteria, Microbial-Sized Microsphere, and Bromide Transport through Aquifer Sediments: Water Resources Research, v. 29, p. 2713-2721.

Headley, J.V., Boldt-Leppin, B.E.J., Haug, M.D., and Peng, J.M., 2001, Determination of diffusion and adsorption coefficients for volatile organics in an organophilic clay-sand-bentonite liner: Canadian Geotechnical Journal, v. 38, p. 809-817.

Helmke, M.F., Simpkins, W.W., and Horton, R., 2005, Experimental determination of effective diffusion parameters in the matrix of fractured till: Vadose Zone Journal, v. 3, p. 1050-1056.

Hendry, M.J., Ranville, J.F., Boldt-Leppin, B.E.J., and Wassenaar, L., 2003a, Geochemical and transport properties of dissolved organic carbon in a clay-rich aquitard: Water Resources Research, v. 39, p. 1194-1203.

Hendry, M.J., Ranville, J.R., Boldt-Leppin, B.E.J., and Wassenaar, L.I., 2003b, Geochemical and transport properties of dissolved organic carbon in a clay-rich aquitard: Water Resources Research, v. 39, p. 1194-1203.

Hendry, M.J., and Wassenaar, L., 1999, Implications of the distribution of delta-D in pore waters for groundwater flow and the timing of geologic events in a thick aquitard system.: Water Resources Research, v. 35, p. 1751-1760.

—, 2000a, Controls on the distribution of major ions in pore waters of a thick surficial aquitard: Water Resources Research, v. 36, p. 503-513.

Hendry, M.J., and Wassenaar, L.I., 2000b, Controls on the distribution of major ions in pore waters of a thick surficial aquitard: Water Resources Research, v. 36, p. 503-513.

—, 2004a, Transport and geochemical controls on the distribution of solutes and stable isotopes in a thick clay-rich till aquitard, Canada: Isotopes in Environmental and Health Studies, v. 40, p. 3-19.

—, 2004b, Transport and geochemical controls on the distribution of solutes and stable isotopes in a thick clay-rich till aquitard, Canada: Isotopes in Environmental and Health Studies, v. 41, p. 3.

—, 2005, Origin and migration of dissolved organic carbon fractions in a clay-rich aquitard: C-14 and delta C-13 evidence: Water Resources Research, v. 41, p. -.

Hendry, M.J., Wassenaar, L.I., and Kotzer, T., 2000, Chloride and chlorine isotopes (Cl-36 and delta Cl-37) as tracers of solute migration in a thick, clay-rich aquitard system: Water Resources Research, v. 36, p. 285-296.

Jorgensen, P.R., McKay, L.D., and Kistrup, J.P., 2004, Aquifer vulnerability to pesticide migration through till aquitards: Ground Water, v. 42, p. 841-855.

Kim, J.I., Buckau, G., Li, G.H., Duschner, H., and Psarros, N., 1990, Characterization of humic and fulvic acids from Gorleben groundwater.: Fresnius Journal of Analytical Chemistry, v. 338.

Kretzschmar, R., Robarge, W.P., and Amoozegar, A., 1994, Filter Efficiency of three sparolites for natural clay and iron oxide colloids: Environmental Science & Technology, v. 28, p. 1907-1915.

—, 1995, Influence of natural organic matter on colloid transport through saprolite: Water Resources Research, v. 31, p. 435-445.

Lawrence, J.R., Hendry, M.J., Wassenaar, L.I., Germida, J.J., Wolfaardt, G.M., Fortin, N., and Greer, C.W., 2000, Distribution and biogeochemical importance of bacterial populations in a thick clay-rich aquitard system: Microbial Ecology, v. 40, p. 273-291.

Litzen, A., and Wahlund, K.-G., 1991, Effects of temperature, carrier composition and sample load in asymmetrical flow field-flow fractionation: Journal of Chromatography A., v. 548, p. 393-406.

Matthess, G., and Peckdeger, A., 1985, Survival and transport of pathogenic bacteria and viruses in groundwater, *in* McCarty, P.L., ed., Ground water quality: New York, John Wiley, p. 472-482.

McCarthy, J.F., McKay, L.D., and Brunner, D.D., 2002, Influence of ionic strength and cation charge on transport of colloidal particles in fractured shale saprolite: Environmental Science & Technology, v. 36, p. 3735-3743.

McKay, L.D., Gillham, R.W., and Cherry, J.A., 1993, Field Experiments in a Fractured Clay Till.2. Solute and Colloid Transport: Water Resources Research, v. 29, p. 3879-3890.

McKay, L.D., Sanford, W.E., and Strong, J.M., 2000, Field-scale migration of colloidal tracers in a fractured shale saprolite: Ground Water, v. 38, p. 139-147.

Moridis, G.J., Hu, Q., Wu, Y.S., and Bodvarsson, G.S., 2003, Preliminary 3-D site-scale studies of radioactive colloid transport in the unsaturated zone at Yucca Mountain, Nevada: Journal of Contaminant Hydrology, v. 60, p. 251-286.

Odiachi, P.C., and Prieve, D.C., 1999, Effect of added salt on the depletion attraction caused by non-adsorbing clay particles: Colloids and Surfaces a-Physicochemical and Engineering Aspects, v. 146, p. 315-328.

Ortega-Guerrero, A., Cherry, J.A., and Rudolph, D.L., 1993, Large-scale aquitard consolidation near Mexico City: Ground Water, v. 31.

Oswald, J.G., and Ibaraki, M., 2001, Migration of colloids in discretely fractured porous media: effect of colloidal matrix diffusion: Journal of Contaminant Hydrology, v. 52, p. 213-244.

Pearson, F.J., 1999, What is the porosity of a mudrock? *in* Fleet, A.J., ed., Muds and Mudstones: Physical and Fluid Flow Properties, Volume 158: Geological Society, London, Special Publications: London, Geological Society of London, p. 9-21.

Perkins, T.K., and Johnston, O.C., 1963, A Review of Diffusion and Dispersion in Porous Media: Transactions of the Society of Petroleum Engineers of Aime, v. 228, p. 70-84.

Quigley, R.M., Fernandez, F., Yanful, E., Helgason, T., Margaritis, A., and Whitby, J.L., 1987, Hydraulic Conductivity of Contaminated Natural Clay Directly Below a Domestic Landfill: Canadian Geotechnical Journal, v. 24, p. 377-383.

Reszat, T.N., and Hendry, M.J., 2005, Characterizing Dissolved Organic Carbon Using Asymmetrical Flow Field-Flow Fractionation with On-Line UV and DOC Detection: Analytical Chemistry, v. 77, p. 4194-4200.

—, 2007, Unpublished Data.

Rowe, R.K., Booker, J.R., and Fraser, M.J., 1997, POLLUTEv6 user's guide: Windsor, Ontario, Canada, GAEA Environmental Engineering.

Ryan, J.N., and Elimelich, M., 1996, Colloid mobilization and transport in groundwater: Colloids and Surfaces A., v. 107, p. 1-56.

Saiers, J.E., and Ryan, J.N., 2006, Introduction to special section on colloid transport in subsurface environments: Water Resources Research, v. 42, p. -.

Sauchyn, D.J., 1990, A Reconstruction of Holocene Geomorphology and Climate, Western Cypress Hills, Alberta and Saskatchewan: Canadian Journal of Earth Sciences, v. 27, p. 1504-1510.

Shackelford, C.D., 1991, Laboratory diffusion testing for waste disposal - A review.: Journal of Contaminant Hydrology, v. 7, p. 177-217.

Shaw, J., and Hendry, M.J., 1998a, Groundwater flow in a thick clay till and clay bedrock sequence in Saskatchewan, Canada: Canadian Geotechnical Journal, v. 35, p. 1041-1052.

Shaw, R.J., and Hendry, M.J., 1998b, Hydrogeology of a thick clay till and Cretaceous clay sequence, Saskatchewan, Canada: Canadian Geotechnical Journal, v. 35, p. 1041-1052.

Smith, D., Pivonka, P., Jungnickel, C., and Fityus, S., 2004, Theoretical analysis of anion exclusion and diffusive transport through platy-clay soils: Transport in Porous Media, v. 57, p. 251-277.

Thang, N.M., Geckeis, H., Kim, J.I., and Beck, H.P., 2001, Application of the flow field flow fractionation (FFFF) to the characterization of aquatic humic colloids: evaluation and optimization of the method: Colloids and Surfaces A., v. 181, p. 289-301.

Thurman, E.M., 1985, Organic Geochemistry of Natural Waters: Dordrecht, Martinus Nijhoff/Dr W. Junk Publishers, 497 p.

van der Kamp, G., Van Stempvoort, D.R., and Wassenaar, L.I., 1996, The radial diffusion method 1. Using intact cores to determine isotopic compostion, chemistry, and effective porosities for groundwater in aquitards: Water Resources Research, v. 32, p. 1815-1822.

Van Loon, L.R., Baeyens, B., and Bradbury, M.H., 2005, Diffusion and retention of sodium and strontium in Opalinus clay: Comparison of sorption data from diffusion and batch sorption measurements, and geochemical calculations: Applied Geochemistry, v. 20, p. 2351-2363.

Wahlund, K.-G., 2000, Asymmetrical Flow-Field Flow Fractionation, *in* Giddings, C.J., ed., Field-Flow Fractionation Handbook: New York, John Wiley & Sons, p. 279-294.

Wahlund, K.-G., and Giddings, C.J., 1987, Properties of an asymmetrical flow field-flow fractionation channel having one permeable wall: Analytical Chemistry, v. 59, p. 1332-1339.

Wassenaar, L.I., and Hendry, M.J., 1999, Improved piezometer construction and sampling techniques to determine pore water chemistry in aquitards: Ground Water, v. 37, p. 564-571.

Wersin, P., Van Loon, L.R., Soler, J.M., Yllera, A., Eikenberg, J., Gimmi, T., Hernan, P., and Boisson, J.Y., 2004, Long-term diffusion experiment at Mont Terri: first results from field and laboratory data: Applied Clay Science, v. 26, p. 123-135.

6.0 SUMMARY AND CONCLUSIONS

The goal of this thesis was to address three important issues concerning DOC within a low permeability ground water environment. Specifically, the objectives were to i) characterize the molecular weight and structural characteristics of the DOC, ii) quantify the complexation of elements with the DOC, and iii) characterize the transport of colloids, including DOC.

The primary study site for this research was the King Site in southern Saskatchewan, Canada. This clay till aquitard was ideal for the study as the site is well characterized with a relatively simple geology and hydrogeology. In addition solute transport mechanisms, inorganic geochemistry, and microbiology of the aquitard are well understood. Sample results from the Warman Site, a clay till aquitard north of Saskatoon and the Chalco basin, a lacustrine clay underlying Mexico City were compared to those from the King Site.

The summary and conclusions from each of the three objectives (see above) are presented below.

6.1 Characterization of the molecular weight and structure of the DOC

To separate and identify DOC within pore waters, an AsFlFFF system was applied. It proved to be an effective method for DOC separation in pore waters. Using AsFlFFF, a method of characterizing dissolved organic carbon (DOC) using on-line UV and DOC detection was developed and applied to aquitard and surface water samples. DOC and UV fractograms obtained with this technique were highly reproducible and were interpreted using a simple molecular weight calibration approach. Results suggest that DOC detection may be a more accurate method to characterize molecular weight of the DOC than UV detection; UV detection may bias molecular weights high because of the method's inability to resolve aliphatics (usually of lower molecular weight).

DOC molecular weights for the King site, determined through DOC detection methods, were consistent with depth. M_w ranged from 1100 to 1308 Da, M_n ranged from 890 to 1206 Da, with a narrow range in molecular weight distribution (polydispersity ranged from 1.08 – 1.30). The molecular weights determined from the UV detection system (at 254 nm) were slightly greater, M_w ranged from 1380 to 1500 Da, M_n ranged from 1100 to 1247 Da (polydispersity ranged from 1.22 – 1.27). Results from the King Research Site were similar to those measured in other aquitards. Warman Site pore waters contain DOC with a M_w ranging from 1540 to 1650 Da and the Chalco lacustrine clay pore waters from Mexico City contain DOC with a M_w ranging from 1470 to 1630.

Coupling of the two detectors (DOC and UV) provided details on the dominant structures (aliphatic vs. aromatic content) in the DOC fractions. Distinct and repeatable differences observed with a normalized intensity comparison (NIC) analysis of different samples supports the ability of this method to characterize the aromaticity of DOC. DOC aromaticity was positively correlated with molecular weight, in both a bulk and molecular weight specific analysis.

6.2 DOC – element complexation

Element speciation experiments to quantify complexation with DOC are few, and the majority of those in literature do not account for complexation in *in-situ* ground water conditions. A coupled AsFlFFF-UV-TOC-ICP-MS technique was developed. It yielded valuable knowledge of DOC-element complexation within a natural aquitard environment. The experiments were conducted under conditions that approach field conditions with only minor alterations (0.45 μm filtration and pH adjustment). This research clearly demonstrates the utility of using AsFlFFF-ICP-MS to determine *in-situ* association constants (K_d) for metal–DOC complexes. It also represents the first attempt to compare elemental speciation modeling to laboratory chromatographic measurements of DOC complexation in porewater samples. The AsFlFFF-ICP-MS technique was shown to be sufficiently sensitive to allow measurement of U–DOC complexation at natural DOC and metal concentrations. This approach is particularly useful if sample volumes are limited (< 1 ml) as might be the case for some porewater studies. Uranium

K_d values were linearly related to NIC (aromaticity) in the DOC samples, suggesting slight changes in DOC properties have an appreciable effect on their complexation capacity.

Modeling results suggest only 23% of carboxylic and 7% of phenolic sites on DOC are occupied by all elements studied at ground water pH conditions (pH 7.9 to 8.3). AsFlFFF-ICP-MS analyses and geochemical modeling suggest less than 4% of total aqueous U and Zn are associated to DOC in these ground waters indicating facilitated transport in this system will be limited. Further, our data suggest DOC facilitated transport of these elements may be of limited importance in ground waters with similar (typical) chemistries. The technique of AsFlFFF coupled with ICP-MS would be a powerful tool to apply to contaminated sites such as mine tailings or landfill waste plumes.

6.3 Transport of DOC in aquitard environments

Studies of the diffusive transport of colloids in low permeability environments are limited. For the first time an in-depth study was conducted to examine the movement of colloids in the macro-molecular/micro-colloidal range (1 – 10 nm). This work is critical to understanding the movement and distribution of colloidal material in diffusion dominated systems, and determining the impact a low permeability matrix has on colloid transport in fractures within a dual porosity system.

The effective pore throat diameter of the glacial till in Saskatchewan was determined to be 2 – 2.2 nm. Mobility in the glacial till was limited to colloids with diameters of 1.5 to 1.8 nm, and movement of larger colloids (>1.80 nm) was restricted, likely by straining in small pore throat constrictions. Other aquitards tested (Warman and Chalco Sites) also have small diameters of mobile DOC, which may indicate comparable effective pore throat diameters. The study suggests that the DOC diameter may be a proxy for the pore throat diameter, at least in low permeability groundwater environments.

Colloid breakthrough time increased with increasing diameter. The D_o^i and D_e^i of the colloids decreased with increasing colloid diameter. D_o^i ranged from 2.62×10^{-10} to 6.31×10^{-11} m s^{-1} (for all colloids) and D_e^i ranged from 2.62×10^{-10} to 2.62×10^{-10} m s^{-1} (for the mobile colloids). From both diffusion coefficients, τ^i ranged from 0.57 – 0.37, decreasing with increasing colloidal diameter. The effective porosity ranged from 0.30 for the 1.45 nm colloid, similar to conservative solutes, to 0.26 for the 1.80 nm fraction of SRFA.

The modeled diffusion parameters of DOC were used to model an approximate time of soil profile formation at the King and Warman sites, Saskatchewan. Best fit models estimate the time of soil zone formation for both sites post-glaciation at 6 ka BP. Colloid migration rates are slower than those of conservative solutes and are controlled by diffusion mechanisms. Models predicting contaminant movement into the aquitard showed 50% of the conservative solute Cl migrating 2.5 m into the glacial till after 1 ka. Colloidal movement is much slower, with the 1.45 nm colloids moving 1.6 m, and SRFA migrating only 0.5 m after 1 ka. Data suggested that straining should prevent the migration of larger colloidal material such as viruses (20 – 250 nm), bacteria (0.2 – 5 μm), and protozoa (10 – 100 μm) in non-fractured low permeability groundwater environments.

6.4 Global Conclusions

The results from this thesis show that the DOC in Saskatchewan clay-rich glacial tills is less reactive and has lower amounts of aromatic carbon than those in surface water environments, thereby having lower complexation capacity. As a result elemental complexation by this DOC is limited and much lower than what has been observed in surface waters. Facilitated transport of contaminants (elements) complexed to DOC is also limited in these glacial tills because the movement of colloids in this environment is limited to diffusion. The migration of larger, and more reactive, DOC, as well as larger colloidal mater which may complex elements, or be contaminants in themselves, is

likely restricted due to sieving through the small pore throat diameters in these materials.

7.0 RECOMMENDATIONS FOR FUTURE WORK

All research conducted in this thesis was performed with unaltered and unconcentrated DOC (DOC concentrations > 10 mg l^{-1}). Several approaches were attempted to characterize the DOC technique at concentrations < 0.5 - 10 mg l^{-1} but were not successful. These included the using the AsFlFFF and ^{13}C Nuclear Magnetic Resonance. These samples could be analyzed with AsFlFFF as well as other techniques by preconcentration techniques, such as ultrafiltration and roto-evaporation. It is believed, however, that using concentration and purification techniques of DOC by harsh methods such as XAD-8 resins will alter the properties of the DOC to such an extent that further characterization will lead to results that are not representative of the true properties. Preconcentration of samples by any method may lead to sample alteration, especially in element complexation studies, which is why these methods were avoided in this thesis. A comparison of the various methods is, however, warranted.

Further characterization of DOC could include voltammetric techniques, and/or molecular mass spectrometry to identify the individual ligands and complexes present in the DOC structure. The complexity of natural DOC would probably necessitate the use of Fourier-Transform mass spectrometry to resolve individual compounds and, possibly, to detect metal-ion complexes by recognition of metal isotope patterns, and mass differences between unbound ligands and the corresponding complex(es).

In future metal complexation studies, the research conducted as part of this thesis could be refined and improved by collecting and analyzing the chemistry (DOC and metal concentrations) of the crossflow pump water from the AsFlFFF system. This should allow a full metal balance.

Elevated background concentrations of Fe, Mn, Ni, Cu, Sr, and Mo in the effluent from the AsFlFFF system may have masked any complexation of these

elements with DOC in the ICP-MS detector, making it impossible to quantify their complexation. This problem could be resolved in future studies. For example, in addition to lower the detection limit (baseline concentration) of the system using ICP-MS, the AsFlFFF could be refitted with inert parts such as PEEK pump pistons and bodies, and the elimination of any stainless steel tubing in the system.

Although studies conducted in this thesis show smaller colloids (DOC) are not a concern in terms of contaminant complexation in the in the aquitards, larger colloidal material, such as Fe- and Al-hydroxides, can be mobile in groundwaters and may have elevated masses of metals complexed to them. Optimization of the AsFlFFF system and subsequent separation of larger colloids should be considered. Preliminary tests (not reported) show that it is feasible to use the coupled AsFlFFF-ICP-MS to characterize these larger colloids.

In the laboratory transport study, the larger colloidal material did not exhibit typical straining and diffusive behavior. The observed transport phenomenon controlling the 3.03, 4.80 and 6.05 nm colloids could not be explained with data collected from the experiments in this study. Although a decrease in colloid concentrations from the source reservoir was observed, a complete understanding of the straining mechanisms in the tills was not possible. This understanding could be acquired using visualization techniques. Visualization of the controlling mechanism could be undertaken by repeating the experiments using fluorescent latex micro-spheres (readily available) instead of the non-fluorescing colloids used in this work. A fluorescent polymer could elucidate where larger polymers are being sieved and trapped in the glacial till. An alternate visualization approach using synchrotron radiation techniques may also prove to be of value.

APPENDIX 1 Supplementary data for thesis.

Appendix 1A – Figure of Postnova Analytics Asymmetrical Flow Field-Flow System.

Appendix 1B – Map of King Site showing locations of piezometers.

Appendix 1C – King Site piezometer details.

Appendix 1D – Map of Warman site showing locations of piezometers.

Appendix 1E – Warman Site piezometer details.

Appendix 1F – Modifications to Sievers Turbo TOC.

Appendix 1G – AsFlFFF system connection to Micromass ICP-MS.

Appendix 1A - Postnova Analytics Asymmetrical Flow Field-Flow Fractionation System

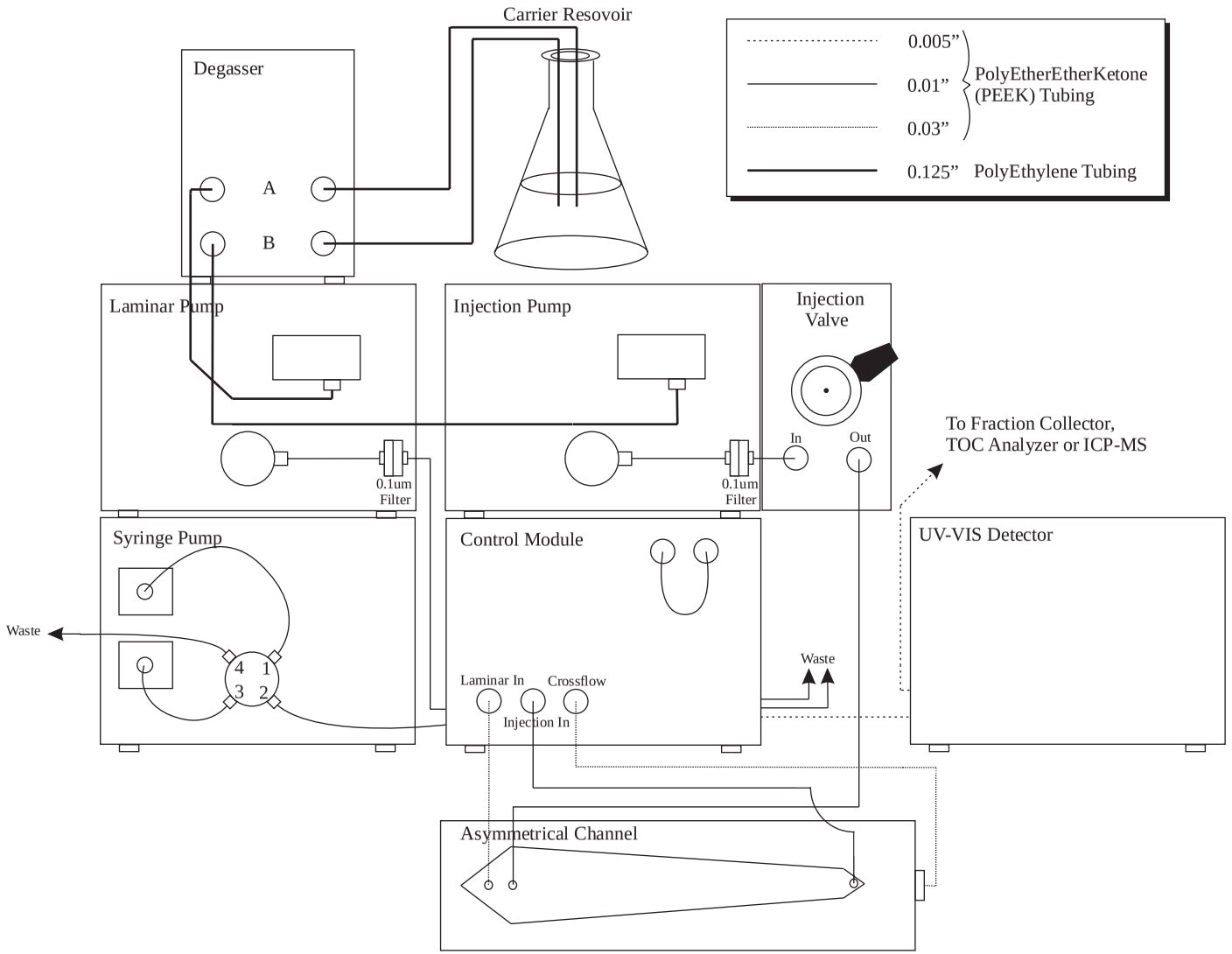

Appendix 1B - Map of King Site showing locations of piezometers. Topography from Harrington and Hendry (2006). Topographic intervals at 0.1 m.

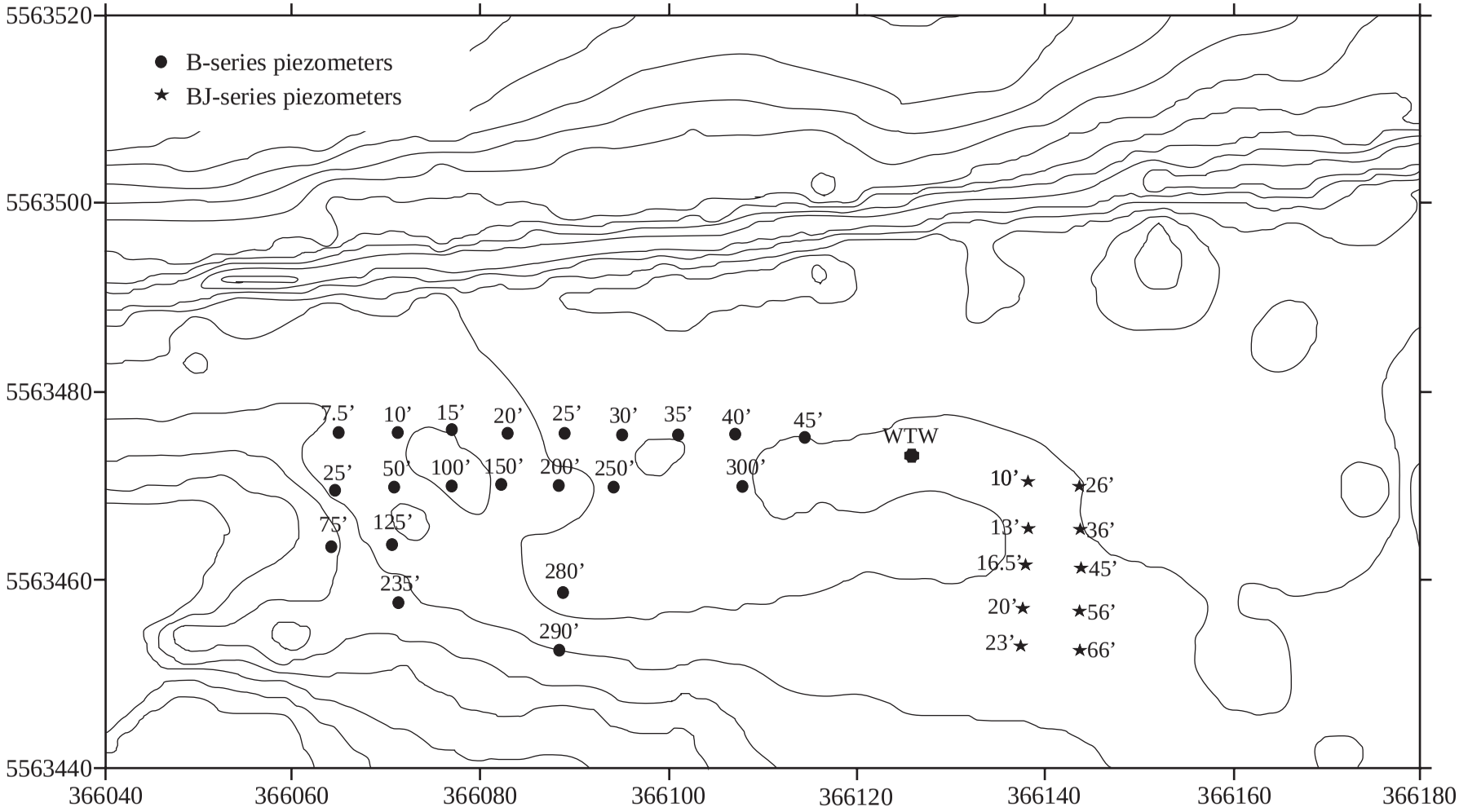

Appendix 1C - King Site Piezometer Details.

Piezometer	Total Depth (m)	Screen Length (m)	Middle of Sandpack (m)	Installation Date
B7.5	1.98	1.52	1.22	Oct-95
B10	2.98	1.52	2.22	Oct-95
WTW	3.20	3.05	1.60	Jul-96
B15	4.49	1.52	3.73	Oct-95
B20	6.02	1.52	5.26	Oct-95
B25	7.68	1.52	6.92	Oct-95
B25L	7.34	3.05	5.82	Oct-95
B30	9.13	1.52	8.37	Oct-95
B35	10.41	1.52	9.65	Oct-95
B40	11.91	1.52	11.15	Oct-95
B45	12.43	1.52	11.67	Oct-95
B50	16.45	3.05	14.93	Nov-95
B75	22.55	3.05	21.03	Nov-95
B100	30.41	3.05	28.89	Nov-95
B125	37.67	3.05	36.15	Nov-95
B150	44.38	3.05	42.86	Nov-95
B200	61.23	3.05	59.71	Nov-95
B235	69.64	3.05	68.12	Jul-96
B250	76.24	3.05	74.72	Nov-95
B280	84.25	3.05	82.73	Jul-96
B290	87.09	3.05	85.57	Jul-96
B300	91.14	3.05	89.62	Nov-95
BJ 10	3.07		3.00	
BJ 13	3.96		3.51	
BJ 16.5	4.99		4.53	
BJ 20	6.25		5.82	
BJ 23	7.01		6.68	
BJ 26	7.95		7.50	
BJ 36	11.07		10.64	
BJ 45	13.80		13.68	
BJ 56	17.08		17.62	
BJ 66	20.25		19.70	

Appendix 1D - Map of Warman Site showing locations of piezometers.

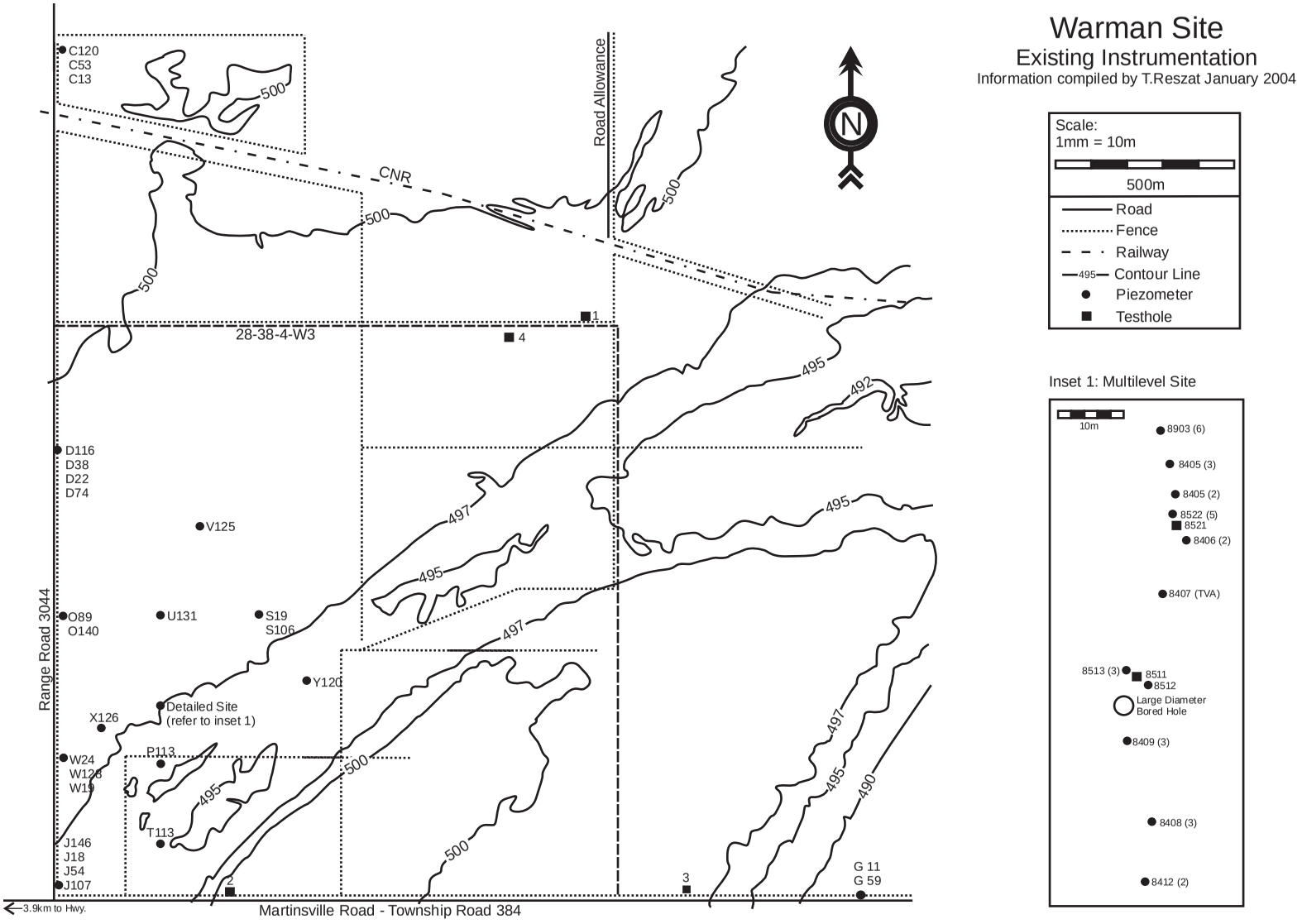

Appendix 1E - Warman Site Piezometer Details.

Piezometer	Total Depth (m)	Screen Length (m)	Middle of Sandpack (m)	Installation Date
C 13	3.96	0.61	3.66	Apr-77
C 25	10.67	0.61	10.37	Apr-77
C 53	16.15	0.61	15.85	Apr-77
D 22	6.71	0.61	6.41	Apr-77
D 38	11.58	0.61	11.28	Apr-77
D 74	22.56	0.61	22.26	Apr-77
D116	35.36	0.61	35.06	Apr-77
J 18	5.49	0.61	5.19	Apr-77
J 54	16.46	0.61	16.16	Apr-77
J107	32.61	0.61	32.31	Apr-77
J146	43.28	0.61	42.98	Apr-77
P113	34.44	0.61	34.14	Jul-77
S 19	5.79	0.61	5.49	Jul-77
S106	32.31	0.61	32.01	Jul-77
U131	39.93	0.61	39.63	Jul-77
W 19	5.79	0.61	5.49	Jul-77
W 24	7.32	0.61	7.02	Jul-77
W128	39.01	0.61	38.71	Jul-77
8405A	32.40	0.40	32.20	Oct-84
8405B	11.90	0.45	11.68	Oct-84
8406A	20.47	0.43	20.26	Oct-84
8406B	6.10	0.43	5.89	Oct-84
8407	77.77	0.50	77.52	Oct-84
8408A	44.02	0.43	43.81	Oct-84
8408B	35.03	0.44	34.81	Oct-84
8408C	6.33	0.44	6.11	Oct-84
8409A	29.98	0.54	29.71	Oct-84
8409B	19.96	0.43	19.75	Oct-84
8409C	5.89	0.43	5.68	Oct-84
8513A	11.02	0.25	10.90	Jun-85
8513B	8.57	0.30	8.42	Jun-85
8513C	6.32	0.29	6.18	Jun-85
8513D	4.18	0.30	4.03	Jun-85
8522A	14.87	0.38	14.68	Sep-85
8522B	12.18	0.37	12.00	Sep-85
8522C	9.21	0.40	9.01	Sep-85
8522D	6.15	0.36	5.97	Sep-85
8522E	4.19	0.35	4.02	Sep-85
8901A	28.50	0.10	28.45	Aug-89
8901B	25.36	0.10	25.31	Aug-89
8901C	22.10	0.10	22.05	Aug-89
8903A	18.84	0.10	18.79	Aug-89
8903B	16.31	0.10	16.26	Aug-89
8903C	13.87	0.10	13.82	Aug-89
8903D	11.40	0.10	11.35	Aug-89
8903E	8.99	0.10	8.94	Aug-89
8903F	7.19	0.10	7.14	Aug-89

Appendix 1F - Modifications to Sievers Turbo TOC

The Sievers Turbo TOC operates by UV-persulphate wet oxidation. Under stock operation influent solution was split into two sample streams, one for inorganic carbon (IC) detection and another for total carbon (TC) detection. The IC sample stream measured the equilibrium CO_2 present in the waters, and the TC stream added acid and oxidizer to the sample, digested all of the carbon in the system to CO_2 using UV oxidation and the resultant total CO_2 was measured. The total organic carbon (TOC) value was determined by subtracting the IC value from the TC value.

1. Initial Modifications

Modification to the system for on-line operation included removal of the entire IC stream from the detector. For the purpose of using the TOC analyzer as a DOC detector the IC value was not needed. Once DOC was separated from the ground water by the AsFlFFF system, the assumption was made that the majority of inorganic carbon (CO_2) was already excluded from the fraction of water which contained the DOC, therefore the TC number was representative of total organic carbon within the sample.

The second modification that was necessary for on-line use was to minimize any plumbing within the system to lessen the effect of peak spreading or band broadening through the TOC system. All of the plumbing in the TOC analyzer was replaced with inert small diameter (0.005” and 0.010” ID) PEEK tubing, with minimized flow lengths to lessen band broadening of the fractionated sample (discussed in detail later).

The input solution to the TOC analyzer (from the UV analyzer) was routed through a 4-way valve to order to route the UV effluent either into the TOC detector or a waste container when not the TOC detector was not in operation. The valve used for this purpose was from Upchurch Scientific (V·101D), rated to 500 PSI, with $1/16^{th}$ OD tubing with a 4 way diagonal flow and bulkhead mounting. See Figure 1 for a plumbing schematic of the valve.

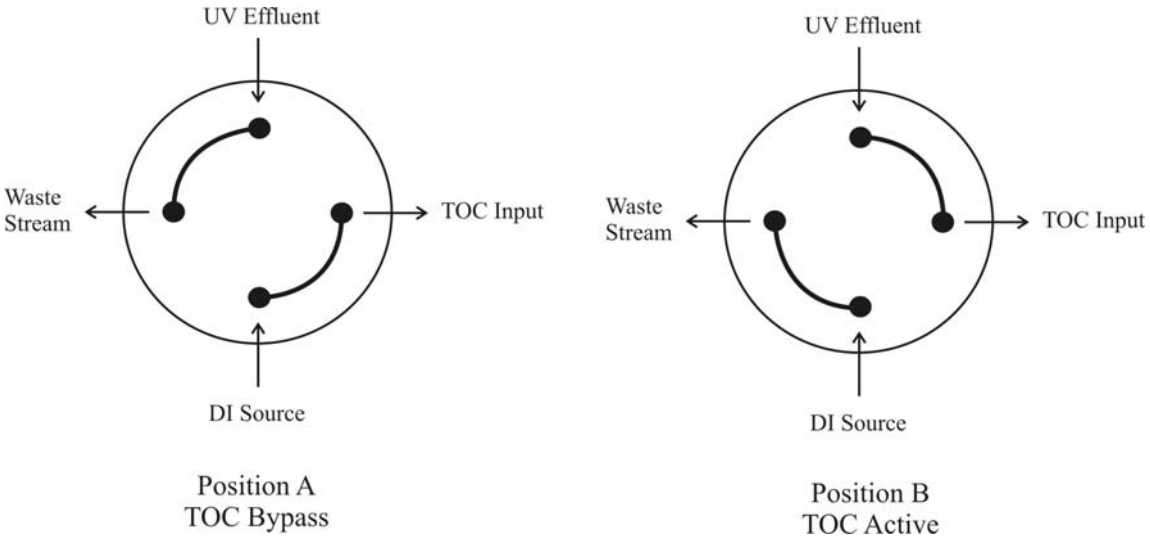

Figure 1: Upchurch Scientific 4-position switching valve setup. Position A is a bypass to run AsFlFFF system without TOC analyzer and Position B running the system with TOC active.

2. Continuous TOC Operation

The TOC instrument cannot be run dry without a flush solution because acid and persulphate are continuously being added to the sample stream. No fluid was being routed to the detectors during rinsing, elution and focusing stages of fractionation in the AsFlFFF, and as a result the TOC instrument needed to be switched on and off at the appropriate times so detection from the AsFlFFF could take place. The TOC instrument has a 230 second warm-up time, and also requires a flush solution during the warm-up period. A fluid flow time delay of approximately 60 seconds between the UV to the TOC detectors posed another problem in timing for instrument initialization and shut down. Due to these issues it was decided that the TOC detector could not be automatically turned on prior to each sample run, and turned off after. Several methods were investigated to automate the detector operation.

a. Manually switching the TOC detector on and off at the appropriate time, which is time consuming and prone to operator error.

b. Turning the TOC detector on/off via a remote signal from the AsFlFFF control module during elution start/stop. The AsFlFFF detector would need to send a TB (tb) and ↵ echo through a digital output cable to TOC detector. To turn off the

detector, a TE (te) and ↵ echo sent to TOC and the instrument would shut off. The RS 232 port on AsFlFFF and the TOC detector can be used for this, however, the AsFlFFF software would need to be formatted to send the signal at the appropriate time(s), and the warm-up time for the TOC detector was longer than most AsFlFFF sequences.

c. Another source of fluid could be sent to the TOC during the AsFlFFF injection, rinsing and focusing stages of operation, preferably de-ionized (DI) water.

The best solution was to route a continuously running fluid source through the detector at all times when sample elution was not occurring (including injection, rinsing and focusing, and times when the AsFlFFF was not running). This would enable the TOC detector to continuously operated without the problem of powering it up and switching it off between sample fractionations. A two way 8 position switching valve in the AsFlFFF control module was examined for possibilities in fluid routing to the TOC detector during injection and focusing. Providing a de-ionized water source to the TOC detector during the injection, rinsing and focusing stages of AsFlFFF operation was done by using a spare port (plug) on a switching valve. The internal Valco (VICI) switching valves in the AsFlFFF alter fluid routing in the channel and the whole AsFlFFF assembly.

The switching valve has two positions (Figure 2). Position A is the position of the valve during elution. Position B is the position of the valve during injection, rinsing and focusing. Under stock configuration of the AsFlFFF, no fluid was being fed to detection systems while in Position B. A source of fluid (DI) was routed through Port 4 on the switching valve. Replacing the plug in this position with a tube (0.010” ID PEEK) provided fluid to the detectors during injection, rinsing, and focusing, and as a result the TOC detector (and UV detector) was provided fluid during all stage of the AsFlFFF run (channel effluent in Position A, and DI during Position B). When the AsFlFFF run changes to elution the switching valve routes DI into the waste container (Position B, hole 5). This gives the TOC time to initialize and warm up before AsFlFFF elution.

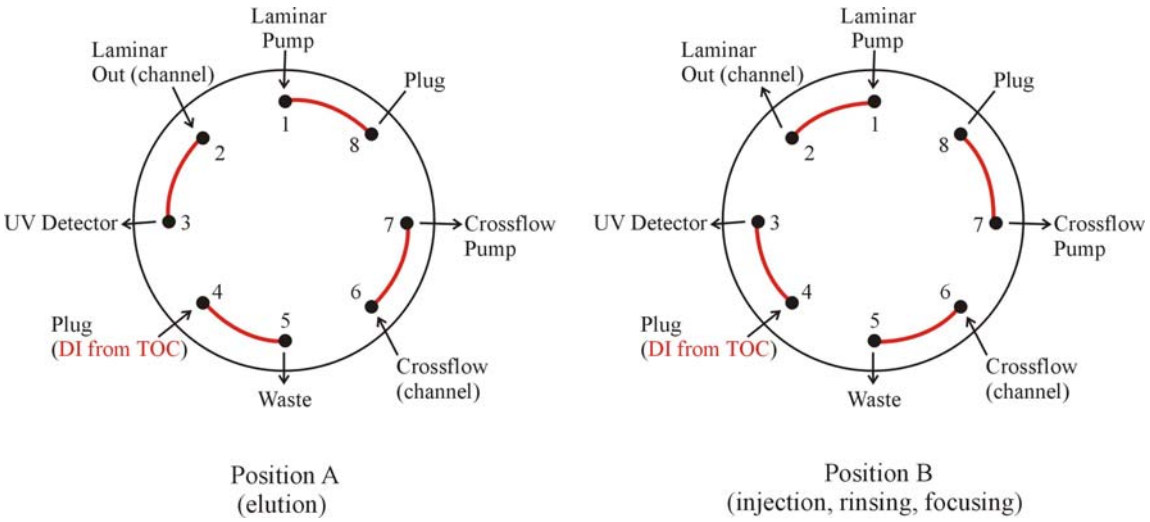

Figure 2: VICI (Valco) 2 Stage 8 Position valve modifications for running of TOC detector. Position A is elution in AsFlFFF and pPosition B is all other FFF operations.

A pump was necessary to route DI to Port 4 on the switching valve. The TOC detector contains a two position peristaltic pump, which operates whenever the instrument needs fluid (Figure 3). As described earlier, the IC line had been removed from the TOC analyzer and therefore one position on the peristaltic pump was available and had the correct flow rate for optimal detector operation.

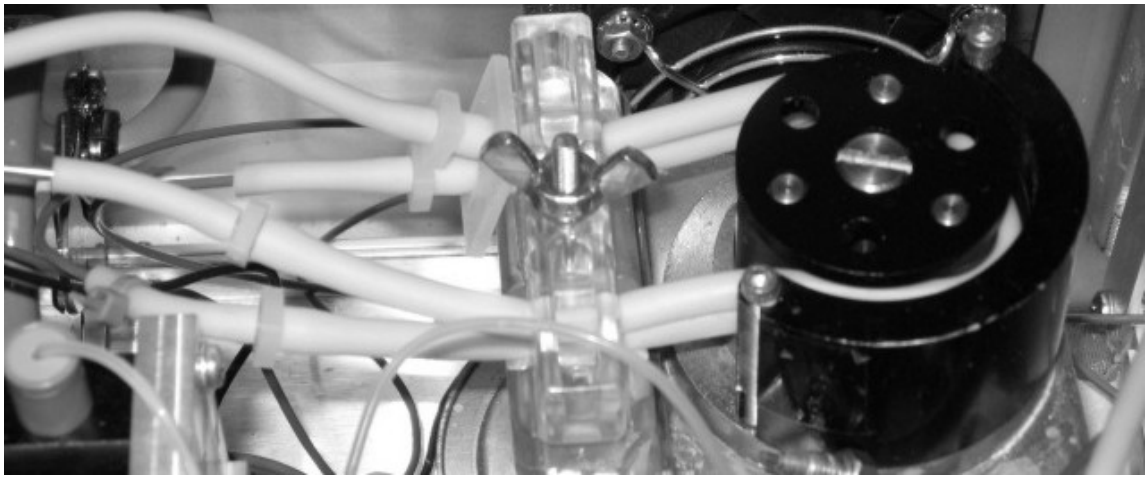

Figure 3 - Two position peristaltic pump in the TOC detector. Lower position was available due to removal of IC line in the detector.

A PEEK tube was run from a DI source container into the TOC analyzer, then through the empty position on the peristaltic pump. This then routed DI through another PEEK tube to Port 4 in the VICI valve in the AsFlFFF control module. The fluid flow rate of this peristaltic pump with the present tubing is 0.97 mL min^{-1}, which is optimal for the TOC detector operation. There are several benefits seen by using the TOC peristaltic; 1) the peristaltic pump is only running when the TOC is on, therefore eliminating the extra task of powering the detector on and off, and the pump is only running when it is needed, 2) no extra pump needs to be purchased and flow rates are always ideal for a TOC feed line, and 3) de-ionized water which is used keeps the tubing in detectors clean and flushed of salts from the carrier solution, which build up with use.

3. Inorganic Carbon Removal

A high inorganic carbon concentration in the carrier solution and/or sample will give a high baseline to the TOC signal and as a result proper peak definition of fractionated DOC samples will not be obtained. Many of the groundwaters examined have a high inorganic carbon content therefore this needed to be remedied. To counteract this, an Inorganic Carbon Removal (ICR) module was placed in line between the acid and persulphate addition and UV reactor in the TOC detector. The ICR uses a vacuum degassing technique to remove CO_2 from the sample. Figure 4 shows a schematic for the tubing routing of the analyzer. The ICR module in this figure is not modified and is in stock configuration.

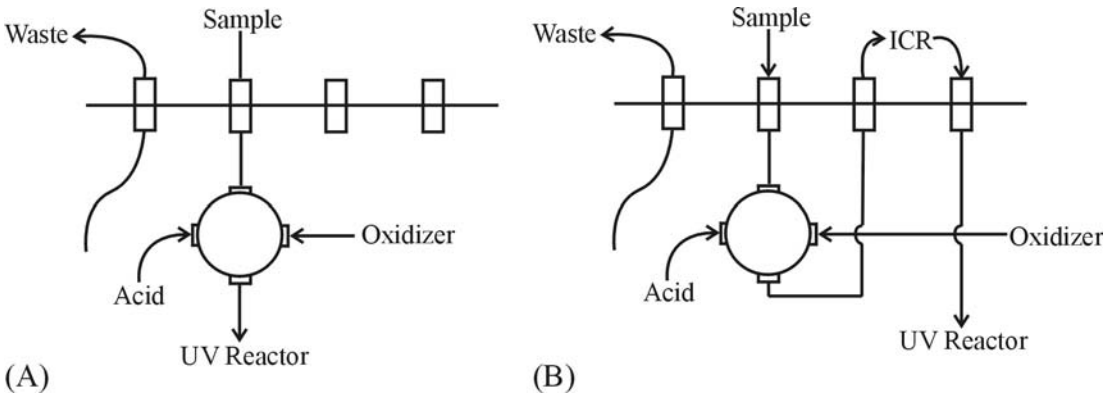

Figure 4: TOC detector tube routing with (B) and without (A) inorganic carbon removal (ICR) module.

Figure 5 shows modifications to the ICR module to eliminate some of the band broadening and sample delay time that the use ICR module presents. The Hollow Fiber Module from the ICR was removed and placed into the TOC enclosure. This results in tubing to and from the ICR being much shorter than in the stock configuration. In addition, when the ICR is on bypass mode the tubing lengths are the same as if the ICR were not present. The vacuum hose and the tube from the chemical trap were extended from the ICR module into the TOC enclosure in order for proper operation.

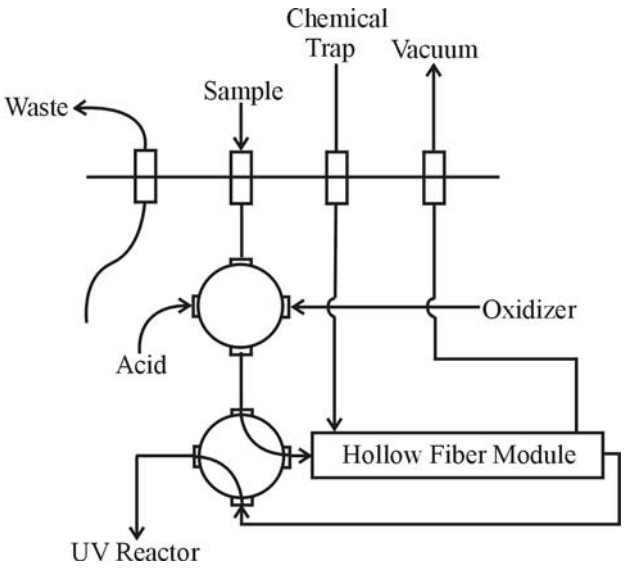

Figure 5: TOC detector tube routing and placement of Hollow Fiber Module inside TOC enclosure. Modifications to ICR Module are outlined.

4. Data Collection

To run the TOC detector system on-line with the AsFlFFF system, it was convenient to have the detector signal transferred to the AsFlFFF software for concurrent data analysis with UV detector signals. This was achieved connecting the TOC detector to the AsFlFFF control module via an analogue out board (0-1 volt or 0-10 volt). Two wires connected to the analog output board on TOC detector writing the output as TC values detected by the TOC analyzer. The output boards for the TOC detector can be seen in Figure 6. The cable connector for the AsFlFFF control module is also shown in the figure. This analogue output is connected into the Detector “1” port on the AsFlFFF control module. The AsFlFFF control module and software has room for

the connection of 3 analogue detector signals. The stock UV detector is “Detector 0”. Detector 1 (the TOC analyzer) is set up to read at ±2.50 volts in the AsFlFFF software.

The analogue output range of the TOC detector was set from 0 – 10,000 ppb C, however this can be easily changed if the DOC concentrations in the samples are too high or low for this signal range. Output values are displayed on the TOC output LCD screen. These are arbitrary TOC values, which are TC – IC, however values sent to the AsFlFFF software and recorded are the Total Carbon (TC) values, which are the ‘real’ results. The IC channel is not connected to the sample stream and read low or zero values.

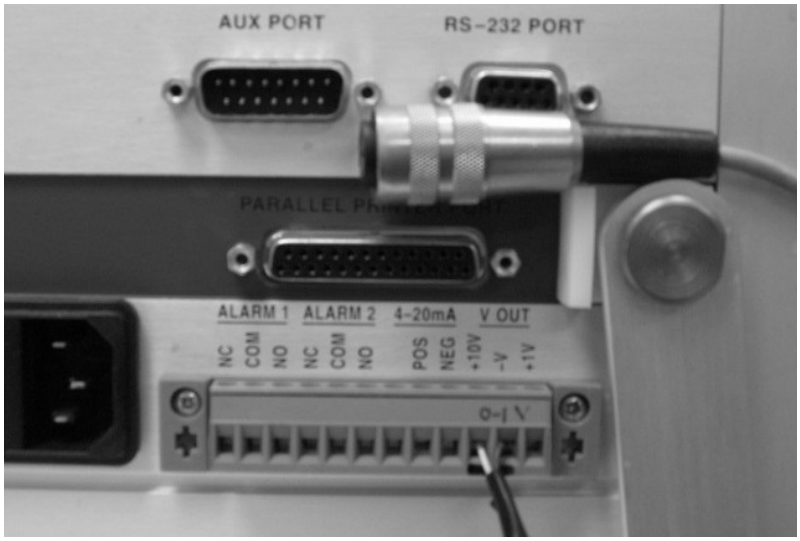

Figure 6: Analogue and digital control communications boards on the TOC detector.

5. Band Broadening

The extra flow lengths between the UV and TOC detection signal, including the void volume in several switching valves and tubing connectors had the potential to create some smearing of the DOC peak (band broadening). To test whether the modifications to the detector eliminated or reduced the amount of band broadening that occurs the width of several poly(styrene) sulphonate (PSS) polymer peaks were compared. The PSS peaks have an identical carbon structure throughout their peak distribution (Figure 7), therefore an identical peak shape should been seen by both the

UV and DOC detection systems. Any differences in peak width between detectors can be attributed to band broadening, and if this exists, could be corrected in subsequent unknown samples. Results from the PSS 4500 polymer are shown in Figure 8. The difference between these peaks is minimal, and band broadening was deemed to not be a concern, so no corrections to the TOC output signal needed to be made.

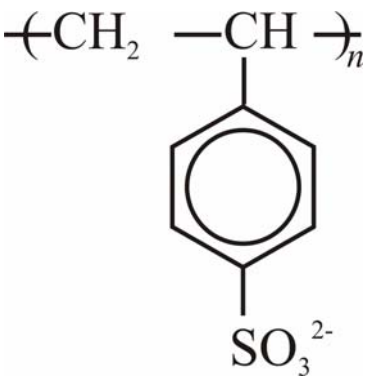

Figure 7: Poly(strene sulphonate) unit cell, which is repeated throughout the polyelectrolyte chain.

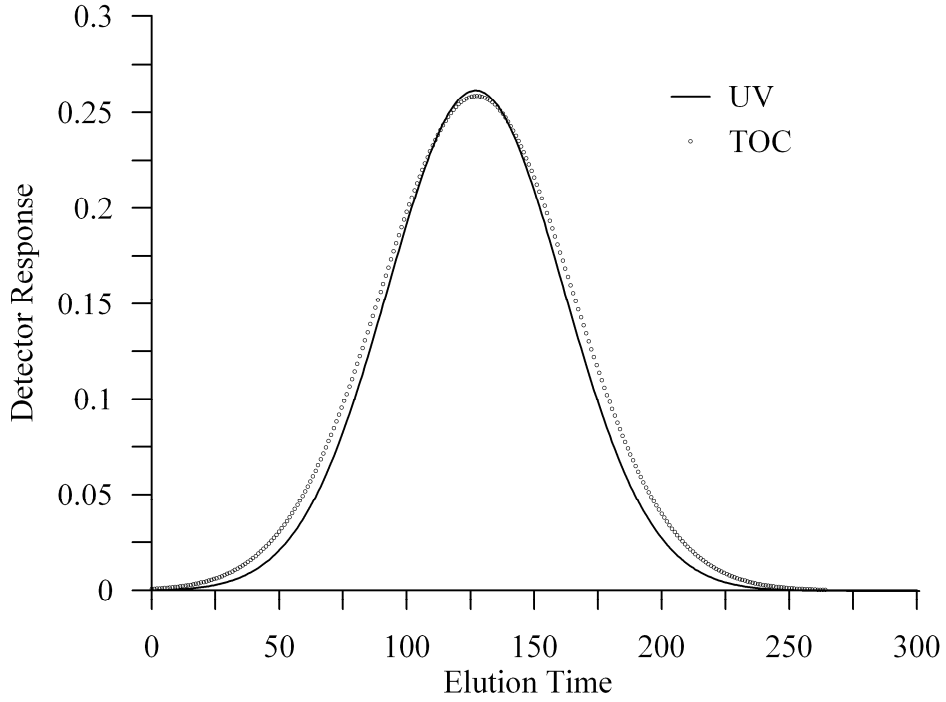

Figure 8: Comparison of UV and TOC responses for poly(styrene) sulphonate polymer, showing minimal band broadening from UV to TOC detector.

Appendix 1G – AsFlFFF system connection to Micromass ICP-MS

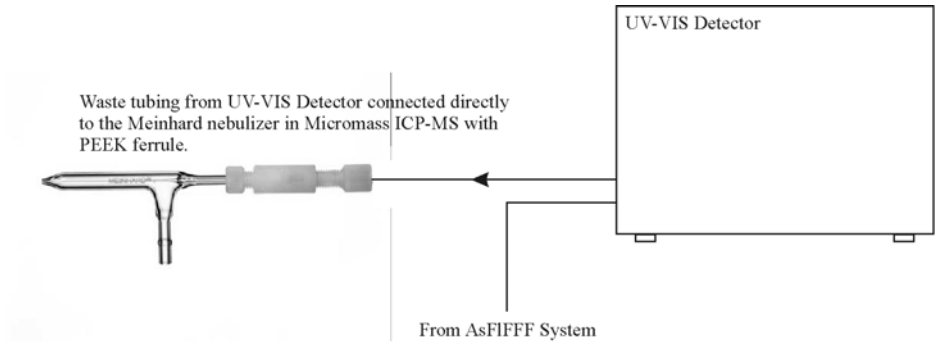

Exploded view of ferrule and tubing connection to nebulizer.

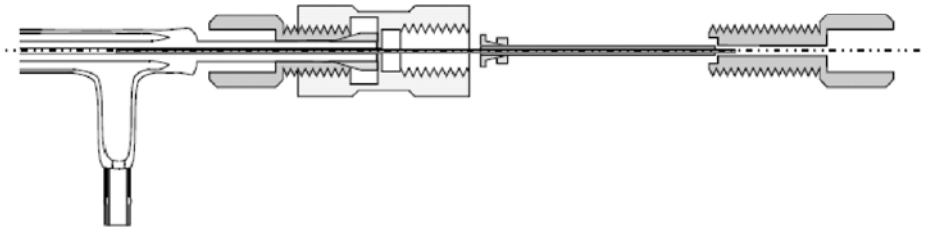

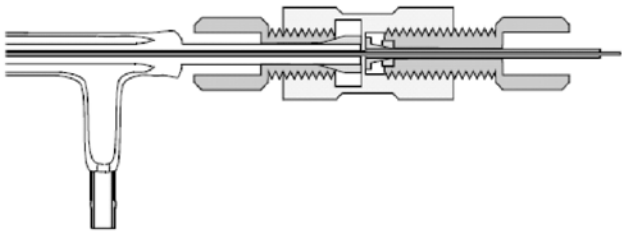

APPENDIX 2 Supplementary data for Chapter 2.

Appendix 2A – UV detector fractograms for King Site ground waters.

Appendix 2B – DOC detector fractograms for King Site ground waters.

Appendix 2C – UV detector fractograms for King Site ground waters (BJ series).

Appendix 2D – DOC detector fractograms for King Site ground waters (BJ series).

Appendix 2E – DOC and UV detector fractograms for surface water samples.

Appendix 2F – DOC and UV detector fractograms for PSS 1430 dalton polymer.

Appendix 2G – UV detector fractograms for Suwannee River humic standards.

Appendix 2H – DOC detector fractograms for Suwannee River humic standards.

Appendix 2I – Data used for calculation of Continuous NIC analysis.

Appendix 2J – NIC and $SUVA_{254}$ vs. depth for all King Site piezometers.

Appendix 2K – Startup procedure for AsFlFFF-UV-TOC system.

Appendix 2A - UV Detector (254 nm) fractograms for King Site Groundwaters. Results of molecular weight calculations at end of table.

Time sec.	MW daltons	B10	B15	B20	B25	B30	B35	B40
0	0	-0.0035	0.0053	-0.0017	-0.0013	-0.0034	-0.0009	-0.0046
1	0	-0.0035	0.0053	-0.0017	-0.0013	-0.0034	-0.0009	-0.0046
2	2	-0.0036	0.0053	-0.0017	-0.0013	-0.0034	-0.0009	-0.0046
3	3	-0.0036	0.0053	-0.0017	-0.0013	-0.0034	-0.0009	-0.0046
4	6	-0.0037	0.0053	-0.0017	-0.0013	-0.0034	-0.0009	-0.0046
5	9	-0.0037	0.0053	-0.0017	-0.0013	-0.0034	-0.0009	-0.0046
6	13	-0.0038	0.0053	-0.0017	-0.0013	-0.0034	-0.0009	-0.0046
7	17	-0.0038	0.0053	-0.0017	-0.0013	-0.0034	-0.0009	-0.0046
8	22	-0.0039	0.0053	-0.0017	-0.0013	-0.0034	-0.0009	-0.0046
9	28	-0.0039	0.0053	-0.0017	-0.0013	-0.0034	-0.0009	-0.0046
10	34	-0.0040	0.0053	-0.0017	-0.0013	-0.0034	-0.0009	-0.0046
11	41	-0.0040	0.0053	-0.0017	-0.0013	-0.0034	-0.0009	-0.0046
12	48	-0.0041	0.0053	-0.0017	-0.0013	-0.0034	-0.0009	-0.0046
13	56	-0.0041	0.0053	-0.0017	-0.0013	-0.0034	-0.0009	-0.0046
14	65	-0.0042	0.0053	-0.0017	-0.0013	-0.0034	-0.0009	-0.0046
15	74	-0.0082	0.0053	-0.0017	-0.0013	-0.0034	-0.0009	-0.0046
16	84	0.0518	0.0053	-0.0017	-0.0013	-0.0034	-0.0009	-0.0046
17	94	0.1656	0.0621	0.0190	0.0234	-0.0034	-0.0008	-0.0046
18	105	0.2501	0.1091	0.0387	0.0449	0.0062	0.0097	-0.0046
19	117	0.2903	0.1335	0.0484	0.0563	0.0174	0.0177	-0.0046
20	129	0.3012	0.1427	0.0520	0.0604	0.0252	0.0234	-0.0046
21	141	0.2987	0.1435	0.0533	0.0618	0.0310	0.0261	-0.0043
22	155	0.2913	0.1415	0.0539	0.0625	0.0330	0.0286	-0.0031
23	168	0.2812	0.1386	0.0545	0.0629	0.0348	0.0305	-0.0017
24	183	0.2704	0.1350	0.0549	0.0630	0.0369	0.0330	0.0009
25	198	0.2581	0.1308	0.0547	0.0627	0.0383	0.0335	0.0031
26	213	0.2452	0.1261	0.0539	0.0618	0.0393	0.0329	0.0048
27	229	0.2322	0.1206	0.0529	0.0606	0.0398	0.0329	0.0062
28	246	0.2194	0.1151	0.0517	0.0589	0.0398	0.0324	0.0071
29	263	0.2069	0.1094	0.0502	0.0574	0.0393	0.0317	0.0079
30	280	0.1953	0.1036	0.0485	0.0546	0.0380	0.0305	0.0083
31	299	0.1834	0.0985	0.0465	0.0523	0.0362	0.0290	0.0085
32	317	0.1723	0.0930	0.0446	0.0505	0.0343	0.0273	0.0084
33	337	0.1624	0.0881	0.0425	0.0473	0.0324	0.0261	0.0082
34	356	0.1538	0.0834	0.0406	0.0451	0.0306	0.0249	0.0079
35	377	0.1470	0.0798	0.0390	0.0429	0.0292	0.0236	0.0076
36	398	0.1407	0.0766	0.0375	0.0411	0.0279	0.0221	0.0072
37	419	0.1356	0.0743	0.0363	0.0396	0.0266	0.0215	0.0069
38	441	0.1320	0.0724	0.0355	0.0388	0.0252	0.0207	0.0065
39	464	0.1296	0.0712	0.0351	0.0378	0.0242	0.0200	0.0063
40	487	0.1283	0.0706	0.0348	0.0373	0.0241	0.0194	0.0061
41	510	0.1280	0.0704	0.0347	0.0370	0.0240	0.0191	0.0060
42	535	0.1285	0.0708	0.0348	0.0370	0.0233	0.0192	0.0059
43	559	0.1297	0.0713	0.0351	0.0372	0.0229	0.0192	0.0059
44	585	0.1315	0.0723	0.0356	0.0374	0.0229	0.0192	0.0059
45	610	0.1337	0.0735	0.0361	0.0378	0.0230	0.0197	0.0060
46	637	0.1366	0.0751	0.0367	0.0384	0.0235	0.0198	0.0060

Appendix 2A - Continued

47	663	0.1400	0.0767	0.0375	0.0390	0.0240	0.0200	0.0062
48	691	0.1437	0.0787	0.0385	0.0398	0.0244	0.0203	0.0063
49	719	0.1475	0.0807	0.0394	0.0406	0.0247	0.0206	0.0065
50	747	0.1515	0.0830	0.0407	0.0415	0.0250	0.0210	0.0066
51	776	0.1556	0.0853	0.0418	0.0424	0.0253	0.0214	0.0069
52	805	0.1602	0.0877	0.0430	0.0433	0.0258	0.0219	0.0070
53	835	0.1647	0.0900	0.0443	0.0444	0.0265	0.0223	0.0071
54	866	0.1691	0.0923	0.0454	0.0453	0.0274	0.0230	0.0073
55	897	0.1733	0.0945	0.0464	0.0462	0.0295	0.0235	0.0074
56	929	0.1774	0.0964	0.0475	0.0472	0.0298	0.0241	0.0074
57	961	0.1810	0.0984	0.0485	0.0480	0.0302	0.0248	0.0075
58	993	0.1844	0.1003	0.0496	0.0487	0.0303	0.0253	0.0076
59	1026	0.1871	0.1020	0.0504	0.0493	0.0310	0.0257	0.0077
60	1060	0.1894	0.1032	0.0511	0.0499	0.0316	0.0262	0.0078
61	1094	0.1908	0.1041	0.0517	0.0504	0.0320	0.0266	0.0079
62	1129	0.1916	0.1048	0.0522	0.0506	0.0324	0.0296	0.0079
63	1164	0.1917	0.1050	0.0526	0.0506	0.0327	0.0302	0.0080
64	1200	0.1910	0.1049	0.0528	0.0506	0.0330	0.0302	0.0080
65	1236	0.1896	0.1044	0.0528	0.0503	0.0332	0.0303	0.0081
66	1273	0.1874	0.1034	0.0526	0.0500	0.0338	0.0299	0.0081
67	1310	0.1843	0.1021	0.0523	0.0495	0.0338	0.0296	0.0080
68	1348	0.1805	0.1004	0.0517	0.0488	0.0339	0.0295	0.0080
69	1386	0.1759	0.0983	0.0510	0.0479	0.0339	0.0293	0.0079
70	1425	0.1710	0.0959	0.0500	0.0469	0.0338	0.0291	0.0078
71	1464	0.1659	0.0931	0.0489	0.0459	0.0336	0.0289	0.0077
72	1504	0.1600	0.0900	0.0477	0.0445	0.0334	0.0285	0.0076
73	1544	0.1534	0.0868	0.0463	0.0435	0.0331	0.0282	0.0074
74	1585	0.1467	0.0835	0.0448	0.0422	0.0325	0.0275	0.0073
75	1626	0.1402	0.0801	0.0433	0.0398	0.0319	0.0270	0.0071
76	1668	0.1329	0.0765	0.0415	0.0383	0.0311	0.0262	0.0068
77	1711	0.1257	0.0728	0.0397	0.0367	0.0304	0.0253	0.0065
78	1754	0.1188	0.0689	0.0377	0.0349	0.0295	0.0249	0.0061
79	1797	0.1116	0.0652	0.0359	0.0332	0.0286	0.0239	0.0058
80	1841	0.1046	0.0617	0.0340	0.0315	0.0277	0.0229	0.0055
81	1885	0.0981	0.0583	0.0322	0.0301	0.0268	0.0218	0.0052
82	1930	0.0916	0.0548	0.0304	0.0283	0.0257	0.0208	0.0049
83	1976	0.0856	0.0515	0.0286	0.0270	0.0245	0.0198	0.0047
84	2022	0.0797	0.0481	0.0268	0.0261	0.0232	0.0187	0.0045
85	2068	0.0740	0.0453	0.0251	0.0235	0.0220	0.0176	0.0043
86	2115	0.0682	0.0424	0.0235	0.0225	0.0207	0.0166	0.0041
87	2162	0.0633	0.0393	0.0219	0.0206	0.0196	0.0155	0.0039
88	2210	0.0583	0.0369	0.0204	0.0192	0.0186	0.0146	0.0038
89	2259	0.0541	0.0342	0.0189	0.0180	0.0177	0.0137	0.0037
90	2308	0.0497	0.0318	0.0175	0.0168	0.0165	0.0130	0.0036
91	2357	0.0462	0.0296	0.0163	0.0158	0.0153	0.0122	0.0034
92	2407	0.0426	0.0275	0.0152	0.0146	0.0141	0.0114	0.0033
93	2458	0.0393	0.0255	0.0140	0.0138	0.0131	0.0108	0.0030
94	2508	0.0362	0.0236	0.0129	0.0126	0.0121	0.0100	0.0038
95	2560	0.0334	0.0222	0.0120	0.0117	0.0112	0.0093	0.0033
96	2612	0.0308	0.0206	0.0110	0.0112	0.0103	0.0086	0.0029
97	2664	0.0286	0.0192	0.0102	0.0102	0.0101	0.0080	0.0027

Appendix 2A - Continued

98	2717	0.0264	0.0179	0.0094	0.0097	0.0092	0.0076	0.0025
99	2771	0.0244	0.0168	0.0086	0.0091	0.0084	0.0069	0.0023
100	2825	0.0226	0.0157	0.0079	0.0085	0.0076	0.0064	0.0022
101	2879	0.0208	0.0147	0.0073	0.0082	0.0069	0.0059	0.0021
102	2934	0.0193	0.0136	0.0067	0.0079	0.0063	0.0053	0.0020
103	2990	0.0180	0.0126	0.0062	0.0070	0.0058	0.0048	0.0019
104	3045	0.0168	0.0118	0.0058	0.0068	0.0051	0.0044	0.0018
105	3102	0.0157	0.0110	0.0054	0.0066	0.0045	0.0039	0.0017
106	3159	0.0147	0.0103	0.0050	0.0059	0.0042	0.0036	0.0015
107	3216	0.0139	0.0096	0.0047	0.0056	0.0038	0.0033	0.0014
108	3274	0.0130	0.0091	0.0043	0.0053	0.0035	0.0031	0.0013
109	3333	0.0122	0.0086	0.0040	0.0050	0.0032	0.0030	0.0012
110	3392	0.0115	0.0080	0.0037	0.0047	0.0029	0.0027	0.0012
111	3451	0.0108	0.0076	0.0034	0.0045	0.0026	0.0025	0.0011
112	3511	0.0103	0.0071	0.0032	0.0043	0.0024	0.0023	0.0010
113	3571	0.0099	0.0066	0.0030	0.0040	0.0022	0.0021	0.0009
114	3632	0.0095	0.0063	0.0028	0.0039	0.0021	0.0018	0.0008
115	3694	0.0091	0.0060	0.0026	0.0036	0.0020	0.0017	0.0008
116	3755	0.0087	0.0057	0.0024	0.0035	0.0018	0.0015	0.0007
117	3818	0.0085	0.0055	0.0022	0.0032	0.0017	0.0013	0.0007
118	3881	0.0082	0.0053	0.0021	0.0031	0.0016	0.0012	0.0007
119	3944	0.0080	0.0051	0.0021	0.0031	0.0016	0.0010	0.0006
120	4008	0.0077	0.0048	0.0020	0.0031	0.0015	0.0008	0.0006
121	4072	0.0075	0.0046	0.0021	0.0029	0.0014	0.0007	0.0006
122	4137	0.0072	0.0044	0.0021	0.0028	0.0013	0.0006	0.0006
123	4202	0.0070	0.0043	0.0020	0.0026	0.0012	0.0006	0.0006
124	4268	0.0068	0.0041	0.0019	0.0025	0.0010	0.0006	0.0006
125	4334	0.0066	0.0038	0.0019	0.0024	0.0009	0.0006	0.0005
126	4401	0.0064	0.0037	0.0018	0.0024	0.0007	0.0007	0.0004
127	4468	0.0063	0.0035	0.0017	0.0023	0.0006	0.0008	0.0004
128	4536	0.0060	0.0033	0.0017	0.0022	0.0005	0.0008	0.0003
129	4604	0.0059	0.0031	0.0016	0.0022	0.0004	0.0009	0.0003
130	4673	0.0057	0.0031	0.0015	0.0022	0.0003	0.0010	0.0003
131	4742	0.0055	0.0030	0.0014	0.0021	0.0002	0.0011	0.0003
132	4812	0.0053	0.0029	0.0013	0.0021	0.0002	0.0012	0.0003
133	4882	0.0052	0.0028	0.0012	0.0020	0.0001	0.0012	0.0004
134	4953	0.0051	0.0026	0.0012	0.0019	0.0000	0.0012	0.0005
135	5024	0.0050	0.0025	0.0013	0.0018	0.0000	0.0012	0.0006
136	5096	0.0048	0.0024	0.0013	0.0017	0.0000	0.0013	0.0007
137	5168	0.0047	0.0023	0.0012	0.0016	0.0000	0.0012	0.0007
138	5240	0.0047	0.0022	0.0012	0.0015	0.0000	0.0012	0.0007
139	5314	0.0047	0.0022	0.0011	0.0015	0.0000	0.0012	0.0008
140	5387	0.0046	0.0021	0.0009	0.0015	0.0000	0.0011	0.0008
141	5461	0.0045	0.0020	0.0008	0.0016	0.0000	0.0010	0.0008
142	5536	0.0041	0.0018	0.0007	0.0016	-0.0001	0.0009	0.0008
143	5611	0.0039	0.0018	0.0008	0.0016	0.0000	0.0008	0.0008
144	5686	0.0036	0.0018	0.0007	0.0016	-0.0001	0.0008	0.0007
145	5762	0.0035	0.0018	0.0007	0.0015	-0.0001	0.0007	0.0006
146	5839	0.0035	0.0018	0.0007	0.0015	0.0001	0.0007	0.0005
147	5916	0.0035	0.0018	0.0007	0.0015	0.0001	0.0008	0.0005
148	5993	0.0034	0.0018	0.0006	0.0015	0.0001	0.0008	0.0004

Appendix 2A - Continued

149	6071	0.0033	0.0018	0.0007	0.0015	0.0001	0.0007	0.0003
150	6150	0.0032	0.0018	0.0007	0.0015	0.0001	0.0007	0.0003
151	6229	0.0031	0.0018	0.0007	0.0015	0.0000	0.0006	0.0003
152	6308	0.0030	0.0019	0.0006	0.0015	0.0000	0.0006	0.0004
153	6388	0.0028	0.0019	0.0006	0.0015	0.0000	0.0005	0.0004
154	6468	0.0027	0.0018	0.0006	0.0015	-0.0001	0.0005	0.0004
155	6549	0.0026	0.0018	0.0006	0.0014	-0.0001	0.0004	0.0004
156	6630	0.0024	0.0017	0.0007	0.0014	-0.0001	0.0005	0.0005
157	6712	0.0023	0.0017	0.0008	0.0014	0.0000	0.0005	0.0006
158	6794	0.0024	0.0017	0.0008	0.0015	0.0001	0.0006	0.0006
159	6877	0.0024	0.0017	0.0007	0.0015	0.0000	0.0007	0.0006
160	6960	0.0024	0.0017	0.0008	0.0015	-0.0001	0.0007	0.0006
161	7044	0.0023	0.0016	0.0008	0.0015	-0.0001	0.0007	0.0006
162	7128	0.0023	0.0015	0.0008	0.0014	-0.0001	0.0007	0.0005
163	7213	0.0023	0.0015	0.0008	0.0015	0.0000	0.0007	0.0006
164	7298	0.0025	0.0015	0.0008	0.0014	0.0000	0.0008	0.0006
165	7384	0.0025	0.0015	0.0008	0.0014	-0.0001	0.0009	0.0006
166	7470	0.0024	0.0015	0.0007	0.0014	-0.0001	0.0010	0.0006
167	7556	0.0025	0.0014	0.0006	0.0013	-0.0001	0.0016	0.0006
168	7644	0.0025	0.0013	0.0006	0.0013	-0.0002	0.0018	0.0013
169	7731	0.0025	0.0012	0.0006	0.0013	-0.0003	0.0019	0.0011
170	7819	0.0025	0.0011	0.0004	0.0013	-0.0003	0.0017	0.0009
171	7908	0.0025	0.0010	0.0004	0.0013	-0.0003	0.0017	0.0008
172	7997	0.0025	0.0009	0.0004	0.0013	-0.0003	0.0017	0.0008
173	8086	0.0025	0.0010	0.0004	0.0013	-0.0004	0.0018	0.0007
174	8176	0.0023	0.0010	0.0003	0.0011	-0.0004	0.0019	0.0008
175	8266	0.0023	0.0009	0.0003	0.0012	-0.0005	0.0020	0.0010
176	8357	0.0021	0.0009	0.0002	0.0011	-0.0004	0.0020	0.0011
177	8449	0.0020	0.0009	0.0003	0.0010	-0.0005	0.0020	0.0009
178	8540	0.0020	0.0008	0.0003	0.0010	-0.0004	0.0020	0.0008
179	8633	0.0020	0.0008	0.0003	0.0010	-0.0004	0.0020	0.0008
180	8725	0.0018	0.0008	0.0003	0.0010	-0.0004	0.0019	0.0008
181	8819	0.0017	0.0008	0.0003	0.0010	-0.0004	0.0019	0.0008
182	8912	0.0017	0.0006	0.0004	0.0010	-0.0002	0.0018	0.0008
183	9007	0.0017	0.0006	0.0004	0.0010	-0.0002	0.0018	0.0009
184	9101	0.0018	0.0006	0.0004	0.0010	0.0000	0.0018	0.0009
185	9196	0.0018	0.0007	0.0003	0.0009	0.0001	0.0018	0.0009
186	9292	0.0017	0.0007	0.0004	0.0007	0.0001	0.0018	0.0009
187	9388	0.0016	0.0007	0.0004	0.0007	0.0001	0.0018	0.0009
188	9485	0.0016	0.0009	0.0003	0.0006	0.0001	0.0018	0.0009
189	9582	0.0017	0.0011	0.0002	0.0005	0.0004	0.0017	0.0007
190	9679	0.0017	0.0010	0.0002	0.0005	0.0004	0.0017	0.0007
191	9777	0.0016	0.0011	0.0002	0.0005	0.0004	0.0017	0.0007
192	9876	0.0017	0.0010	0.0002	0.0006	0.0003	0.0017	0.0006
193	9975	0.0016	0.0009	0.0001	0.0006	0.0003	0.0017	0.0005
194	10074	0.0016	0.0009	0.0000	0.0007	0.0003	0.0018	0.0004
195	10174	0.0015	0.0010	0.0000	0.0007	0.0002	0.0018	0.0003
196	10274	0.0015	0.0010	-0.0001	0.0008	0.0002	0.0019	0.0002
197	10375	0.0015	0.0009	-0.0001	0.0008	0.0001	0.0019	0.0001
198	10476	0.0014	0.0008	0.0000	0.0007	0.0001	0.0019	0.0001
199	10578	0.0014	0.0008	0.0000	0.0006	0.0000	0.0020	0.0000

Appendix 2A - Continued

200	10680	0.0014	0.0007	-0.0001	0.0006	0.0001	0.0020	0.0000
201	10783	0.0014	0.0006	-0.0001	0.0006	0.0001	0.0019	0.0000
202	10886	0.0013	0.0007	-0.0001	0.0005	0.0001	0.0019	0.0000
203	10990	0.0013	0.0007	-0.0001	0.0005	0.0002	0.0017	0.0001
204	11094	0.0013	0.0006	-0.0001	0.0005	0.0002	0.0017	0.0001
205	11199	0.0013	0.0005	-0.0001	0.0005	0.0001	0.0016	0.0001
206	11304	0.0012	0.0005	0.0000	0.0006	0.0001	0.0016	0.0001
207	11409	0.0013	0.0003	-0.0001	0.0006	0.0001	0.0015	0.0001
208	11515	0.0012	0.0003	-0.0001	0.0006	0.0000	0.0015	0.0001
209	11622	0.0011	0.0004	-0.0001	0.0005	0.0000	0.0015	0.0003
210	11729	0.0011	0.0003	0.0000	0.0004	-0.0001	0.0014	0.0001
211	11836	0.0012	0.0002	-0.0001	0.0005	-0.0001	0.0014	0.0001
212	11944	0.0012	0.0002	-0.0002	0.0005	-0.0001	0.0014	0.0001
213	12052	0.0012	0.0002	-0.0002	0.0005	-0.0002	0.0014	0.0001
214	12161	0.0012	0.0002	-0.0002	0.0006	-0.0002	0.0015	0.0000
215	12270	0.0012	0.0001	-0.0003	0.0006	-0.0003	0.0014	0.0000
216	12380	0.0011	0.0002	-0.0003	0.0005	-0.0002	0.0013	0.0000
217	12490	0.0011	0.0003	-0.0003	0.0006	0.0002	0.0012	0.0000
218	12601	0.0010	0.0003	-0.0003	0.0006	0.0001	0.0012	-0.0001
219	12712	0.0010	0.0003	-0.0003	0.0006	0.0000	0.0012	-0.0002
220	12824	0.0009	0.0004	-0.0003	0.0006	0.0000	0.0013	-0.0003
221	12936	0.0008	0.0004	-0.0004	0.0006	0.0002	0.0015	-0.0005
222	13048	0.0008	0.0003	-0.0004	0.0006	0.0001	0.0014	-0.0005
223	13161	0.0008	0.0002	-0.0004	0.0007	0.0002	0.0014	-0.0005
224	13275	0.0006	0.0001	-0.0004	0.0007	0.0004	0.0014	-0.0004
225	13389	0.0006	0.0001	-0.0005	0.0007	0.0005	0.0015	-0.0003
226	13503	0.0005	0.0001	-0.0005	0.0006	0.0005	0.0015	-0.0002
227	13618	0.0005	0.0001	-0.0005	0.0006	0.0004	0.0015	0.0003
228	13733	0.0005	0.0001	-0.0005	0.0007	0.0003	0.0016	0.0004
229	13849	0.0005	0.0001	-0.0005	0.0007	0.0003	0.0015	0.0006
230	13965	0.0005	0.0002	-0.0004	0.0007	0.0006	0.0016	0.0006
231	14082	0.0004	0.0002	-0.0005	0.0007	0.0005	0.0016	0.0007
232	14199	0.0003	0.0002	-0.0005	0.0006	0.0004	0.0017	0.0007
233	14317	0.0003	0.0002	-0.0005	0.0005	0.0011	0.0017	0.0007
234	14435	0.0003	0.0003	-0.0004	0.0005	0.0010	0.0016	0.0006
235	14554	0.0003	0.0003	-0.0004	0.0004	0.0008	0.0015	0.0004
236	14673	0.0003	0.0003	-0.0004	0.0004	0.0007	0.0015	0.0003
237	14792	0.0003	0.0004	-0.0005	0.0004	0.0005	0.0014	0.0002
238	14912	0.0002	0.0004	-0.0005	0.0004	0.0003	0.0012	0.0001
239	15033	0.0003	0.0004	-0.0004	0.0005	0.0010	0.0011	0.0002
240	15154	0.0002	0.0003	-0.0003	0.0006	0.0010	0.0011	0.0009

	B10	**B15**	**B20**	**B25**	**B30**	**B35**
MW (peak)	**1132**	**1132**	**1170**	**1132**	**1327**	**1208**
Mw (calc.)	**1382**	**1416**	**1427**	**1452**	**1406**	**1509**
***Mn* (calc.)**	**1101**	**1121**	**1136**	**1131**	**1150**	**1191**
Mn /Mw	**1.25**	**1.26**	**1.26**	**1.28**	**1.22**	**1.27**

Appendix 2B - DOC detector fractograms for King Site Groundwaters.
Results of molecular weight calculations at end of table.

Time sec.	MW daltons	B10	B15	B20	B25	B30	B35	B40
1	0							
2	0	0.0008	0.0096	0.0110	0.0098	-0.0247	-0.0115	-0.0144
3	0	0.0008	0.0096	0.0110	0.0098	-0.0247	-0.0115	-0.0144
4	0	0.0008	0.0096	0.0110	0.0098	-0.0247	-0.0115	-0.0144
5	0	0.0008	0.0096	0.0110	0.0098	-0.0247	-0.0115	-0.0144
6	0	0.0008	0.0096	0.0110	0.0098	-0.0247	-0.0115	-0.0144
7	0	0.0008	0.0096	0.0110	0.0098	-0.0247	-0.0115	-0.0144
8	0	0.0008	0.0096	0.0110	0.0098	-0.0247	-0.0115	-0.0144
9	0	0.0008	0.0096	0.0110	0.0098	-0.0247	-0.0115	-0.0144
10	0	0.0008	0.0096	0.0110	0.0098	-0.0247	-0.0115	-0.0144
11	1	0.0008	0.0096	0.0110	0.0098	-0.0247	-0.0115	-0.0144
12	1	0.0008	0.0096	0.0110	0.0098	-0.0247	-0.0115	-0.0144
13	1	0.0008	0.0096	0.0110	0.0098	-0.0247	-0.0115	-0.0144
14	1	0.0008	0.0096	0.0110	0.0098	-0.0247	-0.0115	-0.0144
15	1	0.0008	0.0096	0.0110	0.0098	-0.0247	-0.0115	-0.0144
16	2	0.0008	0.0096	0.0110	0.0098	-0.0247	-0.0115	-0.0144
17	2	0.0008	0.0096	0.0110	0.0098	-0.0247	-0.0115	-0.0144
18	2	0.0008	0.0096	0.0110	0.0098	-0.0247	-0.0115	-0.0144
19	3	0.0008	0.0096	0.0110	0.0098	-0.0247	-0.0115	-0.0144
20	3	0.0008	0.0096	0.0110	0.0098	-0.0247	-0.0115	-0.0144
21	4	0.0008	0.0096	0.0110	0.0098	-0.0247	-0.0115	-0.0144
22	5	0.0008	0.0096	0.0110	0.0098	-0.0247	-0.0115	-0.0144
23	5	0.0008	0.0096	0.0110	0.0098	-0.0247	-0.0115	-0.0144
24	6	0.0008	0.0096	0.0110	0.0098	-0.0247	-0.0115	-0.0144
25	7	0.0008	0.0096	0.0110	0.0098	-0.0247	-0.0115	-0.0144
26	8	0.0008	0.0096	0.0110	0.0098	-0.0247	-0.0115	-0.0144
27	9	0.0008	0.0096	0.0110	0.0098	-0.0247	-0.0115	-0.0144
28	10	0.0008	0.0096	0.0110	0.0098	-0.0247	-0.0115	-0.0144
29	11	0.0008	0.0096	0.0110	0.0098	-0.0247	-0.0115	-0.0144
30	12	0.0008	0.0096	0.0110	0.0098	-0.0247	-0.0115	-0.0144
31	14	0.0008	0.0096	0.0110	0.0098	-0.0247	-0.0115	-0.0144
32	15	0.0008	0.0096	0.0110	0.0098	-0.0247	-0.0115	-0.0144
33	17	0.0008	0.0096	0.0110	0.0098	-0.0247	-0.0115	-0.0144
34	18	0.0008	0.0096	0.0110	0.0098	-0.0247	-0.0115	-0.0144
35	20	0.0008	0.0096	0.0110	0.0098	-0.0247	-0.0115	-0.0144
36	22	0.0008	0.0096	0.0110	0.0098	-0.0247	-0.0115	-0.0144
37	24	0.0008	0.0096	0.0110	0.0098	-0.0247	-0.0115	-0.0144
38	26	0.0008	0.0096	0.0110	0.0098	-0.0247	-0.0115	-0.0144
39	28	0.0008	0.0096	0.0110	0.0098	-0.0247	-0.0115	-0.0144
40	30	0.0008	0.0096	0.0110	0.0098	-0.0247	-0.0115	-0.0144
41	33	0.0008	0.0096	0.0110	0.0098	-0.0247	-0.0115	-0.0144
42	35	0.0008	0.0096	0.0110	0.0098	-0.0247	-0.0115	-0.0144
43	38	0.0008	0.0096	0.0110	0.0098	-0.0247	-0.0115	-0.0144
44	41	0.0008	0.0096	0.0110	0.0098	-0.0247	-0.0115	-0.0144
45	44	0.0008	0.0096	0.0110	0.0098	-0.0247	-0.0115	-0.0144
46	47	0.0008	0.0096	0.0110	0.0098	-0.0247	-0.0115	-0.0144
47	50	0.0008	0.0096	0.0110	0.0098	-0.0247	-0.0115	-0.0144

Appendix 2B Continued

48	54	0.0008	0.0096	0.0110	0.0098	-0.0247	-0.0115	-0.0144
49	57	0.0008	0.0096	0.0110	0.0098	-0.0247	-0.0115	-0.0144
50	61	0.0008	0.0096	0.0110	0.0098	-0.0247	-0.0115	-0.0144
51	65	0.0008	0.0096	0.0110	0.0098	-0.0247	-0.0115	-0.0144
52	69	0.0008	0.0100	0.0110	0.0098	-0.0247	-0.0115	-0.0144
53	73	0.0008	0.0103	0.0110	0.0101	-0.0247	-0.0115	-0.0144
54	78	0.0008	0.0106	0.0110	0.0109	-0.0247	-0.0115	-0.0144
55	83	0.0008	0.0109	0.0110	0.0116	-0.0247	-0.0115	-0.0144
56	87	0.0009	0.0132	0.0110	0.0124	-0.0247	-0.0114	-0.0144
57	92	0.0053	0.0170	0.0110	0.0146	-0.0247	-0.0112	-0.0144
58	97	0.0098	0.0207	0.0110	0.0181	-0.0247	-0.0108	-0.0142
59	103	0.0142	0.0246	0.0110	0.0209	-0.0247	-0.0091	-0.0134
60	108	0.0188	0.0346	0.0110	0.0241	-0.0247	-0.0067	-0.0118
61	114	0.0323	0.0450	0.0110	0.0316	-0.0247	-0.0045	-0.0102
62	120	0.0405	0.0532	0.0110	0.0393	-0.0247	-0.0004	-0.0083
63	126	0.0489	0.0634	0.0110	0.0452	-0.0247	0.0049	-0.0041
64	133	0.0662	0.0808	0.0111	0.0518	-0.0247	0.0096	0.0004
65	139	0.0937	0.0946	0.0120	0.0635	-0.0247	0.0135	0.0040
66	146	0.1112	0.1055	0.0194	0.0720	-0.0247	0.0182	0.0082
67	153	0.1296	0.1173	0.0262	0.0787	-0.0247	0.0206	0.0123
68	161	0.1519	0.1321	0.0331	0.0856	-0.0247	0.0209	0.0137
69	168	0.1697	0.1401	0.0400	0.0927	-0.0240	0.0207	0.0142
70	176	0.1762	0.1456	0.0459	0.0950	-0.0231	0.0171	0.0144
71	184	0.1842	0.1506	0.0454	0.0962	-0.0222	0.0105	0.0112
72	192	0.1889	0.1520	0.0454	0.0966	-0.0213	0.0043	0.0076
73	201	0.1862	0.1470	0.0452	0.0913	-0.0200	-0.0015	0.0042
74	209	0.1796	0.1414	0.0405	0.0854	-0.0194	-0.0107	-0.0005
75	218	0.1735	0.1343	0.0361	0.0789	-0.0190	-0.0192	-0.0079
76	227	0.1659	0.1203	0.0318	0.0712	-0.0186	-0.0256	-0.0128
77	237	0.1541	0.1062	0.0269	0.0560	-0.0180	-0.0325	-0.0172
78	247	0.1465	0.0941	0.0187	0.0459	-0.0179	-0.0417	-0.0225
79	257	0.1384	0.0819	0.0153	0.0359	-0.0165	-0.0474	-0.0269
80	267	0.1198	0.0696	0.0115	0.0248	-0.0045	-0.0503	-0.0278
81	278	0.0937	0.0592	0.0064	0.0098	0.0078	-0.0536	-0.0284
82	289	0.0761	0.0528	-0.0082	0.0039	0.0199	-0.0564	-0.0277
83	300	0.0576	0.0459	-0.0182	-0.0016	0.0384	-0.0569	-0.0262
84	311	0.0366	0.0392	-0.0286	-0.0073	0.0629	-0.0577	-0.0248
85	323	0.0249	0.0326	-0.0391	-0.0125	0.0767	-0.0556	-0.0232
86	335	0.0223	0.0321	-0.0495	-0.0125	0.0903	-0.0528	-0.0189
87	348	0.0185	0.0308	-0.0498	-0.0130	0.1051	-0.0481	-0.0162
88	360	0.0255	0.0342	-0.0511	-0.0121	0.1153	-0.0436	-0.0123
89	373	0.0393	0.0390	-0.0499	-0.0080	0.1189	-0.0375	-0.0080
90	387	0.0539	0.0451	-0.0426	-0.0037	0.1224	-0.0335	-0.0017
91	400	0.0684	0.0512	-0.0347	0.0006	0.1264	-0.0269	0.0014
92	414	0.0959	0.0585	-0.0268	0.0069	0.1310	-0.0218	0.0073
93	428	0.1141	0.0650	-0.0157	0.0119	0.1343	-0.0138	0.0123
94	443	0.1275	0.0693	-0.0026	0.0135	0.1368	-0.0050	0.0174
95	458	0.1426	0.0740	0.0038	0.0156	0.1300	0.0064	0.0204
96	473	0.1725	0.0802	0.0110	0.0190	0.1225	0.0149	0.0258
97	489	0.1892	0.0912	0.0224	0.0240	0.1135	0.0244	0.0280
98	505	0.2042	0.1043	0.0347	0.0284	0.1038	0.0330	0.0300

Appendix 2B Continued

99	521	0.2222	0.1172	0.0421	0.0331	0.0823	0.0403	0.0316
100	538	0.2494	0.1304	0.0500	0.0391	0.0711	0.0444	0.0330
101	555	0.2611	0.1452	0.0621	0.0481	0.0600	0.0483	0.0317
102	572	0.2732	0.1570	0.0718	0.0534	0.0487	0.0540	0.0311
103	590	0.2867	0.1627	0.0771	0.0591	0.0376	0.0583	0.0302
104	608	0.3008	0.1690	0.0830	0.0669	0.0379	0.0611	0.0292
105	627	0.3044	0.1761	0.0899	0.0754	0.0375	0.0640	0.0281
106	646	0.3085	0.1807	0.0931	0.0794	0.0375	0.0664	0.0273
107	665	0.3136	0.1821	0.0943	0.0835	0.0403	0.0662	0.0265
108	685	0.3185	0.1842	0.0958	0.0883	0.0426	0.0652	0.0259
109	705	0.3202	0.1866	0.0979	0.0910	0.0455	0.0646	0.0255
110	725	0.3222	0.1879	0.0992	0.0916	0.0484	0.0640	0.0254
111	746	0.3247	0.1885	0.0999	0.0923	0.0508	0.0637	0.0249
112	767	0.3262	0.1893	0.1008	0.0931	0.0505	0.0634	0.0247
113	789	0.3267	0.1897	0.1016	0.0937	0.0506	0.0635	0.0244
114	811	0.3273	0.1896	0.1018	0.0942	0.0506	0.0634	0.0242
115	834	0.3279	0.1895	0.1018	0.0947	0.0506	0.0634	0.0236
116	857	0.3280	0.1892	0.1018	0.0953	0.0505	0.0634	0.0234
117	880	0.3280	0.1884	0.1017	0.0958	0.0504	0.0633	0.0230
118	904	0.3280	0.1878	0.1018	0.0958	0.0503	0.0631	0.0227
119	928	0.3280	0.1871	0.1017	0.0958	0.0503	0.0630	0.0223
120	953	0.3273	0.1857	0.1017	0.0951	0.0505	0.0629	0.0220
121	978	0.3263	0.1835	0.1017	0.0945	0.0506	0.0626	0.0214
122	1003	0.3252	0.1816	0.1012	0.0939	0.0517	0.0624	0.0206
123	1029	0.3236	0.1798	0.1003	0.0932	0.0534	0.0623	0.0198
124	1056	0.3185	0.1764	0.0995	0.0918	0.0548	0.0621	0.0188
125	1083	0.3137	0.1723	0.0986	0.0908	0.0562	0.0616	0.0178
126	1110	0.3094	0.1691	0.0966	0.0895	0.0576	0.0613	0.0171
127	1138	0.3028	0.1661	0.0944	0.0883	0.0582	0.0606	0.0163
128	1166	0.2922	0.1610	0.0926	0.0848	0.0582	0.0597	0.0152
129	1195	0.2847	0.1555	0.0906	0.0822	0.0584	0.0581	0.0143
130	1224	0.2777	0.1517	0.0867	0.0797	0.0584	0.0569	0.0135
131	1254	0.2674	0.1478	0.0835	0.0771	0.0583	0.0552	0.0129
132	1284	0.2538	0.1415	0.0811	0.0725	0.0582	0.0535	0.0125
133	1315	0.2446	0.1351	0.0785	0.0702	0.0581	0.0516	0.0123
134	1346	0.2359	0.1307	0.0739	0.0679	0.0574	0.0505	0.0120
135	1378	0.2238	0.1262	0.0706	0.0654	0.0569	0.0488	0.0116
136	1410	0.2091	0.1195	0.0680	0.0615	0.0564	0.0468	0.0108
137	1443	0.2004	0.1133	0.0653	0.0595	0.0558	0.0450	0.0099
138	1476	0.1916	0.1095	0.0605	0.0575	0.0544	0.0435	0.0091
139	1510	0.1799	0.1055	0.0577	0.0546	0.0530	0.0414	0.0084
140	1544	0.1674	0.1014	0.0555	0.0504	0.0516	0.0399	0.0073
141	1579	0.1609	0.0976	0.0532	0.0480	0.0499	0.0392	0.0067
142	1615	0.1542	0.0959	0.0489	0.0457	0.0474	0.0384	0.0062
143	1651	0.1446	0.0940	0.0465	0.0434	0.0455	0.0376	0.0058
144	1687	0.1346	0.0921	0.0445	0.0409	0.0442	0.0374	0.0051
145	1724	0.1287	0.0866	0.0423	0.0401	0.0423	0.0366	0.0049
146	1762	0.1227	0.0825	0.0384	0.0392	0.0394	0.0348	0.0046
147	1800	0.1146	0.0784	0.0365	0.0382	0.0374	0.0331	0.0040
148	1838	0.1061	0.0742	0.0347	0.0357	0.0355	0.0315	0.0032
149	1878	0.1013	0.0674	0.0328	0.0338	0.0331	0.0292	0.0028

Appendix 2B Continued

150	1917	0.0964	0.0633	0.0295	0.0320	0.0302	0.0268	0.0022
151	1958	0.0894	0.0599	0.0280	0.0301	0.0283	0.0255	0.0015
152	1999	0.0824	0.0565	0.0265	0.0267	0.0266	0.0243	0.0012
153	2040	0.0788	0.0517	0.0250	0.0246	0.0244	0.0222	0.0011
154	2082	0.0750	0.0492	0.0223	0.0229	0.0222	0.0205	0.0009
155	2125	0.0694	0.0477	0.0211	0.0211	0.0212	0.0194	0.0009
156	2168	0.0642	0.0460	0.0198	0.0181	0.0202	0.0183	0.0009
157	2212	0.0612	0.0431	0.0186	0.0165	0.0187	0.0163	0.0009
158	2257	0.0579	0.0403	0.0162	0.0152	0.0173	0.0146	0.0009
159	2302	0.0536	0.0376	0.0152	0.0138	0.0165	0.0134	0.0009
160	2347	0.0498	0.0349	0.0142	0.0116	0.0156	0.0122	0.0008
161	2394	0.0477	0.0317	0.0131	0.0104	0.0143	0.0104	0.0007
162	2441	0.0455	0.0289	0.0114	0.0094	0.0133	0.0094	0.0005
163	2488	0.0423	0.0271	0.0109	0.0083	0.0128	0.0087	0.0005
164	2536	0.0395	0.0256	0.0102	0.0070	0.0121	0.0079	0.0005
165	2585	0.0378	0.0236	0.0096	0.0062	0.0109	0.0069	0.0005
166	2635	0.0360	0.0216	0.0090	0.0057	0.0100	0.0064	0.0005
167	2685	0.0334	0.0202	0.0086	0.0052	0.0093	0.0061	0.0005
168	2735	0.0311	0.0191	0.0082	0.0043	0.0084	0.0056	0.0004
169	2787	0.0297	0.0177	0.0077	0.0039	0.0073	0.0050	0.0003
170	2839	0.0283	0.0162	0.0068	0.0036	0.0067	0.0047	0.0002
171	2892	0.0263	0.0152	0.0060	0.0033	0.0063	0.0044	0.0002
172	2945	0.0248	0.0144	0.0056	0.0030	0.0058	0.0038	0.0002
173	2999	0.0241	0.0134	0.0052	0.0028	0.0054	0.0033	0.0001
174	3054	0.0232	0.0124	0.0048	0.0025	0.0052	0.0029	0.0001
175	3109	0.0224	0.0119	0.0048	0.0023	0.0051	0.0026	0.0001
176	3165	0.0221	0.0115	0.0048	0.0019	0.0050	0.0022	0.0000
177	3222	0.0222	0.0109	0.0048	0.0014	0.0047	0.0021	0.0000
178	3279	0.0222	0.0103	0.0049	0.0010	0.0042	0.0021	-0.0001
179	3337	0.0222	0.0100	0.0048	0.0006	0.0038	0.0021	-0.0002
180	3396	0.0216	0.0097	0.0048	0.0002	0.0033	0.0020	-0.0003
181	3456	0.0207	0.0093	0.0048	-0.0001	0.0028	0.0019	-0.0003
182	3516	0.0195	0.0089	0.0048	-0.0002	0.0023	0.0019	-0.0004
183	3577	0.0183	0.0087	0.0047	-0.0003	0.0021	0.0019	-0.0003
184	3638	0.0169	0.0084	0.0044	-0.0004	0.0019	0.0019	-0.0003
185	3701	0.0157	0.0080	0.0041	-0.0005	0.0016	0.0019	-0.0002
186	3764	0.0149	0.0076	0.0038	-0.0005	0.0014	0.0017	-0.0001
187	3828	0.0143	0.0073	0.0035	-0.0005	0.0014	0.0015	-0.0001
188	3892	0.0134	0.0070	0.0032	-0.0007	0.0014	0.0012	-0.0001
189	3957	0.0125	0.0067	0.0031	-0.0008	0.0013	0.0010	0.0000
190	4023	0.0120	0.0066	0.0030	-0.0008	0.0011	0.0007	0.0001
191	4090	0.0115	0.0066	0.0027	-0.0009	0.0009	0.0006	0.0001
192	4158	0.0107	0.0066	0.0025	-0.0010	0.0007	0.0005	0.0001
193	4226	0.0101	0.0065	0.0023	-0.0008	0.0005	0.0004	0.0000
194	4295	0.0095	0.0063	0.0021	-0.0007	0.0004	0.0005	-0.0002
195	4365	0.0090	0.0061	0.0019	-0.0007	0.0003	0.0005	-0.0003
196	4435	0.0084	0.0059	0.0017	-0.0007	0.0003	0.0006	-0.0004
197	4507	0.0080	0.0057	0.0016	-0.0006	0.0003	0.0006	-0.0005
198	4579	0.0077	0.0056	0.0015	-0.0007	0.0004	0.0006	-0.0005
199	4652	0.0077	0.0056	0.0014	-0.0008	0.0005	0.0005	-0.0005
200	4725	0.0074	0.0056	0.0015	-0.0009	0.0006	0.0004	-0.0004

Appendix 2B Continued

201	4800	0.0070	0.0056	0.0015	-0.0008	0.0006	0.0004	-0.0003
202	4875	0.0067	0.0056	0.0016	-0.0007	0.0004	0.0003	-0.0001
203	4951	0.0064	0.0055	0.0016	-0.0007	0.0003	0.0003	0.0001
204	5028	0.0060	0.0055	0.0015	-0.0006	0.0001	0.0003	0.0002
205	5106	0.0057	0.0055	0.0015	-0.0005	0.0001	0.0005	0.0003
206	5184	0.0055	0.0054	0.0015	-0.0005	0.0001	0.0006	0.0004
207	5263	0.0053	0.0053	0.0014	-0.0005	0.0003	0.0008	0.0003
208	5344	0.0050	0.0052	0.0014	-0.0006	0.0004	0.0008	0.0003
209	5425	0.0049	0.0051	0.0014	-0.0006	0.0006	0.0008	0.0003
210	5506	0.0049	0.0050	0.0014	-0.0006	0.0007	0.0007	0.0003
211	5589	0.0049	0.0050	0.0013	-0.0006	0.0008	0.0005	0.0002
212	5672	0.0048	0.0050	0.0011	-0.0005	0.0008	0.0004	0.0003
213	5757	0.0046	0.0049	0.0009	-0.0005	0.0006	0.0003	0.0003
214	5842	0.0044	0.0048	0.0007	-0.0006	0.0004	0.0003	0.0004
215	5928	0.0042	0.0047	0.0005	-0.0006	0.0001	0.0003	0.0005
216	6015	0.0041	0.0046	0.0004	-0.0006	-0.0002	0.0004	0.0005
217	6103	0.0041	0.0044	0.0003	-0.0006	-0.0003	0.0005	0.0005
218	6191	0.0042	0.0043	0.0003	-0.0005	-0.0002	0.0005	0.0005
219	6281	0.0043	0.0042	0.0002	-0.0005	-0.0002	0.0005	0.0005
220	6371	0.0043	0.0041	0.0002	-0.0004	-0.0002	0.0002	0.0006
221	6462	0.0042	0.0039	0.0002	-0.0002	-0.0003	0.0000	0.0007
222	6554	0.0041	0.0038	0.0002	-0.0001	-0.0003	-0.0003	0.0010
223	6647	0.0040	0.0037	0.0002	0.0000	-0.0004	-0.0005	0.0012
224	6741	0.0038	0.0036	0.0002	0.0000	-0.0005	-0.0006	0.0014
225	6836	0.0037	0.0034	0.0002	0.0000	-0.0005	-0.0004	0.0016
226	6932	0.0036	0.0033	0.0001	-0.0001	-0.0005	-0.0002	0.0017
227	7028	0.0035	0.0033	0.0003	-0.0002	-0.0006	0.0000	0.0017
228	7126	0.0034	0.0032	0.0004	-0.0002	-0.0005	0.0002	0.0016
229	7224	0.0034	0.0032	0.0005	-0.0001	-0.0003	0.0002	0.0017
230	7324	0.0034	0.0032	0.0007	-0.0001	-0.0001	0.0003	0.0017
231	7424	0.0034	0.0031	0.0007	0.0000	0.0000	0.0002	0.0017
232	7525	0.0034	0.0031	0.0007	0.0000	0.0003	0.0001	0.0017
233	7627	0.0033	0.0030	0.0006	0.0000	0.0003	0.0000	0.0016
234	7730	0.0032	0.0027	0.0005	-0.0001	0.0003	-0.0001	0.0015
235	7835	0.0031	0.0025	0.0005	-0.0001	0.0003	0.0000	0.0014
236	7940	0.0030	0.0023	0.0005	-0.0001	0.0003	0.0003	0.0014
237	8045	0.0029	0.0021	0.0005	0.0000	0.0002	0.0006	0.0014
238	8152	0.0029	0.0020	0.0006	0.0000	0.0002	0.0008	0.0014
239	8260	0.0029	0.0020	0.0006	0.0001	0.0002	0.0011	0.0015
240	8369	0.0029	0.0020	0.0007	0.0001	0.0003	0.0011	0.0016

	B10	**B15**	**B20**	**B25**
MW (peak)	**972**	**868**	**972**	**945**
Mw (calc.)	**1142**	**1160**	**1266**	**1105**
***Mn* (calc.)**	**891**	**895**	**1041**	**948**
Mn /Mw	**1.28**	**1.30**	**1.22**	**1.17**

Appendix 2C - UV (254 nm) detector fractograms for King Site ground waters (BJ series). Results of molecular weight calculations at end of table.

Time sec.	MW daltons	BJ10	BJ13	BJ 16.5	BJ20	BJ23	BJ26	BJ36
0	0	0.0019	0.0023	-0.0052	-0.0039	-0.0029	-0.0030	-0.0009
1	0	0.0019	0.0023	-0.0052	-0.0039	-0.0029	-0.0030	-0.0009
2	2	0.0019	0.0023	-0.0052	-0.0039	-0.0029	-0.0030	-0.0009
3	3	0.0019	0.0023	-0.0052	-0.0039	-0.0029	-0.0030	-0.0009
4	6	0.0019	0.0023	-0.0052	-0.0039	-0.0029	-0.0030	-0.0009
5	9	0.0019	0.0023	-0.0052	-0.0039	-0.0029	-0.0030	-0.0009
6	13	0.0019	0.0023	-0.0052	-0.0039	-0.0029	-0.0030	-0.0009
7	17	0.0019	0.0023	-0.0052	-0.0039	-0.0029	-0.0030	-0.0009
8	22	0.0019	0.0023	-0.0052	-0.0039	-0.0029	-0.0030	-0.0009
9	28	0.0019	0.0023	-0.0052	-0.0039	-0.0029	-0.0030	-0.0009
10	34	0.0019	0.0023	-0.0052	-0.0039	-0.0029	-0.0030	-0.0009
11	41	0.0019	0.0023	-0.0052	-0.0039	-0.0029	-0.0030	-0.0009
12	48	0.0019	0.0023	-0.0052	-0.0039	-0.0029	-0.0030	-0.0009
13	56	0.0019	0.0023	-0.0052	-0.0039	-0.0029	-0.0030	-0.0009
14	65	0.0019	0.0023	-0.0052	-0.0039	-0.0029	-0.0030	-0.0009
15	74	0.0019	0.0023	-0.0049	-0.0039	-0.0029	-0.0030	-0.0009
16	84	0.0019	0.0023	-0.0002	0.0023	-0.0029	-0.0030	-0.0009
17	94	0.0416	0.0589	0.0390	0.0431	0.0167	0.0179	-0.0013
18	105	0.1184	0.1460	0.1029	0.1015	0.0549	0.0496	0.0063
19	117	0.1921	0.2166	0.1559	0.1392	0.0856	0.0739	0.0137
20	129	0.2359	0.2568	0.1864	0.1628	0.1034	0.0869	0.0176
21	141	0.2544	0.2736	0.1984	0.1687	0.1111	0.0918	0.0197
22	155	0.2598	0.2767	0.2007	0.1704	0.1131	0.0930	0.0213
23	168	0.2581	0.2732	0.1986	0.1650	0.1158	0.0927	0.0228
24	183	0.2533	0.2669	0.1943	0.1590	0.1149	0.0914	0.0244
25	198	0.2464	0.2586	0.1891	0.1528	0.1115	0.0895	0.0257
26	213	0.2376	0.2488	0.1827	0.1470	0.1078	0.0870	0.0263
27	229	0.2275	0.2379	0.1755	0.1411	0.1040	0.0839	0.0265
28	246	0.2164	0.2263	0.1677	0.1344	0.1001	0.0806	0.0262
29	263	0.2050	0.2144	0.1592	0.1275	0.0955	0.0768	0.0257
30	280	0.1935	0.2023	0.1505	0.1209	0.0909	0.0730	0.0250
31	299	0.1823	0.1904	0.1420	0.1149	0.0863	0.0691	0.0241
32	317	0.1720	0.1790	0.1339	0.1096	0.0818	0.0652	0.0229
33	337	0.1621	0.1682	0.1262	0.1028	0.0773	0.0615	0.0217
34	356	0.1521	0.1584	0.1191	0.0973	0.0732	0.0581	0.0206
35	377	0.1441	0.1495	0.1130	0.0921	0.0697	0.0551	0.0195
36	398	0.1369	0.1420	0.1076	0.0883	0.0664	0.0526	0.0185
37	419	0.1314	0.1358	0.1031	0.0849	0.0639	0.0506	0.0177
38	441	0.1264	0.1307	0.0994	0.0824	0.0618	0.0492	0.0170
39	464	0.1227	0.1269	0.0967	0.0802	0.0603	0.0480	0.0165
40	487	0.1200	0.1241	0.0948	0.0788	0.0601	0.0471	0.0162
41	510	0.1181	0.1224	0.0936	0.0778	0.0595	0.0466	0.0160
42	535	0.1171	0.1214	0.0934	0.0774	0.0589	0.0464	0.0159
43	559	0.1168	0.1214	0.0937	0.0774	0.0586	0.0465	0.0159
44	585	0.1175	0.1218	0.0943	0.0777	0.0588	0.0469	0.0160
45	610	0.1184	0.1229	0.0953	0.0783	0.0593	0.0475	0.0162

Appendix 2C Continued

46	637	0.1199	0.1245	0.0967	0.0793	0.0600	0.0482	0.0165
47	663	0.1218	0.1266	0.0984	0.0805	0.0610	0.0491	0.0168
48	691	0.1241	0.1291	0.1005	0.0821	0.0621	0.0503	0.0171
49	719	0.1266	0.1319	0.1028	0.0839	0.0634	0.0516	0.0175
50	747	0.1296	0.1350	0.1052	0.0859	0.0649	0.0528	0.0180
51	776	0.1327	0.1384	0.1079	0.0880	0.0664	0.0541	0.0190
52	805	0.1362	0.1421	0.1107	0.0902	0.0681	0.0553	0.0196
53	835	0.1397	0.1458	0.1136	0.0925	0.0698	0.0567	0.0200
54	866	0.1435	0.1497	0.1168	0.0949	0.0716	0.0580	0.0204
55	897	0.1473	0.1536	0.1199	0.0974	0.0735	0.0595	0.0209
56	929	0.1511	0.1577	0.1229	0.0999	0.0753	0.0609	0.0214
57	961	0.1549	0.1618	0.1261	0.1024	0.0771	0.0624	0.0220
58	993	0.1585	0.1656	0.1290	0.1049	0.0788	0.0638	0.0225
59	1026	0.1620	0.1692	0.1318	0.1070	0.0805	0.0650	0.0230
60	1060	0.1652	0.1759	0.1344	0.1091	0.0821	0.0662	0.0234
61	1094	0.1681	0.1778	0.1367	0.1109	0.0835	0.0673	0.0237
62	1129	0.1704	0.1796	0.1388	0.1125	0.0847	0.0682	0.0239
63	1164	0.1726	0.1811	0.1406	0.1138	0.0857	0.0689	0.0241
64	1200	0.1739	0.1820	0.1420	0.1147	0.0865	0.0694	0.0247
65	1236	0.1747	0.1825	0.1428	0.1154	0.0870	0.0696	0.0246
66	1273	0.1748	0.1824	0.1433	0.1157	0.0872	0.0697	0.0245
67	1310	0.1744	0.1816	0.1433	0.1156	0.0871	0.0694	0.0244
68	1348	0.1732	0.1802	0.1428	0.1151	0.0868	0.0691	0.0242
69	1386	0.1712	0.1782	0.1416	0.1143	0.0862	0.0685	0.0240
70	1425	0.1686	0.1755	0.1399	0.1130	0.0852	0.0676	0.0237
71	1464	0.1653	0.1721	0.1377	0.1112	0.0840	0.0664	0.0233
72	1504	0.1615	0.1681	0.1349	0.1090	0.0824	0.0651	0.0228
73	1544	0.1570	0.1635	0.1317	0.1065	0.0806	0.0635	0.0223
74	1585	0.1520	0.1585	0.1280	0.1038	0.0786	0.0619	0.0217
75	1626	0.1465	0.1532	0.1240	0.1007	0.0763	0.0599	0.0210
76	1668	0.1407	0.1474	0.1198	0.0973	0.0737	0.0578	0.0202
77	1711	0.1344	0.1416	0.1153	0.0936	0.0710	0.0556	0.0195
78	1754	0.1280	0.1353	0.1106	0.0899	0.0681	0.0532	0.0187
79	1797	0.1214	0.1288	0.1056	0.0859	0.0651	0.0508	0.0178
80	1841	0.1148	0.1223	0.1006	0.0819	0.0620	0.0483	0.0169
81	1885	0.1082	0.1157	0.0956	0.0778	0.0590	0.0459	0.0160
82	1930	0.1016	0.1093	0.0904	0.0738	0.0558	0.0434	0.0151
83	1976	0.0951	0.1029	0.0853	0.0697	0.0529	0.0409	0.0141
84	2022	0.0889	0.0966	0.0803	0.0656	0.0499	0.0385	0.0132
85	2068	0.0827	0.0906	0.0753	0.0615	0.0469	0.0361	0.0123
86	2115	0.0769	0.0848	0.0705	0.0577	0.0441	0.0338	0.0115
87	2162	0.0714	0.0790	0.0660	0.0539	0.0413	0.0315	0.0106
88	2210	0.0659	0.0735	0.0616	0.0502	0.0387	0.0293	0.0099
89	2259	0.0608	0.0682	0.0573	0.0467	0.0361	0.0272	0.0092
90	2308	0.0560	0.0634	0.0533	0.0434	0.0337	0.0252	0.0090
91	2357	0.0516	0.0588	0.0495	0.0403	0.0314	0.0234	0.0081
92	2407	0.0474	0.0545	0.0459	0.0374	0.0291	0.0217	0.0074
93	2458	0.0434	0.0505	0.0426	0.0346	0.0271	0.0201	0.0067
94	2508	0.0397	0.0468	0.0393	0.0320	0.0251	0.0186	0.0061
95	2560	0.0363	0.0433	0.0364	0.0296	0.0232	0.0171	0.0055
96	2612	0.0331	0.0400	0.0338	0.0275	0.0215	0.0157	0.0049

Appendix 2C Continued

97	2664	0.0303	0.0370	0.0313	0.0254	0.0198	0.0145	0.0045
98	2717	0.0278	0.0342	0.0290	0.0234	0.0184	0.0134	0.0041
99	2771	0.0254	0.0317	0.0269	0.0215	0.0170	0.0123	0.0037
100	2825	0.0233	0.0292	0.0249	0.0199	0.0157	0.0114	0.0034
101	2879	0.0214	0.0271	0.0230	0.0186	0.0145	0.0105	0.0031
102	2934	0.0197	0.0251	0.0212	0.0172	0.0135	0.0098	0.0029
103	2990	0.0181	0.0233	0.0196	0.0158	0.0125	0.0091	0.0028
104	3045	0.0166	0.0215	0.0181	0.0147	0.0116	0.0084	0.0026
105	3102	0.0152	0.0200	0.0169	0.0136	0.0108	0.0078	0.0025
106	3159	0.0140	0.0186	0.0156	0.0127	0.0099	0.0072	0.0024
107	3216	0.0130	0.0173	0.0146	0.0119	0.0093	0.0068	0.0023
108	3274	0.0119	0.0163	0.0136	0.0111	0.0086	0.0063	0.0022
109	3333	0.0110	0.0152	0.0126	0.0105	0.0080	0.0058	0.0020
110	3392	0.0102	0.0143	0.0118	0.0098	0.0076	0.0054	0.0019
111	3451	0.0094	0.0134	0.0110	0.0093	0.0071	0.0050	0.0018
112	3511	0.0087	0.0126	0.0103	0.0087	0.0067	0.0046	0.0017
113	3571	0.0081	0.0119	0.0095	0.0082	0.0063	0.0043	0.0016
114	3632	0.0075	0.0112	0.0089	0.0078	0.0059	0.0040	0.0016
115	3694	0.0071	0.0106	0.0083	0.0073	0.0057	0.0038	0.0016
116	3755	0.0067	0.0100	0.0078	0.0068	0.0054	0.0036	0.0015
117	3818	0.0063	0.0093	0.0074	0.0064	0.0051	0.0034	0.0015
118	3881	0.0060	0.0089	0.0070	0.0060	0.0048	0.0032	0.0015
119	3944	0.0057	0.0083	0.0065	0.0056	0.0046	0.0030	0.0014
120	4008	0.0054	0.0078	0.0061	0.0053	0.0043	0.0029	0.0013
121	4072	0.0052	0.0074	0.0057	0.0049	0.0040	0.0027	0.0013
122	4137	0.0049	0.0070	0.0053	0.0047	0.0037	0.0025	0.0012
123	4202	0.0047	0.0067	0.0049	0.0043	0.0035	0.0023	0.0011
124	4268	0.0044	0.0064	0.0046	0.0040	0.0033	0.0021	0.0011
125	4334	0.0042	0.0061	0.0043	0.0038	0.0031	0.0019	0.0010
126	4401	0.0039	0.0058	0.0041	0.0035	0.0029	0.0018	0.0009
127	4468	0.0037	0.0056	0.0039	0.0033	0.0027	0.0017	0.0009
128	4536	0.0035	0.0054	0.0038	0.0032	0.0027	0.0017	0.0009
129	4604	0.0033	0.0052	0.0037	0.0031	0.0026	0.0016	0.0009
130	4673	0.0032	0.0050	0.0036	0.0030	0.0026	0.0016	0.0009
131	4742	0.0031	0.0047	0.0036	0.0030	0.0025	0.0016	0.0009
132	4812	0.0031	0.0046	0.0037	0.0030	0.0025	0.0016	0.0009
133	4882	0.0030	0.0044	0.0038	0.0030	0.0024	0.0015	0.0009
134	4953	0.0029	0.0042	0.0038	0.0029	0.0023	0.0016	0.0009
135	5024	0.0028	0.0040	0.0038	0.0029	0.0023	0.0016	0.0009
136	5096	0.0027	0.0038	0.0037	0.0028	0.0026	0.0015	0.0009
137	5168	0.0026	0.0037	0.0038	0.0027	0.0025	0.0015	0.0008
138	5240	0.0025	0.0035	0.0036	0.0027	0.0023	0.0016	0.0008
139	5314	0.0024	0.0034	0.0036	0.0027	0.0022	0.0016	0.0008
140	5387	0.0023	0.0033	0.0035	0.0027	0.0021	0.0016	0.0009
141	5461	0.0022	0.0032	0.0035	0.0028	0.0020	0.0015	0.0009
142	5536	0.0020	0.0030	0.0034	0.0028	0.0020	0.0014	0.0009
143	5611	0.0019	0.0030	0.0033	0.0028	0.0020	0.0014	0.0009
144	5686	0.0018	0.0028	0.0032	0.0028	0.0019	0.0013	0.0009
145	5762	0.0016	0.0028	0.0030	0.0028	0.0019	0.0013	0.0009
146	5839	0.0015	0.0029	0.0027	0.0027	0.0019	0.0012	0.0009
147	5916	0.0015	0.0028	0.0025	0.0027	0.0018	0.0010	0.0009

Appendix 2C Continued

148	5993	0.0015	0.0027	0.0024	0.0026	0.0018	0.0009	0.0009
149	6071	0.0014	0.0026	0.0023	0.0026	0.0018	0.0009	0.0009
150	6150	0.0014	0.0026	0.0022	0.0025	0.0018	0.0008	0.0008
151	6229	0.0013	0.0026	0.0022	0.0023	0.0017	0.0007	0.0007
152	6308	0.0014	0.0025	0.0022	0.0022	0.0015	0.0007	0.0007
153	6388	0.0015	0.0025	0.0022	0.0021	0.0014	0.0007	0.0007
154	6468	0.0015	0.0024	0.0022	0.0019	0.0013	0.0006	0.0008
155	6549	0.0015	0.0023	0.0023	0.0017	0.0013	0.0005	0.0008
156	6630	0.0015	0.0023	0.0023	0.0015	0.0012	0.0005	0.0009
157	6712	0.0014	0.0022	0.0024	0.0013	0.0011	0.0006	0.0010
158	6794	0.0014	0.0021	0.0024	0.0011	0.0010	0.0005	0.0009
159	6877	0.0013	0.0021	0.0024	0.0009	0.0010	0.0005	0.0009
160	6960	0.0013	0.0020	0.0025	0.0008	0.0009	0.0005	0.0008
161	7044	0.0012	0.0020	0.0025	0.0007	0.0009	0.0005	0.0008
162	7128	0.0012	0.0019	0.0024	0.0008	0.0008	0.0004	0.0008
163	7213	0.0012	0.0020	0.0024	0.0008	0.0009	0.0005	0.0008
164	7298	0.0010	0.0020	0.0022	0.0008	0.0009	0.0004	0.0008
165	7384	0.0010	0.0020	0.0021	0.0009	0.0009	0.0003	0.0008
166	7470	0.0009	0.0019	0.0018	0.0010	0.0008	0.0003	0.0008
167	7556	0.0008	0.0018	0.0016	0.0010	0.0008	0.0003	0.0008
168	7644	0.0007	0.0019	0.0015	0.0009	0.0008	0.0003	0.0007
169	7731	0.0006	0.0018	0.0014	0.0010	0.0007	0.0005	0.0007
170	7819	0.0005	0.0017	0.0014	0.0010	0.0007	0.0005	0.0006
171	7908	0.0004	0.0017	0.0013	0.0011	0.0006	0.0006	0.0005
172	7997	0.0003	0.0017	0.0013	0.0011	0.0006	0.0006	0.0005
173	8086	0.0002	0.0016	0.0014	0.0011	0.0005	0.0006	0.0004
174	8176	0.0002	0.0016	0.0014	0.0012	0.0004	0.0007	0.0004
175	8266	0.0001	0.0015	0.0014	0.0012	0.0003	0.0007	0.0004
176	8357	0.0001	0.0015	0.0015	0.0013	0.0002	0.0008	0.0003
177	8449	0.0001	0.0015	0.0014	0.0013	0.0001	0.0008	0.0003
178	8540	0.0001	0.0015	0.0014	0.0013	0.0000	0.0009	0.0003
179	8633	0.0001	0.0014	0.0014	0.0013	0.0000	0.0010	0.0003
180	8725	0.0002	0.0014	0.0014	0.0013	0.0000	0.0010	0.0003
181	8819	0.0001	0.0014	0.0014	0.0013	0.0000	0.0010	0.0003
182	8912	0.0001	0.0015	0.0014	0.0013	0.0000	0.0010	0.0002
183	9007	0.0000	0.0015	0.0014	0.0012	0.0001	0.0010	0.0002
184	9101	-0.0001	0.0015	0.0014	0.0013	0.0001	0.0010	0.0002
185	9196	-0.0001	0.0016	0.0013	0.0013	0.0001	0.0010	0.0002
186	9292	-0.0001	0.0015	0.0011	0.0014	0.0001	0.0010	0.0002
187	9388	-0.0002	0.0015	0.0009	0.0014	0.0002	0.0009	0.0002
188	9485	-0.0002	0.0015	0.0007	0.0014	0.0002	0.0009	0.0002
189	9582	-0.0002	0.0015	0.0005	0.0014	0.0003	0.0008	0.0002
190	9679	-0.0002	0.0014	0.0005	0.0013	0.0002	0.0009	0.0001
191	9777	-0.0002	0.0013	0.0005	0.0012	0.0001	0.0009	0.0001
192	9876	-0.0002	0.0013	0.0005	0.0011	0.0001	0.0009	0.0001
193	9975	-0.0001	0.0013	0.0005	0.0010	0.0001	0.0009	0.0001
194	10074	-0.0002	0.0013	0.0005	0.0010	0.0001	0.0009	0.0001
195	10174	-0.0003	0.0013	0.0004	0.0009	0.0001	0.0009	0.0001
196	10274	-0.0003	0.0012	0.0004	0.0009	0.0001	0.0009	0.0001
197	10375	-0.0004	0.0012	0.0004	0.0008	0.0000	0.0008	0.0000
198	10476	-0.0003	0.0011	0.0003	0.0008	0.0000	0.0008	0.0000

Appendix 2C Continued

199	10578	-0.0002	0.0010	0.0002	0.0008	-0.0002	0.0008	-0.0001
200	10680	-0.0001	0.0010	0.0000	0.0007	-0.0003	0.0007	-0.0001
201	10783	-0.0001	0.0010	-0.0001	0.0007	-0.0004	0.0006	-0.0001
202	10886	-0.0001	0.0009	-0.0002	0.0006	-0.0005	0.0005	-0.0001
203	10990	0.0000	0.0010	-0.0002	0.0005	-0.0006	0.0004	-0.0001
204	11094	0.0000	0.0009	-0.0001	0.0005	-0.0006	0.0004	-0.0001
205	11199	0.0000	0.0010	0.0000	0.0005	-0.0006	0.0003	0.0000
206	11304	0.0001	0.0010	0.0002	0.0005	-0.0007	0.0002	0.0000
207	11409	0.0001	0.0011	0.0003	0.0005	-0.0006	0.0001	0.0000
208	11515	0.0002	0.0010	0.0004	0.0005	-0.0006	0.0001	0.0001
209	11622	0.0002	0.0009	0.0006	0.0005	-0.0006	0.0001	0.0001
210	11729	0.0002	0.0009	0.0007	0.0006	-0.0006	0.0000	0.0002
211	11836	0.0002	0.0008	0.0008	0.0006	-0.0005	-0.0001	0.0002
212	11944	0.0001	0.0009	0.0009	0.0007	-0.0004	-0.0003	0.0003
213	12052	0.0000	0.0008	0.0009	0.0008	-0.0004	-0.0004	0.0003
214	12161	-0.0001	0.0008	0.0009	0.0008	-0.0003	-0.0004	0.0003
215	12270	-0.0001	0.0008	0.0008	0.0008	-0.0003	-0.0004	0.0004
216	12380	-0.0002	0.0008	0.0007	0.0008	-0.0002	-0.0004	0.0004
217	12490	-0.0003	0.0008	0.0005	0.0007	-0.0002	-0.0003	0.0004
218	12601	-0.0004	0.0006	0.0004	0.0007	-0.0002	-0.0002	0.0003
219	12712	-0.0005	0.0006	0.0003	0.0006	-0.0002	-0.0001	0.0002
220	12824	-0.0005	0.0006	0.0003	0.0006	-0.0002	0.0000	0.0002
221	12936	-0.0006	0.0005	0.0003	0.0005	-0.0003	0.0000	0.0002
222	13048	-0.0006	0.0006	0.0002	0.0004	-0.0003	0.0000	0.0002
223	13161	-0.0006	0.0006	0.0001	0.0002	-0.0003	-0.0001	0.0002
224	13275	-0.0006	0.0007	0.0001	0.0001	-0.0004	-0.0002	0.0003
225	13389	-0.0006	0.0007	0.0001	0.0000	-0.0003	-0.0003	0.0003
226	13503	-0.0006	0.0007	0.0000	-0.0001	-0.0004	-0.0005	0.0003
227	13618	-0.0006	0.0008	0.0000	-0.0001	-0.0005	-0.0005	0.0003
228	13733	-0.0007	0.0008	0.0000	-0.0001	-0.0005	-0.0004	0.0003
229	13849	-0.0006	0.0008	0.0000	0.0000	-0.0006	-0.0003	0.0003
230	13965	-0.0006	0.0008	-0.0001	0.0000	-0.0006	-0.0002	0.0003
231	14082	-0.0005	0.0008	-0.0001	0.0001	-0.0006	-0.0002	0.0003
232	14199	-0.0005	0.0008	-0.0002	0.0000	-0.0005	-0.0001	0.0003
233	14317	-0.0005	0.0007	-0.0002	0.0000	-0.0006	0.0000	0.0003
234	14435	-0.0004	0.0007	-0.0002	0.0001	-0.0005	0.0001	0.0003
235	14554	-0.0004	0.0007	-0.0002	0.0001	-0.0005	0.0001	0.0003
236	14673	-0.0004	0.0006	-0.0002	0.0001	-0.0006	0.0001	0.0003
237	14792	-0.0003	0.0006	-0.0002	0.0001	-0.0006	0.0001	0.0002
238	14912	-0.0003	0.0006	-0.0002	0.0000	-0.0006	0.0002	0.0002
239	15033	-0.0003	0.0005	-0.0002	0.0000	-0.0006	0.0002	0.0001
240	15154	-0.0003	0.0004	-0.0002	-0.0001	-0.0006	0.0003	0.0001
241	15275	-0.0003	0.0004	-0.0003	-0.0001	-0.0006	0.0004	0.0001
242	15397	-0.0004	0.0004	-0.0002	-0.0002	-0.0006	0.0005	0.0001
243	15519	-0.0004	0.0004	-0.0002	-0.0002	-0.0006	0.0005	0.0001
244	15642	-0.0005	0.0004	-0.0003	-0.0003	-0.0006	0.0004	0.0001
245	15765	-0.0006	0.0004	-0.0004	-0.0003	-0.0005	0.0005	0.0001
246	15889	-0.0006	0.0003	-0.0005	-0.0004	-0.0006	0.0005	0.0000
247	16013	-0.0007	0.0003	-0.0005	-0.0004	-0.0006	0.0005	0.0000
248	16138	-0.0008	0.0003	-0.0006	-0.0004	-0.0006	0.0005	0.0000
249	16263	-0.0008	0.0002	-0.0006	-0.0004	-0.0007	0.0004	-0.0001

Appendix 2C Continued

250	16388	-0.0007	0.0001	-0.0005	-0.0004	-0.0007	0.0004	-0.0001
251	16514	-0.0010	0.0002	-0.0005	-0.0004	-0.0007	0.0003	-0.0001
252	16641	-0.0009	0.0001	-0.0004	-0.0004	-0.0007	0.0002	-0.0001
253	16768	-0.0009	0.0001	-0.0004	-0.0004	-0.0008	0.0002	-0.0001
254	16895	-0.0008	0.0000	-0.0005	-0.0003	-0.0009	0.0002	-0.0001
255	17023	-0.0008	0.0000	-0.0005	-0.0003	-0.0010	0.0002	-0.0001
256	17151	-0.0008	0.0000	-0.0005	-0.0003	-0.0010	0.0002	-0.0001
257	17280	-0.0007	-0.0001	-0.0005	-0.0003	-0.0010	0.0002	-0.0001
258	17409	-0.0007	-0.0001	-0.0004	-0.0003	-0.0010	0.0003	-0.0001
259	17539	-0.0007	-0.0001	-0.0003	-0.0003	-0.0009	0.0003	-0.0001
260	17669	-0.0007	-0.0001	-0.0003	-0.0003	-0.0008	0.0003	-0.0001
261	17800	-0.0008	-0.0002	-0.0003	-0.0004	-0.0007	0.0003	-0.0002
262	17931	-0.0008	-0.0002	-0.0003	-0.0003	-0.0007	0.0003	-0.0002
263	18063	-0.0007	-0.0003	-0.0005	-0.0004	-0.0007	0.0003	-0.0002
264	18195	-0.0007	-0.0004	-0.0006	-0.0004	-0.0007	0.0003	-0.0003
265	18327	-0.0007	-0.0003	-0.0009	-0.0004	-0.0006	0.0003	-0.0003
266	18460	-0.0007	-0.0003	-0.0011	-0.0004	-0.0007	0.0002	-0.0003
267	18593	-0.0007	-0.0004	-0.0012	-0.0005	-0.0008	0.0002	-0.0003
268	18727	-0.0007	-0.0004	-0.0011	-0.0005	-0.0009	0.0001	-0.0003
269	18862	-0.0008	-0.0004	-0.0011	-0.0006	-0.0009	0.0001	-0.0003
270	18996	-0.0008	-0.0004	-0.0009	-0.0006	-0.0009	0.0000	-0.0003
271	19132	-0.0009	-0.0005	-0.0008	-0.0004	-0.0009	0.0000	-0.0004
272	19267	-0.0010	-0.0004	-0.0006	-0.0005	-0.0009	-0.0001	-0.0004
273	19403	-0.0010	-0.0004	-0.0005	-0.0005	-0.0009	-0.0002	-0.0005
274	19540	-0.0010	-0.0004	-0.0004	-0.0006	-0.0009	-0.0002	-0.0004
275	19677	-0.0010	-0.0005	-0.0003	-0.0007	-0.0009	-0.0003	-0.0004
276	19815	-0.0010	-0.0005	-0.0001	-0.0008	-0.0009	-0.0003	-0.0003
277	19953	-0.0010	-0.0006	0.0000	-0.0008	-0.0009	-0.0003	-0.0003
278	20091	-0.0009	-0.0006	0.0001	-0.0008	-0.0010	-0.0004	-0.0003
279	20230	-0.0008	-0.0006	0.0002	-0.0008	-0.0010	-0.0005	-0.0003
280	20369	-0.0007	-0.0005	0.0002	-0.0009	-0.0011	-0.0006	-0.0002
281	20509	-0.0006	-0.0005	0.0003	-0.0009	-0.0011	-0.0007	-0.0002
282	20649	-0.0005	-0.0004	0.0004	-0.0009	-0.0011	-0.0007	-0.0002
283	20790	-0.0005	-0.0004	0.0004	-0.0008	-0.0011	-0.0007	-0.0003
284	20931	-0.0004	-0.0004	0.0002	-0.0008	-0.0012	-0.0007	-0.0003
285	21073	-0.0004	-0.0004	0.0001	-0.0008	-0.0012	-0.0007	-0.0003
286	21215	-0.0004	-0.0003	0.0001	-0.0007	-0.0013	-0.0006	-0.0004
287	21358	-0.0004	-0.0003	0.0000	-0.0007	-0.0014	-0.0006	-0.0004
288	21501	-0.0003	-0.0004	-0.0001	-0.0006	-0.0014	-0.0006	-0.0003
289	21644	-0.0004	-0.0005	-0.0002	-0.0007	-0.0015	-0.0007	-0.0003
290	21788	-0.0004	-0.0006	-0.0002	-0.0006	-0.0015	-0.0007	-0.0002

	BJ10	**BJ13**	**BJ 16.5**	**BJ20**	**BJ23**	**BJ26**	**BJ36**
MW (peak)	**1247**	**1208**	**1247**	**1247**	**1247**	**1247**	**1208**
Mw (calc.)	**1429**	**1470**	**1486**	**1488**	**1498**	**1469**	**1483**
***Mn* (calc.)**	**1176**	**1195**	**1207**	**1207**	**1211**	**1196**	**1201**
Mn /Mw	**1.22**	**1.23**	**1.23**	**1.23**	**1.24**	**1.23**	**1.23**

Appendix 2D - DOC detector fractograms for King Site ground waters (BJ series).
Results of molecular weight calculations at end of table.

Time sec.	MW daltons	BJ10	BJ13	BJ16.5	BJ20	BJ23	BJ26	BJ36
0	0	-0.0234	0.0034	-0.0034	0.0003	0.0037	-0.0026	-0.0141
1	0	-0.0234	0.0034	-0.0034	0.0003	0.0037	-0.0026	-0.0141
2	0	-0.0234	0.0034	-0.0034	0.0003	0.0037	-0.0026	-0.0141
3	0	-0.0234	0.0034	-0.0034	0.0003	0.0037	-0.0026	-0.0141
4	0	-0.0234	0.0034	-0.0034	0.0003	0.0037	-0.0026	-0.0141
5	0	-0.0234	0.0034	-0.0034	0.0003	0.0037	-0.0026	-0.0141
6	0	-0.0234	0.0034	-0.0034	0.0003	0.0037	-0.0026	-0.0141
7	0	-0.0234	0.0034	-0.0034	0.0003	0.0037	-0.0026	-0.0141
8	0	-0.0234	0.0034	-0.0034	0.0003	0.0037	-0.0026	-0.0141
9	0	-0.0234	0.0034	-0.0034	0.0003	0.0037	-0.0026	-0.0141
10	0	-0.0234	0.0034	-0.0034	0.0003	0.0037	-0.0026	-0.0141
11	1	-0.0234	0.0034	-0.0034	0.0003	0.0037	-0.0026	-0.0141
12	1	-0.0234	0.0034	-0.0034	0.0003	0.0037	-0.0026	-0.0141
13	1	-0.0234	0.0034	-0.0034	0.0003	0.0037	-0.0026	-0.0141
14	1	-0.0234	0.0034	-0.0034	0.0003	0.0037	-0.0026	-0.0141
15	1	-0.0234	0.0034	-0.0034	0.0003	0.0037	-0.0026	-0.0141
16	2	-0.0234	0.0034	-0.0034	0.0003	0.0037	-0.0026	-0.0141
17	2	-0.0234	0.0034	-0.0034	0.0003	0.0037	-0.0026	-0.0141
18	2	-0.0234	0.0034	-0.0034	0.0003	0.0037	-0.0026	-0.0141
19	3	-0.0234	0.0034	-0.0034	0.0003	0.0037	-0.0026	-0.0141
20	3	-0.0234	0.0034	-0.0034	0.0003	0.0037	-0.0026	-0.0141
21	4	-0.0234	0.0034	-0.0034	0.0002	0.0037	-0.0026	-0.0141
22	5	-0.0234	0.0034	-0.0034	0.0002	0.0037	-0.0026	-0.0141
23	5	-0.0234	0.0034	-0.0034	0.0002	0.0037	-0.0026	-0.0141
24	6	-0.0234	0.0034	-0.0034	0.0002	0.0037	-0.0026	-0.0141
25	7	-0.0234	0.0034	-0.0034	0.0002	0.0037	-0.0026	-0.0141
26	8	-0.0234	0.0034	-0.0034	0.0002	0.0037	-0.0026	-0.0141
27	9	-0.0234	0.0034	-0.0034	0.0002	0.0037	-0.0026	-0.0141
28	10	-0.0234	0.0034	-0.0034	0.0002	0.0037	-0.0026	-0.0141
29	11	-0.0234	0.0034	-0.0034	0.0002	0.0037	-0.0026	-0.0141
30	12	-0.0234	0.0034	-0.0034	0.0002	0.0037	-0.0026	-0.0141
31	14	-0.0234	0.0034	-0.0034	0.0002	0.0037	-0.0026	-0.0141
32	15	-0.0234	0.0034	-0.0034	0.0002	0.0037	-0.0026	-0.0141
33	17	-0.0234	0.0034	-0.0034	0.0002	0.0037	-0.0026	-0.0141
34	18	-0.0234	0.0034	-0.0034	0.0002	0.0037	-0.0026	-0.0141
35	20	-0.0234	0.0034	-0.0034	0.0002	0.0037	-0.0026	-0.0141
36	22	-0.0234	0.0034	-0.0034	0.0002	0.0037	-0.0026	-0.0141
37	24	-0.0234	0.0034	-0.0034	0.0002	0.0037	-0.0026	-0.0141
38	26	-0.0234	0.0034	-0.0034	0.0002	0.0037	-0.0026	-0.0141
39	28	-0.0234	0.0034	-0.0034	0.0002	0.0037	-0.0026	-0.0141
40	30	-0.0234	0.0034	-0.0034	0.0002	0.0037	-0.0026	-0.0141
41	33	-0.0234	0.0034	-0.0034	0.0001	0.0037	-0.0026	-0.0141
42	35	-0.0234	0.0034	-0.0034	0.0001	0.0037	-0.0026	-0.0141
43	38	-0.0234	0.0034	-0.0034	0.0001	0.0037	-0.0026	-0.0141
44	41	-0.0234	0.0034	-0.0034	0.0001	0.0037	-0.0026	-0.0141
45	44	-0.0234	0.0034	-0.0034	0.0001	0.0037	-0.0026	-0.0141
46	47	-0.0234	0.0034	-0.0034	0.0001	0.0037	-0.0026	-0.0141

Appendix 2D Continued

47	50	-0.0234	0.0034	-0.0034	0.0001	0.0037	-0.0026	-0.0141
48	54	-0.0234	0.0034	-0.0034	0.0001	0.0037	-0.0026	-0.0141
49	57	-0.0234	0.0034	-0.0034	0.0001	0.0037	-0.0026	-0.0141
50	61	-0.0233	0.0034	-0.0034	0.0001	0.0037	-0.0026	-0.0141
51	65	-0.0233	0.0034	-0.0034	0.0001	0.0037	-0.0026	-0.0141
52	69	-0.0233	0.0034	-0.0034	0.0001	0.0038	-0.0026	-0.0141
53	73	-0.0234	0.0041	-0.0034	0.0001	0.0039	-0.0026	-0.0141
54	78	-0.0234	0.0047	-0.0034	0.0002	0.0040	-0.0026	-0.0141
55	83	-0.0230	0.0057	-0.0033	0.0003	0.0044	-0.0025	-0.0141
56	87	-0.0222	0.0084	-0.0033	0.0009	0.0051	-0.0022	-0.0141
57	92	-0.0205	0.0111	-0.0021	0.0017	0.0057	-0.0004	-0.0138
58	97	-0.0184	0.0131	0.0005	0.0024	0.0064	0.0016	-0.0129
59	103	-0.0146	0.0182	0.0029	0.0038	0.0085	0.0038	-0.0117
60	108	-0.0088	0.0269	0.0053	0.0070	0.0117	0.0080	-0.0105
61	114	-0.0018	0.0334	0.0134	0.0102	0.0148	0.0149	-0.0083
62	120	0.0056	0.0401	0.0221	0.0131	0.0179	0.0201	-0.0042
63	126	0.0157	0.0539	0.0291	0.0177	0.0235	0.0262	-0.0008
64	133	0.0274	0.0668	0.0363	0.0241	0.0291	0.0334	0.0023
65	139	0.0381	0.0756	0.0505	0.0285	0.0333	0.0403	0.0063
66	146	0.0496	0.0852	0.0591	0.0324	0.0376	0.0441	0.0096
67	153	0.0626	0.1314	0.0659	0.0414	0.0429	0.0529	0.0108
68	161	0.0741	0.1699	0.0730	0.0589	0.0466	0.0741	0.0119
69	168	0.0820	0.2058	0.0912	0.0731	0.0486	0.0964	0.0120
70	176	0.0916	0.2421	0.1016	0.0883	0.0509	0.1169	0.0098
71	184	0.1014	0.2780	0.1120	0.1130	0.0512	0.1424	0.0074
72	192	0.1096	0.2772	0.1260	0.1375	0.0499	0.1733	0.0049
73	201	0.1175	0.2770	0.1491	0.1630	0.0477	0.1904	0.0020
74	209	0.1481	0.2771	0.1775	0.1881	0.0430	0.2072	-0.0002
75	218	0.1919	0.2861	0.2071	0.2157	0.0388	0.2315	-0.0009
76	227	0.2318	0.3520	0.2446	0.2443	0.0372	0.2557	-0.0017
77	237	0.2920	0.4148	0.2855	0.2725	0.0359	0.2695	-0.0041
78	247	0.3690	0.4775	0.3299	0.2890	0.0325	0.2834	-0.0066
79	257	0.4311	0.5561	0.3566	0.3066	0.0269	0.2959	-0.0087
80	267	0.4759	0.6360	0.3827	0.3273	0.0207	0.3011	-0.0109
81	278	0.5356	0.6575	0.4004	0.3370	0.0122	0.3014	-0.0140
82	289	0.5739	0.6823	0.4094	0.3423	0.0026	0.2957	-0.0180
83	300	0.5945	0.7025	0.4059	0.3481	-0.0065	0.2749	-0.0212
84	311	0.6075	0.7069	0.3924	0.3515	-0.0109	0.2508	-0.0246
85	323	0.6207	0.7010	0.3776	0.3487	-0.0152	0.2270	-0.0248
86	335	0.6177	0.6964	0.3624	0.3464	-0.0146	0.1997	-0.0240
87	348	0.6145	0.6685	0.3482	0.3422	-0.0102	0.1756	-0.0206
88	360	0.6077	0.6445	0.3254	0.3360	-0.0046	0.1651	-0.0172
89	373	0.5847	0.6209	0.3012	0.3323	0.0013	0.1563	-0.0106
90	387	0.5488	0.5909	0.2781	0.3178	0.0096	0.1442	-0.0071
91	400	0.5159	0.5092	0.2489	0.2989	0.0144	0.1319	-0.0037
92	414	0.4752	0.4557	0.2165	0.2816	0.0168	0.1181	0.0011
93	428	0.4221	0.4023	0.1838	0.2665	0.0210	0.1061	0.0080
94	443	0.3731	0.3368	0.1641	0.2437	0.0320	0.0951	0.0116
95	458	0.3387	0.2610	0.1472	0.2274	0.0409	0.0857	0.0152
96	473	0.2929	0.2392	0.1392	0.2155	0.0497	0.0753	0.0208
97	489	0.2540	0.2122	0.1375	0.2047	0.0604	0.0701	0.0289

Appendix 2D Continued

98	505	0.2290	0.1939	0.1445	0.1865	0.0770	0.0646	0.0341
99	521	0.2146	0.1880	0.1576	0.1724	0.0861	0.0591	0.0395
100	538	0.2025	0.1985	0.1723	0.1632	0.0948	0.0555	0.0458
101	555	0.2039	0.2069	0.1869	0.1561	0.1053	0.0565	0.0505
102	572	0.2137	0.2260	0.1990	0.1466	0.1168	0.0570	0.0513
103	590	0.2247	0.2366	0.2126	0.1457	0.1208	0.0610	0.0525
104	608	0.2418	0.2465	0.2209	0.1480	0.1252	0.0680	0.0541
105	627	0.2556	0.2575	0.2252	0.1506	0.1298	0.0750	0.0549
106	646	0.2696	0.2722	0.2282	0.1562	0.1329	0.0823	0.0552
107	665	0.2769	0.2761	0.2313	0.1631	0.1338	0.0907	0.0556
108	685	0.2857	0.2804	0.2337	0.1691	0.1349	0.0961	0.0562
109	705	0.2898	0.2859	0.2346	0.1762	0.1362	0.1021	0.0564
110	725	0.2954	0.2915	0.2365	0.1844	0.1374	0.1075	0.0565
111	746	0.2998	0.2932	0.2382	0.1873	0.1389	0.1132	0.0567
112	767	0.3038	0.2953	0.2402	0.1904	0.1397	0.1181	0.0569
113	789	0.3071	0.2976	0.2416	0.1941	0.1408	0.1236	0.0570
114	811	0.3112	0.2988	0.2431	0.1977	0.1422	0.1255	0.0570
115	834	0.3145	0.2990	0.2438	0.1992	0.1436	0.1279	0.0571
116	857	0.3163	0.2994	0.2443	0.2008	0.1449	0.1298	0.0571
117	880	0.3181	0.3012	0.2445	0.2033	0.1462	0.1317	0.0570
118	904	0.3199	0.3027	0.2447	0.2056	0.1476	0.1325	0.0570
119	928	0.3207	0.3041	0.2449	0.2068	0.1488	0.1336	0.0568
120	953	0.3212	0.3051	0.2449	0.2080	0.1500	0.1342	0.0566
121	978	0.3221	0.3051	0.2449	0.2090	0.1509	0.1346	0.0564
122	1003	0.3224	0.3037	0.2449	0.2087	0.1512	0.1345	0.0563
123	1029	0.3219	0.3025	0.2444	0.2081	0.1511	0.1344	0.0558
124	1056	0.3212	0.2998	0.2438	0.2074	0.1512	0.1334	0.0555
125	1083	0.3196	0.2966	0.2433	0.2061	0.1506	0.1324	0.0552
126	1110	0.3164	0.2944	0.2414	0.2040	0.1494	0.1308	0.0549
127	1138	0.3132	0.2921	0.2391	0.2023	0.1484	0.1296	0.0543
128	1166	0.3096	0.2872	0.2373	0.2005	0.1474	0.1278	0.0539
129	1195	0.3051	0.2835	0.2350	0.1975	0.1454	0.1263	0.0536
130	1224	0.3005	0.2807	0.2318	0.1945	0.1429	0.1239	0.0531
131	1254	0.2974	0.2777	0.2301	0.1926	0.1408	0.1221	0.0521
132	1284	0.2929	0.2748	0.2289	0.1902	0.1390	0.1194	0.0511
133	1315	0.2874	0.2745	0.2260	0.1859	0.1355	0.1167	0.0500
134	1346	0.2830	0.2746	0.2231	0.1820	0.1319	0.1129	0.0485
135	1378	0.2795	0.2746	0.2213	0.1790	0.1287	0.1095	0.0465
136	1410	0.2731	0.2747	0.2193	0.1759	0.1254	0.1058	0.0446
137	1443	0.2664	0.2696	0.2140	0.1711	0.1202	0.1021	0.0432
138	1476	0.2617	0.2606	0.2103	0.1670	0.1165	0.0987	0.0415
139	1510	0.2570	0.2521	0.2072	0.1639	0.1131	0.0945	0.0401
140	1544	0.2501	0.2435	0.2039	0.1606	0.1093	0.0910	0.0387
141	1579	0.2435	0.2273	0.1983	0.1546	0.1041	0.0867	0.0378
142	1615	0.2358	0.2150	0.1930	0.1506	0.1001	0.0825	0.0366
143	1651	0.2269	0.2069	0.1870	0.1480	0.0965	0.0775	0.0352
144	1687	0.2164	0.1981	0.1805	0.1445	0.0920	0.0743	0.0332
145	1724	0.2065	0.1816	0.1720	0.1385	0.0871	0.0701	0.0319
146	1762	0.1951	0.1723	0.1617	0.1354	0.0841	0.0663	0.0301
147	1800	0.1856	0.1644	0.1544	0.1324	0.0818	0.0626	0.0281
148	1838	0.1754	0.1549	0.1464	0.1266	0.0783	0.0600	0.0258

Appendix 2D Continued

149	1878	0.1660	0.1377	0.1377	0.1193	0.0754	0.0571	0.0245
150	1917	0.1541	0.1292	0.1265	0.1148	0.0738	0.0545	0.0226
151	1958	0.1450	0.1210	0.1199	0.1100	0.0713	0.0522	0.0207
152	1999	0.1359	0.1110	0.1115	0.1015	0.0668	0.0508	0.0191
153	2040	0.1261	0.0991	0.1028	0.0948	0.0633	0.0488	0.0180
154	2082	0.1144	0.0953	0.0922	0.0905	0.0605	0.0461	0.0168
155	2125	0.1072	0.0908	0.0864	0.0860	0.0563	0.0443	0.0150
156	2168	0.0994	0.0843	0.0783	0.0775	0.0515	0.0428	0.0137
157	2212	0.0920	0.0777	0.0710	0.0728	0.0488	0.0413	0.0125
158	2257	0.0861	0.0744	0.0648	0.0689	0.0463	0.0393	0.0112
159	2302	0.0832	0.0708	0.0617	0.0642	0.0423	0.0382	0.0097
160	2347	0.0787	0.0645	0.0569	0.0566	0.0390	0.0368	0.0090
161	2394	0.0751	0.0597	0.0532	0.0532	0.0369	0.0350	0.0083
162	2441	0.0721	0.0569	0.0503	0.0498	0.0345	0.0320	0.0076
163	2488	0.0699	0.0538	0.0477	0.0457	0.0314	0.0294	0.0070
164	2536	0.0667	0.0482	0.0443	0.0408	0.0292	0.0269	0.0067
165	2585	0.0640	0.0454	0.0410	0.0390	0.0278	0.0243	0.0064
166	2635	0.0618	0.0429	0.0386	0.0370	0.0261	0.0211	0.0060
167	2685	0.0580	0.0403	0.0360	0.0341	0.0245	0.0188	0.0055
168	2735	0.0542	0.0363	0.0330	0.0314	0.0237	0.0169	0.0051
169	2787	0.0509	0.0348	0.0304	0.0301	0.0233	0.0148	0.0048
170	2839	0.0481	0.0334	0.0289	0.0287	0.0226	0.0130	0.0045
171	2892	0.0439	0.0316	0.0269	0.0264	0.0221	0.0117	0.0044
172	2945	0.0419	0.0292	0.0252	0.0246	0.0218	0.0109	0.0044
173	2999	0.0386	0.0282	0.0237	0.0235	0.0209	0.0098	0.0044
174	3054	0.0352	0.0272	0.0227	0.0223	0.0199	0.0088	0.0041
175	3109	0.0309	0.0255	0.0217	0.0206	0.0185	0.0079	0.0038
176	3165	0.0283	0.0236	0.0209	0.0197	0.0172	0.0072	0.0035
177	3222	0.0248	0.0225	0.0200	0.0191	0.0153	0.0061	0.0032
178	3279	0.0219	0.0213	0.0196	0.0184	0.0137	0.0053	0.0026
179	3337	0.0193	0.0198	0.0190	0.0175	0.0120	0.0045	0.0023
180	3396	0.0177	0.0189	0.0184	0.0171	0.0108	0.0038	0.0021
181	3456	0.0154	0.0185	0.0174	0.0167	0.0093	0.0031	0.0018
182	3516	0.0136	0.0181	0.0167	0.0163	0.0083	0.0027	0.0016
183	3577	0.0124	0.0170	0.0160	0.0159	0.0071	0.0024	0.0017
184	3638	0.0115	0.0163	0.0148	0.0157	0.0064	0.0022	0.0017
185	3701	0.0099	0.0157	0.0136	0.0156	0.0056	0.0019	0.0016
186	3764	0.0090	0.0151	0.0131	0.0152	0.0051	0.0017	0.0014
187	3828	0.0082	0.0139	0.0125	0.0145	0.0043	0.0015	0.0012
188	3892	0.0074	0.0134	0.0112	0.0138	0.0039	0.0012	0.0011
189	3957	0.0066	0.0128	0.0104	0.0129	0.0033	0.0010	0.0009
190	4023	0.0065	0.0122	0.0097	0.0118	0.0027	0.0007	0.0008
191	4090	0.0064	0.0115	0.0090	0.0108	0.0023	0.0004	0.0008
192	4158	0.0063	0.0114	0.0082	0.0100	0.0020	0.0001	0.0007
193	4226	0.0063	0.0112	0.0081	0.0092	0.0019	-0.0001	0.0006
194	4295	0.0063	0.0110	0.0080	0.0085	0.0018	-0.0002	0.0005
195	4365	0.0063	0.0109	0.0078	0.0079	0.0018	-0.0001	0.0004
196	4435	0.0063	0.0109	0.0073	0.0075	0.0017	-0.0001	0.0003
197	4507	0.0061	0.0109	0.0069	0.0073	0.0016	-0.0001	0.0003
198	4579	0.0056	0.0109	0.0065	0.0070	0.0014	-0.0002	0.0003
199	4652	0.0052	0.0109	0.0061	0.0066	0.0012	-0.0005	0.0003

Appendix 2D Continued

200	4725	0.0047	0.0109	0.0058	0.0064	0.0007	-0.0007	0.0004
201	4800	0.0042	0.0109	0.0054	0.0061	0.0005	-0.0009	0.0005
202	4875	0.0039	0.0109	0.0051	0.0058	0.0003	-0.0011	0.0004
203	4951	0.0038	0.0109	0.0048	0.0055	0.0001	-0.0012	0.0003
204	5028	0.0037	0.0109	0.0044	0.0053	-0.0001	-0.0012	0.0002
205	5106	0.0034	0.0109	0.0039	0.0051	-0.0002	-0.0012	0.0001
206	5184	0.0032	0.0107	0.0037	0.0047	-0.0003	-0.0011	0.0000
207	5263	0.0030	0.0101	0.0033	0.0044	-0.0004	-0.0010	0.0000
208	5344	0.0027	0.0096	0.0029	0.0041	-0.0006	-0.0010	-0.0001
209	5425	0.0025	0.0091	0.0024	0.0039	-0.0006	-0.0011	-0.0002
210	5506	0.0023	0.0083	0.0021	0.0039	-0.0007	-0.0011	-0.0002
211	5589	0.0023	0.0077	0.0019	0.0039	-0.0006	-0.0011	-0.0002
212	5672	0.0022	0.0074	0.0019	0.0040	-0.0006	-0.0011	0.0000
213	5757	0.0021	0.0071	0.0018	0.0041	-0.0005	-0.0010	0.0001
214	5842	0.0020	0.0064	0.0018	0.0041	-0.0003	-0.0008	0.0003
215	5928	0.0019	0.0060	0.0017	0.0037	-0.0002	-0.0007	0.0004
216	6015	0.0019	0.0056	0.0017	0.0034	-0.0001	-0.0007	0.0005
217	6103	0.0019	0.0052	0.0018	0.0031	-0.0001	-0.0007	0.0007
218	6191	0.0020	0.0045	0.0018	0.0028	-0.0001	-0.0008	0.0009
219	6281	0.0021	0.0042	0.0019	0.0025	-0.0003	-0.0009	0.0010
220	6371	0.0020	0.0040	0.0021	0.0025	-0.0006	-0.0009	0.0010
221	6462	0.0020	0.0037	0.0020	0.0024	-0.0007	-0.0009	0.0010
222	6554	0.0018	0.0034	0.0021	0.0021	-0.0008	-0.0007	0.0009
223	6647	0.0017	0.0033	0.0023	0.0019	-0.0011	-0.0007	0.0008
224	6741	0.0015	0.0032	0.0026	0.0017	-0.0012	-0.0006	0.0005
225	6836	0.0015	0.0030	0.0028	0.0013	-0.0012	-0.0005	0.0003
226	6932	0.0014	0.0026	0.0030	0.0009	-0.0014	-0.0002	0.0001
227	7028	0.0015	0.0023	0.0030	0.0007	-0.0014	-0.0002	0.0001
228	7126	0.0015	0.0020	0.0030	0.0006	-0.0013	0.0000	0.0000
229	7224	0.0014	0.0018	0.0029	0.0004	-0.0011	0.0001	0.0000
230	7324	0.0012	0.0017	0.0027	0.0004	-0.0009	0.0002	0.0000
231	7424	0.0011	0.0018	0.0023	0.0002	-0.0007	0.0002	0.0000
232	7525	0.0009	0.0019	0.0019	0.0000	-0.0007	0.0002	-0.0001
233	7627	0.0007	0.0020	0.0016	-0.0002	-0.0006	0.0002	-0.0002
234	7730	0.0004	0.0020	0.0013	-0.0006	-0.0005	0.0002	-0.0001
235	7835	0.0002	0.0020	0.0009	-0.0009	-0.0005	0.0001	-0.0002
236	7940	-0.0002	0.0021	0.0006	-0.0011	-0.0006	0.0001	-0.0002
237	8045	-0.0005	0.0019	0.0004	-0.0013	-0.0006	0.0000	-0.0002
238	8152	-0.0008	0.0017	0.0002	-0.0014	-0.0006	-0.0002	-0.0002
239	8260	-0.0010	0.0015	-0.0003	-0.0013	-0.0006	-0.0002	-0.0001
240	8369	-0.0012	0.0013	-0.0005	-0.0013	-0.0006	-0.0003	0.0003
241	8479	-0.0012	0.0015	-0.0007	-0.0012	-0.0005	-0.0003	0.0005
242	8590	-0.0011	0.0019	-0.0009	-0.0011	-0.0006	-0.0002	0.0008
243	8701	-0.0011	0.0023	-0.0012	-0.0011	-0.0007	-0.0001	0.0011
244	8814	-0.0010	0.0027	-0.0013	-0.0011	-0.0007	0.0000	0.0012
245	8928	-0.0011	0.0028	-0.0014	-0.0010	-0.0008	0.0002	0.0011
246	9043	-0.0012	0.0026	-0.0015	-0.0009	-0.0008	0.0002	0.0011
247	9158	-0.0012	0.0024	-0.0017	-0.0009	-0.0008	0.0002	0.0011
248	9275	-0.0010	0.0021	-0.0017	-0.0008	-0.0008	0.0002	0.0010
249	9393	-0.0009	0.0019	-0.0018	-0.0009	-0.0007	0.0002	0.0010
250	9512	-0.0007	0.0020	-0.0018	-0.0010	-0.0005	0.0002	0.0011

Appendix 2D Continued

251	9632	-0.0006	0.0020	-0.0018	-0.0011	-0.0004	0.0003	0.0011
252	9752	-0.0007	0.0020	-0.0017	-0.0012	-0.0003	0.0004	0.0011
253	9874	-0.0008	0.0020	-0.0017	-0.0011	-0.0001	0.0006	0.0012
254	9997	-0.0009	0.0020	-0.0016	-0.0009	0.0001	0.0008	0.0013
255	10121	-0.0010	0.0020	-0.0017	-0.0007	0.0002	0.0010	0.0014
256	10246	-0.0009	0.0019	-0.0018	-0.0004	0.0002	0.0011	0.0014
257	10372	-0.0008	0.0019	-0.0019	-0.0002	0.0002	0.0013	0.0015
258	10499	-0.0008	0.0019	-0.0019	-0.0002	0.0002	0.0015	0.0016
259	10627	-0.0008	0.0019	-0.0017	-0.0001	0.0001	0.0016	0.0017
260	10756	-0.0009	0.0019	-0.0013	-0.0001	0.0000	0.0016	0.0018
261	10887	-0.0011	0.0019	-0.0009	-0.0002	0.0001	0.0018	0.0019
262	11018	-0.0012	0.0019	-0.0003	-0.0001	0.0002	0.0019	0.0019
263	11150	-0.0015	0.0020	0.0000	-0.0001	0.0003	0.0020	0.0021
264	11284	-0.0018	0.0020	0.0002	0.0000	0.0004	0.0021	0.0022
265	11418	-0.0020	0.0018	0.0002	-0.0001	0.0006	0.0023	0.0024
266	11554	-0.0022	0.0015	0.0002	-0.0003	0.0007	0.0024	0.0025
267	11691	-0.0022	0.0013	0.0001	-0.0006	0.0008	0.0025	0.0024
268	11828	-0.0020	0.0012	0.0000	-0.0008	0.0009	0.0025	0.0022
269	11967	-0.0019	0.0010	0.0000	-0.0009	0.0009	0.0024	0.0020
270	12107	-0.0018	0.0010	0.0000	-0.0008	0.0009	0.0023	0.0019
271	12249	-0.0019	0.0010	-0.0001	-0.0006	0.0009	0.0021	0.0019
272	12391	-0.0020	0.0010	-0.0002	-0.0005	0.0009	0.0019	0.0021
273	12534	-0.0021	0.0007	-0.0003	-0.0004	0.0009	0.0017	0.0023
274	12679	-0.0023	0.0004	-0.0005	-0.0003	0.0010	0.0016	0.0025
275	12824	-0.0024	0.0001	-0.0007	-0.0004	0.0010	0.0015	0.0026
276	12971	-0.0024	-0.0003	-0.0008	-0.0005	0.0012	0.0015	0.0025
277	13119	-0.0025	-0.0007	-0.0010	-0.0006	0.0013	0.0015	0.0024
278	13268	-0.0025	-0.0008	-0.0012	-0.0007	0.0014	0.0014	0.0022
279	13418	-0.0024	-0.0010	-0.0013	-0.0007	0.0014	0.0014	0.0019
280	13570	-0.0023	-0.0010	-0.0014	-0.0007	0.0013	0.0012	0.0017
281	13722	-0.0022	-0.0010	-0.0015	-0.0006	0.0011	0.0011	0.0015
282	13876	-0.0021	-0.0009	-0.0015	-0.0005	0.0010	0.0011	0.0014
283	14031	-0.0021	-0.0008	-0.0015	-0.0003	0.0008	0.0011	0.0013
284	14187	-0.0022	-0.0008	-0.0015	-0.0002	0.0007	0.0011	0.0013
285	14344	-0.0023	-0.0008	-0.0015	-0.0002	0.0007	0.0012	0.0013
286	14502	-0.0023	-0.0009	-0.0016	-0.0002	0.0007	0.0013	0.0012
287	14662	-0.0022	-0.0010	-0.0016	-0.0002	0.0007	0.0013	0.0012
288	14823	-0.0022	-0.0013	-0.0015	-0.0003	0.0008	0.0014	0.0012
289	14985	-0.0022	-0.0014	-0.0016	-0.0004	0.0008	0.0014	0.0013
290	15148	-0.0024	-0.0015	-0.0017	-0.0004	0.0009	0.0013	0.0014

	BJ10	**BJ13**	**BJ16.5**	**BJ20**	**BJ23**	**BJ26**	**BJ36**
MW (peak)	**1084**	**1055**	**1055**	**1055**	**1084**	**1055**	**893**
Mw (calc.)	**1297**	**1285**	**1274**	**1306**	**1268**	**1267**	**1173**
***Mn* (calc.)**	**1064**	**1037**	**1018**	**1206**	**1024**	**1074**	**964**
Mn*/*Mw	**1.22**	**1.24**	**1.25**	**1.08**	**1.24**	**1.18**	**1.22**

Appendix 2E - DOC and UV (254 nm) detector fractograms for surface water samples. King Site Recharge (KSR) and Hangingstone River (HGSR). Results of molecular weight calculations at end of table.

Time sec.	MW - UV daltons	KSR-2 UV	HGSR-1 UV	MW - TOC daltons	KSR-2 DOC	HGSR-1 DOC
0	0	-0.0022	-0.0036	0		-0.0478
1	0	-0.0022	-0.0095	0		-0.0478
2	2	-0.0022	-0.0095	0	0.0067	-0.0478
3	3	-0.0022	-0.0095	0	0.0067	-0.0478
4	6	-0.0022	-0.0095	0	0.0067	-0.0478
5	9	-0.0022	-0.0095	0	0.0067	-0.0478
6	13	-0.0022	-0.0095	0	0.0067	-0.0478
7	17	-0.0022	-0.0095	0	0.0067	-0.0478
8	22	-0.0022	-0.0095	0	0.0067	-0.0478
9	28	-0.0022	-0.0095	0	0.0067	-0.0478
10	34	-0.0022	-0.0095	0	0.0067	-0.0478
11	41	-0.0022	-0.0095	1	0.0067	-0.0478
12	48	-0.0022	-0.0095	1	0.0067	-0.0478
13	56	-0.0022	-0.0095	1	0.0067	-0.0478
14	65	-0.0022	-0.0095	1	0.0067	-0.0478
15	74	-0.0022	-0.0095	1	0.0067	-0.0478
16	84	-0.0022	-0.0095	2	0.0067	-0.0478
17	94	0.0076	0.0096	2	0.0067	-0.0478
18	105	0.0339	0.0371	2	0.0067	-0.0478
19	117	0.0499	0.0574	3	0.0067	-0.0478
20	129	0.0577	0.0681	3	0.0067	-0.0478
21	141	0.0604	0.0717	4	0.0067	-0.0478
22	155	0.0596	0.0714	5	0.0067	-0.0478
23	168	0.0583	0.0700	5	0.0067	-0.0478
24	183	0.0578	0.0680	6	0.0067	-0.0478
25	198	0.0564	0.0659	7	0.0067	-0.0478
26	213	0.0544	0.0633	8	0.0067	-0.0478
27	229	0.0526	0.0606	9	0.0067	-0.0478
28	246	0.0509	0.0579	10	0.0067	-0.0478
29	263	0.0495	0.0550	11	0.0067	-0.0478
30	280	0.0482	0.0520	12	0.0067	-0.0478
31	299	0.0467	0.0496	14	0.0067	-0.0478
32	317	0.0447	0.0466	15	0.0067	-0.0478
33	337	0.0425	0.0437	17	0.0067	-0.0478
34	356	0.0403	0.0406	18	0.0067	-0.0478
35	377	0.0381	0.0383	20	0.0067	-0.0478
36	398	0.0363	0.0363	22	0.0067	-0.0478
37	419	0.0346	0.0345	24	0.0067	-0.0478
38	441	0.0330	0.0330	26	0.0067	-0.0478
39	464	0.0313	0.0318	28	0.0067	-0.0478
40	487	0.0301	0.0309	30	0.0067	-0.0478
41	510	0.0288	0.0303	33	0.0067	-0.0478
42	535	0.0280	0.0299	35	0.0067	-0.0478
43	559	0.0274	0.0297	38	0.0067	-0.0478
44	585	0.0269	0.0298	41	0.0067	-0.0478
45	610	0.0265	0.0300	44	0.0067	-0.0478

Appendix 2E - Continued

46	637	0.0263	0.0303	47	0.0067	-0.0478
47	663	0.0264	0.0306	50	0.0067	-0.0478
48	691	0.0264	0.0308	54	0.0067	-0.0478
49	719	0.0266	0.0317	57	0.0067	-0.0478
50	747	0.0268	0.0320	61	0.0067	-0.0478
51	776	0.0272	0.0325	65	0.0067	-0.0478
52	805	0.0276	0.0332	69	0.0067	-0.0478
53	835	0.0280	0.0339	73	0.0067	-0.0478
54	866	0.0285	0.0350	78	0.0067	-0.0478
55	897	0.0290	0.0360	83	0.0067	-0.0478
56	929	0.0297	0.0371	87	0.0075	-0.0478
57	961	0.0303	0.0383	92	0.0095	-0.0478
58	993	0.0309	0.0396	97	0.0114	-0.0478
59	1026	0.0316	0.0409	103	0.0132	-0.0480
60	1060	0.0322	0.0420	108	0.0223	-0.0479
61	1094	0.0330	0.0431	114	0.0313	-0.0426
62	1129	0.0338	0.0443	120	0.0390	-0.0427
63	1164	0.0346	0.0454	126	0.0469	-0.0427
64	1200	0.0355	0.0465	133	0.0548	-0.0416
65	1236	0.0364	0.0475	139	0.0555	-0.0167
66	1273	0.0372	0.0486	146	0.0553	-0.0189
67	1310	0.0379	0.0493	153	0.0553	-0.0188
68	1348	0.0386	0.0500	161	0.0553	-0.0128
69	1386	0.0393	0.0506	168	0.0523	-0.0007
70	1425	0.0401	0.0511	176	0.0476	-0.0023
71	1464	0.0409	0.0515	184	0.0432	-0.0022
72	1504	0.0416	0.0518	192	0.0387	-0.0040
73	1544	0.0422	0.0521	201	0.0346	-0.0054
74	1585	0.0428	0.0522	209	0.0335	-0.0053
75	1626	0.0434	0.0522	218	0.0340	-0.0052
76	1668	0.0440	0.0521	227	0.0344	-0.0177
77	1711	0.0446	0.0520	237	0.0305	-0.0202
78	1754	0.0450	0.0517	247	0.0263	-0.0197
79	1797	0.0455	0.0513	257	0.0220	-0.0199
80	1841	0.0459	0.0509	267	0.0178	-0.0199
81	1885	0.0461	0.0505	278	0.0048	-0.0197
82	1930	0.0463	0.0498	289	-0.0034	-0.0198
83	1976	0.0465	0.0490	300	-0.0114	-0.0198
84	2022	0.0466	0.0480	311	-0.0190	-0.0199
85	2068	0.0467	0.0469	323	-0.0247	-0.0147
86	2115	0.0466	0.0457	335	-0.0207	-0.0133
87	2162	0.0465	0.0446	348	-0.0155	-0.0135
88	2210	0.0464	0.0435	360	-0.0102	-0.0135
89	2259	0.0462	0.0425	373	-0.0054	-0.0052
90	2308	0.0459	0.0414	387	-0.0025	-0.0040
91	2357	0.0456	0.0402	400	-0.0005	-0.0043
92	2407	0.0453	0.0388	414	-0.0002	-0.0033
93	2458	0.0450	0.0377	428	0.0000	0.0265
94	2508	0.0446	0.0365	443	0.0002	0.0238
95	2560	0.0443	0.0353	458	0.0003	0.0240
96	2612	0.0438	0.0342	473	0.0005	0.0325

Appendix 2E - Continued

98	2717	0.0429	0.0321	505	0.0020	0.0549
99	2771	0.0424	0.0312	521	0.0033	0.0551
100	2825	0.0418	0.0301	538	0.0052	0.0520
101	2879	0.0413	0.0290	555	0.0080	0.0471
102	2934	0.0407	0.0280	572	0.0108	0.0478
103	2990	0.0401	0.0268	590	0.0140	0.0477
104	3045	0.0394	0.0257	608	0.0172	0.0450
105	3102	0.0388	0.0246	627	0.0206	0.0446
106	3159	0.0382	0.0237	646	0.0236	0.0447
107	3216	0.0375	0.0229	665	0.0272	0.0447
108	3274	0.0367	0.0221	685	0.0304	0.0458
109	3333	0.0361	0.0212	705	0.0338	0.0456
110	3392	0.0354	0.0204	725	0.0370	0.0457
111	3451	0.0347	0.0195	746	0.0406	0.0458
112	3511	0.0341	0.0186	767	0.0436	0.0496
113	3571	0.0334	0.0177	789	0.0466	0.0498
114	3632	0.0328	0.0170	811	0.0494	0.0499
115	3694	0.0321	0.0163	834	0.0520	0.0524
116	3755	0.0314	0.0156	857	0.0540	0.0566
117	3818	0.0308	0.0151	880	0.0560	0.0561
118	3881	0.0301	0.0144	904	0.0579	0.0561
119	3944	0.0295	0.0139	928	0.0601	0.0577
120	4008	0.0289	0.0133	953	0.0620	0.0585
121	4072	0.0282	0.0127	978	0.0635	0.0583
122	4137	0.0277	0.0123	1003	0.0646	0.0584
123	4202	0.0271	0.0119	1029	0.0659	0.0636
124	4268	0.0266	0.0116	1056	0.0663	0.0636
125	4334	0.0260	0.0112	1083	0.0667	0.0635
126	4401	0.0254	0.0108	1110	0.0671	0.0638
127	4468	0.0251	0.0103	1138	0.0686	0.0691
128	4536	0.0243	0.0099	1166	0.0688	0.0687
129	4604	0.0237	0.0096	1195	0.0692	0.0687
130	4673	0.0232	0.0092	1224	0.0701	0.0692
131	4742	0.0227	0.0087	1254	0.0707	0.0710
132	4812	0.0222	0.0087	1284	0.0713	0.0709
133	4882	0.0217	0.0085	1315	0.0719	0.0709
134	4953	0.0212	0.0081	1346	0.0724	0.0731
135	5024	0.0208	0.0078	1378	0.0725	0.0752
136	5096	0.0204	0.0075	1410	0.0730	0.0749
137	5168	0.0200	0.0069	1443	0.0740	0.0751
138	5240	0.0195	0.0064	1476	0.0747	0.0741
139	5314	0.0191	0.0059	1510	0.0757	0.0738
140	5387	0.0187	0.0055	1544	0.0771	0.0740
141	5461	0.0183	0.0050	1579	0.0776	0.0740
142	5536	0.0182	0.0046	1615	0.0780	0.0740
143	5611	0.0177	0.0043	1651	0.0784	0.0740
144	5686	0.0173	0.0041	1687	0.0793	0.0739
145	5762	0.0169	0.0039	1724	0.0797	0.0740
146	5839	0.0164	0.0037	1762	0.0801	0.0739
147	5916	0.0160	0.0036	1800	0.0806	0.0720
148	5993	0.0157	0.0035	1838	0.0814	0.0672

Appendix 2E - Continued

149	6071	0.0154	0.0033	1878	0.0818	0.0677
150	6150	0.0151	0.0031	1917	0.0822	0.0677
151	6229	0.0147	0.0030	1958	0.0824	0.0645
152	6308	0.0143	0.0028	1999	0.0822	0.0633
153	6388	0.0140	0.0026	2040	0.0818	0.0635
154	6468	0.0137	0.0023	2082	0.0814	0.0634
155	6549	0.0133	0.0021	2125	0.0807	0.0546
156	6630	0.0130	0.0019	2168	0.0801	0.0538
157	6712	0.0127	0.0017	2212	0.0797	0.0542
158	6794	0.0123	0.0015	2257	0.0793	0.0541
159	6877	0.0120	0.0013	2302	0.0781	0.0435
160	6960	0.0117	0.0012	2347	0.0770	0.0435
161	7044	0.0115	0.0011	2394	0.0762	0.0437
162	7128	0.0112	0.0010	2441	0.0754	0.0424
163	7213	0.0109	0.0009	2488	0.0732	0.0368
164	7298	0.0107	0.0009	2536	0.0719	0.0374
165	7384	0.0105	0.0009	2585	0.0706	0.0374
166	7470	0.0102	0.0008	2635	0.0693	0.0336
167	7556	0.0100	0.0008	2685	0.0672	0.0285
168	7644	0.0097	0.0009	2735	0.0664	0.0293
169	7731	0.0096	0.0008	2787	0.0655	0.0292
170	7819	0.0093	0.0006	2839	0.0622	0.0255
171	7908	0.0091	0.0006	2892	0.0610	0.0223
172	7997	0.0089	0.0006	2945	0.0597	0.0228
173	8086	0.0087	0.0004	2999	0.0573	0.0230
174	8176	0.0085	0.0003	3054	0.0554	0.0211
175	8266	0.0083		3109	0.0542	0.0207
176	8357	0.0081		3165	0.0530	0.0207
177	8449	0.0080		3222	0.0509	0.0209
178	8540	0.0078		3279	0.0500	0.0152
179	8633	0.0077		3337	0.0492	0.0155
180	8725	0.0076		3396	0.0483	0.0157
181	8819	0.0074		3456	0.0464	0.0155
182	8912	0.0073		3516	0.0453	0.0133
183	9007	0.0071		3577	0.0443	0.0136
184	9101	0.0070		3638	0.0431	0.0135
185	9196	0.0068		3701	0.0414	0.0126
186	9292	0.0066		3764	0.0408	0.0113
187	9388	0.0065		3828	0.0402	0.0115
188	9485	0.0063		3892	0.0394	0.0115
189	9582	0.0061		3957	0.0387	0.0089
190	9679	0.0060		4023	0.0386	0.0082
191	9777	0.0059		4090	0.0384	0.0083
192	9876	0.0059		4158	0.0379	0.0083
193	9975	0.0057		4226	0.0374	0.0075
194	10074	0.0055		4295	0.0370	0.0073
195	10174	0.0054		4365	0.0366	0.0073
196	10274	0.0052		4435	0.0355	0.0072
197	10375	0.0051		4507	0.0347	0.0062
198	10476	0.0051		4579	0.0341	0.0063
199	10578	0.0049		4652	0.0335	0.0062

Appendix 2E - Continued

200	10680	0.0047	4725	0.0323	0.0060
201	10783	0.0046	4800	0.0316	0.0051
202	10886	0.0045	4875	0.0310	0.0051
203	10990	0.0044	4951	0.0304	0.0053
204	11094	0.0043	5028	0.0291	0.0052
205	11199	0.0043	5106	0.0285	0.0051
206	11304	0.0042	5184	0.0279	0.0051
207	11409	0.0042	5263	0.0272	0.0051
208	11515	0.0042	5344	0.0261	0.0052
209	11622	0.0041	5425	0.0257	0.0052
210	11729	0.0040	5506	0.0253	0.0052
211	11836	0.0038	5589	0.0247	0.0053
212	11944	0.0038	5672	0.0239	0.0051
213	12052	0.0039	5757	0.0236	0.0051
214	12161	0.0038	5842	0.0231	0.0052
215	12270	0.0037	5928	0.0224	0.0052
216	12380	0.0036	6015	0.0215	0.0048
217	12490	0.0035	6103	0.0209	0.0040
218	12601	0.0034	6191	0.0202	0.0042
219	12712	0.0033	6281	0.0196	0.0040
220	12824	0.0032	6371	0.0193	0.0021
221	12936	0.0030	6462	0.0193	0.0019
222	13048	0.0030	6554	0.0194	0.0021
223	13161	0.0030	6647	0.0190	0.0021
224	13275	0.0029	6741	0.0185	0.0013
225	13389	0.0029	6836	0.0181	0.0011
226	13503	0.0030	6932	0.0176	0.0011
227	13618	0.0030	7028	0.0172	0.0011
228	13733	0.0030	7126	0.0172	0.0012
229	13849	0.0031	7224	0.0172	0.0011
230	13965	0.0031	7324	0.0172	0.0011
231	14082	0.0031	7424	0.0172	0.0010
232	14199	0.0030	7525	0.0172	0.0000
233	14317	0.0029	7627	0.0167	0.0000
234	14435	0.0029	7730	0.0163	0.0002
235	14554	0.0029	7835	0.0159	0.0008
236	14673	0.0028	7940	0.0152	0.0011
237	14792	0.0028	8045	0.0144	0.0010
238	14912	0.0028	8152	0.0140	0.0010
239	15033	0.0028	8260	0.0136	0.0004
240	15154	0.0027	8369	0.0128	-0.0001

	KSR-2 UV	**HGSR-1 UV**	**KSR-2 DOC**	**HGSR-1 DOC**
MW (peak)	**2115**	**1605**	**2226**	**1584**
***Mw* (calc.)**	**3001**	**2113**	**2784**	**1839**
***Mn* (calc.)**	**2037**	**1558**	**1679**	**1465**
Mw/Mn	**1.47**	**1.36**	**1.66**	**1.26**

Appendix 2F - DOC and UV (254 nm) detector fractograms for PSS 1430 dalton polymer. Results of molecular weight calculations at end of table.

Time sec.	MW - UV daltons	PSS 1430 UV	MW - DOC daltons	PSS 1430 DOC
0	0	0.0058	0	0.0120
1	0	0.0058	0	0.0120
2	1	0.0058	0	0.0120
3	2	0.0058	0	0.0120
4	4	0.0058	0	0.0120
5	6	0.0058	0	0.0120
6	8	0.0058	0	0.0120
7	12	0.0058	0	0.0120
8	15	0.0058	0	0.0120
9	20	0.0058	0	0.0120
10	24	0.0058	0	0.0120
11	30	0.0058	0	0.0120
12	36	0.0058	1	0.0120
13	42	0.0058	1	0.0120
14	49	0.0058	1	0.0120
15	57	0.0058	1	0.0120
16	65	0.0058	1	0.0120
17	74	0.1053	2	0.0120
18	83	0.1861	2	0.0120
19	93	0.2305	2	0.0120
20	103	0.2456	3	0.0120
21	114	0.2474	3	0.0120
22	126	0.2447	4	0.0120
23	138	0.2399	5	0.0120
24	151	0.2344	5	0.0120
25	165	0.2273	6	0.0120
26	179	0.2204	7	0.0120
27	193	0.2119	8	0.0120
28	208	0.2032	9	0.0120
29	224	0.1939	10	0.0120
30	241	0.1838	11	0.0120
31	258	0.1739	12	0.0120
32	275	0.1648	14	0.0120
33	294	0.1549	15	0.0120
34	313	0.1456	17	0.0120
35	332	0.1371	18	0.0120
36	352	0.1299	20	0.0120
37	373	0.1240	22	0.0120
38	394	0.1196	24	0.0120
39	416	0.1158	26	0.0120
40	439	0.1135	28	0.0120
41	462	0.1116	31	0.0120
42	486	0.1104	33	0.0120
43	510	0.1100	36	0.0120
44	535	0.1106	39	0.0120
45	561	0.1117	42	0.0120
46	587	0.1135	45	0.0120

Appendix 2F - Continued

47	614	0.1153	48	0.0120
48	642	0.1175	51	0.0120
49	670	0.1201	55	0.0120
50	699	0.1228	59	0.0120
51	728	0.1263	63	0.0120
52	759	0.1302	67	0.0120
53	789	0.1343	71	0.0120
54	821	0.1393	75	0.0120
55	853	0.1441	80	0.0120
56	885	0.1492	85	0.0120
57	919	0.1542	90	0.0120
58	953	0.1594	95	0.0120
59	987	0.1648	101	0.0197
60	1022	0.1701	106	0.0378
61	1058	0.1751	112	0.0390
62	1095	0.1792	118	0.0466
63	1132	0.1844	125	0.0599
64	1170	0.1880	131	0.0841
65	1208	0.1912	138	0.0822
66	1247	0.1937	145	0.0929
67	1287	0.1949	153	0.1040
68	1328	0.1952	160	0.1241
69	1369	0.1947	168	0.1222
70	1410	0.1934	176	0.1264
71	1453	0.1914	185	0.1295
72	1496	0.1886	193	0.1305
73	1540	0.1853	202	0.1303
74	1584	0.1812	211	0.1235
75	1629	0.1760	221	0.1123
76	1674	0.1705	231	0.0974
77	1721	0.1643	241	0.0990
78	1768	0.1572	251	0.0823
79	1815	0.1499	262	0.0684
80	1864	0.1427	273	0.0629
81	1913	0.1350	284	0.0637
82	1962	0.1273	296	0.0636
83	2012	0.1201	308	0.0534
84	2063	0.1123	320	0.0467
85	2115	0.1052	333	0.0476
86	2167	0.0982	346	0.0475
87	2220	0.0909	359	0.0475
88	2274	0.0841	373	0.0475
89	2328	0.0780	387	0.0475
90	2383	0.0719	401	0.0475
91	2439	0.0666	416	0.0434
92	2495	0.0609	431	0.0338
93	2552	0.0558	446	0.0330
94	2609	0.0506	462	0.0180
95	2668	0.0459	478	0.0145
96	2726	0.0417	495	0.0137
97	2786	0.0375	512	0.0247

Appendix 2F - Continued

98	2846	0.0337	530	0.0218
99	2907	0.0304	548	0.0290
100	2969	0.0272	566	0.0343
101	3031	0.0239	585	0.0467
102	3094	0.0216	604	0.0562
103	3158	0.0193	623	0.0707
104	3222	0.0178	643	0.0802
105	3287	0.0158	664	0.0938
106	3353	0.0145	685	0.1014
107	3419	0.0131	706	0.1149
108	3486	0.0122	728	0.1228
109	3554	0.0113	750	0.1243
110	3622	0.0107	773	0.1396
111	3691	0.0096	796	0.1463
112	3761	0.0088	820	0.1512
113	3831	0.0083	844	0.1590
114	3902	0.0075	869	0.1635
115	3974	0.0066	894	0.1656
116	4047	0.0058	920	0.1704
117	4120	0.0056	946	0.1749
118	4194	0.0050	972	0.1781
119	4268	0.0047	1000	0.1802
120	4343	0.0046	1027	0.1828
121	4419	0.0046	1056	0.1872
122	4496	0.0041	1084	0.1898
123	4573	0.0036	1114	0.1903
124	4651	0.0034	1144	0.1925
125	4730	0.0033	1174	0.1951
126	4809	0.0031	1205	0.1961
127	4889	0.0030	1237	0.1966
128	4969	0.0028	1269	0.1972
129	5051	0.0048	1302	0.1979
130	5133	0.0058	1335	0.1986
131	5216	0.0049	1369	0.1975
132	5299	0.0044	1403	0.1976
133	5383	0.0039	1438	0.1968
134	5468	0.0034	1474	0.1953
135	5553	0.0032	1510	0.1928
136	5640	0.0031	1547	0.1896
137	5727	0.0030	1585	0.1868
138	5814	0.0030	1623	0.1855
139	5902	0.0030	1662	0.1807
140	5991	0.0030	1701	0.1764
141	6081	0.0030	1741	0.1766
142	6171	0.0032	1782	0.1753
143	6262	0.0035	1823	0.1698
144	6354	0.0037	1865	0.1704
145	6447	0.0033	1908	0.1703
146	6540	0.0030	1951	0.1668
147	6633	0.0027	1995	0.1544
148	6728	0.0025	2040	0.1557

Appendix 2F - Continued

150	6919	0.0018	2132	0.1400
151	7016	0.0017	2179	0.1372
152	7113	0.0015	2226	0.1376
153	7211	0.0016	2274	0.1277
154	7310	0.0018	2323	0.1197
155	7409	0.0022	2373	0.1185
156	7509	0.0024	2424	0.1186
157	7610	0.0029	2475	0.1091
158	7711	0.0027	2527	0.1009
159	7814	0.0027	2579	0.1002
160	7917	0.0026	2633	0.1003
161	8020	0.0025	2687	0.0910
162	8124	0.0023	2742	0.0795
163	8229	0.0019	2798	0.0738
164	8335	0.0021	2854	0.0742
165	8442	0.0026	2912	0.0689
166	8549	0.0028	2970	0.0570
167	8657	0.0029	3029	0.0543
168	8765	0.0026	3088	0.0543
169	8874	0.0025	3149	0.0506
170	8984	0.0025	3210	0.0405
171	9095	0.0025	3272	0.0388
172	9206	0.0027	3335	0.0391
173	9318	0.0028	3399	0.0354
174	9431	0.0029	3464	0.0265
175	9544	0.0029	3530	0.0257
176	9659	0.0030	3596	0.0251
177	9773	0.0030	3663	0.0233
178	9889	0.0027	3731	0.0205
179	10005	0.0025	3800	0.0204
180	10122	0.0023	3870	0.0200
181	10240	0.0021	3941	0.0190
182	10358	0.0021	4013	0.0163
183	10478	0.0020	4085	0.0163
184	10597	0.0018	4159	0.0160
185	10718	0.0016	4233	0.0146
186	10839	0.0017	4308	0.0132
187	10961	0.0019	4385	0.0132
188	11084	0.0022	4462	0.0127
189	11207	0.0027	4540	0.0120
190	11331	0.0028	4619	0.0108
191	11456	0.0029	4699	0.0109
192	11582	0.0030	4780	0.0105
193	11708	0.0030	4862	0.0101
194	11835	0.0026	4945	0.0091
195	11962	0.0022	5029	0.0092
196	12091	0.0019	5113	0.0088
197	12220	0.0013	5199	0.0083
198	12350	0.0010	5286	0.0079
199	12480	0.0009	5374	0.0080
200	12611	0.0012	5463	0.0077

Appendix 2F - Continued

201	12743	0.0015	5553	0.0077
202	12876	0.0016	5644	0.0072
203	13009	0.0019	5735	0.0073
204	13143	0.0021	5828	0.0073
205	13278	0.0024	5922	0.0073
206	13414	0.0025	6017	0.0070
207	13550	0.0025	6113	0.0064
208	13687	0.0023	6211	0.0064
209	13825	0.0020	6309	0.0064
210	13963	0.0016	6408	0.0055
211	14102	0.0012	6508	0.0053
212	14242	-0.0003	6610	0.0053
213	14382	-0.0014	6712	0.0053
214	14524	-0.0022	6816	0.0052
215	14666	-0.0029	6921	0.0049
216	14808	-0.0032	7027	0.0049
217	14952	-0.0032	7134	0.0049
218	15096	-0.0032	7242	0.0046
219	15241	-0.0030	7351	0.0041
220	15386	-0.0028	7461	0.0041
221	15533	-0.0026	7573	0.0040
222	15680	-0.0024	7685	0.0037
223	15828	-0.0024	7799	0.0034
224	15976	-0.0022	7914	0.0034
225	16125	-0.0020	8030	0.0034
226	16275	-0.0019	8148	0.0035
227	16426	-0.0017	8266	0.0034
228	16577	-0.0018	8386	0.0031
229	16729	-0.0021	8507	0.0030
230	16882	-0.0026	8629	0.0028
231	17035	-0.0030	8752	0.0029
232	17190	-0.0034	8877	0.0028
233	17345	-0.0038	9003	0.0028
234	17500	-0.0039	9130	0.0027
235	17657	-0.0039	9258	0.0026
236	17814	-0.0039	9387	0.0026
237	17972	-0.0040	9518	0.0025
238	18130	-0.0041	9650	0.0023
239	18290	-0.0039	9783	0.0023
240	18450	-0.0038	9918	0.0023

	UV Results	**DOC Results**
MW (peak)	**1400**	**1400**
***Mw* (calc.)**	**1461**	**1480**
***Mn* (calc.)**	**1228**	**1237**
Mw/Mn	**1.19**	**1.20**

Appendix 2G - UV (254 nm) detector fractograms for Suwannee River humic standards. Results of molecular weight calculations at end of table.

Time sec.	MW daltons	SRFA Run 1	SRFA Run2	SRFA avg.	SRHA Run 1	SRHA Run2	SRHA avg.	SRNOM Run 1	SRNOM Run2	SRNOM avg.
0	0	-0.0092	-0.0114	-0.0103	0.0157	0.0082	0.0061	0.0053	0.0113	0.0083
1	0	-0.0092	-0.0114	-0.0103	0.0157	0.0082	0.0061	0.0053	0.0113	0.0083
2	1	-0.0092	-0.0114	-0.0103	0.0157	0.0082	0.0061	0.0053	0.0113	0.0083
3	2	-0.0092	-0.0114	-0.0103	0.0157	0.0082	0.0061	0.0053	0.0113	0.0083
4	4	-0.0092	-0.0114	-0.0103	0.0157	0.0082	0.0061	0.0053	0.0113	0.0083
5	6	-0.0092	-0.0114	-0.0103	0.0157	0.0082	0.0061	0.0053	0.0113	0.0083
6	8	-0.0092	-0.0114	-0.0103	0.0157	0.0082	0.0061	0.0053	0.0113	0.0083
7	12	-0.0092	-0.0114	-0.0103	0.0157	0.0082	0.0061	0.0053	0.0113	0.0083
8	15	-0.0092	-0.0114	-0.0103	0.0157	0.0082	0.0061	0.0053	0.0113	0.0083
9	20	-0.0092	-0.0114	-0.0103	0.0157	0.0082	0.0061	0.0053	0.0113	0.0083
10	24	-0.0092	-0.0114	-0.0103	0.0157	0.0082	0.0061	0.0053	0.0113	0.0083
11	30	-0.0092	-0.0114	-0.0103	0.0157	0.0082	0.0061	0.0053	0.0113	0.0083
12	36	-0.0092	-0.0114	-0.0103	0.0157	0.0082	0.0061	0.0053	0.0113	0.0083
13	42	-0.0092	-0.0114	-0.0103	0.0157	0.0082	0.0061	0.0053	0.0113	0.0083
14	49	-0.0092	-0.0114	-0.0103	0.0157	0.0082	0.0061	0.0053	0.0113	0.0083
15	57	-0.0092	-0.0114	-0.0103	0.0157	0.0082	0.0061	0.0053	0.0113	0.0083
16	65	0.0145	0.0063	0.0104	0.0157	0.0082	0.0228	0.0053	0.0113	0.0083
17	74	0.0577	0.0479	0.0528	0.0855	0.0720	0.0889	0.0484	0.0495	0.0490
18	83	0.0911	0.0777	0.0844	0.1520	0.1132	0.1362	0.0849	0.0768	0.0809
19	93	0.1066	0.0928	0.0997	0.1857	0.1290	0.1545	0.1004	0.0908	0.0956
20	103	0.1092	0.0968	0.1030	0.1907	0.1277	0.1530	0.1034	0.0927	0.0980
21	114	0.1059	0.0944	0.1002	0.1813	0.1203	0.1434	0.0998	0.0893	0.0946
22	126	0.1010	0.0904	0.0957	0.1677	0.1114	0.1322	0.0945	0.0849	0.0897
23	138	0.0963	0.0858	0.0911	0.1560	0.1034	0.1225	0.0894	0.0807	0.0851
24	151	0.0919	0.0822	0.0870	0.1444	0.0968	0.1142	0.0847	0.0773	0.0810
25	165	0.0876	0.0782	0.0829	0.1340	0.0911	0.1066	0.0803	0.0739	0.0771
26	179	0.0836	0.0759	0.0798	0.1251	0.0865	0.1003	0.0760	0.0706	0.0733
27	193	0.0797	0.0727	0.0762	0.1179	0.0822	0.0948	0.0721	0.0675	0.0698
28	208	0.0758	0.0679	0.0718	0.1122	0.0785	0.0902	0.0689	0.0650	0.0669
29	224	0.0718	0.0647	0.0683	0.1075	0.0750	0.0861	0.0656	0.0624	0.0640
30	241	0.0683	0.0610	0.0647	0.1035	0.0716	0.0823	0.0624	0.0597	0.0610
31	258	0.0645	0.0579	0.0612	0.0991	0.0682	0.0785	0.0591	0.0569	0.0580
32	275	0.0607	0.0549	0.0578	0.0946	0.0649	0.0749	0.0558	0.0542	0.0550
33	294	0.0574	0.0517	0.0546	0.0899	0.0616	0.0710	0.0525	0.0516	0.0521
34	313	0.0543	0.0491	0.0517	0.0849	0.0586	0.0673	0.0493	0.0491	0.0492
35	332	0.0516	0.0468	0.0492	0.0805	0.0557	0.0639	0.0463	0.0467	0.0465
36	352	0.0495	0.0445	0.0470	0.0762	0.0532	0.0609	0.0436	0.0447	0.0441
37	373	0.0478	0.0429	0.0453	0.0724	0.0511	0.0582	0.0416	0.0430	0.0423
38	394	0.0463	0.0413	0.0438	0.0693	0.0492	0.0560	0.0397	0.0416	0.0406
39	416	0.0453	0.0404	0.0428	0.0663	0.0477	0.0540	0.0384	0.0404	0.0394
40	439	0.0445	0.0395	0.0420	0.0637	0.0465	0.0524	0.0372	0.0396	0.0384
41	462	0.0440	0.0391	0.0415	0.0616	0.0457	0.0512	0.0363	0.0390	0.0376
42	486	0.0436	0.0389	0.0413	0.0601	0.0452	0.0504	0.0356	0.0386	0.0371
43	510	0.0437	0.0389	0.0413	0.0590	0.0449	0.0499	0.0352	0.0385	0.0369
44	535	0.0440	0.0392	0.0416	0.0580	0.0449	0.0496	0.0351	0.0386	0.0368
45	561	0.0446	0.0396	0.0421	0.0575	0.0451	0.0496	0.0351	0.0388	0.0369
46	587	0.0453	0.0405	0.0429	0.0573	0.0455	0.0498	0.0354	0.0391	0.0372

Appendix 2G Continued

47	614	0.0461	0.0414	0.0437	0.0573	0.0460	0.0501	0.0358	0.0395	0.0376
48	642	0.0470	0.0423	0.0446	0.0575	0.0466	0.0506	0.0364	0.0400	0.0382
49	670	0.0480	0.0432	0.0456	0.0579	0.0473	0.0512	0.0371	0.0406	0.0388
50	699	0.0492	0.0445	0.0469	0.0586	0.0482	0.0521	0.0376	0.0413	0.0395
51	728	0.0505	0.0457	0.0481	0.0595	0.0493	0.0531	0.0384	0.0420	0.0402
52	759	0.0517	0.0474	0.0496	0.0602	0.0505	0.0541	0.0392	0.0429	0.0411
53	789	0.0529	0.0489	0.0509	0.0614	0.0517	0.0553	0.0402	0.0440	0.0421
54	821	0.0544	0.0505	0.0524	0.0625	0.0530	0.0566	0.0412	0.0449	0.0430
55	853	0.0560	0.0519	0.0540	0.0638	0.0544	0.0580	0.0422	0.0460	0.0441
56	885	0.0580	0.0536	0.0558	0.0651	0.0558	0.0595	0.0432	0.0471	0.0452
57	919	0.0599	0.0554	0.0577	0.0665	0.0573	0.0609	0.0443	0.0483	0.0463
58	953	0.0616	0.0575	0.0595	0.0679	0.0590	0.0625	0.0455	0.0495	0.0475
59	987	0.0635	0.0592	0.0614	0.0694	0.0607	0.0642	0.0467	0.0508	0.0487
60	1022	0.0652	0.0611	0.0632	0.0711	0.0625	0.0659	0.0481	0.0520	0.0500
61	1058	0.0670	0.0631	0.0651	0.0728	0.0644	0.0678	0.0496	0.0533	0.0514
62	1095	0.0686	0.0648	0.0667	0.0747	0.0663	0.0697	0.0510	0.0546	0.0528
63	1132	0.0705	0.0668	0.0687	0.0765	0.0684	0.0716	0.0523	0.0559	0.0541
64	1170	0.0721	0.0686	0.0703	0.0784	0.0704	0.0736	0.0537	0.0572	0.0555
65	1208	0.0738	0.0702	0.0720	0.0804	0.0725	0.0756	0.0551	0.0583	0.0567
66	1247	0.0753	0.0718	0.0735	0.0821	0.0745	0.0776	0.0564	0.0595	0.0579
67	1287	0.0767	0.0732	0.0750	0.0841	0.0766	0.0796	0.0577	0.0605	0.0591
68	1328	0.0780	0.0746	0.0763	0.0862	0.0788	0.0816	0.0587	0.0616	0.0602
69	1369	0.0791	0.0757	0.0774	0.0883	0.0810	0.0839	0.0597	0.0627	0.0612
70	1410	0.0803	0.0768	0.0786	0.0904	0.0831	0.0861	0.0608	0.0637	0.0622
71	1453	0.0813	0.0779	0.0796	0.0923	0.0852	0.0881	0.0616	0.0646	0.0631
72	1496	0.0819	0.0787	0.0803	0.0944	0.0874	0.0902	0.0625	0.0654	0.0639
73	1540	0.0827	0.0795	0.0811	0.0965	0.0893	0.0922	0.0633	0.0660	0.0646
74	1584	0.0833	0.0800	0.0817	0.0985	0.0914	0.0942	0.0638	0.0664	0.0651
75	1629	0.0837	0.0805	0.0821	0.1005	0.0934	0.0961	0.0642	0.0669	0.0656
76	1674	0.0838	0.0806	0.0822	0.1024	0.0953	0.0981	0.0646	0.0673	0.0659
77	1721	0.0838	0.0806	0.0822	0.1043	0.0970	0.0998	0.0648	0.0677	0.0662
78	1768	0.0837	0.0807	0.0822	0.1061	0.0988	0.1015	0.0650	0.0679	0.0664
79	1815	0.0835	0.0804	0.0819	0.1078	0.1005	0.1032	0.0652	0.0679	0.0666
80	1864	0.0829	0.0799	0.0814	0.1093	0.1020	0.1048	0.0654	0.0678	0.0666
81	1913	0.0824	0.0795	0.0810	0.1106	0.1035	0.1060	0.0656	0.0677	0.0666
82	1962	0.0818	0.0791	0.0804	0.1120	0.1047	0.1074	0.0654	0.0675	0.0665
83	2012	0.0808	0.0783	0.0795	0.1133	0.1059	0.1086	0.0652	0.0673	0.0663
84	2063	0.0801	0.0777	0.0789	0.1145	0.1070	0.1096	0.0649	0.0670	0.0659
85	2115	0.0788	0.0767	0.0778	0.1157	0.1079	0.1107	0.0645	0.0666	0.0656
86	2167	0.0777	0.0757	0.0767	0.1168	0.1088	0.1117	0.0642	0.0661	0.0651
87	2220	0.0766	0.0746	0.0756	0.1179	0.1097	0.1126	0.0638	0.0656	0.0647
88	2274	0.0754	0.0734	0.0744	0.1187	0.1104	0.1133	0.0632	0.0650	0.0641
89	2328	0.0741	0.0721	0.0731	0.1193	0.1110	0.1139	0.0628	0.0644	0.0636
90	2383	0.0731	0.0708	0.0720	0.1199	0.1115	0.1144	0.0622	0.0636	0.0629
91	2439	0.0711	0.0693	0.0702	0.1202	0.1120	0.1147	0.0617	0.0630	0.0623
92	2495	0.0698	0.0677	0.0688	0.1206	0.1124	0.1150	0.0611	0.0622	0.0616
93	2552	0.0683	0.0662	0.0673	0.1208	0.1127	0.1152	0.0606	0.0615	0.0610
94	2609	0.0667	0.0646	0.0657	0.1211	0.1128	0.1154	0.0599	0.0606	0.0603
95	2668	0.0651	0.0630	0.0641	0.1212	0.1128	0.1154	0.0591	0.0599	0.0595
96	2726	0.0635	0.0613	0.0624	0.1212	0.1127	0.1153	0.0582	0.0590	0.0586
97	2786	0.0618	0.0595	0.0607	0.1211	0.1126	0.1152	0.0573	0.0580	0.0577

Appendix 2G Continued

98	2846	0.0602	0.0579	0.0590	0.1210	0.1124	0.1150	0.0564	0.0572	0.0568
99	2907	0.0588	0.0564	0.0576	0.1208	0.1121	0.1154	0.0555	0.0562	0.0559
100	2969	0.0569	0.0548	0.0559	0.1205	0.1118	0.1151	0.0545	0.0554	0.0550
101	3031	0.0553	0.0531	0.0542	0.1201	0.1114	0.1145	0.0533	0.0545	0.0539
102	3094	0.0537	0.0515	0.0526	0.1196	0.1109	0.1139	0.0521	0.0537	0.0529
103	3158	0.0522	0.0501	0.0512	0.1191	0.1104	0.1133	0.0510	0.0527	0.0519
104	3222	0.0505	0.0485	0.0495	0.1186	0.1098	0.1126	0.0499	0.0518	0.0509
105	3287	0.0490	0.0469	0.0480	0.1180	0.1091	0.1119	0.0490	0.0510	0.0500
106	3353	0.0475	0.0455	0.0465	0.1173	0.1085	0.1111	0.0481	0.0502	0.0491
107	3419	0.0461	0.0441	0.0451	0.1167	0.1078	0.1104	0.0472	0.0492	0.0482
108	3486	0.0449	0.0427	0.0438	0.1159	0.1070	0.1096	0.0463	0.0482	0.0473
109	3554	0.0434	0.0412	0.0423	0.1151	0.1062	0.1088	0.0454	0.0473	0.0464
110	3622	0.0421	0.0397	0.0409	0.1142	0.1054	0.1079	0.0443	0.0464	0.0453
111	3691	0.0409	0.0385	0.0397	0.1133	0.1046	0.1070	0.0432	0.0455	0.0443
112	3761	0.0395	0.0371	0.0383	0.1124	0.1038	0.1061	0.0421	0.0445	0.0433
113	3831	0.0384	0.0359	0.0372	0.1115	0.1029	0.1051	0.0412	0.0436	0.0424
114	3902	0.0369	0.0347	0.0358	0.1107	0.1021	0.1043	0.0402	0.0427	0.0415
115	3974	0.0358	0.0334	0.0346	0.1097	0.1010	0.1033	0.0393	0.0418	0.0406
116	4047	0.0342	0.0322	0.0332	0.1087	0.1001	0.1023	0.0384	0.0409	0.0397
117	4120	0.0328	0.0311	0.0319	0.1077	0.0992	0.1013	0.0376	0.0401	0.0388
118	4194	0.0317	0.0300	0.0309	0.1066	0.0980	0.1002	0.0368	0.0393	0.0380
119	4268	0.0303	0.0290	0.0296	0.1054	0.0970	0.0991	0.0359	0.0385	0.0372
120	4343	0.0292	0.0280	0.0286	0.1044	0.0961	0.0981	0.0353	0.0377	0.0365
121	4419	0.0281	0.0271	0.0276	0.1033	0.0953	0.0972	0.0345	0.0369	0.0357
122	4496	0.0270	0.0260	0.0265	0.1022	0.0944	0.0962	0.0336	0.0360	0.0348
123	4573	0.0258	0.0251	0.0254	0.1011	0.0934	0.0952	0.0328	0.0352	0.0340
124	4651	0.0250	0.0242	0.0246	0.1000	0.0924	0.0941	0.0321	0.0346	0.0333
125	4730	0.0239	0.0234	0.0237	0.0987	0.0914	0.0930	0.0315	0.0338	0.0326
126	4809	0.0230	0.0225	0.0228	0.0974	0.0903	0.0918	0.0309	0.0330	0.0320
127	4889	0.0221	0.0216	0.0218	0.0961	0.0891	0.0906	0.0304	0.0323	0.0313
128	4969	0.0212	0.0208	0.0210	0.0950	0.0880	0.0894	0.0299	0.0317	0.0308
129	5051	0.0203	0.0201	0.0202	0.0940	0.0869	0.0884	0.0294	0.0310	0.0302
130	5133	0.0194	0.0193	0.0194	0.0927	0.0858	0.0872	0.0288	0.0304	0.0296
131	5216	0.0185	0.0185	0.0185	0.0915	0.0847	0.0861	0.0281	0.0297	0.0289
132	5299	0.0178	0.0178	0.0178	0.0904	0.0836	0.0849	0.0274	0.0290	0.0282
133	5383	0.0170	0.0172	0.0171	0.0890	0.0824	0.0837	0.0267	0.0283	0.0275
134	5468	0.0163	0.0166	0.0165	0.0877	0.0812	0.0825	0.0262	0.0277	0.0269
135	5553	0.0156	0.0160	0.0158	0.0863	0.0802	0.0813	0.0257	0.0271	0.0264
136	5640	0.0151	0.0152	0.0152	0.0851	0.0789	0.0801	0.0252	0.0265	0.0258
137	5727	0.0145	0.0145	0.0145	0.0838	0.0777	0.0789	0.0247	0.0258	0.0252
138	5814	0.0138	0.0139	0.0139	0.0825	0.0764	0.0776	0.0241	0.0253	0.0247
139	5902	0.0133	0.0133	0.0133	0.0812	0.0753	0.0764	0.0237	0.0246	0.0242
140	5991	0.0128	0.0128	0.0128	0.0800	0.0740	0.0752	0.0232	0.0241	0.0236
141	6081	0.0124	0.0122	0.0123	0.0796	0.0728	0.0743	0.0226	0.0236	0.0231
142	6171	0.0118	0.0116	0.0117	0.0798	0.0718	0.0737	0.0220	0.0230	0.0225
143	6262	0.0114	0.0112	0.0113	0.0791	0.0706	0.0727	0.0213	0.0224	0.0218
144	6354	0.0110	0.0107	0.0109	0.0781	0.0695	0.0716	0.0207	0.0217	0.0212
145	6447	0.0107	0.0104	0.0106	0.0771	0.0683	0.0705	0.0201	0.0212	0.0206
146	6540	0.0104	0.0101	0.0103	0.0759	0.0672	0.0694	0.0194	0.0206	0.0200
147	6633	0.0100	0.0100	0.0100	0.0747	0.0659	0.0682	0.0188	0.0200	0.0194
148	6728	0.0096	0.0098	0.0097	0.0735	0.0647	0.0670	0.0182	0.0196	0.0189

Appendix 2G Continued

149	6823	0.0092	0.0096	0.0094	0.0721	0.0635	0.0657	0.0178	0.0191	0.0184
150	6919	0.0088	0.0093	0.0091	0.0710	0.0626	0.0647	0.0174	0.0187	0.0180
151	7016	0.0083	0.0091	0.0087	0.0697	0.0616	0.0636	0.0169	0.0183	0.0176
152	7113	0.0079	0.0088	0.0084	0.0686	0.0604	0.0625	0.0165	0.0179	0.0172
153	7211	0.0074	0.0084	0.0079	0.0674	0.0593	0.0614	0.0160	0.0174	0.0167
154	7310	0.0070	0.0079	0.0075	0.0662	0.0582	0.0603	0.0155	0.0169	0.0162
155	7409	0.0065	0.0076	0.0071	0.0650	0.0572	0.0592	0.0149	0.0165	0.0157
156	7509	0.0062	0.0072	0.0067	0.0639	0.0561	0.0582	0.0145	0.0161	0.0153
157	7610	0.0059	0.0070	0.0065	0.0628	0.0549	0.0571	0.0140	0.0158	0.0149
158	7711	0.0056	0.0067	0.0062	0.0616	0.0538	0.0559	0.0137	0.0155	0.0146
159	7814	0.0055	0.0062	0.0059	0.0605	0.0529	0.0549	0.0134	0.0151	0.0142
160	7917	0.0053	0.0058	0.0056	0.0594	0.0519	0.0539	0.0131	0.0148	0.0140
161	8020	0.0051	0.0054	0.0052	0.0582	0.0509	0.0528	0.0127	0.0145	0.0136
162	8124	0.0048	0.0051	0.0050	0.0572	0.0499	0.0518	0.0122	0.0142	0.0132
163	8229	0.0048	0.0048	0.0048	0.0561	0.0489	0.0508	0.0116	0.0138	0.0127
164	8335	0.0044	0.0046	0.0045	0.0551	0.0479	0.0497	0.0110	0.0134	0.0122
165	8442	0.0042	0.0043	0.0043	0.0540	0.0470	0.0489	0.0105	0.0131	0.0118
166	8549	0.0039	0.0040	0.0040	0.0530	0.0462	0.0479	0.0101	0.0127	0.0114
167	8657	0.0037	0.0037	0.0037	0.0521	0.0454	0.0470	0.0097	0.0124	0.0110
168	8765	0.0036	0.0035	0.0035	0.0511	0.0446	0.0461	0.0093	0.0121	0.0107
169	8874	0.0035	0.0034	0.0034	0.0500	0.0437	0.0452	0.0089	0.0118	0.0103
170	8984	0.0032	0.0034	0.0033	0.0491	0.0428	0.0443	0.0086	0.0116	0.0101
171	9095	0.0030	0.0034	0.0032	0.0481	0.0419	0.0434	0.0083	0.0113	0.0098
172	9206	0.0028	0.0034	0.0031	0.0472	0.0409	0.0424	0.0079	0.0111	0.0095
173	9318	0.0026	0.0034	0.0030	0.0462	0.0401	0.0415	0.0077	0.0108	0.0093
174	9431	0.0025	0.0032	0.0029	0.0453	0.0393	0.0407	0.0074	0.0106	0.0090
175	9544	0.0022	0.0030	0.0026	0.0443	0.0384	0.0399	0.0072	0.0103	0.0087
176	9659	0.0022	0.0029	0.0026	0.0434	0.0378	0.0391	0.0069	0.0102	0.0085
177	9773	0.0021	0.0028	0.0024	0.0424	0.0371	0.0382	0.0066	0.0100	0.0083
178	9889	0.0021	0.0026	0.0024	0.0417	0.0363	0.0374	0.0063	0.0098	0.0080
179	10005	0.0019	0.0025	0.0022	0.0408	0.0356	0.0366	0.0060	0.0096	0.0078
180	10122	0.0018	0.0023	0.0021	0.0400	0.0349	0.0359	0.0058	0.0093	0.0075
181	10240	0.0018	0.0022	0.0020	0.0393	0.0342	0.0352	0.0055	0.0091	0.0073
182	10358	0.0017	0.0021	0.0019	0.0385	0.0335	0.0345	0.0058	0.0089	0.0074
183	10478	0.0015	0.0020	0.0018	0.0377	0.0327	0.0337	0.0055	0.0086	0.0070
184	10597	0.0014	0.0019	0.0017	0.0371	0.0321	0.0331	0.0051	0.0085	0.0068
185	10718	0.0013	0.0018	0.0015	0.0365	0.0315	0.0325	0.0049	0.0082	0.0065
186	10839	0.0012	0.0015	0.0014	0.0358	0.0309	0.0319	0.0046	0.0080	0.0063
187	10961	0.0010	0.0015	0.0013	0.0351	0.0304	0.0312	0.0044	0.0079	0.0061
188	11084	0.0010	0.0013	0.0012	0.0342	0.0297	0.0305	0.0040	0.0077	0.0058
189	11207	0.0009	0.0012	0.0011	0.0335	0.0292	0.0299	0.0037	0.0075	0.0056
190	11331	0.0009	0.0012	0.0011	0.0328	0.0287	0.0293	0.0034	0.0074	0.0054
191	11456	0.0007	0.0010	0.0009	0.0321	0.0281	0.0286	0.0032	0.0072	0.0052
192	11582	0.0006	0.0009	0.0008	0.0315	0.0276	0.0280	0.0030	0.0070	0.0050
193	11708	0.0005	0.0010	0.0008	0.0309	0.0269	0.0275	0.0030	0.0069	0.0049
194	11835	0.0004	0.0009	0.0007	0.0303	0.0263	0.0269	0.0028	0.0067	0.0048
195	11962	0.0003	0.0008	0.0005	0.0298	0.0258	0.0265	0.0027	0.0066	0.0047
196	12091	0.0002	0.0007	0.0005	0.0292	0.0251	0.0259	0.0026	0.0065	0.0045
197	12220	0.0000	0.0007	0.0004	0.0288	0.0245	0.0254	0.0024	0.0064	0.0044
198	12350	-0.0001	0.0007	0.0003	0.0282	0.0241	0.0249	0.0023	0.0063	0.0043
199	12480	-0.0002	0.0006	0.0002	0.0276	0.0237	0.0244	0.0021	0.0062	0.0041

Appendix 2G Continued

200	12611	0.0000	0.0006	0.0003	0.0271	0.0232	0.0239	0.0019	0.0061	0.0040
201	12743	0.0001	0.0005	0.0003	0.0265	0.0228	0.0235	0.0018	0.0060	0.0039
202	12876	0.0002	0.0004	0.0003	0.0260	0.0224	0.0230	0.0018	0.0059	0.0039
203	13009	0.0003	0.0003	0.0003	0.0254	0.0221	0.0226	0.0019	0.0058	0.0038
204	13143	0.0004	0.0003	0.0003	0.0249	0.0218	0.0222	0.0019	0.0058	0.0038
205	13278	0.0005	0.0001	0.0003	0.0244	0.0214	0.0217	0.0019	0.0057	0.0038
206	13414	0.0005	-0.0001	0.0002	0.0239	0.0209	0.0212	0.0019	0.0057	0.0038
207	13550	0.0004	-0.0002	0.0001	0.0234	0.0205	0.0208	0.0018	0.0055	0.0036
208	13687	0.0002	-0.0003	0.0000	0.0231	0.0201	0.0204	0.0017	0.0054	0.0035
209	13825	0.0003	-0.0005	-0.0001	0.0225	0.0197	0.0200	0.0018	0.0053	0.0035
210	13963	0.0003	-0.0006	-0.0001	0.0220	0.0192	0.0195	0.0019	0.0052	0.0035
211	14102	0.0002	-0.0006	-0.0002	0.0216	0.0188	0.0191	0.0019	0.0051	0.0035
212	14242	0.0002	-0.0005	-0.0001	0.0212	0.0184	0.0188	0.0018	0.0051	0.0035
213	14382	0.0002	-0.0005	-0.0002	0.0209	0.0180	0.0184	0.0016	0.0050	0.0033
214	14524	0.0000	-0.0006	-0.0003	0.0206	0.0177	0.0181	0.0014	0.0048	0.0031
215	14666	-0.0001	-0.0005	-0.0003	0.0201	0.0174	0.0177	0.0012	0.0048	0.0030
216	14808	-0.0002	-0.0005	-0.0004	0.0196	0.0171	0.0173	0.0011	0.0047	0.0029
217	14952	-0.0002	-0.0006	-0.0004	0.0191	0.0166	0.0168	0.0010	0.0046	0.0028
218	15096	-0.0004	-0.0006	-0.0005	0.0187	0.0163	0.0164	0.0010	0.0044	0.0027
219	15241	-0.0005	-0.0006	-0.0005	0.0184	0.0160	0.0161	0.0010	0.0044	0.0027
220	15386	-0.0006	-0.0007	-0.0006	0.0181	0.0157	0.0158	0.0011	0.0044	0.0027
221	15533	-0.0006	-0.0006	-0.0006	0.0177	0.0154	0.0155	0.0011	0.0044	0.0027
222	15680	-0.0006	-0.0007	-0.0006	0.0174	0.0152	0.0152	0.0012	0.0044	0.0028
223	15828	-0.0007	-0.0006	-0.0007	0.0171	0.0148	0.0149	0.0012	0.0044	0.0028
224	15976	-0.0008	-0.0005	-0.0006	0.0168	0.0145	0.0146	0.0011	0.0043	0.0027
225	16125	-0.0008	-0.0003	-0.0005	0.0164	0.0143	0.0142	0.0011	0.0043	0.0027
226	16275	-0.0009	0.0000	-0.0004	0.0162	0.0139	0.0139	0.0010	0.0042	0.0026
227	16426	-0.0008	0.0003	-0.0003	0.0159	0.0136	0.0136	0.0008	0.0042	0.0025
228	16577	-0.0008	0.0006	-0.0001	0.0155	0.0134	0.0133	0.0006	0.0041	0.0024
229	16729	-0.0009	0.0008	0.0000	0.0152	0.0132	0.0131	0.0005	0.0040	0.0023
230	16882	-0.0008	0.0009	0.0000	0.0149	0.0130	0.0128	0.0004	0.0040	0.0022
231	17035	-0.0008	0.0009	0.0001	0.0146	0.0127	0.0126	0.0003	0.0040	0.0021
232	17190	-0.0008	0.0010	0.0001	0.0143	0.0124	0.0124	0.0003	0.0038	0.0021
233	17345	-0.0008	0.0011	0.0002	0.0140	0.0122	0.0121	0.0003	0.0037	0.0020
234	17500	-0.0008	0.0012	0.0002	0.0138	0.0120	0.0119	0.0004	0.0035	0.0019
235	17657	-0.0008	0.0012	0.0002	0.0135	0.0117	0.0117	0.0005	0.0034	0.0020
236	17814	-0.0009	0.0009	0.0000	0.0133	0.0115	0.0114	0.0006	0.0034	0.0020
237	17972	-0.0009	0.0007	-0.0001	0.0130	0.0114	0.0112	0.0008	0.0034	0.0021
238	18130	-0.0010	0.0006	-0.0002	0.0128	0.0112	0.0110	0.0010	0.0035	0.0022
239	18290	-0.0010	0.0007	-0.0001	0.0126	0.0110	0.0108	0.0011	0.0035	0.0023
240	18450	-0.0010	0.0008	-0.0001	0.0124	0.0107	0.0106	0.0012	0.0034	0.0023
241	18611	-0.0009	0.0009	0.0000	0.0121	0.0105	0.0103	0.0013	0.0034	0.00233
242	18772	-0.0009	0.0007	-0.0001	0.0118	0.0104	0.0102	0.0013	0.0034	0.00233
243	18934	-0.0010	0.0007	-0.0001	0.0117	0.0103	0.0100	0.0014	0.0034	0.002365

	SRFA	**SRHA**	**SRNOM**
MW (peak)	**1720**	**2726**	**1864**
Mw (calc.)	**2364**	**3792**	**2945**
***Mn* (calc.)**	**1658**	**2389**	**1885**
Mn /Mw	**1.43**	**1.59**	**1.56**

Appendix 2H - DOC detector fractograms for Suwannee River humic standards.
Results of molecular weight calculations at end of table.

Time sec.	MW daltons	SRFA Run 1	SRFA Run 2	SRFA avg.	SRHA Run 1	SRHA Run 2	SRHA avg.	SRNOM Run 1	SRNOM Run 2	SRNOM avg.
0	0	0.0005	0.0068	0.0037	0.0118	0.0327	0.0153	-0.0048	0.0080	0.0016
1	0	0.0005	0.0068	0.0037	0.0118	0.0327	0.0153	-0.0048	0.0080	0.0016
2	0	0.0005	0.0068	0.0037	0.0118	0.0327	0.0153	-0.0048	0.0080	0.0016
3	0	0.0005	0.0068	0.0037	0.0118	0.0327	0.0153	-0.0048	0.0080	0.0016
4	0	0.0005	0.0068	0.0037	0.0118	0.0327	0.0153	-0.0048	0.0080	0.0016
5	0	0.0005	0.0068	0.0037	0.0118	0.0327	0.0153	-0.0048	0.0080	0.0016
6	0	0.0005	0.0068	0.0037	0.0118	0.0327	0.0153	-0.0048	0.0080	0.0016
7	0	0.0005	0.0068	0.0037	0.0118	0.0327	0.0153	-0.0048	0.0080	0.0016
8	0	0.0005	0.0068	0.0037	0.0118	0.0327	0.0153	-0.0048	0.0080	0.0016
9	0	0.0005	0.0068	0.0037	0.0118	0.0327	0.0153	-0.0048	0.0080	0.0016
10	0	0.0005	0.0068	0.0037	0.0118	0.0327	0.0153	-0.0048	0.0080	0.0016
11	0	0.0005	0.0068	0.0037	0.0118	0.0327	0.0153	-0.0048	0.0080	0.0016
12	1	0.0005	0.0068	0.0037	0.0118	0.0327	0.0153	-0.0048	0.0080	0.0016
13	1	0.0005	0.0068	0.0037	0.0118	0.0327	0.0153	-0.0048	0.0080	0.0016
14	1	0.0005	0.0068	0.0037	0.0118	0.0327	0.0153	-0.0048	0.0080	0.0016
15	1	0.0005	0.0068	0.0037	0.0118	0.0327	0.0153	-0.0048	0.0080	0.0016
16	1	0.0005	0.0068	0.0037	0.0118	0.0327	0.0153	-0.0048	0.0080	0.0016
17	2	0.0005	0.0068	0.0037	0.0118	0.0327	0.0153	-0.0048	0.0080	0.0016
18	2	0.0005	0.0068	0.0037	0.0118	0.0327	0.0153	-0.0048	0.0080	0.0016
19	2	0.0005	0.0068	0.0037	0.0118	0.0327	0.0153	-0.0048	0.0080	0.0016
20	3	0.0005	0.0068	0.0037	0.0118	0.0327	0.0153	-0.0048	0.0080	0.0016
21	3	0.0005	0.0068	0.0037	0.0118	0.0327	0.0153	-0.0048	0.0080	0.0016
22	4	0.0005	0.0068	0.0037	0.0118	0.0327	0.0153	-0.0048	0.0080	0.0016
23	5	0.0005	0.0068	0.0037	0.0118	0.0327	0.0153	-0.0048	0.0080	0.0016
24	5	0.0005	0.0068	0.0037	0.0118	0.0327	0.0153	-0.0048	0.0080	0.0016
25	6	0.0005	0.0068	0.0037	0.0118	0.0327	0.0153	-0.0048	0.0080	0.0016
26	7	0.0005	0.0068	0.0037	0.0118	0.0327	0.0153	-0.0048	0.0080	0.0016
27	8	0.0005	0.0068	0.0037	0.0118	0.0327	0.0153	-0.0048	0.0080	0.0016
28	9	0.0005	0.0068	0.0037	0.0118	0.0327	0.0153	-0.0048	0.0080	0.0016
29	10	0.0005	0.0068	0.0037	0.0118	0.0327	0.0153	-0.0048	0.0080	0.0016
30	11	0.0005	0.0068	0.0037	0.0118	0.0327	0.0153	-0.0048	0.0080	0.0016
31	12	0.0005	0.0068	0.0037	0.0118	0.0327	0.0153	-0.0048	0.0080	0.0016
32	14	0.0005	0.0068	0.0037	0.0118	0.0327	0.0153	-0.0048	0.0080	0.0016
33	15	0.0005	0.0068	0.0037	0.0118	0.0327	0.0153	-0.0048	0.0080	0.0016
34	17	0.0005	0.0068	0.0037	0.0118	0.0327	0.0153	-0.0048	0.0080	0.0016
35	18	0.0005	0.0068	0.0037	0.0118	0.0327	0.0153	-0.0048	0.0080	0.0016
36	20	0.0005	0.0068	0.0037	0.0118	0.0327	0.0153	-0.0048	0.0080	0.0016
37	22	0.0005	0.0068	0.0037	0.0118	0.0327	0.0153	-0.0048	0.0080	0.0016
38	24	0.0005	0.0068	0.0037	0.0118	0.0327	0.0153	-0.0048	0.0080	0.0016
39	26	0.0005	0.0068	0.0037	0.0118	0.0327	0.0153	-0.0048	0.0080	0.0016
40	28	0.0005	0.0068	0.0037	0.0118	0.0327	0.0153	-0.0048	0.0080	0.0016
41	31	0.0005	0.0068	0.0037	0.0118	0.0327	0.0153	-0.0048	0.0080	0.0016
42	33	0.0005	0.0068	0.0037	0.0118	0.0327	0.0153	-0.0048	0.0080	0.0016
43	36	0.0005	0.0068	0.0037	0.0118	0.0327	0.0153	-0.0048	0.0080	0.0016
44	39	0.0005	0.0068	0.0037	0.0118	0.0327	0.0153	-0.0048	0.0080	0.0016
45	42	0.0005	0.0068	0.0037	0.0118	0.0327	0.0153	-0.0048	0.0080	0.0016
46	45	0.0005	0.0068	0.0037	0.0118	0.0327	0.0153	-0.0048	0.0080	0.0016

Appendix 2H Continued

47	48	0.0005	0.0068	0.0037	0.0118	0.0327	0.0152	-0.0048	0.0080	0.0016
48	51	0.0005	0.0068	0.0037	0.0118	0.0327	0.0156	-0.0048	0.0080	0.0016
49	55	0.0005	0.0068	0.0037	0.0118	0.0310	0.0160	-0.0048	0.0080	0.0016
50	59	0.0005	0.0068	0.0037	0.0118	0.0314	0.0166	-0.0048	0.0080	0.0016
51	63	0.0004	0.0069	0.0037	0.0118	0.0313	0.0174	-0.0048	0.0083	0.0019
52	67	0.0007	0.0070	0.0045	0.0118	0.0353	0.0205	-0.0048	0.0082	0.0028
53	71	0.0006	0.0071	0.0056	0.0118	0.0354	0.0228	-0.0048	0.0110	0.0041
54	75	0.0060	0.0086	0.0067	0.0118	0.0354	0.0269	0.0007	0.0116	0.0052
55	80	0.0060	0.0126	0.0077	0.0118	0.0354	0.0310	0.0042	0.0114	0.0082
56	85	0.0058	0.0122	0.0127	0.0120	0.0589	0.0410	0.0037	0.0115	0.0130
57	90	0.0059	0.0123	0.0177	0.0122	0.0586	0.0482	0.0039	0.0287	0.0181
58	95	0.0273	0.0298	0.0222	0.0200	0.0583	0.0593	0.0207	0.0343	0.0227
59	101	0.0255	0.0397	0.0270	0.0194	0.0585	0.0723	0.0299	0.0331	0.0311
60	106	0.0256	0.0381	0.0367	0.0194	0.1146	0.0904	0.0286	0.0332	0.0415
61	112	0.0271	0.0384	0.0420	0.0321	0.1131	0.1020	0.0289	0.0702	0.0504
62	118	0.0765	0.0384	0.0466	0.0487	0.1123	0.1194	0.0645	0.0724	0.0583
63	125	0.0723	0.0383	0.0541	0.0462	0.1130	0.1366	0.0715	0.0717	0.0713
64	131	0.0724	0.0383	0.0646	0.0464	0.1904	0.1544	0.0701	0.0718	0.0850
65	138	0.1012	0.0383	0.0699	0.0640	0.1838	0.1674	0.0704	0.1215	0.0953
66	145	0.1322	0.0384	0.0757	0.0842	0.1843	0.1843	0.1167	0.1198	0.1048
67	153	0.1293	0.0383	0.0844	0.0815	0.2055	0.1974	0.1201	0.1195	0.1179
68	160	0.1297	0.0383	0.0918	0.0818	0.2543	0.2067	0.1191	0.1197	0.1284
69	168	0.1601	0.0383	0.0957	0.1129	0.2484	0.2125	0.1193	0.1531	0.1344
70	176	0.1746	0.0383	0.1000	0.1144	0.2489	0.2192	0.1453	0.1519	0.1401
71	185	0.1720	0.0384	0.1033	0.1139	0.2542	0.2175	0.1445	0.1518	0.1458
72	193	0.1723	0.0383	0.1020	0.1140	0.2815	0.2130	0.1443	0.1519	0.1448
73	202	0.1622	0.0383	0.0991	0.1064	0.2787	0.2081	0.1442	0.1518	0.1416
74	211	0.1570	0.0282	0.0965	0.1070	0.2790	0.2024	0.1109	0.1518	0.1385
75	221	0.1579	0.0264	0.0874	0.1069	0.2672	0.1867	0.1131	0.1519	0.1353
76	231	0.1578	0.0268	0.0770	0.1069	0.2602	0.1743	0.1131	0.1519	0.1322
77	241	0.0928	0.0268	0.0679	0.0566	0.2613	0.1612	0.1130	0.1519	0.1324
78	251	0.0919	0.0042	0.0589	0.0602	0.2612	0.1469	0.1130	0.1519	0.1324
79	262	0.0927	0.0013	0.0411	0.0600	0.2230	0.1267	0.1130	0.1519	0.1324
80	273	0.0922	0.0019	0.0278	0.0456	0.2118	0.1142	0.1129	0.1520	0.1324
81	284	0.0056	0.0018	0.0167	-0.0066	0.2138	0.1015	0.1130	0.1519	0.1324
82	296	0.0087	-0.0227	0.0058	-0.0007	0.2134	0.0883	0.1130	0.1519	0.1324
83	308	0.0091	-0.0241	-0.0119	-0.0013	0.1837	0.0749	0.1130	0.1519	0.1277
84	320	0.0089	-0.0238	-0.0227	-0.0288	0.1687	0.0682	0.1130	0.1518	0.1233
85	333	-0.0584	-0.0238	-0.0312	-0.0635	0.1711	0.0618	0.1130	0.1048	0.1190
86	346	-0.0627	-0.0379	-0.0397	-0.0589	0.1708	0.0567	0.1131	0.1083	0.1145
87	359	-0.0618	-0.0380	-0.0481	-0.0594	0.1708	0.0533	0.1130	0.1082	0.1065
88	373	-0.0619	-0.0380	-0.0462	-0.0700	0.1709	0.0519	0.1130	0.1074	0.0997
89	387	-0.0604	-0.0379	-0.0427	-0.0858	0.1709	0.0502	0.1126	0.0722	0.0929
90	401	-0.0604	-0.0030	-0.0385	-0.0839	0.1708	0.0472	0.0747	0.0751	0.0860
91	416	-0.0604	-0.0056	-0.0305	-0.0841	0.1709	0.0432	0.0779	0.0750	0.0758
92	431	-0.0515	-0.0056	-0.0184	-0.0840	0.1495	0.0405	0.0778	0.0747	0.0659
93	446	-0.0147	-0.0054	-0.0102	-0.0840	0.1251	0.0376	0.0776	0.0406	0.0597
94	462	-0.0186	0.0406	-0.0017	-0.0840	0.1285	0.0335	0.0428	0.0428	0.0530
95	478	-0.0182	0.0371	0.0071	-0.0840	0.1281	0.0300	0.0456	0.0427	0.0439
96	495	-0.0183	0.0373	0.0151	-0.0840	0.1087	0.0283	0.0455	0.0407	0.0368
97	512	-0.0183	0.0492	0.0185	-0.0840	0.0976	0.0263	0.0431	0.0179	0.0332

Appendix 2H Continued

98	530	-0.0183	0.0779	0.0222	-0.0840	0.0991	0.0238	0.0275	0.0200	0.0299
99	548	-0.0183	0.0744	0.0264	-0.0841	0.0989	0.0232	0.0290	0.0199	0.0308
100	566	-0.0183	0.0748	0.0343	-0.0840	0.0909	0.0233	0.0289	0.0265	0.0360
101	585	-0.0183	0.0786	0.0397	-0.0841	0.0791	0.0233	0.0358	0.0595	0.0423
102	604	0.0263	0.0836	0.0453	-0.0840	0.0804	0.0243	0.0571	0.0559	0.0490
103	623	0.0309	0.0830	0.0510	-0.0840	0.0803	0.0263	0.0546	0.0563	0.0562
104	643	0.0295	0.0831	0.0609	-0.0540	0.0652	0.0279	0.0548	0.0608	0.0606
105	664	0.0298	0.0830	0.0654	-0.0539	0.0609	0.0294	0.0580	0.0698	0.0631
106	685	0.0761	0.0831	0.0696	-0.0543	0.0617	0.0331	0.0706	0.0686	0.0659
107	706	0.0723	0.0830	0.0744	-0.0541	0.0615	0.0346	0.0693	0.0687	0.0686
108	728	0.0724	0.0831	0.0811	-0.0175	0.0581	0.0356	0.0694	0.0697	0.0702
109	750	0.0738	0.0873	0.0831	-0.0198	0.0573	0.0369	0.0705	0.0722	0.0706
110	773	0.0917	0.0885	0.0854	-0.0198	0.0574	0.0409	0.0716	0.0717	0.0713
111	796	0.0901	0.0883	0.0883	-0.0164	0.0574	0.0417	0.0715	0.0718	0.0725
112	820	0.0903	0.0882	0.0913	0.0217	0.0610	0.0438	0.0715	0.0735	0.0736
113	844	0.0906	0.0945	0.0922	0.0180	0.0617	0.0469	0.0751	0.0763	0.0745
114	869	0.0957	0.0946	0.0933	0.0183	0.0615	0.0517	0.0769	0.0760	0.0758
115	894	0.0952	0.0942	0.0958	0.0338	0.0615	0.0541	0.0767	0.0760	0.0775
116	920	0.0953	0.0945	0.0978	0.0575	0.0667	0.0575	0.0767	0.0799	0.0787
117	946	0.1000	0.1029	0.0993	0.0544	0.0669	0.0612	0.0791	0.0826	0.0797
118	972	0.1029	0.1029	0.1010	0.0548	0.0666	0.0644	0.0812	0.0822	0.0809
119	1000	0.1024	0.1027	0.1039	0.0602	0.0668	0.0660	0.0808	0.0823	0.0824
120	1027	0.1026	0.1032	0.1057	0.0613	0.0732	0.0671	0.0808	0.0842	0.0834
121	1056	0.1087	0.1105	0.1072	0.0610	0.0731	0.0689	0.0856	0.0855	0.0842
122	1084	0.1112	0.1101	0.1088	0.0610	0.0730	0.0710	0.0862	0.0854	0.0853
123	1114	0.1108	0.1100	0.1107	0.0696	0.0730	0.0731	0.0860	0.0853	0.0868
124	1144	0.1108	0.1100	0.1114	0.0706	0.0818	0.0747	0.0860	0.0886	0.0877
125	1174	0.1142	0.1101	0.1118	0.0703	0.0814	0.0768	0.0899	0.0898	0.0885
126	1205	0.1162	0.1100	0.1124	0.0705	0.0814	0.0787	0.0903	0.0896	0.0896
127	1237	0.1161	0.1100	0.1133	0.0760	0.0815	0.0802	0.0903	0.0896	0.0908
128	1269	0.1161	0.1100	0.1143	0.0755	0.0882	0.0814	0.0903	0.0924	0.0914
129	1302	0.1206	0.1100	0.1150	0.0755	0.0877	0.0831	0.0933	0.0928	0.0921
130	1335	0.1203	0.1134	0.1157	0.0771	0.0876	0.0850	0.0935	0.0927	0.0928
131	1369	0.1203	0.1131	0.1165	0.0846	0.0877	0.0867	0.0934	0.0928	0.0935
132	1403	0.1202	0.1131	0.1171	0.0839	0.0954	0.0883	0.0935	0.0937	0.0938
133	1438	0.1203	0.1133	0.1174	0.0840	0.0949	0.0904	0.0957	0.0938	0.0941
134	1474	0.1203	0.1166	0.1177	0.0875	0.0950	0.0924	0.0955	0.0937	0.0944
135	1510	0.1202	0.1162	0.1179	0.0940	0.0956	0.0941	0.0954	0.0937	0.0943
136	1547	0.1202	0.1164	0.1176	0.0933	0.1004	0.0956	0.0953	0.0937	0.0941
137	1585	0.1193	0.1160	0.1171	0.0933	0.0999	0.0969	0.0933	0.0937	0.0939
138	1623	0.1182	0.1128	0.1163	0.0968	0.0999	0.0981	0.0934	0.0937	0.0937
139	1662	0.1182	0.1131	0.1150	0.0976	0.1003	0.0989	0.0934	0.0938	0.0934
140	1701	0.1155	0.1131	0.1134	0.0975	0.1033	0.0998	0.0933	0.0938	0.0932
141	1741	0.1139	0.1100	0.1123	0.0975	0.1030	0.1007	0.0934	0.0922	0.0930
142	1782	0.1140	0.1053	0.1106	0.1030	0.1030	0.1016	0.0935	0.0916	0.0928
143	1823	0.1140	0.1059	0.1087	0.1028	0.1040	0.1024	0.0935	0.0917	0.0923
144	1865	0.1084	0.1059	0.1070	0.1028	0.1065	0.1033	0.0934	0.0917	0.0913
145	1908	0.1064	0.1028	0.1058	0.1028	0.1062	0.1038	0.0934	0.0885	0.0905
146	1951	0.1067	0.1004	0.1038	0.1060	0.1062	0.1043	0.0891	0.0873	0.0896
147	1995	0.1067	0.1006	0.1013	0.1058	0.1062	0.1045	0.0892	0.0875	0.0884
148	2040	0.0991	0.1007	0.0991	0.1058	0.1062	0.1046	0.0892	0.0874	0.0868

Appendix 2H Continued

149	2086	0.0970	0.0922	0.0972	0.1055	0.1062	0.1046	0.0893	0.0833	0.0858
150	2132	0.0973	0.0902	0.0944	0.1048	0.1061	0.1045	0.0837	0.0821	0.0847
151	2179	0.0972	0.0904	0.0915	0.1048	0.1062	0.1044	0.0839	0.0824	0.0831
152	2226	0.0893	0.0903	0.0895	0.1048	0.1062	0.1042	0.0840	0.0822	0.0812
153	2274	0.0882	0.0823	0.0878	0.1047	0.1052	0.1042	0.0840	0.0766	0.0800
154	2323	0.0882	0.0819	0.0849	0.1047	0.1051	0.1041	0.0773	0.0760	0.0787
155	2373	0.0876	0.0821	0.0822	0.1048	0.1052	0.1039	0.0777	0.0761	0.0769
156	2424	0.0768	0.0820	0.0804	0.1048	0.1051	0.1037	0.0778	0.0761	0.0749
157	2475	0.0777	0.0748	0.0786	0.1048	0.1041	0.1034	0.0777	0.0702	0.0737
158	2527	0.0778	0.0747	0.0769	0.1046	0.1041	0.1031	0.0712	0.0697	0.0725
159	2579	0.0778	0.0747	0.0751	0.1036	0.1041	0.1026	0.0715	0.0698	0.0706
160	2633	0.0777	0.0747	0.0741	0.1038	0.1041	0.1020	0.0715	0.0698	0.0688
161	2687	0.0777	0.0636	0.0731	0.1038	0.1019	0.1015	0.0714	0.0636	0.0677
162	2742	0.0778	0.0643	0.0720	0.1026	0.1019	0.1010	0.0659	0.0635	0.0665
163	2798	0.0778	0.0643	0.0700	0.1016	0.1020	0.1000	0.0664	0.0636	0.0648
164	2854	0.0777	0.0641	0.0693	0.1017	0.1019	0.0990	0.0663	0.0636	0.0631
165	2912	0.0777	0.0553	0.0685	0.1017	0.0978	0.0981	0.0655	0.0586	0.0620
166	2970	0.0777	0.0561	0.0675	0.0983	0.0980	0.0973	0.0596	0.0583	0.0609
167	3029	0.0777	0.0561	0.0659	0.0973	0.0980	0.0961	0.0601	0.0584	0.0592
168	3088	0.0777	0.0551	0.0653	0.0975	0.0979	0.0952	0.0601	0.0584	0.0574
169	3149	0.0777	0.0482	0.0646	0.0975	0.0958	0.0946	0.0597	0.0532	0.0563
170	3210	0.0778	0.0488	0.0622	0.0953	0.0959	0.0941	0.0533	0.0531	0.0551
171	3272	0.0778	0.0488	0.0594	0.0954	0.0959	0.0930	0.0539	0.0531	0.0534
172	3335	0.0639	0.0464	0.0574	0.0955	0.0955	0.0921	0.0538	0.0532	0.0517
173	3399	0.0639	0.0409	0.0545	0.0953	0.0903	0.0914	0.0515	0.0492	0.0507
174	3464	0.0642	0.0416	0.0508	0.0943	0.0908	0.0906	0.0470	0.0489	0.0496
175	3530	0.0558	0.0415	0.0486	0.0943	0.0908	0.0893	0.0476	0.0490	0.0478
176	3596	0.0512	0.0385	0.0469	0.0943	0.0898	0.0883	0.0475	0.0489	0.0464
177	3663	0.0518	0.0360	0.0440	0.0932	0.0862	0.0874	0.0459	0.0433	0.0456
178	3731	0.0517	0.0363	0.0414	0.0887	0.0866	0.0864	0.0430	0.0437	0.0446
179	3800	0.0408	0.0362	0.0394	0.0892	0.0866	0.0849	0.0434	0.0437	0.0430
180	3870	0.0389	0.0326	0.0377	0.0891	0.0853	0.0838	0.0434	0.0437	0.0418
181	3941	0.0393	0.0306	0.0351	0.0872	0.0821	0.0831	0.0410	0.0393	0.0409
182	4013	0.0392	0.0310	0.0330	0.0858	0.0824	0.0822	0.0378	0.0396	0.0400
183	4085	0.0312	0.0310	0.0314	0.0860	0.0824	0.0806	0.0382	0.0396	0.0384
184	4159	0.0285	0.0275	0.0300	0.0861	0.0804	0.0795	0.0382	0.0396	0.0374
185	4233	0.0288	0.0266	0.0280	0.0826	0.0768	0.0785	0.0363	0.0351	0.0367
186	4308	0.0287	0.0269	0.0270	0.0817	0.0772	0.0774	0.0349	0.0354	0.0360
187	4385	0.0243	0.0268	0.0265	0.0819	0.0773	0.0755	0.0350	0.0354	0.0346
188	4462	0.0245	0.0268	0.0261	0.0818	0.0750	0.0744	0.0351	0.0354	0.0338
189	4540	0.0245	0.0268	0.0254	0.0755	0.0727	0.0734	0.0330	0.0309	0.0331
190	4619	0.0246	0.0269	0.0251	0.0755	0.0730	0.0722	0.0318	0.0313	0.0323
191	4699	0.0213	0.0269	0.0248	0.0756	0.0730	0.0705	0.0320	0.0313	0.0309
192	4780	0.0215	0.0270	0.0240	0.0755	0.0712	0.0698	0.0320	0.0310	0.0300
193	4862	0.0215	0.0265	0.0228	0.0723	0.0674	0.0690	0.0279	0.0279	0.0291
194	4945	0.0213	0.0223	0.0220	0.0724	0.0679	0.0681	0.0265	0.0282	0.0283
195	5029	0.0169	0.0227	0.0210	0.0725	0.0678	0.0666	0.0269	0.0281	0.0274
196	5113	0.0173	0.0226	0.0194	0.0713	0.0659	0.0658	0.0268	0.0282	0.0272
197	5199	0.0173	0.0212	0.0181	0.0669	0.0646	0.0650	0.0259	0.0282	0.0272
198	5286	0.0160	0.0160	0.0172	0.0674	0.0647	0.0637	0.0257	0.0282	0.0270
199	5374	0.0141	0.0164	0.0162	0.0673	0.0647	0.0621	0.0257	0.0282	0.0269

Appendix 2H Continued

200	5463	0.0142	0.0164	0.0150	0.0647	0.0615	0.0613	0.0257	0.0282	0.0268
201	5553	0.0142	0.0156	0.0145	0.0617	0.0603	0.0604	0.0257	0.0282	0.0264
202	5644	0.0130	0.0142	0.0141	0.0621	0.0605	0.0592	0.0257	0.0268	0.0261
203	5735	0.0121	0.0144	0.0135	0.0621	0.0605	0.0580	0.0257	0.0249	0.0258
204	5828	0.0122	0.0144	0.0127	0.0606	0.0587	0.0574	0.0258	0.0250	0.0252
205	5922	0.0122	0.0127	0.0120	0.0599	0.0573	0.0567	0.0257	0.0251	0.0243
206	6017	0.0104	0.0111	0.0114	0.0600	0.0574	0.0557	0.0252	0.0225	0.0236
207	6113	0.0090	0.0114	0.0106	0.0600	0.0575	0.0547	0.0212	0.0218	0.0228
208	6211	0.0090	0.0114	0.0097	0.0558	0.0575	0.0541	0.0216	0.0220	0.0218
209	6309	0.0090	0.0096	0.0092	0.0558	0.0575	0.0536	0.0216	0.0219	0.0207
210	6408	0.0070	0.0091	0.0088	0.0558	0.0574	0.0526	0.0211	0.0196	0.0202
211	6508	0.0069	0.0092	0.0083	0.0558	0.0574	0.0520	0.0182	0.0187	0.0195
212	6610	0.0070	0.0092	0.0080	0.0501	0.0574	0.0517	0.0185	0.0188	0.0187
213	6712	0.0070	0.0092	0.0079	0.0506	0.0574	0.0514	0.0185	0.0188	0.0179
214	6816	0.0059	0.0092	0.0078	0.0505	0.0574	0.0510	0.0184	0.0166	0.0175
215	6921	0.0060	0.0093	0.0074	0.0506	0.0574	0.0510	0.0173	0.0155	0.0171
216	7027	0.0060	0.0092	0.0068	0.0505	0.0574	0.0508	0.0174	0.0157	0.0165
217	7134	0.0059	0.0064	0.0063	0.0506	0.0575	0.0505	0.0174	0.0157	0.0157
218	7242	0.0038	0.0060	0.0057	0.0505	0.0573	0.0498	0.0163	0.0148	0.0152
219	7351	0.0039	0.0061	0.0051	0.0506	0.0573	0.0490	0.0129	0.0146	0.0147
220	7461	0.0038	0.0060	0.0047	0.0506	0.0516	0.0479	0.0132	0.0146	0.0141
221	7573	0.0038	0.0051	0.0046	0.0492	0.0511	0.0470	0.0132	0.0146	0.0135
222	7685	0.0038	0.0050	0.0045	0.0484	0.0513	0.0458	0.0129	0.0139	0.0134
223	7799	0.0037	0.0051	0.0043	0.0485	0.0512	0.0445	0.0121	0.0136	0.0132
224	7914	0.0039	0.0050	0.0042	0.0485	0.0461	0.0431	0.0122	0.0136	0.0128
225	8030	0.0038	0.0041	0.0040	0.0421	0.0459	0.0420	0.0122	0.0136	0.0125
226	8148	0.0038	0.0040	0.0038	0.0421	0.0459	0.0407	0.0118	0.0127	0.0123
227	8266	0.0029	0.0040	0.0035	0.0422	0.0460	0.0393	0.0111	0.0126	0.0121
228	8386	0.0028	0.0040	0.0033	0.0422	0.0398	0.0381	0.0112	0.0126	0.0116
229	8507	0.0029	0.0029	0.0029	0.0377	0.0396	0.0371	0.0112	0.0125	0.0111
230	8629	0.0027	0.0030	0.0026	0.0381	0.0397	0.0357	0.0101	0.0106	0.0107
231	8752	0.0008	0.0030	0.0023	0.0381	0.0397	0.0345	0.0089	0.0104	0.0102
232	8877	0.0007	0.0030	0.0021	0.0380	0.0345	0.0336	0.0091	0.0105	0.0097
233	9003	0.0007	0.0029	0.0017	0.0358	0.0345	0.0330	0.0090	0.0105	0.0095
234	9130	0.0007	0.0030	0.0014	0.0360	0.0345	0.0321	0.0091	0.0094	0.0094
235	9258	-0.0014	0.0030	0.0010	0.0360	0.0345	0.0314	0.0090	0.0094	0.0093
236	9387	-0.0014	0.0027	0.0006	0.0344	0.0322	0.0307	0.0090	0.0095	0.0090
237	9518	-0.0014	0.0008	0.0003	0.0315	0.0324	0.0301	0.0091	0.0095	0.0087
238	9650	-0.0012	0.0008	0.0002	0.0320	0.0324	0.0294	0.0082	0.0084	0.0084
239	9783	-0.0002	0.0009	0.0001	0.0319	0.0324	0.0290	0.0068	0.0084	0.0081
240	9918	-0.0002	0.0008	0.0002	0.0319	0.0302	0.0286	0.0070	0.0084	0.0076
241	10054	-0.0004	0.0008	0.0001	0.0319	0.0303	0.0283	0.0070	0.0084	0.0072
242	10191	-0.0007	0.0008	0.0000	0.0319	0.0303	0.0279	0.0064	0.0074	0.0071
243	10329	-0.0014	0.0009	-0.0001	0.0319	0.0303	0.0275	0.0058	0.0072	0.0068

	SRFA	**SRHA**	**SRNOM**
MW (peak)	**1510**	**2040**	**1474**
Mw (calc.)	**1900**	**3199**	**2263**
***Mn* (calc.)**	**1518**	**2039**	**1454**
Mn /Mw	**1.25**	**1.57**	**1.56**

Appendix 2I - Data used for the calculation of Continuous Normalized Intensity Comparasin (NIC) for Suwannee River Natural Organic Matter (SRNOM) and King Site 2.2 m ground water sample (B10).

SRNOM					B10				
MW	UV	MW	DOC	NIC	MW	UV	MW	TOC	NIC
535	0.0368	530	0.0299	1.099	462	0.1280	462	0.1275	1.090
		548	0.0308		486	0.1285	478	0.1426	0.978
561	0.0369	566	0.0360	0.915			495	0.1725	
587	0.0372	585	0.0423	0.786	510	0.1297	512	0.1892	0.744
614	0.0376	604	0.0490	0.687	535	0.1315	530	0.2042	0.698
		623	0.0562				548	0.2222	
642	0.0382	643	0.0606	0.564	561	0.1337	566	0.2494	0.580
670	0.0388	664	0.0631	0.552	587	0.1366	585	0.2611	0.565
699	0.0395	685	0.0659	0.538	614	0.1400	604	0.2732	0.553
		706	0.0686				623	0.2867	
728	0.0402	728	0.0702	0.516	642	0.1437	643	0.3008	0.514
759	0.0411	750	0.0706	0.525	670	0.1475	664	0.3044	0.521
789	0.0421	773	0.0713	0.534	699	0.1515	685	0.3085	0.527
		796	0.0725				706	0.3136	
821	0.0430	820	0.0736	0.531	728	0.1556	728	0.3185	0.523
853	0.0441	844	0.0745	0.538	759	0.1602	750	0.3202	0.535
		869	0.0758				773	0.3222	
885	0.0452	894	0.0775	0.531	789	0.1647	796	0.3247	0.541
919	0.0463	920	0.0787	0.537	821	0.1691	820	0.3262	0.552
953	0.0475	946	0.0797	0.546	853	0.1733	844	0.3267	0.564
987	0.0487	972	0.0809	0.553			869	0.3273	
		1000	0.0824		885	0.1774	894	0.3279	0.574
1022	0.0500	1027	0.0834	0.552	919	0.1810	920	0.3280	0.585
1058	0.0514	1056	0.0842	0.563	953	0.1844	946	0.3280	0.596
1095	0.0528	1084	0.0853	0.572	987	0.1871	972	0.3280	0.604
		1114	0.0868				1000	0.3280	0.034
1132	0.0541	1144	0.0877	0.571	1022	0.1894	1027	0.3273	0.612
1170	0.0555	1174	0.0885	0.581	1058	0.1908	1056	0.3263	0.619
1208	0.0567	1205	0.0896	0.588	1095	0.1916	1084	0.3252	0.623
1247	0.0579	1237	0.0908	0.594			1114	0.3236	
1287	0.0591	1269	0.0914	0.602	1132	0.1917	1144	0.3185	0.636
		1302	0.0921		1170	0.1910	1174	0.3137	0.644
1328	0.0602	1335	0.0928	0.605	1208	0.1896	1205	0.3094	0.648
1369	0.0612	1369	0.0935	0.612	1247	0.1874	1237	0.3028	0.655
1410	0.0622	1403	0.0938	0.621	1287	0.1843	1269	0.2922	0.668
1453	0.0631	1438	0.0941	0.628			1302	0.2847	
1496	0.0639	1474	0.0944	0.635	1328	0.1805	1335	0.2777	0.689
		1510	0.0943		1369	0.1759	1369	0.2674	0.699
1540	0.0646	1547	0.0941	0.644	1410	0.1710	1403	0.2538	0.717
1584	0.0651	1585	0.0939	0.651	1453	0.1659	1438	0.2446	0.723
1629	0.0656	1623	0.0937	0.657	1496	0.1600	1474	0.2359	0.730
1674	0.0659	1662	0.0934	0.663			1510	0.2238	
1721	0.0662	1701	0.0932	0.668	1540	0.1534	1547	0.2091	0.750
1768	0.0664	1741	0.0930	0.671	1584	0.1467	1585	0.2004	0.770
		1782	0.0928		1629	0.1402	1623	0.1916	0.780
1815	0.0666	1823	0.0923	0.678	1674	0.1329	1662	0.1799	0.800

Appendix 2I - Continued

1864	0.0666	1865	0.0913	0.686			1701	0.1674	
1913	0.0666	1908	0.0905	0.692	1721	0.1257	1741	0.1609	0.820
1962	0.0665	1951	0.0896	0.697	1768	0.1188	1782	0.1542	0.830
2012	0.0663	1995	0.0884	0.704	1815	0.1116	1823	0.1446	0.848
2063	0.0659	2040	0.0868	0.714	1864	0.1046	1865	0.1346	0.859
		2086	0.0858		1913	0.0981	1908	0.1287	0.860
2115	0.0656	2132	0.0847	0.727	1962	0.0916	1951	0.1227	0.870
2167	0.0651	2179	0.0831	0.736	2012	0.0856	1995	0.1146	0.880
2220	0.0647	2226	0.0812	0.747			2040	0.1061	
2274	0.0641	2274	0.0800	0.751	2063	0.0797	2086	0.1013	0.890
2328	0.0636	2323	0.0787	0.756	2115	0.0740	2132	0.0964	0.900
2383	0.0629	2373	0.0769	0.766	2167	0.0682	2179	0.0894	0.905
2439	0.0623	2424	0.0749	0.778	2220	0.0633	2226	0.0824	0.910
2495	0.0616	2475	0.0737	0.782	2274	0.0583	2274	0.0788	0.915
2552	0.0610	2527	0.0725	0.786	2328	0.0541	2323	0.0750	0.900
		2579	0.0706		2383	0.0497	2373	0.0694	0.910
2609	0.0603	2633	0.0688	0.819	2439	0.0462	2424	0.0642	0.915
2668	0.0595	2687	0.0677	0.820			2475	0.0612	
2726	0.0586	2742	0.0665	0.821	2495	0.0426	2527	0.0579	0.925
2786	0.0577	2798	0.0648	0.828	2552	0.0393	2579	0.0536	0.939
2846	0.0568	2854	0.0631	0.837	2609	0.0362	2633	0.0498	0.948
2907	0.0559	2912	0.0620	0.837	2668	0.0334	2687	0.0477	0.930
2969	0.0550	2970	0.0609	0.837	2726	0.0308	2742	0.0455	0.919
3031	0.0539	3029	0.0592	0.843	2786	0.0286	2798	0.0423	0.936
3094	0.0529	3088	0.0574	0.852	2846	0.0264	2854	0.0395	0.948
3158	0.0519	3149	0.0563	0.850	2907	0.0244	2912	0.0378	0.936
3222	0.0509	3210	0.0551	0.850	2969	0.0226	2970	0.0360	0.933
3287	0.0500	3272	0.0534	0.863	3031	0.0208	3029	0.0334	0.952
3353	0.0491	3335	0.0517	0.874	3094	0.0193	3088	0.0311	0.974
		3399	0.0507		3158	0.0180	3149	0.0297	0.974
3486	0.0473	3464	0.0496	0.872	3222	0.0168	3210	0.0283	0.984
3554	0.0464	3530	0.0478	0.885	3287	0.0157	3272	0.0263	1.015
		3596	0.0464		3353	0.0147	3335	0.0248	1.037
3622	0.0453	3663	0.0456	0.907	3419	0.0139	3399	0.0241	1.034
3761	0.0433	3731	0.0446	0.881	3486	0.0130	3464	0.0232	1.034
3831	0.0424	3800	0.0430	0.893	3554	0.0122	3530	0.0224	1.034
3902	0.0415	3870	0.0418	0.896	3622	0.0115	3596	0.0221	1.017
3974	0.0406	3941	0.0409	0.893	3691	0.0108	3663	0.0222	0.984
4047	0.0397	4013	0.0400	0.892	3761	0.0103	3731	0.0222	0.960
4120	0.0388	4085	0.0384	0.906	3831	0.0099	3800	0.0222	0.942
4194	0.0380	4159	0.0374	0.909	3902	0.0095	3870	0.0216	0.949
4268	0.0372	4233	0.0367	0.903	3974	0.0091	3941	0.0207	0.972
4343	0.0365	4308	0.0360	0.901	4047	0.0087	4013	0.0195	1.013
		4385	0.0346						
4496	0.0348	4462	0.0338	0.911					
4573	0.0340	4540	0.0331	0.906					
4651	0.0333	4619	0.0323	0.907					
4730	0.0326	4699	0.0309	0.927					
4809	0.0320	4780	0.0300	0.934					
4889	0.0313	4862	0.0291	0.937					
4969	0.0308	4945	0.0283	0.945					

Appendix 2I - Continued

5051	0.0302	5029	0.0274	0.954
5133	0.0296	5113	0.0272	0.939
5216	0.0289	5199	0.0272	0.917
5299	0.0282	5286	0.0270	0.894
5383	0.0275	5374	0.0269	0.872
5468	0.0269	5463	0.0268	0.856
5553	0.0264	5553	0.0264	0.846
5640	0.0258	5644	0.0261	0.835
5727	0.0252	5735	0.0258	0.823
5814	0.0247	5828	0.0252	0.821
5902	0.0242	5922	0.0243	0.831
5991	0.0236	6017	0.0236	0.833
6081	0.0231	6113	0.0228	0.836
6262	0.0218	6211	0.0218	0.818
6354	0.0212	6309	0.0207	0.830
6447	0.0206	6408	0.0202	0.823
6540	0.0200	6508	0.0195	0.819
6633	0.0194	6610	0.0187	0.823
6728	0.0189	6712	0.0179	0.832
6823	0.0184	6816	0.0175	0.824
6919	0.0180	6921	0.0171	0.820
7016	0.0176	7027	0.0165	0.826
7113	0.0172	7134	0.0157	0.837
7211	0.0167	7242	0.0152	0.833
7310	0.0162	7351	0.0147	0.830
7409	0.0157	7461	0.0141	0.832
7509	0.0153	7573	0.0135	0.836
7711	0.0146	7685	0.0134	0.000
7814	0.0142	7799	0.0132	0.000

Appendix 2J - Normalized Intensity Comparison (NIC) with depth for all King Site piezometers, compared with $SUVA_{254}$ analysis. $SUVA_{254}$ values in part from Hendry, et al. (2003).

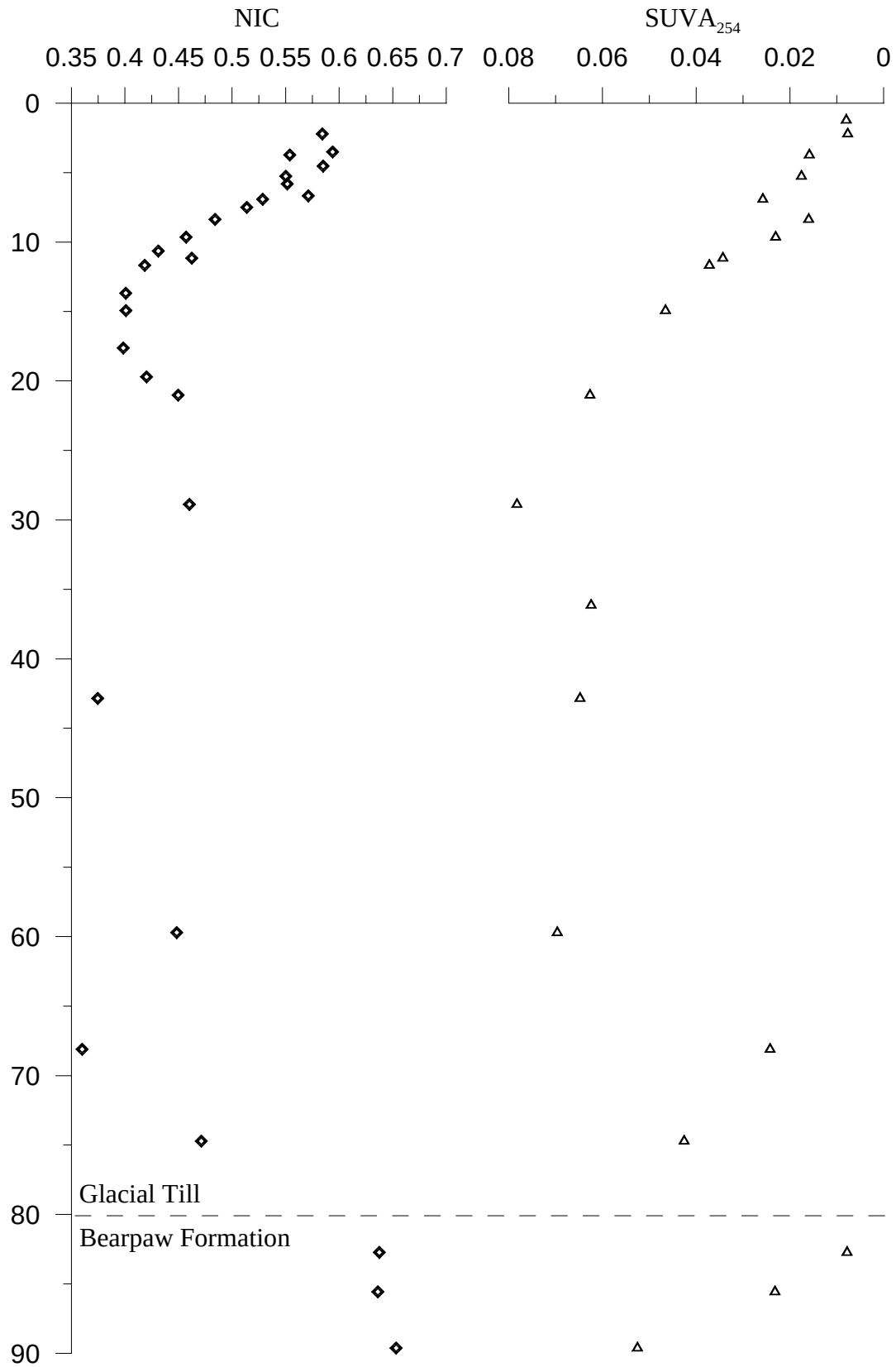

Appendix 2K - Startup Procedure for AsFlFFF – UV – TOC System

1. Check all fluid levels
   - Empty waste containers
     i. AsFlFFF waste
     ii. UV – TOC waste
   - Check reservoir levels
     i. AsFlFFF Carrier Solution reservoir
     ii. TOC D.I. feed reservoir
     iii. TOC internal D.I. reservoir
     iv. TOC acid/reagent cartridge levels

2. Power up instruments
   - Power on AsFlFFF and computer
   - Power on TOC

3. Flush AsFlFFF system
   - Check to make sure that the UV to TOC 4-way valve is set to *GRAB* from the UV detector. DO NOT route fluid into the TOC Detector
   - Select appropriate sequence and method for runs on AsFlFFF software
   - Rinse AsFlFFF channel at low flow rates (in manual mode) 0.5 mL min^{-1} on both pumps (rinsing and injection pumps)
   - Switch AsFlFFF to elution mode at low flow rates (in manual mode) 0.3 to 0.4 mL min^{-1} on both pumps. Ensure pressure does not exceed 1.5 kPa on either pump
   - When UVA signal does not fluctuate, auto-zero the detector

4. Prepare TOC for operation
   - Remove plug on air cleaner from the ICR
   - Turn off the pumps on the AsFlFFF
   - Switch TOC 4-way valve to *INLINE*
   - Start the TOC detector

5. Start run on AsFlFFF
   - Enter filename for run on AsFlFFF software
   - Begin run procedure

APPENDIX 3 Supplementary data for Chapter 3.

Appendix 3 – UV and ICP-MS fractograms.

Appendix 3 - DOC response (UV) and uranium counts (ICP-MS) for King Site porewaters. Samples collected on August 29, 02 are labeled-1 and samples collected on June 5, 02 are labeled -2.

Time	B10-2		B10-1		B15-2		B15-1		B20-2		B30-2	
Sec.	UV	ICP-MS	UV	ICP-MS	UV	ICP-MS	UV	ICP-MS	UV	ICP-MS	UV	ICP-MS
0	-0.0944		-0.0162		0.1037		0.0911		-0.0950		0.1776	
1	-0.0865		0.0019		0.1251		0.1052		0.0190		0.2180	
2	-0.0715		0.0219		0.1601		0.1389		0.1419		0.2577	
3	-0.0268	10	0.0612	20	0.2235	394	0.2012	0	0.3707	10335	0.3127	5
4	0.0007		0.0638		0.2265		0.1978		0.3538		0.3005	
5	-0.0115		0.0305		0.1656		0.1372		0.1628		0.2200	
6	-0.0254	0	0.0001	5	0.1039	21512	0.0800	3	0.0038	9462	0.1428	3
7	-0.0370		-0.0226		0.0550		0.0342		-0.1108		0.0821	
8	-0.0460		-0.0385		0.0185		0.0034		-0.1886		0.0370	
9	-0.0501	3	-0.0469	8	-0.0057	200415	-0.0178	2372	-0.2283	8596	0.0063	5
10	-0.0489		-0.0482		-0.0186		-0.0285		-0.2285		-0.0117	
11	-0.0429		-0.0438		-0.0228		-0.0305		-0.2022		-0.0192	
12	-0.0081	3	-0.0171	13470	-0.0127	123855	-0.0189	1905	-0.1448	139074	-0.0153	8
13	0.3266		0.3218		0.1574		0.1552		0.0249		0.0638	
14	0.8133		0.8336		0.4426		0.4461		0.2235		0.2125	
15	1.0242	0	1.0511	10381	0.5752	62103	0.5779	1453	0.3077	143022	0.2907	0
16	1.0058		1.0230		0.5602		0.5600		0.2984		0.2857	
17	0.9012		0.9070		0.4883		0.4846		0.2508		0.2460	
18	0.7866	0	0.7827	6360	0.4107	135920	0.4048	173792	0.1966	22463	0.2026	0
19	0.6857		0.6759		0.3460		0.3397		0.1486		0.1676	
20	0.6033		0.5903		0.2973		0.2911		0.1128		0.1416	
21	0.5390	0	0.5240	253219	0.2623	110696	0.2565	92768	0.0864	162896	0.1239	3
22	0.4905		0.4751		0.2387		0.2334		0.0689		0.1123	
23	0.4553		0.4391		0.2235		0.2186		0.0587		0.1046	
24	0.4305	3	0.4143	163043	0.2142	36022	0.2095	11391	0.0553	154792	0.1003	3
25	0.4131		0.3962		0.2085		0.2038		0.0537		0.0975	
26	0.4004		0.3829		0.2046		0.1998		0.0534		0.0959	
27	0.3908	3	0.3728	29216	0.2016	46076	0.1968	111744	0.0530	80522	0.0949	3
28	0.3843		0.3653		0.1993		0.1950		0.0525		0.0940	

Appendix 3 Continued

29	0.3802		0.3599		0.1979		0.1940		0.0521		0.0941	
30	0.3796	11851	0.3572	142486	0.1977	279304	0.1939	349440	0.0525	88608	0.0946	0
31	0.3818		0.3579		0.1989		0.1955		0.0530		0.0956	
32	0.3884		0.3618		0.2016		0.1987		0.0528		0.0977	
33	0.3993	4262	0.3700	680282	0.2063	232144	0.2039	203872	0.0562	120800	0.1005	886
34	0.4141		0.3823		0.2128		0.2104		0.0608		0.1040	
35	0.4327		0.3982		0.2210		0.2192		0.0677		0.1082	
36	0.4541	3249	0.4176	465010	0.2307	146280	0.2296	111456	0.0741	71360	0.1126	505
37	0.4769		0.4398		0.2416		0.2414		0.0802		0.1175	
38	0.5006		0.4640		0.2534		0.2537		0.0848		0.1222	
39	0.5233	149376	0.4893	248752	0.2655	109872	0.2667	61896	0.0893	44386	0.1271	700
40	0.5437		0.5155		0.2771		0.2794		0.0935		0.1315	
41	0.5603		0.5384		0.2882		0.2918		0.0959		0.1354	
42	0.5716	98560	0.5591	359040	0.2974	96192	0.3028	51160	0.1000	37616	0.1388	3307
43	0.5769		0.5755		0.3043		0.3120		0.1031		0.1412	
44	0.5754		0.5861		0.3084		0.3194		0.1074		0.1423	
45	0.5671	11098	0.5904	176896	0.3095	87512	0.3244	47584	0.1095	37480	0.1422	182880
46	0.5521		0.5890		0.3078		0.3260		0.1100		0.1410	
47	0.5320		0.5818		0.3030		0.3243		0.1092		0.1383	
48	0.5072	41528	0.5678	107122	0.2957	83648	0.3197	55251	0.1082	43856	0.1347	42164
49	0.4788		0.5482		0.2857		0.3123		0.1063		0.1300	
50	0.4479		0.5336		0.2738		0.3020		0.1030		0.1244	
51	0.4157	411520	0.4966	576992	0.2602	80400	0.2896	66692	0.0980	47824	0.1177	4131
52	0.3828		0.4682		0.2452		0.2756		0.0920		0.1107	
53	0.3500		0.4422		0.2292		0.2601		0.0873		0.1030	
54	0.3183	293888	0.4037	668928	0.2126	79576	0.2438	80702	0.0818	55192	0.0952	64184
55	0.2877		0.3722		0.1962		0.2270		0.0763		0.0874	
56	0.2590		0.3413		0.1801		0.2100		0.0705		0.0796	
57	0.2319	152000	0.3109	434400	0.1640	80664	0.1932	138832	0.0655	59560	0.0721	83184
58	0.2069		0.2906		0.1490		0.1768		0.0598		0.0649	
59	0.1841		0.2551		0.1345		0.1609		0.0536		0.0580	
60	0.1630	92096	0.2309	324800	0.1210	77426	0.1459	105990	0.0478	61376	0.0521	38632
61	0.1440		0.2060		0.1088		0.1319		0.0422		0.0475	

Appendix 3 Continued

62	0.1269		0.1841		0.0973		0.1186		0.0384		0.0429	
63	0.1116	74240	0.1666	281248	0.0870	69250	0.1064	96612	0.0320	58656	0.0387	20600
64	0.0981		0.1467		0.0776		0.0949		0.0265		0.0345	
65	0.0860		0.1304		0.0691		0.0843		0.0208		0.0304	
66	0.0753	69952	0.1157	259008	0.0614	59570	0.0751	236896	0.0161	55864	0.0265	13752
67	0.0660		0.1017		0.0543		0.0666		0.0108		0.0230	
68	0.0575		0.0905		0.0479		0.0588		0.0075		0.0199	
69	0.0500	80928	0.0815	243904	0.0426	51472	0.0518	340800	0.0044	46848	0.0169	12258
70	0.0435		0.0767		0.0376		0.0459		0.0024		0.0142	
71	0.0378		0.0616		0.0334		0.0404		0.0034		0.0119	
72	0.0328	94051	0.0552	231008	0.0295	39844	0.0357	203320	0.0043	36802	0.0098	13260
73	0.0282		0.0491		0.0259		0.0315		0.0036		0.0083	
74	0.0244		0.0426		0.0228		0.0278		0.0046		0.0071	
75	0.0215	108896	0.0368	231904	0.0199	31524	0.0241	122040	0.0039	28780	0.0057	15018
76	0.0188		0.0331		0.0174		0.0212		0.0057		0.0045	
77	0.0164		0.0283		0.0153		0.0185		0.0076		0.0037	
78	0.0144	116352	0.0247	234688	0.0135	22113	0.0161	83648	0.0092	21810	0.0029	18500
79	0.0128		0.0219		0.0121		0.0141		0.0103		0.0023	
80	0.0113		0.0192		0.0106		0.0121		0.0085		0.0018	
81	0.0103	115712	0.0168	224496	0.0094	16158	0.0105	71280	0.0075	15536	0.0013	21566
82	0.0093		0.0144		0.0084		0.0091		0.0073		0.0009	
83	0.0083		0.0123		0.0073		0.0079		0.0067		0.0006	
84	0.0074	105760	0.0105	208488	0.0065	11478	0.0067	63712	0.0058	12976	0.0003	25196
85	0.0067		0.0089		0.0060		0.0059		0.0059		0.0001	
86	0.0061		0.0075		0.0055		0.0050		0.0054		-0.0002	
87	0.0051	86400	0.0063	190816	0.0051	8467	0.0044	66336	0.0052	9499	-0.0002	26930
88	0.0044		0.0052		0.0045		0.0037		0.0035		-0.0004	
89	0.0040		0.0043		0.0038		0.0031		0.0019		-0.0006	
90	0.0036	69024	0.0034	167056	0.0031	5941	0.0026	70244	-0.0004	7997	-0.0007	25898
91	0.0034		0.0028		0.0027		0.0024		-0.0025		-0.0007	
92	0.0034		0.0023		0.0024		0.0023		-0.0054		-0.0010	
93	0.0032	48504	0.0018	130048	0.0021	4907	0.0022	77964	-0.0075	6715	-0.0011	23316
94	0.0030		0.0015		0.0020		0.0020		-0.0095		-0.0011	

Appendix 3 Continued

95	0.0030		0.0011		0.0018		0.0019		-0.0100		-0.0012	
96	0.0029	34928	0.0010	105296	0.0017	3808	0.0018	84048	-0.0108	6256	-0.0011	18068
97	0.0030		0.0007		0.0014		0.0015		-0.0122		-0.0009	
98	0.0031		0.0002		0.0014		0.0011		-0.0126		-0.0007	
99	0.0031	26584	0.0001	80894	0.0013	3417	0.0007	88586	-0.0140	5113	-0.0006	13902
100	0.0032		0.0000		0.0011		0.0003		-0.0155		-0.0006	
101	0.0034		0.0000		0.0014		0.0000		-0.0147		-0.0005	
102	0.0037	17114	0.0001	65274	0.0013	2921	-0.0006	87006	-0.0137	5096	-0.0003	10524
103	0.0035		-0.0001		0.0017		-0.0008		-0.0124		-0.0003	
104	0.0034		-0.0002		0.0018		-0.0011		-0.0119		0.0000	
105	0.0033	12651	-0.0002	47264	0.0018	2705	-0.0014	79268	-0.0108	4206	0.0000	7559
106	0.0034		-0.0003		0.0016		-0.0017				0.0003	
107	0.0032		-0.0003		0.0015		-0.0019				0.0004	
108	0.0031	7825	-0.0002	39292	0.0011	3046	-0.0021	67109		3969	0.0005	5350
109	0.0031		0.0000		0.0009		-0.0022				0.0005	
110	0.0029		0.0001		0.0007		-0.0021				0.0006	
111	0.0028	29764	0.0002	25458	0.0005	2424	-0.0020	54277		3710	0.0006	4503
112	0.0028		0.0007		0.0005		-0.0018				0.0007	
113	0.0028		0.0009		0.0004		-0.0019				0.0009	
114	0.0028	25441	0.0014	22066	0.0001	2233	-0.0019	43457		4117	0.0011	3066
115	0.0029		0.0016		-0.0002		-0.0020				0.0012	
116	0.0029		0.0019		-0.0004		-0.0019				0.0012	
117	0.0028	5045	0.0021	16084	-0.0005	2019	-0.0018	30886		3976	0.0014	3075
118	0.0029		0.0023		-0.0006		-0.0015				0.0013	
119	0.0026		0.0026		-0.0005		-0.0016				0.0012	
120	0.0022	17736	0.0026	12091	-0.0004	2229	-0.0016	23655		3161	0.0013	2209
121	0.0019		0.0028		-0.0002		-0.0015				0.0014	
122	0.0017		0.0027		-0.0001		-0.0013				0.0013	
123	0.0017	331355	0.0027	10990	-0.0002	2045	-0.0013	17008		3469	0.0014	2144
124	0.0020		0.0023		-0.0002		-0.0011				0.0015	
125	0.0021		0.0021		-0.0001		-0.0011				0.0015	
126	0.0023	270972	0.0016	8151	0.0000	2491	-0.0011	11614		2127	0.0014	1998
127	0.0023		0.0012		0.0002		-0.0011				0.0011	

Appendix 3 Continued

128	0.0024		0.0008		0.0002		-0.0014			0.0009	
129	0.0022	137930	0.0006	6966	0.0003	2159	-0.0017	8547	1796	0.0006	1953
130	0.0021		0.0003		0.0002		-0.0019			0.0006	
131	0.0020		0.0002		0.0003		-0.0019			0.0005	
132	0.0016	85483	0.0002	6775	0.0004	1898	-0.0019	6542	2091	0.0005	1664
133	0.0013		-0.0001		0.0005		-0.0020			0.0007	
134	0.0015		-0.0002		0.0006		-0.0018			0.0011	
135	0.0018	67281	-0.0002	6596	0.0006	2059		5240	2916	0.0011	1671
136	0.0019		-0.0009		0.0007						
137	0.0021		-0.0012		0.0010						
138	0.0024	69905	-0.0014	5489	0.0013	1819		4278	3492		1507
139	0.0026		-0.0016		0.0017						
140	0.0025		-0.0017		0.0019						
141	0.0024	73040	-0.0020	4774	0.0022	1734		3868	2958		1586
142	0.0024		-0.0019		0.0021						
143	0.0026		-0.0017		0.0021						
144	0.0026	87640	-0.0016	5195	0.0022	1760		3184	2965		1393
145	0.0027		-0.0017		0.0022						
146	0.0027		-0.0016		0.0019						
147	0.0026	98103	-0.0019	4418	0.0019	1890		3172	2918		1266
148	0.0024		-0.0018		0.0021						
149	0.0019		-0.0017		0.0021						
150	0.0015	110711	-0.0014	4650	0.0022	1772		2830	2984		1211
151	0.0010		-0.0014		0.0023						
152	0.0007		-0.0012		0.0021						
153		105899	-0.0011	4881	0.0023	1644		2688	2948		1263
154			-0.0009		0.0024						
155			-0.0007		0.0024						
156		96520	-0.0007	4388	0.0023	1771		2508	2732		1224
157			-0.0007		0.0022						
158			-0.0008		0.0022						
159		76232	-0.0007	4597	0.0022	1559		2418	3032		1158

Appendix 3 Continued

Time	B35-2		B40-2		B45-2		B50-2		B100-2		B125-2	
Sec.	UV	ICP-MS	UV	ICP-MS	UV	ICP-MS	UV	ICP-MS	UV	ICP-MS	UV	ICP-MS
0	-0.0455		-0.2153		-0.0244		-0.0415		-0.3753		-0.2765	
1	-0.0384		-0.1868		-0.0053		-0.0308		-0.2726		-0.2329	
2	-0.0182		-0.1546		0.0164		-0.0129		-0.1163		-0.0730	
3	0.0245	0	-0.0460	0	0.0630	5	0.0317	3	0.2734	10	0.3396	0
4	0.0447		0.0132		0.0783		0.0451		0.3591		0.4408	
5	0.0225		-0.0237		0.0474		0.0176		0.1006		0.2960	
6	0.0001	3	-0.0622	3	0.0164	0	-0.0077	0	-0.1274	8	0.0492	0
7	-0.0171		-0.0920		-0.0075		-0.0265		-0.2940		-0.1413	
8	-0.0299		-0.1147		-0.0256		-0.0400		-0.4061		-0.2822	
9	-0.0377	1722	-0.1260	0	-0.0363	990	-0.0468	1132	-0.4579	20	-0.3609	3
10	-0.0384		-0.1232		-0.0397		-0.0475		-0.4458		-0.3729	
11	-0.0350		-0.1087		-0.0374		-0.0430		-0.3877		-0.3318	
12	-0.0249	1668	-0.0810	423	-0.0254	463	-0.0332	1642	-0.2816	3174	-0.2412	1357
13	0.0402		0.0162		0.0792		-0.0057		-0.0546		-0.0411	
14	0.1510		0.1448		0.2422		0.0298		0.2069		0.2131	
15	0.2058	1767	0.2059	491	0.3155	388	0.0471	559	0.3332	8248	0.3484	2411
16	0.2006		0.2036		0.3064		0.0469		0.3380		0.3615	
17	0.1709		0.1737		0.2661		0.0393		0.2856		0.3100	
18	0.1389	91809	0.1396	484	0.2223	27648	0.0302	27179	0.2180	53472	0.2441	11758
19	0.1128		0.1087		0.1855		0.0218		0.1535		0.1793	
20	0.0941		0.0855		0.1577		0.0153		0.1022		0.1274	
21	0.0830	105678	0.0690	64496	0.1377	22121	0.0106	20402	0.0632	174213	0.0900	133696
22	0.0753		0.0587		0.1242		0.0073		0.0369		0.0626	
23	0.0710		0.0526		0.1157		0.0057		0.0218		0.0450	
24	0.0690	12462	0.0491	17120	0.1106	2160	0.0054	19415	0.0197	39317	0.0376	37728
25	0.0683		0.0484		0.1075		0.0054		0.0188		0.0384	
26	0.0683		0.0483		0.1054		0.0057		0.0215		0.0391	
27	0.0688	3936	0.0489	1201	0.1043	1285	0.0059	1682	0.0214	5127	0.0405	3683
28	0.0697		0.0501		0.1032		0.0061		0.0220		0.0437	
29	0.0709		0.0517		0.1030		0.0067		0.0246		0.0443	
30	0.0722	49554	0.0528	1201	0.1034	55032	0.0073	1074	0.0267	6145	0.0493	2411

Appendix 3 Continued

31	0.0737		0.0542		0.1043		0.0077		0.0285		0.0519	
32	0.0757		0.0567		0.1061		0.0084		0.0282		0.0557	
33	0.0778	31980	0.0594	1949	0.1092	8642	0.0096	1244	0.0321	4494	0.0582	1792
34	0.0804		0.0625		0.1130		0.0106		0.0369		0.0605	
35	0.0836		0.0656		0.1175		0.0116		0.0433		0.0609	
36	0.0869	13766	0.0694	1190	0.1228	1104	0.0126	821	0.0497	3088	0.0598	13052
37	0.0903		0.0733		0.1287		0.0136		0.0552		0.0580	
38	0.0939		0.0768		0.1351		0.0146		0.0588		0.0560	
39	0.0972	8457	0.0800	642	0.1415	1206	0.0154	525	0.0618	2390	0.0565	18613
40	0.1006		0.0834		0.1476		0.0162		0.0657		0.0571	
41	0.1037		0.0858		0.1533		0.0168		0.0678		0.0599	
42	0.1058	6421	0.0875	469	0.1579	1259	0.0173	381	0.0716	11705	0.0633	2909
43	0.1076		0.0891		0.1610		0.0177		0.0748		0.0672	
44	0.1087		0.0898		0.1625		0.0179		0.0793		0.0704	
45	0.1089	5980	0.0889	417	0.1625	842	0.0179	422	0.0824	3980	0.0731	1253
46	0.1084		0.0884		0.1610		0.0176		0.0837		0.0747	
47	0.1068		0.0865		0.1579		0.0174		0.0840		0.0762	
48	0.1043	6122	0.0841	337	0.1536	733	0.0172	427	0.0828	3286	0.0765	1681
49	0.1011		0.0813		0.1478		0.0167		0.0813		0.0792	
50	0.0973		0.0776		0.1415		0.0161		0.0782		0.0781	
51	0.0927	7161	0.0738	606	0.1342	541	0.0155	378	0.0746	88417	0.0790	1430
52	0.0877		0.0696		0.1261		0.0146		0.0700		0.0755	
53	0.0822		0.0658		0.1175		0.0137		0.0660		0.0752	
54	0.0767	8267	0.0605	1125	0.1086	456	0.0125	337	0.0620	91530	0.0755	927
55	0.0712		0.0553		0.0998		0.0112		0.0575		0.0720	
56	0.0658		0.0507		0.0914		0.0102		0.0526		0.0682	
57	0.0602	9877	0.0460	1071	0.0830	565	0.0090	370	0.0492	12692	0.0630	870
58	0.0550		0.0416		0.0751		0.0080		0.0450		0.0577	
59	0.0500		0.0376		0.0677		0.0071		0.0393		0.0512	
60	0.0454	11008	0.0336	75277	0.0609	496	0.0064	317	0.0370	3527	0.0452	736
61	0.0413		0.0299		0.0544		0.0051		0.0335		0.0385	
62	0.0367		0.0268		0.0484		0.0041		0.0307		0.0312	
63	0.0328	10947	0.0244	28481	0.0431	463	0.0032	350	0.0247	3972	0.0257	830

Appendix 3 Continued

64	0.0291		0.0219		0.0382		0.0024		0.0198		0.0196	
65	0.0260		0.0192		0.0339		0.0017		0.0159		0.0164	
66	0.0232	10926	0.0177	2816	0.0300	525	0.0012	479	0.0125	3785	0.0133	843
67	0.0206		0.0156		0.0265		0.0009		0.0069		0.0108	
68	0.0186		0.0141		0.0231		0.0005		0.0029		0.0104	
69	0.0166	9906	0.0128	1557	0.0202	502	0.0000	367	-0.0008	2602	0.0096	694
70	0.0149		0.0123		0.0177		-0.0003		-0.0022		0.0103	
71	0.0135		0.0114		0.0158		-0.0003		-0.0018		0.0090	
72	0.0121	7789	0.0112	2802	0.0136	503	-0.0006	320	-0.0012	2373	0.0058	731
73	0.0111		0.0105		0.0116		-0.0007		-0.0011		0.0061	
74	0.0101		0.0104		0.0099		-0.0010		-0.0002		0.0038	
75	0.0093	6282	0.0097	1703	0.0084	488	-0.0011	340	0.0006	2322	0.0000	658
76	0.0087		0.0091		0.0071		-0.0013		0.0025		-0.0008	
77	0.0082		0.0091		0.0061		-0.0013		0.0056		-0.0025	
78	0.0077	4911	0.0082	1180	0.0052	478	-0.0014	315	0.0085	2006	-0.0011	788
79	0.0075		0.0072		0.0046		-0.0016		0.0110		-0.0011	
80	0.0073		0.0063		0.0038		-0.0015		0.0110		-0.0008	
81	0.0071	3638	0.0055	900	0.0034	425	-0.0014	299	0.0120	1987	0.0007	724
82	0.0068		0.0053		0.0030		-0.0013		0.0138		0.0008	
83	0.0065		0.0053		0.0023		-0.0016		0.0147		0.0005	
84	0.0063	2639	0.0055	851	0.0018	458	-0.0017	340	0.0159	2005	-0.0002	692
85	0.0061		0.0061		0.0017		-0.0018		0.0175		-0.0002	
86	0.0060		0.0058		0.0016		-0.0019		0.0179		-0.0017	
87	0.0060	2130	0.0055	740	0.0015	422	-0.0021	251	0.0170	2084	-0.0035	661
88	0.0060		0.0061		0.0014		-0.0022		0.0141		-0.0045	
89	0.0059		0.0060		0.0011		-0.0023		0.0112		-0.0046	
90	0.0060	1670	0.0054	740	0.0009	412	-0.0022	227	0.0071	2398	-0.0024	602
91	0.0060		0.0048		0.0007		-0.0021		0.0042		-0.0011	
92	0.0058		0.0039		0.0007		-0.0021		-0.0002		0.0013	
93	0.0057	1714	0.0039	747	0.0006	438	-0.0022	364	-0.0017	1892	0.0031	705
94	0.0055		0.0022		0.0007		-0.0020		-0.0033		0.0040	
95	0.0053		0.0021		0.0008		-0.0017		-0.0040		0.0060	
96	0.0053	1308	0.0020	733	0.0008	370	-0.0015	235	-0.0056	3263	0.0080	706

Appendix 3 Continued

97	0.0052		0.0017		0.0007		-0.0016		-0.0071		0.0122	
98	0.0051		0.0005		0.0009		-0.0014		-0.0073		0.0150	
99	0.0050	1379	-0.0003	691	0.0008	368	-0.0014	291	-0.0102	2034	0.0182	755
100	0.0050		-0.0020		0.0006		-0.0013		-0.0117		0.0201	
101	0.0048		-0.0028		0.0010		-0.0010		-0.0110		0.0220	
102	0.0048	1340	-0.0031	780	0.0009	402	-0.0009	239	-0.0078	2266	0.0244	902
103	0.0048		-0.0028		0.0011		-0.0006		-0.0047		0.0268	
104	0.0048		-0.0026		0.0014		-0.0001		-0.0032		0.0287	
105	0.0051	1302	-0.0028	739	0.0014	372	0.0000	244	-0.0004	2208	0.0288	662
106	0.0052		-0.0034		0.0011		0.0001		0.0020		0.0309	
107	0.0052		-0.0036		0.0009		0.0001		0.0040		0.0312	
108	0.0054	1232	-0.0034	829	0.0006	342	-0.0001	280	0.0076	2059	0.0300	644
109	0.0054		-0.0037		0.0005		-0.0001		0.0112		0.0290	
110	0.0055		-0.0037		0.0005		-0.0002		0.0138		0.0274	
111	0.0055	1174	-0.0037	931	0.0003	413	-0.0003	292	0.0151	1984	0.0255	823
112	0.0056		-0.0041		0.0003		0.0000		0.0161		0.0237	
113	0.0056		-0.0041		0.0003		0.0001		0.0172		0.0222	
114	0.0055	987	-0.0044	690	-0.0002	451	-0.0001	302	0.0185	2023	0.0222	675
115	0.0056		-0.0040		-0.0004		-0.0005		0.0193		0.0211	
116	0.0055		-0.0045		-0.0006		-0.0003		0.0191		0.0201	
117	0.0054	1028	-0.0051	556	-0.0007	419	-0.0001	213	0.0186	2039	0.0205	784
118	0.0053		-0.0060		-0.0008		-0.0002		0.0184		0.0197	
119	0.0052		-0.0069		-0.0006		0.0000		0.0189		0.0203	
120	0.0051	965	-0.0071	540	-0.0005	403	0.0000	434	0.0162	2047	0.0196	648
121	0.0050		-0.0074		-0.0007		-0.0001		0.0132		0.0194	
122	0.0050		-0.0076		-0.0006		-0.0002		0.0113		0.0188	
123	0.0051	1060	-0.0082	573	-0.0004	316	-0.0001	237	0.0086	1803	0.0177	628
124	0.0049		-0.0089		-0.0003		0.0001		0.0071		0.0162	
125	0.0047		-0.0092		-0.0003		0.0000		0.0066		0.0170	
126	0.0045	1060	-0.0094	475	-0.0001	402	0.0002	262	0.0047	2384	0.0173	911
127	0.0043		-0.0095		0.0000		0.0003		0.0031		0.0172	
128	0.0042		-0.0098		-0.0001		0.0004		0.0034		0.0157	
129	0.0043	1053	-0.0095	590	0.0002	279	0.0008	282	0.0021	2106	0.0160	771

Appendix 3 Continued

130	0.0045		-0.0084		0.0002		0.0010		0.0003		0.0165	
131	0.0044		-0.0076		0.0002		0.0012		0.0009		0.0159	
132	0.0048	1110	-0.0068	477	0.0004	369	0.0015	331	0.0000	1769	0.0146	887
133	0.0048		-0.0062		0.0004		0.0016		-0.0001		0.0135	
134	0.0049		-0.0046		0.0004		0.0019		0.0002		0.0127	
135	0.0051	804	-0.0043	499	0.0000	449	0.0019	339	0.0021	1803	0.0111	1506
136	0.0055		-0.0041		-0.0001		0.0019		0.0029		0.0099	
137	0.0058		-0.0037		-0.0001		0.0020		0.0029		0.0102	
138	0.0060	858	-0.0037	496	0.0002	388	0.0023	338	0.0006	1679	0.0108	730
139	0.0060		-0.0042		0.0003		0.0023		-0.0021		0.0127	
140	0.0061		-0.0046		0.0004		0.0022		-0.0057		0.0136	
141	0.0060	1007	-0.0054	603	0.0005	344	0.0021	344	-0.0075	1980	0.0154	712
142	0.0059		-0.0054		0.0004		0.0019		-0.0098		0.0175	
143	0.0058		-0.0054		0.0005		0.0015		-0.0110		0.0190	
144	0.0056	809	-0.0054	587	0.0005	374	0.0011	344	-0.0114	1781	0.0203	778
145	0.0055		-0.0051		0.0003		0.0008		-0.0122		0.0210	
146	0.0057		-0.0050		0.0003		0.0005		-0.0133		0.0225	
147	0.0060	1018	-0.0052	466	0.0003	338	0.0003	267	-0.0123	1961	0.0243	711
148	0.0059		-0.0048		0.0003		0.0000		-0.0124		0.0255	
149	0.0060		-0.0043		0.0000		-0.0003		-0.0109		0.0254	
150	0.0063	900	-0.0040	607	-0.0002	364	-0.0005	235	-0.0084	1671	0.0251	664
151	0.0066		-0.0039		-0.0004		-0.0007		-0.0066		0.0234	
152	0.0064		-0.0033		-0.0005		-0.0006		-0.0048		0.0225	
153	0.0068	907	-0.0026	524	-0.0002	394	-0.0003	228	-0.0013	1521	0.0221	578
154	0.0069		-0.0018		-0.0004		-0.0004		0.0023		0.0214	
155	0.0069		-0.0011		-0.0002		-0.0001		0.0058		0.0225	
156	0.0070	817	0.0000	501	0.0000	349	0.0003	287	0.0095	1448	0.0214	665
157	0.0070		0.0009		0.0000		0.0003		0.0135		0.0192	
158	0.0071		0.0005		0.0002		0.0005		0.0186		0.0185	
159	0.0068	880	0.0009	547	0.0003	430	0.0007	256	0.0224	1783	0.0192	727

APPENDIX 4 Supplementary data for Chapter 4.

Appendix 4A – Uranium ICP-MS counts for King Site ground waters.

Appendix 4B – Zinc ICP-MS counts for King Site ground waters.

Appendix 4C – UV fractograms for King Site ground waters.

Appendix 4D – Uranium ICP-MS counts for titration experiment.

Appendix 4E – Zinc ICP-MS counts for titration experiment.

Appendix 4F – King Site ground water chemistry.

Appendix 4G – Data for Uranium and Zinc kinetic experiment.

Appendix 4A - Uranium ICP-MS counts for King Site groundwaters for experiments in in Chapter 4. Note time scale difference for B10 and B15. Values averages of several runs.

Time min	B10	B15	Time min	B7.5	B20	B25	B30	B35	B40
0.11	5560780	1079532	0.106	21280	130582	8180	3756	99310	244438
0.13	3136588	1292556	0.113	20880	78412	10180	7252	264950	157334
0.14	1588604	1364876	0.121	12976	117830	80300	26308	460910	98710
0.16	1401724	1560460	0.128	16288	251375	235796	133604	553974	86678
0.17	2449148	1075916	0.135	64160	517801	430284	404308	474510	53462
0.19	3467388	477164	0.143	292352	628303	520700	766532	341822	36230
0.20	3801852	172908	0.150	742528	610176	483020	899492	209534	28742
0.22	3544700	86652	0.157	1284544	558196	346604	950596	184198	24102
0.23	3076604	50852	0.165	1650240	432574	223564	954564	250054	18054
0.25	2904956	28612	0.172	1764160	203092	137012	962884	387110	12758
0.26	3623420	19812	0.179	1530560	275386	82924	825060	472526	14198
0.28	4709372	30756	0.187	1162560	67963	108020	608580	480150	10598
0.29	5306364	200548	0.194	805824	35197	281732	392132	335070	11942
0.30	5366268	615796	0.201	498912	16519	553844	241508	224014	7590
0.32	4866044	1043212	0.209	310880	10749	723420	140644	135734	6790
0.33	4446716	1581452	0.216	186336	4003	690428	82572	83438	6262
0.35	3719292	2073612	0.223	115192	-8178	510012	55420	48550	7654
0.36	3351036	2078988	0.231	85536	-4620	323444	42436	40198	6006
0.38	2949244	1807372	0.238	65312	2011	178804	26348	31534	8246
0.39	2649724	1524492	0.245	56504	55655	93444	21476	27222	17318
0.41	2347900	1430668	0.253	38184	136080	61428	21772	21894	28390
0.42	2154492	1161100	0.260	22496	245080	38796	21628	16662	40758
0.44	1977468	982668	0.267	14256	363167	32572	15020	12582	50550
0.45	1858684	891404	0.275	14224	422495	15332	11980	10990	57926
0.47	1784060	827020	0.282	4776	479573	6668	8524	10854	57174
0.48	1697532	774924	0.289	5776	508423	5308	6716	18614	59622
0.50	1658492	657932	0.297	1992	530651	5924	4036	33734	53606
0.51	1624444	629132	0.304	9632	503026	24524	6748	62334	51142
0.53	1679228	623372	0.311	10592	529200	70116	20836	84118	50054
0.54	1686396	583308	0.319	38344	585720	136436	52652	101166	45878
0.56	1688316	595980	0.326	127360	711966	217436	97420	112286	41478
0.57	1638524	598924	0.333	307048	745785	274476	155164	108646	35814
0.58	1720060	582796	0.341	633920	820853	290692	222148	111102	34070
0.60	1696124	568332	0.348	982688	845296	327052	281444	122062	34646
0.61	1760124	578316	0.355	1348416	758880	329124	363684	139206	26614
0.63	1787004	610700	0.363	1619776	709273	322380	417316	163526	25878
0.64	1836796	570892	0.370	1801024	686330	313556	423588	175782	24294
0.66	1848572	597388	0.377	1976128	668564	312084	438436	184262	23734
0.67	1905532	582796	0.385	2034368	579727	356628	413220	181574	22038
0.69	1928572	644364	0.392	1858240	534413	400372	407332	167078	22390
0.70	1953020	665612	0.399	1847232	508560	443188	348036	159334	20342
0.72	2011260	654476	0.407	1788608	447573	468116	334980	149798	18774
0.73	1980156	693772	0.414	1626560	436503	460084	302852	129174	20742
0.75	1985148	710668	0.421	1531200	410987	447732	261732	125094	20278
0.76	1985276	730508	0.429	1418816	412054	413652	244260	113222	17398
0.78	2031612	753420	0.436	1310784	356931	387284	221828	106782	18678

Appendix 4A Continued

0.79	2021884	774668	0.443	1225536	376197	352788	209636	99062	15750
0.80	2050812	793868	0.451	1100736	317222	329204	198084	90238	16454
0.82	2060284	834444	0.458	1068480	314670	300404	186916	83182	16838
0.83	1933308	792716	0.466	1011264	310151	271028	176900	80742	17046
0.85	1978876	795532	0.473	951744	299178	256628	170276	71518	16742
0.86	1923452	849932	0.480	922816	308183	242868	163332	97718	15846
0.88	1933564	880524	0.488	890304	269773	231956	161956	68918	14486
0.89	1825660	848652	0.495	859328	270096	219604	155012	66966	16102
0.91	1758844	861324	0.502	816960	282010	208436	152996	71406	13238
0.92	1749884	848524	0.510	794688	274807	203540	152548	61702	17190
0.94	1719036	921740	0.517	767424	258644	192788	143876	60622	15158
0.95	1653628	867468	0.524	739904	280619	189940	140228	58854	15398
0.97	1568892	863372	0.532	714048	267973	180340	140292	60142	15190
0.98	1492348	827916	0.539	709696	257183	177268	137636	58022	12486
1.00	1415164	842636	0.546	676032	254065	173940	127940	54782	18022
1.01	1369212	817932	0.554	671424	256267	169460	131972	52622	21686
1.02	1281276	789388	0.561	673344	253362	164724	128036	53478	14374
1.04	1187964	828556	0.568	660416	242084	164052	128100	54126	13974
1.05	1157884	819468	0.576	655040	256505	169396	128868	56686	14182
1.07	1085052	768780	0.583	650176	275409	166836	144996	56246	15878
1.08	1022332	686348	0.590	642496	261184	161204	129316	55622	13542
1.10	972028	674444	0.598	646976	263925	165556	130756	56278	16374
1.11	889468	709900	0.605	630080	269794	160244	127492	56078	17014
1.13	840060	659084	0.612	624192	263924	167668	132324	53990	14278
1.14	779516	658828	0.620	622144	279088	158900	129636	55214	14854
1.16	727036	594188	0.627	617152	298688	161300	130820	54878	15878
1.17	677884	569228	0.634	639936	275938	157556	127428	59478	15766
1.19	653564	522572	0.642	638784	295624	159764	128644	57486	16326
1.20	591612	515308	0.649	622656	284411	161300	130884	59526	17606
1.22	557436	521612	0.656	632896	311840	168532	132708	57398	16502
1.23	525500	457292	0.664	650048	295025	169620	132612	56622	12278
1.25	494876	417964	0.671	656064	305615	175828	134212	57806	14374
1.26	471900	448172	0.678	658112	297079	169236	135620	59470	15958
1.27	419708	377612	0.686	663616	336674	170388	139044	59174	17046
1.29	395068	375500	0.693	670912	334873	173332	141380	62198	20054
1.30	357372	342444	0.701	672448	325688	178356	150244	59254	15158
1.32	337916	335180	0.708	673984	312424	181524	140644	59494	19302
1.33	305532	305580	0.715	675904	328059	188244	153988	59734	17270
1.35	291740	276332	0.723	687040	315746	184852	151780	63118	18582
1.36	263964	277996	0.730	708928	344690	191252	155300	65254	20582
1.38	239548	254700	0.737	731712	348758	192948	163108	69934	16454
1.39	223676	233196	0.745	723392	381025	190996	163716	67638	18806
1.41	208700	202156	0.752	744768	394290	196532	163780	66870	19478
1.42	192156	189868	0.759	734400	417559	201812	163940	69646	18166
1.44	184092	201356	0.767	772288	384572	202804	169828	72910	21366
1.45	162332	187468	0.774	765888	399416	207060	169924	70070	18422
1.47	153372	163820	0.781	761408	353774	206964	168452	72574	20102
1.48	137948	143948	0.789	786880	412001	219700	176068	76718	21334
1.49	128156	131852	0.796	787776	409358	208916	174724	74518	18950
1.51	118844	132268	0.803	794304	395888	213780	175428	77446	20374
1.52	111772	112428	0.811	817728	407164	223604	180868	79078	18838

Appendix 4A Continued

1.54	104284	108204	0.818	839744	435808	230292	184868	82902	19622
1.55	93372	111660	0.825	860096	417328	230036	187972	78446	20614
1.57	102396	93708	0.833	838208	427589	232628	199332	80742	19638
1.58	84796	100844	0.840	852672	438986	231508	194660	82342	21814
1.60	76252	70172	0.847	863680	444451	238612	203556	84702	22934
1.61	79868	75948	0.855	851136	433931	241652	209444	84374	24822
1.63	62844	75020	0.862	875840	407521	252340	208548	87158	21830
1.64	62972	57788	0.869	877632	414388	252052	209636	86846	23190
1.66	57788	55108	0.877	890816	439112	250356	194308	84662	22118
1.67	53596	55756	0.884	889792	451629	254964	212964	87358	21318
1.69	52540	52708	0.891	888896	447119	252212	213124	102502	24982
1.70	51036	42108	0.899	896832	426246	261076	218148	92702	22374
1.72	47260	50404	0.906	873920	448976	266356	214980	92830	20854
1.73	40220	53356	0.914	910784	453644	265876	216900	93566	23926
1.74	36876	38836	0.921	912448	445770	267604	218852	95038	22918
1.76	38044	42276	0.928	880576	459350	271220	231460	92750	24678
1.77	36540	35892	0.936	885184	472120	273492	221444	96454	24182
1.79	29628	29444	0.943	887616	449773	269780	227908	93006	21270
1.80	30220	28364	0.950	882240	429889	280788	220932	94150	22902
1.82	28292	23212	0.958	897600	422152	272980	232708	98214	24150
1.83	27476	29028	0.965	889152	392184	280916	231684	100326	23398
1.85	26076	25636	0.972	890048	426485	277620	231972	102246	23622
1.86	25332	21548	0.980	869696	454616	288788	241604	100518	23878
1.88	25940	18468	0.987	884288	456939	285300	235812	98950	25126
1.89	23492	18620	0.994	880064	471894	283892	241092	101446	24582
1.91	23460	18988	1.002	856384	442755	280660	241508	99750	23046
1.92	22300	19788	1.009	872128	467862	281300	226980	101158	23606
1.94	20044	9820	1.016	860224	441401	287700	229060	99046	28022
1.95	17844	17564	1.024	836160	439759	282420	218564	101222	21734
1.97	16164	14572	1.031	826560	454259	285108	228708	102982	25382
1.98	15684	13780	1.038	817600	426431	280692	228388	100806	21030
1.99	14516	8004	1.046	812480	446764	284948	223940	109094	20518
2.01	16404	6132	1.053	787008	416382	277780	223300	100518	21190
2.02	12380	5572	1.060	780736	409662	280756	232612	103814	20534
2.04	13780	11004	1.068	769728	403887	279220	224868	99846	20870
2.05	12668	2036	1.075	730944	421333	276180	227588	94726	21142
2.07	13164	6332	1.082	735296	400793	274164	217124	97094	19558
2.08	8868	7596	1.090	737600	378036	274900	218148	98790	18822
2.10	11284	5820	1.097	719936	356437	269876	214660	92838	17238
2.11	8988	6740	1.105	736448	363760	265492	207876	96006	20742
2.13	7996	1692	1.112	704064	369964	266164	204228	99654	18022
2.14	9980	4548	1.119	693440	341995	260532	208900	95078	20790
2.16	12244	4188	1.127	675008	331955	259828	203684	93222	20214
2.17	5172	2460	1.134	652352	341848	252628	204228	91590	18310
2.19	6684	3444	1.141	630080	331521	253716	204804	91014	17366
2.20	3988	4404	1.149	621504	350595	250292	202116	89190	15750
2.21	6316	1924	1.156	610112	323616	245748	188612	90054	19286
2.23	7620	1940	1.163	593856	342449	239668	185636	87270	13046
2.24	5380	1796	1.171	587840	329930	233428	186116	83206	16086
2.26	4508	7836	1.178	569792	300504	232212	182212	82918	15542
2.27	3012	5116	1.185	565056	288643	224436	177540	83670	23814

Appendix 4A Continued

2.29	6172	-804	1.193	546496	280898	215284	177764	81846	17110
2.30	2748	-148	1.200	528960	285209	219732	166660	80542	16854
2.32	7172	4108	1.207	512064	273617	209972	167908	79494	14502
2.33	2796	-756	1.215	493888	254610	210612	162788	77110	13942
2.35	5556	-1684	1.222	491328	265471	209940	159812	76550	13638
2.36	884	1012	1.229	469312	278187	204148	158276	75446	12022
2.38	1788	1156	1.237	459936	242289	199508	152196	71342	12262
2.39	820	4012	1.244	435104	240999	190292	148484	70094	13670
2.41	-1988	-3228	1.251	426624	217828	187028	145348	70686	12774
2.42	5164	436	1.259	409696	221206	178676	138884	66534	14118
2.44	1780	716	1.266	398624	225013	177908	142212	66086	11494
2.45	1652	932	1.273	393216	185650	180564	132868	64534	11542
2.46	3572	-2532	1.281	366496	199150	170228	132004	66694	9942
2.48	1172	-1420	1.289	360192	191568	166996	129956	63342	10934
2.49	2668	724	1.296	349024	195006	164116	119556	60030	10406
2.51	-796	2812	1.303	334432	207994	158036	118660	57294	12374
2.52	1476	4804	1.311	328544	172128	152948	114564	56718	12358
2.54	28	-5244	1.318	320256	173348	150164	113380	53758	10566
2.55	2124	7540	1.325	310176	162627	143380	110308	51326	11014
2.57	-820	2716	1.333	307776	169662	140980	108420	51254	6902
2.58	-2220	2772	1.340	287424	151396	140948	102180	50190	7862
2.60	-1892	-3092	1.347	286400	158661	136916	100068	48550	8326
2.61	-84	172	1.355	266368	151624	130484	100900	45630	4294
2.63	-1028	-5804	1.362	259680	138535	123796	90692	45870	9734
2.64	-1452	1644	1.369	252480	140866	120788	90788	45118	9318
2.66	-1300	60	1.377	235072	149767	118484	87460	41830	7974
2.67	692	-996	1.384	228864	130345	114708	85444	43510	3846
2.69	-3340	-2764	1.391	226464	123408	105524	81956	40678	5862
2.70	28	-1772	1.399	211520	112923	108340	79332	39542	6182
2.71	364	2572	1.406	210432	106005	106516	76836	37430	5670
2.73	-1916	-3052	1.413	202400	104699	102036	73700	38206	4374
2.74	-1220	-596	1.421	195520	111615	101236	68156	36918	6486
2.76	-1180	-3380	1.428	185632	95177	98324	67292	37758	3846
2.77	-2460	-3180	1.435	176672	101021	93780	65772	33886	5302
2.79	-4564	-1308	1.443	171712	91765	89460	65932	34510	4598
2.80	-3636	-276	1.450	166240	80213	82300	64660	31134	3686
2.82	-428	-756	1.457	159808	80650	85516	67428	28782	6390
2.83	3148	-1220	1.465	156544	76325	77908	57340	28798	5190
2.85	324	-532	1.472	147936	78944	78116	55756	29070	8486
2.86	-4036	76	1.479	141696	77452	73732	51524	26166	6166
2.88	-3092	-180	1.487	133760	74078	71132	48484	26542	2310
2.89	-1308	-1900	1.494	127680	72196	71572	48796	26766	2998
2.91	-1412	6820	1.501	120512	67298	66700	46604	25094	3574
2.92	-972	-2636	1.509	117824	67423	66988	43156	23902	2870
2.93	-1668	2156	1.516	110048	64644	63700	40148	24014	3798
2.95	-652	-340	1.523	112672	65157	62212	40412	21326	2390
2.96	-3340	2300	1.531	101984	54799	58436	39628	21270	3430
2.98	-2148	2676	1.538	100480	49161	56740	34532	19870	3814
2.99	-2260	1604	1.545	95424	58242	51196	37308	19862	3910
			1.553	89792	54305	49252	35828	18702	3526
			1.560	85824	48502	49380	33364	18614	1302

Appendix 4A Continued

1.567	81984	48749	48044	31500	17566	4006
1.575	75296	45490	46316	30956	18478	1430
1.582	72448	46817	45388	29276	16630	1910
1.589	73120	42906	41372	28212	19502	3222
1.597	66976	34334	42668	24644	14694	998
1.604	65504	42379	40052	27012	15726	2806
1.611	60552	47060	37236	24620	14198	2038
1.619	58264	33202	37724	24636	14038	6246
1.626	56448	35040	37012	24508	14374	3398
1.633	55104	37768	33284	22700	13310	2342
1.641	51864	25113	31284	20668	13470	2550
1.648	48536	25455	29908	18628	13326	358
1.655	44848	26010	31388	19436	11390	1670
1.663	45528	28583	28716	20060	13302	2246
1.670	43696	22803	26284	20420	10094	2390
1.677	43552	27276	24636	19020	12598	2358
1.685	39800	25117	28468	18132	9070	3302
1.692	36240	29715	24132	15924	10582	838
1.699	35952	29709	25588	15500	9606	7590
1.707	33384	20383	23740	15492	9102	2150
1.714	30600	18016	22060	12436	8854	1542
1.722	28544	20379	21308	14340	7294	2166
1.729	26392	21595	19380	15020	8630	1238
1.736	24896	22383	21588	12076	9734	3126
1.744	24392	21775	18884	13612	8646	1654
1.751	22008	18294	18660	12788	5438	1766
1.758	22072	18091	16780	9716	6702	1302
1.766	22480	13329	16100	11500	7542	4550
1.773	19472	24675	15188	10396	5910	934
1.780	18160	20943	16204	10756	7198	694
1.788	18792	12745	16188	10644	7102	1606
1.795	16296	9755	15980	10484	6238	3142
1.802	14336	22518	14668	9996	6486	-26
1.810	15392	16075	12940	7956	6254	4294
1.817	13840	20885	13564	9036	4342	1766
1.824	11480	20127	14556	8236	6766	5574
1.832	13400	12011	13252	7812	6062	3110
1.839	10176	15341	10388	7644	5406	2342
1.846	11920	13373	9172	9468	5030	3302
1.854	10240	6843	10788	6404	7126	3526
1.861	7568	12537	8500	7932	6222	406
1.868	7600	8055	7556	6996	5094	1494
1.876	8960	11163	8548	6948	6622	390
1.883	7808	4827	9364	6084	8374	1414
1.891	9376	9338	8460	7044	6678	582
1.898	4448	9236	8260	4348	4110	2006
1.905	3768	12244	8444	6924	3590	3974
1.913	5120	13613	7364	4900	7446	3238
1.920	5984	10409	8900	5372	6862	1046
1.927	5552	12101	7460	6428	5590	1126
1.935	4152	9865	8188	5012	3286	1462

Appendix 4A Continued

1.942	4656	8968	6740	7844	3758	1686
1.949	720	8556	5836	2924	3622	-186
1.957	2048	6311	5924	4884	3694	1926
1.964	2320	4824	4148	4788	3022	1430
1.971	2040	9339	5372	3204	3382	2550
1.979	200	7961	6468	3188	3582	1206
1.986	1016	8040	4444	3612	3078	-266
1.994	-1776	13396	4636	1676	3054	3078
2.001	-1976	6670	3324	2356	4214	2502
2.008	-408	4070	3932	6420	4342	3286
2.016	8	4457	4588	5396	5438	3238
2.023	-96	5685	4948	4156	3590	934
2.030	784	853	5524	4452	4950	2566
2.038	-1864	8426	3452	7004	3934	774
2.045	-1872	2693	3372	4580	3590	1846
2.052	-944	2892	5308	2716	2334	-346
2.060	-3744	13900	1948	3820	4886	2022
2.067	-2408	7990	3452	420	3558	438
2.074	-4320	4466	4124	3004	2854	1926
2.082	-2920	2705	2284	2596	3246	486
2.089	-2456	4245	3500	1716	4150	2710
2.096	-3832	4000	1876	3588	2686	-298
2.104	-2368	7526	2820	4052	3350	-378
2.111	-2128	6558	4772	3500	3718	774
2.118	-2880	4005	2004	1940	4014	1126
2.126	-4784	6045	3660	3676	2678	-346
2.133	-5352	6726	1132	4204	1318	2006
2.140	-5400	7862	2964	1252	1806	3094
2.148	-6856	1819	1316	292	1134	3734
2.155	-5360	6177	3852	932	4622	1174
2.162	-6912	-4066	3420	2252	3094	2230
2.170	-5408	4829	1076	3444	3942	-522
2.177	-2624	7826	1020	1804	4006	2630
2.184	-1760	-1467	2812	1964	2806	1542
2.192	-7808	8641	3084	3492	3798	3302
2.199	-6480	7293	3628	3212	2382	1302
2.206	-6848	2413	2284	1444	1190	678
2.214	-4456	819	2124	2244	3990	4502
2.221	-4624	2830	1092	1052	2502	1286
2.228	-4984	1535	1556	1668	3422	-826
2.236	-6504	8743	764	1476	3446	1270
2.243	-5544	357	1308	892	3622	870
2.251	-8216	-456	836	116	3494	1462
2.258	-8072	2359	2180	2772	2382	214
2.265	-5960	8130	-460	1276	3134	2374
2.273	-9000	5441	-212	1748	3070	758
2.280	-7384	2482	1172	2148	2062	2054
2.287	-8464	-3133	380	4428	2446	3254
2.295	-8168	1948	276	2132	2334	2390
2.302	-7880	10921	1308	644	1758	422
2.309	-5552	-125	1148	3740	3550	1462

Appendix 4A Continued

2.317	-7192	3998	-844	3228	2958	310
2.324	-8736	4406	948	1740	1998	1286
2.331	-9080	5337	1948	2036	606	3046
2.339	-7336	5796	2324	2340	1382	950
2.346	-5048	3906	1420	1460	3326	-106
2.353	-7512	6328	-1444	1028	2198	694
2.361	-7504	6531	564	2356	3438	86
2.368	-7032	5866	-348	196	1854	1366
2.375	-7168	2930	1580	844	3438	-170
2.383	-8184	2690	860	1292	1278	502
2.390	-8816	6807	-132	1996	2726	582
2.397	-8504	370	580	2316	3438	3734
2.405	-9504	-2472	1284	412	2854	3638
2.412	-7720	7649	484	4124	2478	2006
2.419	-7504	3678	1932	1996	870	1190
2.427	-7888	4766	-396	2684	574	854
2.434	-8304	6614	1412	-100	1182	1142
2.441	-7984	3444	-564	556	2966	1430
2.449	-8112	1432	-1436	932	4134	1846
2.456	-8480	5315	-404	2124	2534	1862
2.463	-6440	-2103	84	3796	3006	-1338
2.471	-8808	3134	948	2068	2262	1190
2.478	-8664	1320	2196	1260	1470	2342
2.485	-7104	2003	244	2252	2102	-842
2.493	-9840	7673	996	580	3134	-842
2.500	-10304	3382	-44	-140	1862	-730
2.507	-9376	8091	-532	-156	2686	982
2.515	-9144	1984	356	2068	5814	1350
2.522	-9104	1653	36	2364	430	1478
2.530	-10592	2653	-124	2964	1742	2278
2.537	-8848	2774	52	2980	5638	1446
2.544	-9984	3674	-1692	2852	2486	1526
2.552	-9568	-685	-396	1292	2254	7030
2.559	-11376	2008	-2324	1404	1766	2310
2.566	-9840	3093	1084	-372	934	2374
2.574	-7792	-335	-12	1364	1462	-762
2.581	-10344	3845	4	1852	4654	1190
2.588	-12480	4905	148	2164	3382	2070
2.596	-9224	5233	-1916	2284	2326	662
2.603	-9528	428	196	588	2422	358
2.610	-8200	8303	468	1460	2038	3350
2.618	-9336	7727	-740	660	2654	934
2.625	-9832	-2135	-36	3172	3366	1078
2.632	-10048	846	-908	2788	2598	806
2.640	-10464	2116	420	1412	3294	3430
2.647	-9528	2809	-788	740	1414	3014
2.654	-9328	3186	116	3196	6	1894
2.662	-9232	1103	700	2788	1054	326
2.669	-8880	288	-596	1404	2190	854
2.676	-9928	1891	84	532	1526	1830
2.684	-9464	6102	-1852	284	1678	1350

Appendix 4A Continued

2.691	-9224	3163	-1276	276	1510	134
2.698	-10184	3848	-468	804	2238	3046
2.706	-11056	5330	-2300	396	2254	3782
2.713	-9160	1484	-100	-708	998	774
2.720	-10976	4685	-236	332	1478	3030
2.728	-9160	-434	-1404	220	1622	1958
2.735	-9280	-253	-1468	1156	702	2518
2.742	-9912	1885	-2340	-596	646	2502
2.750	-10344	5378	-804	1132	1630	1110
2.757	-8280	1546	308	716	1558	1430
2.765	-10840	1539	-292	-476	1222	-1242
2.772	-10336	2140	1020	2468	2702	-570
2.779	-12072	4552	292	1884	2238	22
2.787	-8712	695	-196	-1188	1798	406
2.794	-9968	3274	-804	-1692	2294	534
2.801	-9920	-588	-1828	1796	1086	1238
2.809	-9240	902	-228	1084	1990	1862
2.816	-10616	456	-1668	244	2582	-250
2.823	-11368	289	-516	740	126	2150
2.831	-11448	-4467	100	-308	3302	1158
2.838	-10088	6455	428	-84	1686	-730
2.845	-9608	-771	-1596	1556	2526	-906
2.853	-9328	3308	412	1420	1142	2054
2.860	-10040	1209	-1068	2660	1494	1462
2.867	-9752	3437	-2372	1980	1630	2982
2.875	-10416	919	-2748	684	470	854
2.882	-10512	-2325	-1524	1204	1638	-1242
2.889	-10040	-2581	-700	1132	382	2166
2.897	-9376	5195	-580	1140	230	3174
2.904	-10432	1445	-828	2148	1870	1446
2.911	-8984	-60	68	692	2782	550
2.919	-9408	-1942	-244	2660	3094	582
2.926	-11248	-5632	-892	-356	838	1270
2.933	-11352	3310	-668	3196	622	1078

Appendix 4B - Zinc ICP-MS counts for King Site groundwaters for experiments in in Chapter 4. Values averages of several runs.

Time min	B7.5	B10	B15	B20	B25	B30	B35	B40
0.11	44	2276	9456	-4800	-1642	540	6552	4712
0.13	6796	10564	23896	-2032	-330	4300	10912	10152
0.14	16596	25636	33376	656	5694	7316	18552	15032
0.16	29972	33084	47680	7024	14982	13036	22328	17464
0.17	46580	44668	50592	21168	24806	20436	26040	24376
0.19	56404	47068	42144	32240	30182	26580	28408	22712
0.20	64596	39388	36704	39600	34022	32596	27352	25720
0.22	62196	33116	38432	42544	35526	37524	27608	27000
0.23	63060	29516	34856	45232	39590	36820	26520	24504
0.25	58132	28964	33824	47792	38310	37844	24984	21944
0.26	54644	30108	33824	43184	34214	40084	23736	23928
0.28	53812	28932	33968	44656	32486	38868	24856	22712
0.29	51892	29132	31496	40880	32070	36372	22200	19000
0.30	49172	28324	27848	40496	28294	35924	21816	19256
0.32	50452	27996	29464	33648	28582	35220	22936	22328
0.33	49108	27228	25384	34672	29286	34740	24024	18168
0.35	49716	25372	22032	33584	30310	35188	22520	18680
0.36	47860	24108	21840	31152	28518	35476	20536	19896
0.38	48372	23412	19664	29360	29222	34676	19928	16312
0.39	44276	23636	19240	29488	29382	31540	20504	18552
0.41	42164	21236	17384	27824	28614	31892	17976	18296
0.42	42708	20364	15000	28144	25606	28532	17240	16056
0.44	41076	22820	17520	27696	24422	28884	15352	15480
0.45	40308	21780	14736	26672	23974	30036	16056	11480
0.47	39412	23236	16224	26864	22342	27444	14696	13592
0.48	39124	20124	19248	23728	22470	27028	14008	12904
0.50	36692	23756	17440	21616	22246	25524	12640	13304
0.51	33716	22372	18904	20464	19270	25332	13272	12744
0.52	32500	22092	26320	18672	18534	23540	10872	13768
0.54	31124	23588	19536	16816	19174	22452	10232	11160
0.55	29492	29244	24816	15216	18214	21236	11072	8856
0.57	28500	27772	25288	16816	17222	19956	9288	6984
0.58	27476	29812	22696	13296	14950	18804	8552	8648
0.60	25908	27396	24432	13680	14118	15572	8984	8648
0.61	25012	31036	27448	12336	12710	17652	7784	6664
0.63	23316	32348	26312	9776	12318	15764	6064	3832
0.64	21140	33020	27456	9584	12806	14324	5504	5080
0.66	21140	35868	29376	6128	11142	13076	3904	4568
0.67	22740	35132	29376	9968	10182	12980	6608	6360
0.69	20724	36060	31112	4656	10814	12492	4520	2648
0.70	20020	35420	31416	7152	8014	11956	5360	1448
0.72	20340	36476	34624	6704	9302	12212	6136	408
0.73	20692	36764	31544	9072	6942	10676	2368	2376
0.75	18676	35772	30048	4400	7878	8732	3592	696
0.76	19860	37820	34088	5936	8382	11444	3840	200
0.77	21748	38300	32632	8496	10518	8740	2952	4648
0.79	19156	40924	30888	7152	7422	7996	3352	-760

Appendix 4B Continued

0.80	21780	39740	34464	6448	8390	10292	2592	136
0.82	22228	36668	33440	6640	7478	7964	2768	3048
0.83	21428	39548	30608	6832	8470	9756	2056	1208
0.85	23988	37500	30208	7088	8550	9644	4544	-184
0.86	22004	37692	28760	7856	7662	9844	4880	3480
0.88	25268	36444	28888	7472	9614	12620	3760	-856
0.89	25172	33980	29936	10288	10510	11876	4512	2488
0.91	26612	33532	25712	9584	10342	10164	5000	1448
0.92	26676	34268	28376	9840	10662	12020	5160	1784
0.94	28084	32732	28632	9328	10502	11532	4592	808
0.95	30420	29244	27352	12400	9486	11716	4840	216
0.97	31412	28668	21952	10352	11894	11892	4760	-1784
0.98	31476	28540	24824	10032	12006	12116	6544	2184
0.99	32468	26236	24408	13936	12870	12180	5728	88
1.01	35028	25476	22168	12016	12710	12692	6000	-648
1.02	35316	25092	21600	16688	13102	14324	6872	-168
1.04	40500	22588	16408	15472	11750	13844	6512	3320
1.05	37172	23932	16960	17200	12998	13428	6376	3032
1.07	37652	19572	21096	17712	15526	14004	8736	712
1.08	40852	19132	16264	17968	14726	17204	8568	1288
1.10	39124	18164	18008	13360	14630	13940	7504	2936
1.11	41972	15052	18440	21744	17350	14484	7792	376
1.13	42644	15548	15176	22640	17510	17236	8312	-424
1.14	43092	15644	15344	17648	19206	18068	8024	2088
1.16	44276	12204	11136	19632	21638	18964	8816	1928
1.17	44180	14356	14416	21232	18982	19796	9528	3992
1.19	44372	11212	14568	20784	19622	19540	9224	2296
1.20	46612	11332	4696	22320	22086	19572	8832	4344
1.22	49044	11652	11704	22768	20486	19124	8064	1224
1.23	48724	9860	8536	24304	20198	20724	9856	2232
1.24	49236	10836	10320	28080	21414	20788	9488	504
1.26	49780	7796	11392	27632	22950	20116	11248	3544
1.27	50676	8620	10016	26928	22278	22132	11512	2312
1.29	49332	8452	10744	28720	22150	22132	12544	3032
1.30	52724	7452	10096	31216	23366	21780	11696	2824
1.32	53236	6020	7584	25392	22566	22580	11168	808
1.33	54452	5900	7104	31216	22022	22228	12408	2760
1.35	52948	6892	4288	29360	23718	22388	9712	5128
1.36	51668	3916	7712	29680	23654	21524	10888	536
1.38	53844	4132	6176	28848	24614	23924	11408	1000
1.39	53652	1996	3920	31664	23366	22228	11304	2408
1.41	54836	3652	6088	34544	25478	22868	11144	1768
1.42	55156	5572	6968	33008	23974	24436	9800	4216
1.44	55316	3364	6336	33008	23974	23700	10368	1288
1.45	56276	3004	6160	33264	24902	22484	11360	1944
1.47	54708	1444	5624	31024	23238	21908	8528	2392
1.48	55764	228	5424	31920	22854	22932	11112	3976
1.49	56596	3476	7376	33072	23590	21460	11440	1672
1.51	53268	2420	3800	33264	23526	22964	10888	4424
1.52	51892	2452	3384	32624	23430	22516	11808	1080
1.54	52948	2948	3480	34800	22470	23156	11184	3464

Appendix 4B Continued

1.55	52084	1740	5560	33520	22086	20916	10440	3176
1.57	50420	2404	4600	30448	23558	21588	8960	1432
1.58	50292	1444	2616	27376	22214	20180	8808	2424
1.60	49748	372	5024	33776	22214	19284	8832	3560
1.61	49300	2236	5280	31856	20838	19636	9776	5384
1.63	50228	1388	2832	31344	21894	19444	8552	3992
1.64	51860	3044	1848	32624	20966	21204	7912	3128
1.66	49748	2020	1696	28784	20582	21332	8040	1160
1.67	48116	860	1432	29552	20710	19348	7360	2792
1.69	49076	3356	3720	29680	20710	17748	8176	1592
1.70	48372	-924	3232	29808	20774	18388	6392	3096
1.71	45428	1956	6848	28720	18502	16852	6136	2280
1.73	47252	460	6064	25456	17574	15700	8704	3400
1.74	44660	580	6360	25392	18054	17012	7640	2776
1.76	44980	-220	2864	25904	15910	16020	5640	1928
1.77	42356	1540	3528	25264	16102	16212	7640	3656
1.79	44020	908	120	27632	16966	14612	8072	1096
1.80	41332	1460	1832	25968	15654	14420	8120	-280
1.82	41620	1276	-848	23536	14854	17012	9408	4248
1.83	43732	1996	2568	25328	13222	14548	6232	2472
1.85	38260	2012	-160	23216	12038	12788	5704	680
1.86	37972	1796	-2064	21104	14022	12692	5712	2312
1.88	38580	2588	7600	20720	13222	12404	6120	2920
1.89	38996	1796	1976	18864	13542	12116	5040	-1192
1.91	35828	2356	-40	20208	13766	11604	5232	3192
1.92	34836	2308	1768	20208	13990	11828	5808	2472
1.94	32436	1396	1784	19504	12390	11572	4856	1192
1.95	32628	3572	400	16688	10878	11796	3456	2072
1.96	32468	2348	1368	15856	10350	10292	4808	2136
1.98	32852	1308	-1360	16944	10478	10260	3352	1720
1.99	30676	596	-1216	15216	10806	8748	4600	648
2.01	30228	1668	3176	14896	7998	8980	5232	1624
2.02	28980	1676	3992	15280	9094	8404	3392	2952
2.04	27700	3268	3824	13744	10398	8604	4152	1864
2.05	27700	836	608	13488	7974	5972	2488	2760
2.07	26868	700	1040	11824	9190	7100	2936	1464
2.08	24180	1692	4232	11760	8486	5548	3408	632
2.10	23412	1956	3800	9328	5910	6788	2528	1928
2.11	25076	2348	4304	13616	6934	5780	2872	1864
2.13	23572	3340	-1616	10608	6462	5884	2160	2440
2.14	22164	2564	3608	10864	6814	5612	2072	1816
2.16	23444	1348	-344	9456	4518	6076	2016	3240
2.17	22420	700	2288	9072	4934	4716	2656	568
2.19	19796	1508	3008	10608	5422	3700	1688	4744
2.20	18644	2540	4104	9136	3886	3932	2576	-904
2.21	19860	772	-560	8560	3214	3524	432	4056
2.23	20308	1628	4928	7856	5470	4388	1040	1224
2.24	18516	1252	2152	7152	5774	3276	1792	776
2.26	16724	3204	2888	6640	2894	5772	2080	6648
2.27	16884	1116	-1120	7344	2446	6324	2112	3832
2.29	17172	1436	5312	7984	4462	6948	2448	-296

Appendix 4B Continued

2.30	15700	1828	2256	2224	2478	5036	1200	1560
2.32	15732	1884	1704	6960	1958	6348	1448	376
2.33	14356	2340	5248	4912	4238	4796	1992	2248
2.35	14804	2684	2872	6768	2054	3748	2432	-472
2.36	13844	2588	1024	5296	2126	2540	1920	840
2.38	12052	548	4160	5808	2014	3388	2536	1608
2.39	11428	2348	4368	3376	14	2308	1976	984
2.41	11284	2036	3808	3376	1630	2884	-72	2600
2.42	11540	4012	648	4080	1382	2980	528	-344
2.43	9900	2508	4568	5296	830	-108	816	1976
2.45	9852	3332	3640	1072	1566	4828	-640	1192
2.46	9284	4492	3512	656	462	3172	912	728
2.48	9924	1604	2208	3312	1534	2348	2024	-1464
2.49	8740	964	1792	2416	-330	1852	2680	1368
2.51	8972	1012	2080	3056	1846	2476	232	712
2.52	8180	3276	3552	3248	894	1468	760	936
2.54	7940	2628	2848	2608	1838	1444	1104	2200
2.55	6908	3484	2352	3632	-218	3244	968	1976
2.57	8196	2916	3312	-976	-90	2268	1296	1496
2.58	5908	3460	5288	1776	902	1636	968	2936
2.60	5204	2972	-672	2544	-186	2708	616	2552
2.61	6004	3196	2128	1776	230	2748	-88	2824
2.63	6092	1892	2624	-256	534	420	2000	1064
2.64	7092	3660	3496	944	-242	2724	2488	1512
2.66	5860	3660	2768	-224	854	732	-568	2760
2.67	6292	2708	1840	-176	-1938	2876	1272	-904
2.68	5420	3820	-760	1264	-2682	1820	1256	968
2.70	6876	4132	5528	-2144	-18	1444	1992	2664
2.71	3380	3236	1160	1840	-1042	92	784	1848
2.73	3484	1684	-520	2288	-2458	724	1792	2168
2.74	3828	2748	1952	-608	38	-644	-768	2312
2.76	3844	2764	4536	240	-714	-252	-368	1800
2.77	4044	3644	2984	416	-1418	924	792	840
2.79	3196	2556	1880	-1408	-746	-164	1944	1416
2.80	4188	3540	3856	976	-826	1156	2256	3832
2.82	3660	3276	2288	768	-674	836	704	1752
2.83	3636	3452		112	182	1132	-152	3480
2.85	2268	3100		-672	-114	1084	984	888
2.86	2284	3772		-688	-1658	1428	64	-296
2.88	4308	2692		-1072	-722	692	1864	-200
2.89	1892	4716		352	-1234	964	-336	3080
2.90	2412	4596		1904	-2770	1780	608	2168
2.92	2956	4228		-1552	926	1140	688	904
2.93	1468	3964		784	1430	356	3376	2440
2.95	1372	2700		-960	-162	-340	-504	1112
2.96	3916	3636		-1904	-346	516	880	4328
2.98	2036	3844		720	-2226	1052	1504	-1272
2.99	3332	4108		-912	-1266	1796	224	-312

Appendix 4C - UV intensity (254 nm) for King Site groundwaters for experiments in in Chapter 4. Values averages of several runs.

Time Min	B7.5	B10	B15	B20	B25	B30	B35	B40
0.00	-0.0240	0.0234	-0.0271	-0.0239	-0.0340	-0.0314	-0.0346	-0.0355
0.02	-0.0240	0.0234	-0.0271	-0.0239	-0.0340	-0.0314	-0.0346	-0.0355
0.03	-0.0240	0.0234	-0.0271	-0.0239	-0.0340	-0.0314	-0.0346	-0.0355
0.05	-0.0240	0.0234	-0.0271	-0.0239	-0.0340	-0.0314	-0.0346	-0.0355
0.07	-0.0240	0.0234	-0.0271	-0.0239	-0.0340	-0.0314	-0.0346	-0.0355
0.08	-0.0240	0.0234	-0.0271	-0.0239	-0.0340	-0.0314	-0.0346	-0.0355
0.10	-0.0240	0.0234	-0.0271	-0.0239	-0.0340	-0.0314	-0.0346	-0.0355
0.12	-0.0240	0.0234	-0.0271	-0.0239	-0.0340	-0.0314	-0.0346	-0.0355
0.13	-0.0240	0.0234	-0.0271	-0.0239	-0.0340	-0.0314	-0.0346	-0.0355
0.15	-0.0240	0.0234	-0.0271	-0.0239	-0.0340	-0.0314	-0.0346	-0.0355
0.17	-0.0240	0.0234	-0.0271	-0.0239	-0.0340	-0.0314	-0.0346	-0.0355
0.18	-0.0240	0.0234	-0.0271	-0.0239	-0.0340	-0.0314	-0.0346	-0.0355
0.20	-0.0240	0.0234	-0.0271	-0.0239	-0.0340	-0.0314	-0.0346	-0.0355
0.22	-0.0240	0.0234	-0.0271	-0.0239	-0.0339	-0.0314	-0.0316	-0.0355
0.23	0.0775	0.4430	0.0866	0.0261	0.0140	0.0072	-0.0081	-0.0355
0.25	0.3407	1.0214	0.3225	0.1574	0.1249	0.1055	0.0575	-0.0288
0.27	0.5943	1.2827	0.4514	0.2329	0.1849	0.1597	0.0913	-0.0282
0.28	0.7048	1.2925	0.4684	0.2441	0.1911	0.1657	0.0935	-0.0308
0.30	0.7083	1.2053	0.4409	0.2287	0.1776	0.1551	0.0862	-0.0303
0.32	0.6683	1.1088	0.4052	0.2110	0.1643	0.1446	0.0815	-0.0238
0.33	0.6257	1.0244	0.3776	0.2001	0.1568	0.1400	0.0817	-0.0137
0.35	0.5884	0.9571	0.3592	0.1959	0.1555	0.1390	0.0878	-0.0031
0.37	0.5585	0.9010	0.3460	0.1965	0.1628	0.1404	0.0914	0.0077
0.38	0.5329	0.8522	0.3353	0.1946	0.1601	0.1420	0.0945	0.0171
0.40	0.5107	0.8087	0.3254	0.1928	0.1582	0.1423	0.0969	0.0244
0.42	0.4909	0.7696	0.3155	0.1891	0.1558	0.1420	0.0987	0.0299
0.43	0.4725	0.7361	0.3063	0.1849	0.1532	0.1406	0.0997	0.0332
0.45	0.4570	0.7076	0.2976	0.1811	0.1514	0.1391	0.1002	0.0358
0.47	0.4438	0.6827	0.2906	0.1821	0.1493	0.1383	0.1006	0.0377
0.48	0.4333	0.6629	0.2853	0.1783	0.1474	0.1380	0.1006	0.0393
0.50	0.4254	0.6480	0.2812	0.1751	0.1463	0.1381	0.1007	0.0406
0.52	0.4201	0.6381	0.2787	0.1734	0.1460	0.1392	0.1013	0.0413
0.53	0.4178	0.6332	0.2782	0.1733	0.1467	0.1431	0.1022	0.0419
0.55	0.4185	0.6333	0.2793	0.1735	0.1477	0.1436	0.1029	0.0425
0.57	0.4219	0.6380	0.2821	0.1750	0.1496	0.1451	0.1042	0.0434
0.58	0.4282	0.6472	0.2868	0.1780	0.1523	0.1472	0.1060	0.0444
0.60	0.4373	0.6603	0.2929	0.1808	0.1557	0.1508	0.1083	0.0449
0.62	0.4485	0.6774	0.3010	0.1848	0.1601	0.1545	0.1109	0.0457
0.63	0.4621	0.6980	0.3105	0.1902	0.1648	0.1591	0.1139	0.0462
0.65	0.4778	0.7212	0.3206	0.1954	0.1701	0.1641	0.1178	0.0469
0.67	0.4944	0.7460	0.3314	0.2016	0.1755	0.1697	0.1212	0.0481
0.68	0.5118	0.7714	0.3436	0.2096	0.1812	0.1752	0.1252	0.0491
0.70	0.5301	0.7973	0.3548	0.2158	0.1869	0.1806	0.1287	0.0496
0.72	0.5483	0.8220	0.3656	0.2216	0.1927	0.1862	0.1329	0.0503
0.73	0.5666	0.8455	0.3768	0.2274	0.1981	0.1915	0.1363	0.0501
0.75	0.5838	0.8671	0.3866	0.2329	0.2029	0.1964	0.1392	0.0511
0.77	0.5994	0.8853	0.3959	0.2383	0.2069	0.2015	0.1420	0.0509

Appendix 4C Continued

0.78	0.6131	0.8998	0.4044	0.2432	0.2109	0.2065	0.1442	0.0517
0.80	0.6246	0.9104	0.4108	0.2473	0.2145	0.2097	0.1463	0.0523
0.82	0.6333	0.9161	0.4158	0.2504	0.2168	0.2112	0.1476	0.0524
0.83	0.6392	0.9170	0.4185	0.2524	0.2185	0.2118	0.1491	0.0522
0.85	0.6410	0.9130	0.4198	0.2532	0.2192	0.2115	0.1487	0.0518
0.87	0.6400	0.9030	0.4186	0.2528	0.2186	0.2101	0.1476	0.0512
0.88	0.6354	0.8883	0.4149	0.2511	0.2169	0.2079	0.1458	0.0504
0.90	0.6274	0.8681	0.4091	0.2481	0.2139	0.2048	0.1433	0.0491
0.92	0.6159	0.8434	0.4012	0.2439	0.2100	0.2006	0.1401	0.0478
0.93	0.6011	0.8146	0.3912	0.2383	0.2054	0.1955	0.1366	0.0466
0.95	0.5836	0.7827	0.3798	0.2319	0.1991	0.1896	0.1325	0.0453
0.97	0.5635	0.7479	0.3670	0.2245	0.1923	0.1829	0.1278	0.0433
0.98	0.5409	0.7104	0.3529	0.2161	0.1849	0.1757	0.1227	0.0422
1.00	0.5166	0.6716	0.3378	0.2072	0.1768	0.1680	0.1174	0.0414
1.02	0.4913	0.6307	0.3214	0.1978	0.1677	0.1598	0.1119	0.0390
1.03	0.4652	0.5891	0.3044	0.1882	0.1588	0.1511	0.1057	0.0366
1.05	0.4379	0.5479	0.2870	0.1780	0.1493	0.1424	0.0992	0.0343
1.07	0.4101	0.5079	0.2694	0.1675	0.1400	0.1330	0.0926	0.0319
1.08	0.3827	0.4685	0.2515	0.1571	0.1302	0.1241	0.0864	0.0295
1.10	0.3555	0.4306	0.2340	0.1462	0.1214	0.1152	0.0806	0.0269
1.12	0.3288	0.3944	0.2166	0.1360	0.1123	0.1067	0.0743	0.0245
1.13	0.3029	0.3592	0.1999	0.1259	0.1038	0.0981	0.0683	0.0223
1.15	0.2779	0.3266	0.1840	0.1160	0.0955	0.0901	0.0626	0.0202
1.17	0.2545	0.2961	0.1689	0.1063	0.0881	0.0823	0.0571	0.0182
1.18	0.2322	0.2677	0.1548	0.0970	0.0803	0.0748	0.0521	0.0162
1.20	0.2112	0.2415	0.1416	0.0886	0.0735	0.0679	0.0472	0.0146
1.22	0.1915	0.2168	0.1291	0.0807	0.0669	0.0613	0.0427	0.0131
1.23	0.1736	0.1944	0.1177	0.0731	0.0603	0.0555	0.0388	0.0119
1.25	0.1570	0.1738	0.1069	0.0667	0.0545	0.0500	0.0354	0.0107
1.27	0.1418	0.1558	0.0971	0.0603	0.0491	0.0451	0.0315	0.0096
1.28	0.1277	0.1393	0.0879	0.0548	0.0441	0.0404	0.0288	0.0085
1.30	0.1151	0.1238	0.0798	0.0491	0.0399	0.0361	0.0261	0.0073
1.32	0.1034	0.1106	0.0724	0.0444	0.0356	0.0323	0.0230	0.0063
1.33	0.0927	0.0990	0.0657	0.0399	0.0317	0.0290	0.0211	0.0058
1.35	0.0830	0.0887	0.0598	0.0357	0.0288	0.0259	0.0191	0.0048
1.37	0.0744	0.0795	0.0545	0.0319	0.0260	0.0231	0.0169	0.0044
1.38	0.0669	0.0713	0.0497	0.0285	0.0234	0.0209	0.0156	0.0040
1.40	0.0600	0.0636	0.0454	0.0254	0.0210	0.0187	0.0138	0.0037
1.42	0.0541	0.0570	0.0417	0.0228	0.0187	0.0168	0.0123	0.0035
1.43	0.0486	0.0510	0.0381	0.0206	0.0170	0.0150	0.0108	0.0032
1.45	0.0437	0.0461	0.0350	0.0187	0.0153	0.0133	0.0098	0.0032
1.47	0.0391	0.0410	0.0322	0.0164	0.0142	0.0118	0.0093	0.0035
1.48	0.0349	0.0374	0.0295	0.0152	0.0126	0.0104	0.0082	0.0031
1.50	0.0312	0.0340	0.0270	0.0135	0.0114	0.0090	0.0071	0.0028
1.52	0.0283	0.0301	0.0252	0.0126	0.0103	0.0075	0.0062	0.0023
1.53	0.0253	0.0275	0.0233	0.0116	0.0099	0.0065	0.0055	0.0021
1.55	0.0230	0.0251	0.0221	0.0123	0.0092	0.0055	0.0050	0.0018
1.57	0.0207	0.0228	0.0205	0.0116	0.0084	0.0045	0.0045	0.0018
1.58	0.0190	0.0207	0.0193	0.0102	0.0077	0.0038	0.0038	0.0019
1.60	0.0170	0.0192	0.0183	0.0091	0.0070	0.0031	0.0036	0.0013
1.62	0.0151	0.0176	0.0168	0.0084	0.0062	0.0022	0.0032	0.0008

Appendix 4C Continued

1.63	0.0136	0.0159	0.0158	0.0083	0.0056	0.0016	0.0029	0.0007
1.65	0.0119	0.0146	0.0145	0.0074	0.0053	0.0012	0.0024	0.0008
1.67	0.0104	0.0135	0.0137	0.0067	0.0051	0.0006	0.0023	0.0006
1.68	0.0096	0.0126	0.0128	0.0061	0.0050	0.0001	0.0015	0.0004
1.70	0.0083	0.0122	0.0120	0.0051	0.0049	-0.0003	0.0012	0.0004
1.72	0.0071	0.0116	0.0115	0.0049	0.0046	-0.0005	0.0012	0.0003
1.73	0.0064	0.0111	0.0107	0.0047	0.0045	-0.0006	0.0008	0.0003
1.75	0.0057	0.0108	0.0100	0.0045	0.0046	-0.0009	0.0007	0.0004
1.77	0.0053	0.0100	0.0093	0.0039	0.0048	-0.0010	0.0007	0.0004
1.78	0.0048	0.0098	0.0090	0.0036	0.0047	-0.0010	0.0003	0.0004
1.80	0.0044	0.0087	0.0087	0.0033	0.0045	-0.0009	0.0001	0.0004
1.82	0.0041	0.0084	0.0087	0.0028	0.0043	-0.0004	0.0001	0.0010
1.83	0.0036	0.0083	0.0083	0.0025	0.0039	-0.0008	0.0001	0.0011
1.85	0.0029	0.0080	0.0080	0.0020	0.0033	-0.0007	0.0002	0.0012
1.87	0.0024	0.0077	0.0077	0.0019	0.0029	-0.0006	0.0003	0.0015
1.88	0.0021	0.0077	0.0074	0.0017	0.0025	-0.0004	0.0003	0.0013
1.90	0.0017	0.0074	0.0072	0.0019	0.0020	-0.0003	0.0004	0.0016
1.92	0.0012	0.0071	0.0066	0.0019	0.0016	-0.0003	0.0004	0.0020
1.93	0.0012	0.0070	0.0066	0.0018	0.0013	-0.0004	0.0003	0.0013
1.95	0.0018	0.0064	0.0067	0.0014	0.0011	-0.0004	0.0003	0.0016
1.97	0.0012	0.0058	0.0066	0.0013	0.0009	-0.0002	0.0002	0.0015
1.98	0.0006	0.0055	0.0065	0.0010	0.0011	-0.0001	0.0001	0.0018
2.00	0.0005	0.0054	0.0060	0.0007	0.0008	-0.0007	0.0000	0.0021
2.02	0.0004	0.0051	0.0057	0.0005	0.0007	-0.0006	-0.0002	0.0022
2.03	0.0002	0.0046	0.0055	0.0005	0.0008	0.0006	-0.0002	0.0019
2.05	-0.0001	0.0043	0.0051	0.0003	0.0006	0.0004	-0.0003	0.0019
2.07	-0.0003	0.0040	0.0049	-0.0001	0.0003	0.0000	-0.0004	0.0012
2.08	-0.0006	0.0037	0.0047	-0.0004	0.0003	-0.0003	-0.0005	0.0006
2.10	-0.0008	0.0036	0.0044	-0.0002	0.0011	-0.0011	-0.0004	0.0005
2.12	-0.0010	0.0037	0.0045	-0.0002	0.0010	-0.0014	-0.0002	0.0003
2.13	-0.0012	0.0040	0.0047	-0.0004	0.0005	-0.0015	-0.0001	0.0000
2.15	-0.0013	0.0039	0.0048	-0.0007	0.0005	-0.0013	-0.0001	0.0001
2.17	-0.0013	0.0036	0.0049	-0.0005	0.0005	-0.0013	-0.0001	-0.0003
2.18	-0.0014	0.0036	0.0043	-0.0004	0.0005	-0.0011	-0.0001	-0.0004
2.20	-0.0015	0.0035	0.0042	-0.0004	0.0005	-0.0008	0.0001	-0.0006
2.22	-0.0017	0.0031	0.0041	-0.0003	0.0008	-0.0008	0.0004	-0.0006
2.23	-0.0018	0.0030	0.0037	0.0000	0.0009	-0.0005	0.0001	-0.0008
2.25	-0.0019	0.0032	0.0034	0.0003	0.0010	-0.0006	0.0000	-0.0008
2.27	-0.0020	0.0033	0.0030	0.0003	0.0019	-0.0006	-0.0002	-0.0013
2.28	-0.0020	0.0031	0.0025	0.0005	0.0017	-0.0009	-0.0001	-0.0015
2.30	-0.0018	0.0031	0.0025	0.0006	0.0014	-0.0010	0.0004	-0.0015
2.32	-0.0021	0.0031	0.0025	0.0005	0.0010	-0.0010	0.0003	-0.0015
2.33	-0.0022	0.0036	0.0021	0.0008	0.0004	-0.0012	0.0003	-0.0015
2.35	-0.0022	0.0035	0.0023	0.0009	0.0000	-0.0013	0.0007	-0.0012
2.37	-0.0021	0.0037	0.0023	0.0010	-0.0003	-0.0012	0.0007	-0.0012
2.38	-0.0023	0.0037	0.0026	0.0010	-0.0003	-0.0010	0.0006	-0.0011
2.40	-0.0024	0.0040	0.0027	0.0009	-0.0008	-0.0008	0.0006	-0.0002
2.42	-0.0023	0.0038	0.0026	0.0009	-0.0012	-0.0008	0.0005	-0.0001
2.43	-0.0026	0.0036	0.0023	0.0009	-0.0016	-0.0009	0.0005	0.0000
2.45	-0.0027	0.0031	0.0024	0.0006	-0.0019	-0.0008	0.0007	0.0003
2.47	-0.0028	0.0031	0.0024	0.0003	-0.0019	-0.0007	0.0008	0.0006

Appendix 4C Continued

2.48	-0.0027	0.0029	0.0023	-0.0001	-0.0020	-0.0006	0.0007	0.0005
2.50	-0.0025	0.0029	0.0024	-0.0003	-0.0020	-0.0003	0.0007	0.0005
2.52	-0.0025	0.0028	0.0025	-0.0009	-0.0021	-0.0001	0.0007	0.0006
2.53	-0.0027	0.0028	0.0029	-0.0011	-0.0022	0.0000	0.0010	0.0003
2.55	-0.0027	0.0028	0.0030	-0.0010	-0.0024	0.0001	0.0010	0.0001
2.57	-0.0027	0.0024	0.0031	-0.0011	-0.0025	0.0001	0.0009	-0.0001
2.58	-0.0023	0.0019	0.0033	-0.0015	-0.0026	0.0008	0.0008	0.0004
2.60	-0.0022	0.0013	0.0036	-0.0015	-0.0023	0.0007	0.0007	0.0003
2.62	-0.0019	0.0014	0.0039	-0.0014	-0.0021	0.0003	0.0003	0.0000
2.63	-0.0012	0.0017	0.0037	-0.0015	-0.0022	0.0002	0.0003	-0.0003
2.65	-0.0009	0.0019	0.0035	-0.0014	-0.0017	0.0002	0.0002	-0.0004
2.67	-0.0005	0.0020	0.0032	-0.0013	-0.0016	0.0001	-0.0001	-0.0002
2.68	-0.0002	0.0020	0.0026	-0.0013	-0.0012	0.0002	-0.0004	0.0000
2.70	-0.0004	0.0022	0.0022	-0.0010	-0.0009	0.0000	-0.0005	-0.0006
2.72	-0.0004	0.0021	0.0014	-0.0010	-0.0007	-0.0003	-0.0006	-0.0005
2.73	-0.0002	0.0018	0.0009	-0.0005	-0.0011	-0.0007	-0.0007	-0.0002
2.75	-0.0001	0.0019	0.0004	-0.0004	-0.0011	-0.0005	-0.0008	-0.0002
2.77	-0.0001	0.0018	0.0000	-0.0002	-0.0013	-0.0006	-0.0009	-0.0002
2.78	-0.0002	0.0018	-0.0001	-0.0004	-0.0015	-0.0008	-0.0007	-0.0001
2.80	-0.0003	0.0020	-0.0002	-0.0003	-0.0015	-0.0013	-0.0007	0.0000
2.82	-0.0004	0.0021	-0.0003	-0.0001	-0.0015	-0.0014	-0.0009	-0.0001
2.83	-0.0006	0.0017	-0.0004	0.0000	-0.0015	-0.0015	-0.0011	-0.0005
2.85	-0.0004	0.0019	-0.0003	0.0002	-0.0014	-0.0019	-0.0010	-0.0001
2.87	-0.0004	0.0023	-0.0001	0.0001	-0.0014	-0.0021	-0.0012	0.0005
2.88	-0.0007	0.0021	-0.0002	0.0002	-0.0011	-0.0020	-0.0014	0.0008
2.90	-0.0010	0.0027	-0.0004	0.0006	-0.0009	-0.0020	-0.0014	0.0006
2.92	-0.0011	0.0030	-0.0002	0.0008	-0.0010	-0.0019	-0.0013	0.0009
2.93	-0.0011	0.0030	0.0001	0.0008	-0.0011	-0.0018	-0.0012	0.0000
2.95	-0.0009	0.0028	0.0004	0.0007	-0.0014	-0.0017	-0.0011	0.0004
2.97	-0.0006	0.0023	0.0003	0.0008	-0.0013	-0.0018	-0.0008	-0.0001
2.98	-0.0003	0.0019	-0.0002	0.0002	-0.0012	-0.0019	-0.0010	-0.0005
3.00	-0.0004	0.0018	-0.0005	0.0003	-0.0011	-0.0017	-0.0011	0.0001
3.02	0.0000	0.0014	-0.0004	0.0002	-0.0013	-0.0014	-0.0009	0.0009
3.03	0.0000	0.0010	-0.0002	0.0004	-0.0012	-0.0011	-0.0009	0.0013
3.05	0.0000	0.0008	-0.0004	0.0009	-0.0014	-0.0012	-0.0010	0.0014
3.07	0.0001	0.0008	-0.0006	0.0012	-0.0016	-0.0015	-0.0010	0.0021
3.08	0.0001	0.0007	-0.0005	0.0013	-0.0015	-0.0017	-0.0011	0.0019
3.10	0.0001	0.0006	-0.0002	0.0014	-0.0016	-0.0001	-0.0025	0.0017
3.12	-0.0002	0.0004	-0.0004	0.0015	-0.0016	0.0000	-0.0035	0.0016
3.13	-0.0005	0.0002	-0.0007	0.0014	0.0020	0.0002	-0.0041	0.0019
3.15	-0.0009	0.0006	-0.0009	0.0008	0.0017	0.0011	-0.0041	0.0014
3.17	-0.0016	0.0006	-0.0014	0.0003	0.0021	0.0008	-0.0047	0.0013
3.18	-0.0019	0.0005	-0.0019	0.0001	0.0017	0.0004	-0.0049	0.0019
3.20	-0.0021	0.0008	-0.0021	-0.0003	0.0013	0.0003	-0.0049	0.0024
3.22	-0.0024	0.0006	-0.0024	-0.0004	0.0007	-0.0002	-0.0047	0.0020

Appendix 4D - Uranium ICP-MS counts for pH titration experiment in Chaper 4. Values are averag of multiple runs.

Time		9.75	9.56	9.02	8.54	7.99	7.41	7.02
min	sec							
0.03	2	-183662	-100064.5	-108968	-109857.5	-173377	-84136.5	-116328.5
0.04	2	-183449.5	-75314.5	-109331	-108041.5	-173287.5	-85102	-116403.5
0.05	3	-178798.5	-75704.5	-109960.5	-109864	-174452.5	-84496	-116308
0.06	3	-129433	-87498	-109390	-107350.5	-174767.5	-88128.5	-116802.5
0.06	4	-73779	-96583	-108907	-108873.5	-174541	-70738	-116664.5
0.07	4	-46528.5	-100914.5	-111115.5	-105787	-174506.5	-72233.5	-114060
0.08	5	-43691	-98618	-112765	-106804	-169122.5	-80167	-112821
0.08	5	10058	-100545	-114581	-109971	-160863.5	-89387.5	-114399.5
0.09	5	238290	-100259	-115441	-109942.5	-144151.5	-89572.5	-113889
0.10	6	302546	-101653	-107517.5	-111943	-138623.5	-88931.5	-95012
0.11	6	206482	-20266	169355	-113291.5	-132032	-92837.5	-54453
0.11	7	120066	212582	959290	-69558	-90230	-97933.5	-16589
0.12	7	73850	552038	1197622	12527	-81462	-98086	2459
0.13	8	59954	744998	1007638	46838	-89150	196222	-6901
0.14	8	112818	846502	788150	77904	32986	563110	-20949
0.14	9	300658	863430	587926	136224	80594	349174	-26101
0.15	9	680754	763782	526582	95744	24266	182686	-17733
0.16	9	1167154	630342	428694	56192	-10734	106246	-6341
0.17	10	1414226	458502	301878	33432	-27678	70062	10115
0.17	10	1413458	300326	187702	27656	-38694	39686	21371
0.18	11	1293778	192102	106390	13872	-41102	38982	30675
0.19	11	1288402	105254	145750	888	-26742	53326	94171
0.19	12	1314770	72550	536206	2624	-9326	68302	554091
0.20	12	1270354	121222	1197006	33136	189202	88462	1669579
0.21	13	1188690	470062	1979382	372336	652658	91158	3488843
0.22	13	936530	1039494	2546582	1278928	1441746	110422	5121995
0.22	13	652178	1556414	2852886	2516872	2295538	361462	5380555
0.23	14	428818	1775606	2830870	3423992	3157874	1290614	4687819
0.24	14	283058	1614526	2418710	3742880	3928562	3074038	3475403
0.25	15	175178	1293214	1788566	3322944	4763634	5172854	2237387
0.25	15	65858	886646	1212182	2812352	4930546	6584950	1369675
0.26	16	2786	586326	764822	2447168	4219378	6461046	759627
0.27	16	-26870	358886	470294	2131008	2991218	4898934	482923
0.28	17	4938	211350	292054	1618368	1883794	3226742	318667
0.28	17	-44966	138982	177462	1103296	1085330	1904118	242347
0.29	17	-62038	87966	117142	693952	686258	1145846	161931
0.30	18	-71502	122758	86422	437472	448850	732534	116043
0.30	18	-72222	460198	73014	280352	313746	513142	89259
0.31	19	-59886	1307206	39966	225920	207794	425910	74763
0.32	19	3858	2928262	24526	151424	144786	363222	57539
0.33	20	471346	5526182	17846	111744	113522	297462	44643
0.33	20	1287218	8426534	10262	93568	75410	260150	60395
0.34	20	3052242	11669734	470	57280	90290	218486	46387
0.35	21	5559250	14339398	-8378	51072	76210	165846	26795
0.36	21	8789074	15916262	-12074	34112	68466	235126	29387
0.36	22	12715474	17075974	9854	16184	30514	264694	16467
0.37	22	15938130	16974502	175110	9920	15858	100982	67411

Appendix 4D Continued

0.38	23	19443282	15604870	815782	16056	119378	88118	407483
0.39	23	20766290	15678758	1958582	139656	572050	80182	1432459
0.39	24	23178834	15869094	4138262	598960	1719218	80534	3766475
0.40	24	24438354	16772262	7260694	1434600	3245778	144182	6656459
0.41	24	24979026	18705062	11441174	2801808	5042034	549686	9910219
0.42	25	25970258	20863654	15338006	4380608	7130610	1764982	13101515
0.42	25	25896530	23321254	19288598	6235328	9342962	4398710	14465483
0.43	26	25499218	25211558	22020630	8412480	11040242	7469174	16269771
0.44	26	24196690	25717414	24185366	10775360	12479986	10515574	16273867
0.44	27	23250514	25608870	23597590	13062976	13360626	12846198	15628747
0.45	27	21730898	24101542	22956566	15131456	13731314	14507126	15376843
0.46	28	21077586	23155366	22491670	16376640	13305330	15144054	13826507
0.47	28	19916370	21906086	20865558	17384256	12656114	15461494	13074891
0.47	28	19232338	20636326	19591702	18025280	11894258	14965878	11905483
0.48	29	18083410	19290790	18635286	17795904	11527666	14228598	11166155
0.49	29	16805458	17439398	17496598	17091392	11073010	13276278	10219979
0.50	30	15586898	16116390	16106006	15657792	10087922	12131446	9331147
0.50	30	14761554	15135398	15114774	15096640	9422322	11326582	9134539
0.51	31	13389394	13847206	13822486	13841216	8620530	10880118	8688075
0.52	31	12498514	12839590	12980758	12366656	7974898	10122358	8211403
0.53	32	11550290	11731622	12243478	11261760	7501810	9426550	7645643
0.53	32	10640978	10566310	11235862	10255680	6905842	8795766	7367115
0.54	32	9350738	9886374	9814550	9222464	6424562	8202358	7167947
0.55	33	8454226	9084070	9014294	8166208	6138354	7816310	6955467
0.55	33	7557714	8158374	8282646	7291200	5862386	7240310	6699467
0.56	34	6806610	7265958	7066646	6700864	5464562	6830198	6445515
0.57	34	6105682	6531238	6182934	5874496	5252594	6569590	6315979
0.58	35	5554258	5776550	5356566	5327168	4899314	6342774	6040011
0.58	35	5007442	5039782	4658198	4764480	4739058	6041718	5834699
0.59	35	4261458	4526246	4076054	4489024	4492274	5699702	5805515
0.60	36	3835986	4084902	3505174	4036928	4295666	5394038	5674443
0.61	36	3406418	3935398	3018262	3654976	4331506	5110390	5435851
0.61	37	3239506	3647142	2839574	3317056	4058098	4986998	5457867
0.62	37	2787922	3175462	2536982	3088192	3948018	4800630	5475275
0.63	38	2493522	2847270	2303510	2898240	3902962	4761718	5275083
0.64	38	2222674	2574886	2171926	2727232	3771378	4466806	5205451
0.64	39	2056274	2319270	1951254	2945344	3725298	4377718	5257675
0.65	39	1882194	2149414	1824918	2501952	3649010	4216950	5172683
0.66	39	1870290	2044582	1723414	2480960	3578866	4260982	5057483
0.66	40	1812946	1934886	1719318	2343232	3522034	4109430	4990411
0.67	40	1618130	1861798	1613078	2334528	3440626	4066422	5014475
0.68	41	1546962	1815590	1669270	2248512	3475954	3981942	5117899
0.69	41	1402194	1844390	1580822	2179392	3488754	4040310	5036491
0.69	42	1435218	1849382	1567510	2139968	3412466	3937910	5192139
0.70	42	1388498	1839782	1547030	2083648	3382770	3935350	5016523
0.71	42	1335890	1818534	1501462	2107712	3346930	3835510	5028299
0.72	43	1295058	1787686	1526934	2110272	3487730	3864182	5107147
0.72	43	1264850	1810982	1544854	2118464	3532274	3831926	5269963
0.73	44	1268946	1825702	1535510	2088768	3539442	3834998	5220811
0.74	44	1278162	1787814	1559702	2089792	3491314	3965558	5260235
0.75	45	1326290	1802790	1515670	2124608	3505138	4019318	5204427

Appendix 4D Continued

0.75	45	1328978	1867174	1593494	2107200	3524594	4036214	5270475
0.76	46	1330258	1926822	1620630	2093888	3599346	3972726	5407691
0.77	46	1343954	1918886	1646102	2179392	3602418	3991158	5439435
0.78	47	1395410	2002982	1679510	2185536	3698674	4038774	5504971
0.78	47	1410386	2061222	1645718	2195264	3680754	4045942	5693387
0.79	47	1452370	2058150	1713942	2233664	3698162	4154486	5558731
0.80	48	1448274	2078630	1744662	2294080	3810802	4055158	5648331
0.80	48	1465554	2123558	1790742	2336064	3877874	4110454	5670347
0.81	49	1516242	2136742	1788566	2291520	3894258	4130422	5910475
0.82	49	1522514	2195238	1856790	2325824	3885554	4250742	5828043
0.83	50	1573458	2201382	1874582	2394944	3971570	4262006	5942731
0.83	50	1606866	2273446	1908118	2474304	4070386	4400758	6000587
0.84	50	1606610	2291238	1928086	2466112	4097522	4456054	6003147
0.85	51	1618770	2314022	1949462	2518336	4169202	4555382	6328267
0.86	51	1647442	2357798	2013206	2605376	4155890	4610678	6374859
0.86	52	1696850	2391718	2010134	2665280	4193266	4625014	6416843
0.87	52	1683026	2383526	2043926	2618688	4322290	4518006	6560715
0.88	53	1676242	2492070	2147862	2708800	4293106	4622966	6527947
0.89	53	1630162	2500262	2169366	2709824	4315122	4703862	6778827
0.89	54	1696082	2493094	2163734	2784576	4433906	4734582	6814667
0.90	54	1720658	2508966	2193430	2758976	4431858	4793974	6774731
0.91	54	1792082	2564262	2229782	2828096	4530162	4844150	6761931
0.91	55	1777618	2531494	2273302	2881856	4517874	4917878	6960075
0.92	55	1794898	2564774	2255382	2891072	4619250	4965494	6940619
0.93	56	1781202	2562726	2216470	2927424	4543474	4955766	6994379
0.94	56	1792210	2620070	2264598	2945344	4681714	5127798	7022539
0.94	57	1781970	2612390	2329622	3031360	4686322	5033078	7178187
0.95	57	1809746	2630310	2314262	3073344	4852210	5123702	7036363
0.96	57	1822034	2692774	2382358	3027776	4811762	5123190	7215563
0.97	58	1785298	2712230	2359830	3068224	4769778	5203574	7298507
0.97	58	1796178	2707622	2433046	3062592	4791282	5186166	7513547
0.98	59	1764946	2626726	2369558	3023168	4891122	5342326	7483339
0.99	59	1804626	2653350	2348054	3056960	5067762	5455478	7446475
1.00	60	1746258	2654374	2451990	3031872	4963826	5450870	7353291
1.00	60	1707986	2605734	2402326	3126592	4852722	5480054	7224267
1.01	61	1697362	2628262	2393622	3150144	4842994	5324406	7305675
1.02	61	1671378	2664102	2392086	3123520	4798450	5242486	7360459
1.02	61	1686866	2594470	2423830	3165504	4887538	5257334	7450059
1.03	62	1695186	2550438	2385430	3145024	4822514	5203062	7375819
1.04	62	1612498	2529958	2377750	3143488	4798962	5286006	7240651
1.05	63	1593938	2523302	2374678	3125056	4768754	5293686	7230411
1.05	63	1583826	2510502	2375190	3088704	4732914	5340790	7350731
1.06	64	1562962	2452134	2342422	3089728	4691442	5359734	7038411
1.07	64	1590354	2438822	2354198	3060032	4701170	5434486	7182283
1.08	65	1633490	2405542	2288662	3024704	4635634	5446774	7219659
1.08	65	1516242	2357926	2255382	3077440	4551154	5313654	7029195
1.09	65	1472850	2351270	2252310	3005248	4538866	5170294	7025611
1.10	66	1438290	2355366	2192406	2921792	4545522	5089398	6726603
1.11	66	1444946	2294950	2173974	2901312	4577778	5201014	6877643
1.11	67	1400530	2306726	2183190	2941248	4397042	5140598	6696395
1.12	67	1341010	2247846	2095510	2828608	4338162	4998774	6476235

Appendix 4D Continued

1.13	68	1336018	2153638	2117654	2800960	4298738	4956278	6429131
1.14	68	1326418	2139302	2067862	2763584	4242418	4956790	6373323
1.14	69	1291090	2119334	2013846	2789696	4111858	4928630	6351819
1.15	69	1245778	2103334	1976854	2713920	4013554	4826230	6162379
1.16	69	1218258	2049702	1950998	2683200	3980786	4697718	6061003
1.16	70	1195090	1975846	1914262	2603840	3849714	4512374	5942731
1.17	70	1164114	1911974	1878550	2552128	3787250	4423286	5839819
1.18	71	1123410	1871270	1855766	2578752	3823602	4481654	5687755
1.19	71	1109714	1824806	1835542	2476864	3701234	4336758	5542859
1.19	72	1068882	1778854	1765398	2378560	3659762	4242038	5367243
1.20	72	1051218	1725094	1724950	2342208	3499506	4156022	5225931
1.21	72	1044946	1720486	1686934	2335552	3353586	4082806	5102539
1.22	73	970194	1697062	1687830	2246464	3329522	3959414	5033931
1.22	73	971602	1642662	1649430	2232640	3274738	3825270	4817867
1.23	74	946642	1577894	1590166	2182976	3209202	3794550	4734411
1.24	74	943314	1559718	1528470	2131776	3081202	3751030	4631499
1.25	75	917458	1510438	1476630	2043712	3044338	3656822	4348875
1.25	75	889298	1446054	1444246	2014144	2996210	3563126	4404683
1.26	76	869202	1434918	1417622	1922368	2786290	3380342	4234699
1.27	76	834002	1403046	1402006	1910080	2775538	3297398	4163531
1.27	76	813138	1390246	1326742	1839552	2651122	3214966	3989963
1.28	77	801746	1275686	1306134	1802944	2573810	3119734	3899851
1.29	77	787410	1263654	1264406	1739712	2478578	3057270	3784139
1.30	78	758482	1242278	1277462	1674304	2394610	2945654	3686347
1.30	78	759634	1185446	1160470	1596224	2330098	2912886	3593675
1.31	79	730066	1166118	1123862	1569472	2266098	2840694	3400139
1.32	79	714578	1118374	1108502	1549504	2200050	2690678	3259339
1.33	80	696402	1050406	1079318	1489600	2147826	2652790	3222987
1.33	80	670034	1045542	1037334	1464768	2052082	2501238	3073995
1.34	80	626130	1005862	1016470	1399872	2002034	2494582	3003851
1.35	81	625234	984230	971030	1351104	1928178	2376822	2823627
1.36	81	615506	979878	953494	1316544	1871986	2339446	2773963
1.36	82	600786	918694	928278	1277248	1882738	2244214	2627019
1.37	82	581458	879782	882582	1212992	1695986	2142838	2578891
1.38	83	572242	850470	837782	1200448	1644146	2076534	2466251
1.38	83	562002	840998	821654	1128128	1583602	2063350	2339275
1.39	84	556754	817446	790038	1119424	1596018	1962870	2206155
1.40	84	517202	778278	764566	1061184	1523314	1910902	2130891
1.41	84	503794	737830	779286	1016896	1431922	1866230	2083403
1.41	85	503634	703014	736022	995648	1395314	1803894	2003915
1.42	85	474354	696614	716566	974912	1346290	1751414	1883467
1.43	86	458226	672806	670230	932416	1324658	1699702	1823179
1.44	86	452658	644390	650390	922432	1289458	1620982	1815755
1.44	87	445138	617638	633238	894528	1196914	1562230	1729355
1.45	87	434258	581798	605974	852800	1148146	1518454	1662155
1.46	87	435154	557350	576150	801472	1118578	1441398	1629899
1.47	88	413970	546854	560790	786624	1063538	1390198	1513547
1.47	88	410130	535078	531094	764992	1016690	1311734	1443275
1.48	89	385906	503334	516758	753600	987122	1297142	1358795
1.49	89	384850	499622	511254	703040	905586	1250166	1330507
1.50	90	364626	471974	483222	673216	886898	1233270	1290059

Appendix 4D Continued

1.50	90	345586	452518	460182	666048	871154	1187830	1199435
1.51	91	340402	443686	438614	640192	842482	1132534	1166155
1.52	91	335730	425766	424214	607168	805618	1076086	1133259
1.52	91	314610	389190	404182	583872	781554	1050998	1128267
1.53	92	297682	383718	378358	571328	732786	1007222	1052107
1.54	92	298994	372166	390614	545472	705138	963446	984267
1.55	93	304498	362918	390358	509760	676850	955638	966475
1.55	93	288626	350758	363094	502336	668530	939254	938315
1.56	94	270162	318182	349366	472896	607218	872438	885195
1.57	94	258450	302438	329302	454720	588146	838902	850251
1.58	95	248242	288454	323222	449600	562290	810486	837323
1.58	95	240882	291110	287190	438464	570738	759414	802251
1.59	95	251826	281606	273718	405664	541938	734838	762699
1.60	96	232946	273414	266230	400000	525810	700918	741451
1.61	96	221490	257062	241366	389472	497266	671222	699211
1.61	97	211122	253862	236470	354816	469106	658038	657995
1.62	97	200210	236614	233238	349056	431986	651382	631371
1.63	98	199218	215078	225142	348128	438514	644598	615499
1.63	98	192690	203718	232758	314336	414066	607734	587723
1.64	99	190578	191590	214294	307328	395250	591606	547659
1.65	99	174386	188006	196822	298656	371186	569334	532043
1.66	99	183026	189286	186486	293792	374514	550774	517195
1.66	100	182898	184038	210358	284480	357170	534134	511947
1.67	100	164882	184358	191414	272736	352754	511350	494923
1.68	101	162130	163590	171766	265344	331058	494710	490443
1.69	101	148946	146214	156502	257184	316818	488822	463179
1.69	102	158034	140966	149270	239200	316114	459766	448203
1.70	102	153266	129702	136918	228128	297266	448502	424395
1.71	102	154130	117478	132566	229792	293522	434422	406315
1.72	103	142546	131110	130006	214432	265554	418550	400843
1.72	103	126994	125126	121974	198432	256466	400182	385675
1.73	104	123538	117350	114038	192000	259570	393494	366315
1.74	104	136306	112166	106358	197408	243314	372502	342411
1.74	105	131602	99142	107510	187712	232914	368630	352523
1.75	105	125682	99654	103926	172160	210226	350582	342315
1.76	106	117490	102182	102198	160192	209106	345750	328747
1.77	106	128914	81958	106550	156448	204530	340054	332171
1.77	106	112882	84678	92598	148544	215666	321718	331179
1.78	107	115218	80870	90774	142976	197746	319830	330379
1.79	107	111410	79398	88502	143040	176978	298262	294315
1.80	108	139314	72582	72342	144832	165714	301558	276011
1.80	108	110642	74502	65782	144448	160114	300502	271019
1.81	109	99218	75334	65782	128576	159858	295894	270539
1.82	109	101170	66886	61430	117184	152626	283478	249483
1.83	110	91570	53510	53302	111744	139730	271734	234667
1.83	110	100242	49862	47222	103456	134770	265942	237771
1.84	110	86674	49222	42390	102848	136626	257814	244811
1.85	111	81970	66502	43638	99936	140466	259318	224459
1.85	111	78994	55846	42710	100320	129554	254646	222955
1.86	112	80722	53254	51606	96288	137778	247190	205803
1.87	112	83634	53990	52310	91808	116242	238998	193739

Appendix 4D Continued

1.88	113	82194	47238	40822	90336	108370	229686	195499
1.88	113	66194	46886	39830	90400	111794	216214	193995
1.89	114	68274	38022	38742	86880	108722	211574	196939
1.90	114	73970	38022	50134	87168	97010	208950	198411
1.91	114	78706	31238	46134	81568	94386	209302	191691
1.91	115	84850	32902	38294	78112	94130	206646	179211
1.92	115	63242	28870	40694	75680	96978	202390	166219
1.93	116	67858	25990	34134	69408	85650	207222	158827
1.94	116	70706	29286	24150	70912	90866	202390	165995
1.94	117	69458	34150	25382	71424	107762	199638	165387
1.95	117	61586	32838	19782	68544	122770	190710	152747
1.96	117	63498	26470	12358	76288	93330	195094	152843
1.97	118	78290	14342	16806	67008	78130	193782	153611
1.97	118	60018	11878	17302	65184	68082	179542	159051
1.98	119	56370	9094	16926	57536	69298	175190	150923
1.99	119	59794	8134	19262	56128	61426	174550	148363
1.99	120	60850	7246	19486	49120	61938	168022	143691
2.00	120	62674	10182	20790	49152	64626	173238	152107
2.01	121	57850	13158	17446	49312	70578	169078	149067
2.02	121	57250	9190	7950	47584	63282	165078	160555
2.02	121	64002	6326	3502	49920	55122	158358	149899
2.03	122	70706	5246	46	49056	45170	156854	141547
2.04	122	69810	8438	1486	44288	50738	164374	146027
2.05	123	57746	3542	12030	46944	60530	160662	140939
2.05	123	66482	3366	3494	40416	62898	155798	128939
2.06	124	51138	9918	1574	41984	58546	154102	124427
2.07	124	59778	7110	-74	42176	49010	170582	120075
2.08	125	51882	-1618	4238	42432	52978	153846	115115
2.08	125	54066	2454	14	41792	42930	147030	115147
2.09	125	49890	6270	-3770	36608	33778	148694	114027
2.10	126	44626	-1674	-946	36480	42258	151030	110635
2.11	126	41786	-3490	7854	51232	59346	172150	113995
2.11	127	54706	2134	1350	46816	44242	154614	107083
2.12	127	53218	5230	2910	38816	45330	156310	105867
2.13	128	57002	-3634	-1746	35968	36434	138966	116043
2.13	128	53474	-8706	-2898	34112	40338	131862	111755
2.14	128	49706	-4450	7726	35200	42898	131062	114187
2.15	129	54922	-5426	-5378	43232	38930	130390	112331
2.16	129	56634	-2666	-7730	35776	36722	126646	114763
2.16	130	47842	-4050	-5490	29472	35090	126806	115243
2.17	130	43570	-4490	-11490	35328	28402	128214	111179
2.18	131	42242	-7826	-10754	33248	31122	126294	109195
2.19	131	41842	-13786	-13018	37088	31090	130486	109163
2.19	132	39074	-14274	-15242	35008	39474	127350	119115
2.20	132	32698	-16434	-14690	24104	25778	122262	120683
2.21	132	53658	-15890	-13578	21984	30002	125782	107179
2.22	133	45058	-13834	-3802	23272	37714	133110	95371
2.22	133	46698	-2202	-5738	22592	30194	127510	98443
2.23	134	44650	-450	-14282	29952	23026	123830	93931
2.24	134	44250	-6274	-10506	24016	27026	115030	88203
2.24	135	52794	-8770	-1762	19856	30994	119414	88683

Appendix 4D Continued

2.25	135	62794	-4458	-10378	20920	34866	114742	91723
2.26	136	51362	-9226	-11290	20896	27794	111606	99051
2.27	136	53122	-8698	-14442	20520	22322	118934	110027
2.27	136	56010	-12514	-12938	12688	29842	135286	105547
2.28	137	50082	-8370	-14802	16064	26034	136118	100683
2.29	137	43314	-11578	-15154	18408	22322	119670	95051
2.30	138	44346	-11762	-10642	21392	19762	117238	84715
2.30	138	45362	-11074	-12930	24840	22290	122870	83979
2.31	139	49658	-14402	-13530	20472	26738	113910	89515
2.32	139	45138	-21714	-16362	17184	25010	108214	90539
2.33	140	42546	-23354	-13274	16696	28050	110390	87275
2.33	140	52146	-19538	-21610	16928	21874	109366	81387
2.34	140	40426	-14714	-6314	14032	24722	114038	74827
2.35	141	44026	-13850	-5434	18096	18290	120566	82283
2.36	141	41354	-17810	-16986	14704	20242	113718	91947
2.36	142	35170	-15658	-10242	23504	19122	107734	83243
2.37	142	33218	-18602	-10226	21864	22258	113718	79147
2.38	143	45146	-18754	-7482	20736	28594	112214	80555
2.38	143	45642	-16690	-19842	17904	25362	100342	107851
2.39	143	46746	-14538	-12090	16040	17682	112150	93579
2.40	144	44378	-4138	-21322	13392	20562	110678	78251
2.41	144	38946	-13658	-23754	14880	13970	102390	83787
2.41	145	37474	-11354	-13474	9632	20402	101974	85547
2.42	145	40282	-21786	-7834	17032	18226	106390	74507
2.43	146	49370	-24554	-14930	11304	18674	104566	69355
2.44	146	48778	-19498	-22442	10256	30034	103094	72619
2.44	147	47010	-13858	-22162	13192	34162	101334	71947
2.45	147	50290	-25010	-19274	13336	18994	103734	67691
2.46	147	45498	-26866	-21418	10856	19538	99862	74571
2.47	148	48522	-22466	-18442	15896	24946	96278	78923
2.47	148	47226	-24066	-13354	16560	17618	100726	80715
2.48	149	45986	-22042	-13682	10656	11250	99574	78731
2.49	149	47418	-22490	-21546	9512	6450	101654	80587
2.49	150	53162	-24266	-19722	13976	7506	98614	86091
2.50	150	46058	-23242	-22274	9120	12562	100342	79243
2.51	151	56762	-25474	-23626	10632	8210	102742	72587
2.52	151	60154	-20218	-26314	10640	8082	102038	122667
2.52	151	46202	-18170	-16362	14984	6418	102902	94187
2.53	152	47730	-17442	-21058	18464	11410	100374	93035
2.54	152	48122	-11314	-24058	13456	2866	98006	86219
2.55	153	43770	53150	-27202	8888	5554	94262	97963
2.55	153	45130	159174	-15354	10240	8114	92758	101611
2.56	154	95098	252502	-20970	8992	15730	97142	79435
2.57	154	45258	308862	-21738	14096	18834	105686	76843
2.58	155	48394	311790	-26146	7664	19698	101526	64587
2.58	155	51634	293982	-27746	4304	18930	117334	67403
2.59	155	52562	272654	-27170	5776	14674	100502	60971
2.60	156	50802	229494	-26482	6696	13810	103254	60331
2.60	156	51714	181486	-22722	9672	10674	105750	66635
2.61	157	64866	144646	-26234	12904	7730	104150	70891
2.62	157	60922	142830	-24914	10248	10930	101398	65835

Appendix 4D Continued

2.63	158	48322	117886	-27530	11304	7378	104438	58699
2.63	158	45074	100246	-27034	6768	4114	104662	62347
2.64	158	46938	94334	-24410	9184	10514	102006	62443
2.65	159	45442	85182	-17050	3416	12530	95318	63339
2.66	159	50674	75502	-23130	4768	15634	93174	59403
2.66	160	58306	54198	-24978	14480	11858	95894	61899
2.67	160	56194	44390	-29474	15712	16562	95382	56363
2.68	161	45874	51030	-27178	8424	10354	101686	68619
2.69	161	48698	35630	-26330	6032	1074	95958	61931
2.69	162	46202	27406	-26154	5208	5746	95094	62635
2.70	162	41482	26886	-28770	5568	10514	103030	60651
2.71	162	43506	32958	-30762	2344	12018	107926	60043
2.72	163	38722	32718	-19450	8400	5042	108342	60683
2.72	163	51090	21142	-15258	2984	6258	94006	68235
2.73	164	46866	6814	-22002	2944	6450	98710	62027
2.74	164	47786	7494	-22818	5464	1298	98550	56683
2.74	165	50578	14	-23938	7568	-1806	89078	55595
2.75	165	49394	-1506	-30218	2872	4370	95670	57579
2.76	166	52514	-770	-32538	976	7442	84406	56139
2.77	166	56106	-3578	-27930	5728	6546	86454	53579
2.77	166	49314	-9490	-27890	3672	15410	94806	53323
2.78	167	56610	-5554	-31090	4344	8082	108342	53707
2.79	167	51674	1366	-29266	10528	498	90710	63435
2.80	168	50074	-3610	-23266	8824	786	88758	58923
2.80	168	50122	-570	-24218	3784	-1582	97302	64395
2.81	169	53074	-9706	-27914	3536	1682	96278	55755
2.82	169	47434	-14010	-29450	2976	1906	88566	51755
2.83	170	47042	-14610	-31562	48	4338	89462	51787
2.83	170	58058	-12602	-30898	2856	-4718	88758	51851
2.84	170	46290	-4554	-30186	-24	2546	86134	52011
2.85	171	42954	-6090	-33858	-984	2450	98454	55979
2.85	171	40418	-6386	-33842	-344	-1582	88118	56203
2.86	172	48490	-11266	-32850	2256	-1166	90262	59563
2.87	172	36234	-20706	-29602	6848	3122	86326	55883
2.88	173	42474	-21090	-27210	1288	2770	88534	54475
2.88	173	44322	-21634	-27762	2232	-5454	91894	57003

Appendix 4D Continued

5.98	4.99	3.91	2.99	2.49	2.05	1.59	1.32
-240391.5	-484873	-479443	-294975	-297104.5	-265697.5	-213627.5	-234767.5
-240968.5	-485200.5	-479693	-294880	-297331.5	-265584.5	-214185.5	-236076
-241012.5	-484569.5	-479664.5	-294463	-297371	-265048	-214149.5	-235802.5
-241095	-484247	-479468	-294833.5	-297198.5	-265195.5	-214057	-235743
-241133.5	-484749.5	-479260.5	-294793.5	-297424.5	-265776.5	-213394.5	-235983.5
-240634.5	-484773.5	-479478.5	-295003.5	-297487.5	-266165.5	-213289.5	-236151
-240797	-484951.5	-479140	-295077.5	-297700.5	-266445.5	-213485	-235892
-240789	-470848	-479134	-295286.5	-297467	-266563.5	-213712	-236056
-239145.5	-362016.5	-479241.5	-295174.5	-297683	-266556	-213804.5	-236291
-232754	-291110.5	-479078.5	-295084.5	-290165.5	-266407	-213761.5	-235989.5
-228676.5	-300876.5	-479273.5	-292220.5	-245439	-266330.5	-213851.5	-234792
-223898	-338518	-479554.5	-276491.5	-212889	-265959	-214225.5	-203960.5
-203554	-374996	-479503.5	-261277.5	-205719	-250597.5	-213957	-160040
-163766	-398794	-479476	-254120	-212138.5	-215111	-213708.5	-145548.5
-147362	-402449.5	-471220.5	-196712	-215041.5	-204623	-214125	-140607
-153850	-396772.5	-450907.5	-138336	-222066.5	-209579.5	-213800.5	-129718
-162944	-396666.5	-436586	-142608	-227159	-208678	-214028	-74588
-164342	-399390.5	-419206	-160656	-223450	-174254	-203432	-18940
-166452	-374110	-377630	-167592	-185724	-143766	-158522	-20828
-158990	-299102	-365134	-183368	-118820	-135070	-121862	-18972
-132684	-126014	-370278	-178472	-99276	-134030	-97118	-22364
-6404	346082	-371734	-166056	-90540	-124550	-82326	2724
306844	1246818	-366494	-145328	-95588	-122798	-93238	-1372
541020	2460994	-361622	-113968	10276	-122094	-79814	36036
799036	2928706	-359190	-40520	401780	-111982	-98718	175332
1207484	2553058	-334534	198584	962612	-42830	-93350	343780
1726780	1756194	-277302	549464	1745604	311346	-78614	333940
2398268	928002	-57750	1120728	2315828	1002066	-60934	297148
2578748	452994	376394	1793368	2014708	1896210	-48262	359364
2202108	179074	913482	2402264	1362580	2506994	-19630	638660
1392124	59106	1541290	2759384	726900	2488242	179058	987460
772700	171906	1963818	2580568	519252	2099634	478898	1252388
396028	676418	2254122	2025560	696980	1931442	792018	1265380
187324	1794754	2779946	1226328	1251220	2180274	1072722	1122372
84476	3168834	2648874	665720	2045780	2158770	1451730	845316
23308	4168290	1932714	349144	2479700	1604402	2084306	548132
-21828	3832546	1072074	178520	2061332	1016178	2498642	323332
-55300	2806722	469994	79352	1374196	577938	2334930	189572
-70876	1695138	179754	5432	730228	343634	1585490	105380
-66652	844130	11850	-12904	377940	199122	947154	57348
-84700	399810	-85462	-45896	200692	104850	540242	13956
-88620	166082	-161110	-68456	88180	69138	352914	-13052
-96884	6018	-204118	-90632	18164	43538	203634	-28732
-119356	-75518	-237526	-106792	4788	16850	121170	-38780
-116252	-100926	-253142	-123528	-33324	8722	81202	-44796
-21828	295042	-274358	-124968	-59756	-14158	38418	-52604
523132	1770306	-272086	-131432	-70476	-10702	30354	-57980

Appendix 4D Continued

2078332	4827970	-286806	-139936	-57932	-24942	10386	-61788
4286652	8542114	-272374	-144160	-16364	-29134	-7790	-59580
7157948	12278690	-281430	-119592	341524	-13614	-9678	-30172
10961084	15016642	-258102	92152	1274388	193586	-22158	133956
14107836	16063330	59754	891576	2748372	881714	-21294	519972
17468604	17002882	1255082	2623448	4513524	2107570	-7950	1208132
19330236	17130946	3886762	5401816	6231028	3646322	-7214	1999140
20739260	16368898	6948330	8692184	7308084	4958450	54866	2837476
20559036	15478146	10481706	12316632	7376692	6277042	354706	4139076
19825852	14666914	13790762	15851480	7936276	7643698	1088306	5678788
18244796	13419170	16386090	17698776	9046036	9020978	2352178	8001604
17251516	13567650	20819498	17989592	10747924	11083314	4050258	10651716
15871164	15718050	23754282	18976728	12000788	12748338	5995858	13104708
14603452	17719970	26209834	18603992	13565460	13805106	7961426	15775812
13724860	21293730	27000362	17436632	14845460	14364210	10088274	19079236
12612796	24193698	27266602	16797656	15035924	14124594	11989330	20197444
11787452	25180834	27242026	15466456	14622228	14011954	13154642	22773828
11068604	25858722	25757226	14043096	13936148	13671986	14465362	24705092
10687676	26841762	24376874	13365208	13506068	13405746	16140626	26253380
10378428	26405538	22644266	12715992	12955156	12109362	17693010	25411652
9974972	25389730	21237290	11966424	12068372	11810354	18164050	24643652
9663676	23669410	19836458	11309016	11304468	11124274	17537362	22980676
9424060	22766242	18400810	10880984	10437140	10367026	17066322	20672580
9026748	21770914	17626666	10493912	10027540	9816114	16134482	18124868
8794300	20720290	16911914	9936856	9515540	9069618	14522706	15329348
8647356	19593890	15992362	9572312	9055252	8510514	12734802	13306948
8408764	19065506	15574570	9205720	8765972	8075826	11368786	11080772
8300220	18324130	14923306	8988632	8382996	7466546	10113874	9375812
8009916	17904290	14466602	8650200	7976980	6904882	8958802	8348228
7769276	16964258	14274090	8511448	7687700	6621746	8124242	7330884
7645372	16671394	13325866	8337368	7281684	6144050	7078226	6344772
7557308	16063138	13055530	8167384	7084052	5886002	6361938	5439044
7378108	15467170	12801578	7589336	6870036	5646898	5722450	4754500
7440060	15016610	12095018	7428056	6721044	5485618	5221714	4278340
7107772	14545570	11595306	7341528	6477844	5174834	4839762	3747396
7196348	14547618	11271722	7112664	6134804	4875826	4479826	3470916
7072444	14215842	10829354	6954968	6082580	4692530	4085074	3183684
7027900	13957794	10432042	6853080	5995540	4439090	3870546	2956868
7031484	14064290	9836074	6538712	5882900	4400178	3646802	2722884
6995132	13185698	9277994	6530008	5693972	4143154	3561298	2526788
6941884	13347490	9169450	6351320	5632020	4085810	3423570	2569668
6945980	13329058	8943146	6269912	5466132	4030002	3302738	2478020
6919868	13699746	8637482	6165464	5308948	3976242	3072850	2350660
7132348	13271714	8910378	6203352	5160468	3981874	2949970	2093892
7171772	12821154	8648746	6080984	5209620	3760690	2789202	1905988
7129788	12724898	8627242	5952984	5047316	3763762	2757458	1837252
7258300	12950178	8517162	5858776	4999700	3702322	2656594	1778500
7171260	12792482	8528426	5831128	4966932	3666994	2634578	1760580
7304380	12851874	8552490	5790168	4937236	3525682	2552146	1685572
7200444	12917410	8748586	5848024	4894740	3494450	2476370	1649092
7462588	12962466	8848938	5816280	4810260	3540018	2466642	1548612

Appendix 4D Continued

7434428	12532386	8887850	5930968	4912660	3477554	2470738	1535172
7602876	12841634	8939050	5907928	4962324	3438130	2367314	1550020
7817916	12982946	9309738	5812184	4812308	3454514	2433362	1491524
7863484	13146786	9391658	5820888	4809748	3473458	2324306	1494596
7791804	13200034	8992298	6007256	4762132	3328050	2314066	1436356
7927996	13247138	9504298	5880280	4798996	3442738	2283858	1429060
8079548	13535906	9836074	6070232	4846100	3513394	2312018	1371076
8029372	13320866	9883178	6000088	4858900	3564594	2350418	1358276
8240316	13669026	10092074	6076376	4897300	3559474	2320722	1344196
8459964	13683362	10194474	6073304	4933652	3642418	2281298	1345860
8563900	13857442	10169898	6303704	5022228	3556402	2224978	1339844
8697020	13939362	10487338	6219736	5066772	3580466	2263890	1321156
9024700	14183074	10438186	6327768	5013012	3644466	2333522	1337668
9223356	14203554	10657322	6246872	5043220	3682866	2359634	1306692
9389244	14766754	11064874	6369752	5060116	3658290	2384210	1318468
9530556	14944930	10991146	6583768	5153300	3697202	2359634	1310916
9561276	15065762	11093546	6677464	5255188	3807282	2383698	1374020
9522364	15211170	11492906	6866392	5167124	3844658	2375506	1314628
9909436	15858338	11839018	6849496	5370900	3883058	2468690	1373764
9999548	16097954	12070442	6897112	5489684	3952690	2382674	1367748
10108092	16442018	12047914	6986200	5527572	4018226	2369362	1348164
10060988	16657058	12336682	7222744	5613588	3964978	2426706	1363140
10280124	16798370	12484138	7691224	5775892	4083250	2424658	1376964
10577084	16917154	12758570	7387608	5756948	4119602	2449234	1412548
10763452	17267362	13157930	7533016	5935124	4147762	2518354	1449156
10765500	17597090	13268522	7611864	5857812	4237874	2587986	1479620
10798268	17767074	13336106	7870936	5855764	4141618	2657618	1454916
11044028	18227874	13450794	7923160	6057492	4318258	2672466	1473860
11357372	18213538	13872682	7911896	6114324	4380210	2730322	1462852
11398332	19169954	13895210	8143832	6173204	4507698	2773330	1451844
11441340	18930338	14560810	8089560	6333972	4482610	2809682	1513924
11361468	19636898	14394922	8092632	6195220	4637746	2748242	1537220
11304124	19616418	14888490	8418776	6408724	4589618	2847058	1543364
11490492	20134562	15001130	8682456	6580244	4596274	2877266	1552196
11527356	20023970	14710314	8675800	6629908	4769330	2842450	1638084
11674812	19694242	15310378	8849368	6771732	4686898	2909010	1672900
11494588	20406946	15283754	8771544	6849556	4716082	3017042	1670596
11398332	20923042	15478314	8919000	6765588	4699698	3075410	1694148
11498684	20394658	15877674	9021400	7058452	4815410	3093842	1693508
11664572	20626082	16043562	9119704	6905364	4932658	3158354	1660612
11427004	20363938	15828522	9091032	7075348	4986930	3237714	1690948
11326652	20935330	16059946	9244632	7149076	4796978	3263826	1729988
11416764	21574306	16408106	9256920	7204372	4953138	3208018	1772612
11398332	21512866	16152106	9224152	7140372	4960818	3191122	1830724
11582652	22016674	16313898	9486296	7224852	4961330	3183442	1813188
11308220	21926562	16049706	9353176	7148052	4892210	3225426	1850948
11187388	21920418	16127530	9525208	7403540	4984882	3250514	1885892
11160764	22258338	16387626	9564120	7401492	5041202	3305810	1926084
10970300	21940898	16250410	9109464	7400468	4965938	3325266	1898820
10882236	22059682	16295466	9359320	7440916	4966962	3257682	1932356
10636476	21809826	16422442	9617368	7499284	4996146	3350866	1965636

Appendix 4D Continued

10314940	22114978	16709162	9461720	7194644	4904498	3401042	1933892
10589372	21648034	16389674	9504728	7378452	5059634	3478866	1998916
10251452	21791394	16248362	9474008	7316500	5118514	3286866	2029124
10226876	22284962	15975978	9428952	7224340	4923954	3341650	2011204
9835708	21994146	16066090	9588696	7226900	4861490	3349330	2008644
9964732	21400226	15982122	9418712	7332372	4793394	3265362	2105412
9530556	21203618	15322666	9318360	7184404	4785714	3290962	2132036
9278652	21361314	15533610	9060312	7152660	4765234	3362130	2150980
9202876	21553826	15293994	9007064	7082516	4688434	3298130	2154052
9114812	21349026	15076906	9140184	7163412	4734514	3312466	2155588
8998076	21287586	14913066	9048024	7070740	4730930	3384146	2162244
8753852	20259490	14747178	9320408	6880788	4645938	3369810	2183236
8511164	20789922	14904874	8787928	7045652	4617266	3234130	2284612
8271036	20058786	14587434	8648664	6875668	4644402	3191122	2179140
7990972	20146850	14454314	8410072	6685204	4343346	3238738	2196036
7692988	19585698	14186026	8260568	6589460	4374066	3185490	2155588
7299260	19786402	13678122	8341464	6508052	4217906	3134802	2163780
7287484	19352226	13680170	8089560	6433812	4184626	3156818	2230340
7096508	19344034	13303338	8005080	6347796	4163122	3150162	2275908
6862524	18553506	13192746	7792600	6254100	4014130	3064658	2253892
6587068	18453154	12996138	7661016	6174228	4010034	3017042	2252356
6408380	17941154	12670506	7480792	6042132	3951666	2978130	2266180
6277308	18637474	12394026	7449560	6024212	3836466	2981202	2244676
6018236	17371810	12287530	7199192	5681172	3785778	2914130	2241604
5672636	17488546	11781674	7067608	5634068	3756594	2861906	2254916
5587644	16943778	11716138	7103960	5638676	3600434	2805074	2296388
5439164	16138914	11224618	6884312	5546004	3546162	2754898	2228292
5206716	15729314	10692138	6719448	5461524	3362354	2690386	2205764
5001404	15608482	10245674	6464472	5303828	3328050	2639698	2180164
4964540	15141538	10294826	6148056	5236244	3219506	2645330	2123844
4573884	14881442	9972266	6000600	5152276	3187762	2540882	2144324
4453052	14783138	9725482	5737432	4926996	3145266	2483538	2201668
4181692	14140066	9423914	5708248	4763668	3077682	2454866	2187844
4149436	13767330	9161770	5514200	4628500	2935346	2452306	2181700
3919036	13490850	8903722	5329368	4557844	2849330	2344786	2126404
3810492	12798626	8722474	5098968	4432916	2806834	2276178	2147780
3655868	12681890	8334378	5002712	4324372	2697266	2225490	2139076
3519164	12497570	8007722	4958168	4205588	2618418	2152786	2115012
3452092	11836578	7640618	4864472	4120596	2543154	2094418	2016324
3268284	11418786	7531050	4578264	3904020	2490930	2063186	2018500
3089596	11277986	7173674	4560856	3768340	2435634	2011474	2066756
2927292	10774690	6964778	4354008	3667476	2350642	1983826	1945796
2866364	10387618	6975018	4292056	3553812	2294834	1921106	1909060
2753212	10144930	6672938	4060632	3416084	2251314	1869522	1910724
2592444	9866914	6258730	3894744	3373588	2046514	1869010	1935044
2505916	9595042	6209066	3781592	3343892	2094130	1783378	1916740
2388668	9099426	5923370	3693016	3184660	1972146	1693906	1887172
2319548	8911522	5749802	3427288	3118100	1904434	1618258	1856708
2226876	8531618	5564458	3335128	2955284	1896370	1601234	1816772
2161340	8243874	5263402	3234776	2845204	1783602	1526738	1763012
2039484	7983778	5022250	3131352	2740244	1714738	1484114	1829828

Appendix 4D Continued

1944380	7805090	4894762	3032024	2626068	1650994	1470546	1737796
1833916	7392418	4789802	2921944	2571796	1612850	1399122	1718980
1759932	7247010	4555818	2815448	2550804	1582514	1376850	1700292
1669692	7016610	4322858	2717656	2384404	1541810	1303378	1679684
1667260	6867106	4210730	2562008	2270740	1407922	1282002	1635140
1586492	6369954	4042282	2440664	2218516	1385266	1216850	1585860
1499580	6151330	3884074	2344920	2134036	1334450	1198674	1586756
1441724	5947042	3642922	2218968	2104340	1310642	1174482	1546948
1401404	5707426	3555370	2191832	2023060	1259954	1121362	1516100
1321276	5427874	3290154	2048472	1944212	1175986	1053266	1475396
1271100	5131938	3170858	2008536	1890452	1175474	1045074	1452868
1185596	5001890	3151914	1909720	1817620	1127474	991954	1443524
1152700	5007522	2995754	1829336	1711636	1070898	978386	1426116
1085116	4784802	2872362	1782616	1698196	993586	899922	1384516
1024700	4587682	2745898	1717080	1591828	988466	888658	1348420
993084	4383394	2597034	1633880	1514772	958898	860754	1300804
968380	4136098	2519082	1575512	1461524	914994	834386	1257156
922300	4015778	2392106	1471192	1489556	870706	807122	1272772
876476	3797666	2306986	1480024	1370900	836658	788562	1216964
844604	3659426	2211370	1397720	1320340	794290	762834	1192900
831932	3657378	2138922	1320536	1254164	788274	731218	1199684
769852	3218082	2014506	1268696	1253652	753970	713170	1148868
751548	3219106	1948202	1243608	1195540	755762	677714	1124932
735676	3094818	1918506	1221976	1140116	723122	649938	1103940
689596	3088290	1823018	1147352	1077012	716082	634194	1078980
695228	2872994	1714090	1128152	1036692	682802	621522	1087428
884412	2743970	1660330	1077976	1019156	637874	585682	1008964
630076	2644386	1604010	1019736	950932	628146	549202	988996
592316	2505506	1575210	992472	931476	593202	516690	966468
582716	2423074	1463082	947160	867476	587698	500178	938692
569404	2324898	1370026	904536	854804	560050	472786	960964
564924	2338594	1301930	846424	814484	529586	472018	904516
546364	2265378	1270058	847960	782356	521906	451282	872004
537404	2110114	1219242	799448	747540	486578	443346	841796
536124	1929378	1198634	777560	738196	457266	414418	811716
492604	1898658	1214506	736088	683796	458802	403154	793924
483900	1841826	1115946	734680	664980	428082	415314	763844
484284	1819298	1087402	692440	660884	418610	393938	770500
449212	1739810	1040426	671064	640404	408754	386258	756420
424124	1660066	980010	649048	646548	381746	369362	717124
405948	1567906	914090	620632	601236	382386	367698	699332
418492	1469858	901674	613464	564500	373426	354642	679492
398908	1384098	854826	584280	541204	347954	342610	669508
384956	1404962	843434	588632	503572	346418	316114	643268
353340	1381154	836138	546008	513428	331314	294450	636356
342940	1274274	774442	541784	509204	317490	281874	598852
357564	1223202	729386	502744	492180	318386	260498	596676
352828	1177250	736042	488408	473620	309938	263538	592324
335100	1151522	676906	473688	428436	289490	253426	581060
294524	1089058	663210	454232	419732	291154	246290	547396
299932	1031458	654634	455768	420756	269074	233778	546756

Appendix 4D Continued

309948	967842	633002	447448	405780	277074	237586	531844
287868	991522	682922	427352	366484	266994	234962	490308
264636	952610	641322	412888	381460	245650	230546	493252
253276	966818	578346	407640	387988	245010	208370	468708
242460	879010	524330	407896	368404	234418	184690	476516
237340	829346	518442	386008	390548	225906	204146	461892
219804	807330	479530	387928	377364	218066	186034	437540
221916	764450	469418	378968	358804	223218	187058	433668
258332	747682	457642	353624	308244	209202	175826	408228
261756	752034	431018	325464	308372	219314	173106	394916
256572	713506	426026	303832	288532	197522	158322	384420
211772	708258	393002	304600	303252	193970	146258	383012
193052	630434	390826	316632	267668	186770	149810	366404
193148	681122	376490	292056	269204	198514	147538	361668
199100	658082	370346	287320	263700	165106	164402	347524
196476	625058	384170	269528	254228	170386	147314	334404
186556	572834	355114	270040	252564	160978	130962	333636
175164	557730	306730	258488	229172	156850	123922	320740
165980	553762	294826	248696	238356	158578	134738	314308
175644	509602	309418	235672	213428	151026	115154	311044
161052	511266	332714	237752	207892	165266	111442	293668
153692	491170	315050	222840	222868	135570	109138	287204
140028	467490	315306	221240	213524	141490	111346	274180
147452	446242	286122	208376	213716	125522	110482	270340
119964	421026	267818	209784	193236	116498	100946	268516
123132	410530	271402	225528	191572	127218	101810	262660
123932	429858	233770	202872	178388	120946	105778	255172
117756	428066	214186	198168	187092	126322	92690	250084
114140	397474	225322	215736	173652	124978	87826	248164
123932	423714	213162	207672	175892	123730	95730	233220
125532	362274	239914	193400	177396	116658	89522	230564
121404	338594	234794	183928	162964	119794	89842	218884
106716	338850	218922	172024	158132	116978	76434	210532
103740	319138	160938	165336	157780	126258	79666	208292
94236	295202	188202	169976	161780	104242	75410	209924
127612	302882	180522	172568	149908	101554	64338	196196
141372	301730	178986	165464	143828	90290	70514	194116
126748	322978	165034	152888	133972	92402	59698	186980
112124	329378	169002	146520	127700	89746	64402	187780
116892	304930	169770	148088	144852	90738	83474	181060
98556	278050	165290	134456	149076	90866	75442	170692
87356	248354	144042	139608	129684	87506	67282	157540
83868	290082	143786	132760	121172	94450	66066	169092
98812	287138	165034	134904	130548	83506	60114	162916
92124	255522	167722	120888	108628	97042	52850	156836
79900	245026	120170	122040	131508	86130	48530	162660
74940	212770	107914	145368	119508	65234	47442	145924
64700	231586	117610	138072	130324	66994	55570	144068
64060	240802	114698	148568	119092	71890	57010	142500
75900	210082	105322	139544	104436	70322	48818	131268
61180	200738	122794	131224	107924	79346	40818	126436

Appendix 4D Continued

59388	202786	116522	117144	104884	64050	44178	133348
61596	187554	108074	115928	104852	106290	45490	125188
65180	156578	102218	120504	93300	90130	35570	125220
49852	171554	106730	105368	85300	71442	36562	125060
69852	177954	100138	101112	76916	72754	34674	115140
63452	136610	116906	90392	85940	76882	42354	120324
74940	143778	58890	95384	88340	66546	47154	112772
78012	146850	68234	100536	107700	60882	40402	118404
83772	145826	76458	89528	102548	57330	50418	101188
60988	152610	61258	95352	78260	51634	37010	92964
46716	156706	68394	89880	74484	59730	36562	91076
46780	157730	56266	91000	77204	53586	38162	101764
52604	172194	59722	97240	69588	61970	29842	83684
55740	147490	35594	87704	83668	75218	27890	95044
59996	118658	59530	84504	70612	56594	33426	80036
58876	126178	113290	86936	77236	49778	32978	84068
44828	154530	68202	71800	72212	45714	29426	86916
36124	118210	59722	74744	80212	46354	19474	80932
33148	115010	27562	78936	60852	39666	15282	76004
35964	114338	22186	89144	72340	44402	22482	69028
35996	106690	47818	71608	70996	48274	21842	75396
33372	110338	28522	60440	79732	37266	16658	81380
35004	106274	24330	77368	64020	44306	27698	77316
36956	91138	31626	75160	59924	36850	23570	65060
35100	87490	28970	63000	46420	39474	17234	66756
33244	108194	29258	59864	58772	36946	17618	65476
34236	141474	14474	58744	55444	33106	17490	69444
38492	95554	24682	58808	50580	34610	17458	59012
37148	71586	11370	65624	43988	37330	11346	64004
31100	73314	15114	65624	45844	29138	6706	66276
30012	70434	9546	77720	58932	32274	7826	52708
27420	62818	11786	63928	42836	34066	15186	51236
24764	72706	7146	53272	42932	35762	23538	53124
37212	41762	5130	44856	40756	43634	8658	41892
24124	44258	-4182	42104	35572	34642	4850	52868
29244	47490	-9046	49240	31444	33682	5426	40996
34876	45346	15466	38808	46068	37330	8146	53284
41276	42402	40394	49944	36468	32498	17010	44900
22844	52514	36522	55800	30644	25682	15794	52708
24444	58466	14410	50872	30196	23858	13042	55332
29212	62722	-12374	32088	31220	22546	19794	50628
34716	61442	5386	44824	30516	22194	12754	42404
20636	57026	-16918	32664	37204	19826	8690	31428
17084	96802	-18518	35672	30836	21586	10002	27684
19036	94914	-6966	30488	41460	32882	-2190	29924
21340	60258	-19446	37656	33620	27922	4722	25348
39804	44322	-21654	36920	22676	26770	7506	27172
36316	30178	-19158	43352	28436	22546	5106	26628
17020	24546	-25334	42648	24372	11794	-4814	27332
23036	32962	-17718	38200	18036	11442	-2318	26308
24156	50850	-32022	33496	29972	14098	754	20932

Appendix 4D Continued

17020	27138	-15606	41624	45204	20338	-9934	17124
11228	27138	-4790	46040	20052	27282	5298	19460
10748	20834	-22102	33208	22132	20178	5010	17028
13596	15586	-35094	35000	20116	27218	10610	21412
23740	30626	-28918	28952	12724	25458	-5262	15908
23164	1602	-18134	25752	23220	11858	-7278	18756
11932	13314	-33910	21944	27828	13618	-5358	12580
27388	1378	-38582	21656	22100	16498	-974	11172
11388	1570	-44790	15192	24788	9458	-910	19620
11068	4002	-33110	12472	19732	8722	-8782	22116
8572	3682	-54998	7992	11380	16050	-3278	14404
6876	2690	-60598	16632	20980	9074	-9198	8100
2204	7202	-59094	13176	11220	10930	-7182	6020
4348	4130	-66486	10200	15284	11090	-9646	18980
2908	4514	-53110	6136	14100	6898	-12846	7300
-1348	1090	-57942	4568	5524	10354	434	4996
-1188	-12318	-69398	8440	15508	9106	-2222	10436
6524	-15678	-67830	5304	3540	11666	-6670	2212
-1156	-8126	-64534	9944	1204	6354	-9934	3364
156	-12606	-55318	11416	5716	9298	-13838	-5212
2236	-3806	-28918	17144	8308	9234	-3150	4164
-5028	-11678	-58614	14616	7252	8818	-9486	6020
-452	31234	-57782	14328	5556	15186	-10830	5732
540	20258	-48150	13976	15060	-494	-17550	8388
-5124	-9470	-39318	6264	8116	1842	-18222	13988
2780	-11710	-59478	11960	244	3282	-15246	-8508
-1508	-8670	-63126	-72	-3692	-398	-17422	-1372
-10916	-11742	-72662	1528	6228	3186	-20334	-12156
-8228	-6718	-77910	3672	500	3570	-22062	-9820
2684	6626	-82518	6808	-3884	-366	-22126	-2236
4924	-7806	-75766	216	-2028	-5902	-14862	-9628
-5924	6530	-76022	-3560	-9900	-8878	-11854	-9500
-8676	-5150	-73590	-9800	-14924	-6830	-19566	-11068
-7460	-21278	-49590	-9672	-7980	-11118	-18318	-12572
-7812	-17214	-48598	-4168	-780	-5422	-14478	-892
-2116	-14718	-62230	-1448	-14156	1106	-18830	6532

Appendix 4E - Zinc ICP-MS counts for pH titration experiment in Chaper 4. Values are averages of multiple runs.

Time		9.75	9.56	9.02	8.54	7.99	7.41	7.02
min	sec							
0.033	1.98	-21248	-4932	662	2226	2168	4684	5784
0.04	2.4	-18496	6668	2894	4226	3328	6884	6248
0.047	2.82	-14120	13796	3950	2842	4512	7292	7304
0.055	3.3	14240	14716	2814	4890	5088	8164	8040
0.062	3.72	38936	13124	2398	3170	4240	7628	7184
0.069	4.14	54296	11700	1470	4162	4536	6468	7464
0.077	4.62	74448	12516	1822	3898	4072	5444	7056
0.084	5.04	79720	17204	1486	3074	4312	7380	6608
0.091	5.46	99440	18164	3038	4098	3232	6876	6864
0.099	5.94	109232	17540	2278	3898	5336	6788	9776
0.106	6.36	103632	16660	9998	2610	6504	8700	14152
0.113	6.78	96528	22476	30126	3578	15008	6052	27688
0.121	7.26	86768	26452	66894	9458	31144	8204	42472
0.128	7.68	80240	23748	112558	26226	37784	9772	51360
0.135	8.1	80912	15372	112078	36442	36512	23020	46960
0.143	8.58	72144	10044	92494	42426	38872	47780	41416
0.15	9	53008	8492	78286	56986	45640	58380	38728
0.157	9.42	29136	7444	70190	66994	48456	59996	44816
0.165	9.9	14008	13604	66734	68530	54952	55076	54168
0.172	10.32	7352	23988	66638	72178	57640	50588	54680
0.179	10.74	1040	32924	63342	73458	55864	44220	51672
0.187	11.22	760	33404	57214	69074	57632	51292	48472
0.194	11.64	4264	37684	47406	66578	60424	61996	43432
0.201	12.06	12480	36332	35766	72658	61672	72300	38104
0.209	12.54	19440	33524	27102	77330	53328	72268	25416
0.216	12.96	29384	23988	15846	67634	42992	71084	10200
0.223	13.38	30528	13684	7190	54402	33680	68844	1992
0.231	13.86	28432	7356	870	45562	27080	60716	-1048
0.238	14.28	28816	4836	1182	39978	22336	46260	2024
0.245	14.7	31680	3972	3878	32242	18392	30132	8112
0.253	15.18	35808	5132	12734	25274	22904	17076	14432
0.26	15.6	35240	6380	22598	19194	28472	13620	28160
0.267	16.02	38672	9820	35958	20538	33312	20524	30488
0.275	16.5	39888	15900	45062	29018	37024	28700	35728
0.282	16.92	37008	19476	48990	33578	40240	42460	37360
0.289	17.34	35728	21660	48726	42538	40112	49396	31696
0.297	17.82	33832	25868	46294	47322	38088	52748	30256
0.304	18.24	31568	28860	40358	48042	33800	51844	27384
0.311	18.66	27872	31908	37406	47954	29048	47452	23984
0.319	19.14	26304	38028	31262	43266	26464	43044	20080
0.326	19.56	30288	37852	28158	38154	23240	36116	19672
0.333	19.98	37392	38460	25854	34402	17224	29092	17144
0.341	20.46	47144	30660	22878	30362	17280	24428	17288
0.348	20.88	43760	27940	20326	25602	14440	19668	16008
0.355	21.3	41336	23164	17062	22058	13136	19588	14208
0.363	21.78	37360	17772	16462	18914	13544	16724	11848
0.371	22.26	41968	18612	17782	16050	11248	13644	15432

Appendix 4E Continued

0.378	22.68	47696	18780	22326	16330	10288	14012	14136
0.385	23.1	49088	17036	32166	16058	16128	13140	22808
0.393	23.58	40864	20620	39734	20434	23032	15108	37176
0.4	24	30048	27276	43510	26570	31664	13444	56344
0.407	24.42	20864	29852	43390	31554	43432	16724	77176
0.415	24.9	16072	25804	38718	36450	55936	26076	93592
0.422	25.32	9480	20772	30854	38226	61192	37580	107096
0.429	25.74	7632	14580	23414	42274	68488	53420	108888
0.437	26.22	5264	11244	17966	48354	70536	67788	109496
0.444	26.64	552	9300	14990	49714	71304	74380	112120
0.451	27.06	-176	8924	12110	48394	69448	77932	106456
0.459	27.54	-3776	7596	7662	43410	68040	73452	109368
0.466	27.96	-5448	4092	7206	38170	68136	72844	105784
0.473	28.38	-8728	1388	4518	31514	66728	71724	104120
0.481	28.86	-9248	388	3238	26698	65640	69964	102520
0.488	29.28	-10712	-932	-322	24962	62576	70828	102488
0.495	29.7	-10704	-1580	-954	25498	64936	66380	104568
0.503	30.18	-13744	-2732	-1354	25226	66440	65260	101976
0.51	30.6	-13736	-2212	-2058	25442	62568	64876	101912
0.517	31.02	-15392	-3180	-3106	28458	65224	66508	97240
0.525	31.5	-16184	-3500	-3226	26994	62920	67564	98072
0.532	31.92	-18048	-628	-1082	27186	63784	64812	96248
0.539	32.34	-20088	-812	-4010	29554	65384	65132	94328
0.547	32.82	-21080	-4	-1954	34306	63784	63660	93656
0.554	33.24	-21832	1356	-2242	36066	62472	64148	90232
0.561	33.66	-20440	3452	-762	37466	61192	65644	86648
0.569	34.14	-21456	5476	-1042	42194	59368	63340	85240
0.576	34.56	-22176	9876	3038	43842	58216	62420	80376
0.584	35.04	-21856	12844	3622	45762	57480	62572	76248
0.591	35.46	-20200	15548	7358	47394	56072	59780	77496
0.598	35.88	-18376	20284	12358	44618	56480	58100	74968
0.606	36.36	-19104	21700	17726	48602	54672	57748	68856
0.613	36.78	-17440	26508	25006	47850	53960	57460	68376
0.62	37.2	-14760	28500	29334	47802	52624	54108	65656
0.628	37.68	-14296	30884	35366	50626	52192	52012	64984
0.635	38.1	-10872	34748	40454	48482	51272	50092	63544
0.642	38.52	-6816	36964	48430	47738	51304	50460	60976
0.65	39	-2432	42068	49454	51962	47352	50908	57184
0.657	39.42	2136	42108	54094	50418	48400	51308	56968
0.664	39.84	6008	45692	56846	51506	46104	48324	55840
0.672	40.32	10008	49580	57614	51322	45504	47188	54240
0.679	40.74	19048	54532	60334	50258	45456	46764	54120
0.686	41.16	25680	58620	60654	49610	44592	43348	52792
0.694	41.64	33360	58092	60718	51394	44984	42772	50440
0.701	42.06	43112	61204	61614	51338	45624	41780	50768
0.708	42.48	49248	61652	61230	48722	43528	42684	49952
0.716	42.96	56072	65044	59566	49482	44504	44708	51984
0.723	43.38	64248	67508	57902	51570	41080	43348	50536
0.73	43.8	76976	67668	60366	49986	41440	41460	50232
0.738	44.28	85584	67924	59566	50770	41624	45500	52184
0.745	44.7	91408	69044	59790	52914	42008	41156	46976

Appendix 4E Continued

0.752	45.12	96304	69652	59950	51762	42528	40924	48712
0.76	45.6	103600	69780	60654	55858	46784	41148	47736
0.768	46.08	107856	67892	55982	55730	46016	41588	48440
0.775	46.5	106992	67988	61934	53042	43520	44140	49960
0.782	46.92	111088	68020	61006	55698	44848	42700	52024
0.79	47.4	114256	68084	61710	55986	45536	41292	54248
0.797	47.82	113776	68308	60238	54834	44000	41764	52864
0.804	48.24	115024	68116	63150	54162	44184	44308	53464
0.812	48.72	111792	67796	62926	58162	43640	44316	53280
0.819	49.14	112432	66772	62062	57586	44544	43996	55224
0.826	49.56	107920	67060	62990	58194	46664	44524	54616
0.834	50.04	106064	67732	62190	59090	44544	46076	53688
0.841	50.46	108976	67764	63470	58418	45120	44924	56184
0.848	50.88	111440	66420	66830	58098	46536	44764	56728
0.856	51.36	102000	67636	61646	58482	47040	47004	55896
0.863	51.78	103792	65556	64302	60114	49576	48924	56568
0.87	52.2	104336	68404	65582	60146	51384	49884	56600
0.878	52.68	101488	67284	63374	59698	51208	48660	60344
0.885	53.1	102512	67348	62062	61618	53056	49772	60888
0.892	53.52	98928	66324	66030	62130	54784	50324	58104
0.9	54	101296	66036	63086	61106	55736	52100	58936
0.907	54.42	99536	67476	64238	62194	54032	51100	59704
0.914	54.84	99248	66612	63342	60498	55360	48596	60024
0.922	55.32	97968	67540	63726	59570	57184	49820	62392
0.929	55.74	97232	68788	65614	60658	58152	52292	61464
0.936	56.16	99856	69204	64846	61906	55912	50292	62808
0.944	56.64	93392	69108	65038	62450	56816	52988	62424
0.951	57.06	94512	67636	65774	63506	55048	55204	64280
0.958	57.48	93648	68788	66126	64370	57352	56908	62968
0.966	57.96	93680	66036	63726	62802	56808	58436	63064
0.973	58.38	92464	64756	63182	63474	57928	57612	62520
0.98	58.8	94000	63348	64942	65234	56744	57804	64152
0.988	59.28	95184	67956	66222	65394	53576	54092	65496
0.995	59.7	93232	66004	66478	62930	56520	56284	63672
1.002	60.12	90640	65812	64910	63954	58184	55300	65304
1.01	60.6	92240	66388	61902	66546	61608	56596	67096
1.017	61.02	90640	64116	63694	65138	59880	59020	66616
1.024	61.44	90384	63252	65198	64658	58280	56412	65208
1.032	61.92	90480	65076	64974	65170	60424	57308	66648
1.039	62.34	88944	65364	62606	64722	59656	59884	66872
1.046	62.76	87472	62068	63662	65074	57832	57772	67096
1.054	63.24	85776	62228	60718	65394	58856	58764	64440
1.061	63.66	87344	61716	60814	65490	56424	55580	62936
1.068	64.08	84528	62164	59182	65170	58088	55804	65240
1.076	64.56	82416	60564	58990	63442	57704	55004	64216
1.083	64.98	81328	59636	60174	66130	60008	55364	62328
1.09	65.4	80784	57652	58894	63826	57448	55308	61016
1.098	65.88	80976	56116	56846	64658	54632	56980	65336
1.105	66.3	78352	54068	58798	60146	53768	54260	62008
1.112	66.72	79120	54356	55758	61970	53224	53540	60056
1.12	67.2	74448	52500	57774	60402	55720	55628	61624

Appendix 4E Continued

1.127	67.62	74672	53876	56142	60818	54216	54988	59928
1.135	68.1	72976	52788	52270	60530	53064	56684	57016
1.142	68.52	72368	50452	53646	56466	51752	52900	56280
1.149	68.94	70480	48436	52718	55986	52736	51100	56184
1.157	69.42	68528	47796	52046	56050	54184	49164	55672
1.164	69.84	69392	47612	50606	54210	51496	50748	53176
1.171	70.26	66512	46468	47790	53762	49776	51796	53976
1.179	70.74	63952	44604	49326	53162	50496	48756	51040
1.186	71.16	65104	43932	45742	53786	48408	49324	50288
1.193	71.58	63632	44212	46102	53274	45056	49652	49424
1.201	72.06	60240	42900	42430	53042	44000	47420	49984
1.208	72.48	60592	42308	43430	49338	44528	46692	48560
1.215	72.9	54896	40892	42966	47794	40464	45644	48264
1.223	73.38	55792	40660	40326	46530	39864	45532	44744
1.23	73.8	55664	40332	37486	44242	41568	44620	46984
1.237	74.22	51792	38660	38614	44730	40864	41268	46696
1.245	74.7	50512	36572	37542	43458	37424	40980	46464
1.252	75.12	46960	34932	38326	42906	36504	39788	43720
1.259	75.54	51312	32140	36446	42610	37080	40572	39496
1.267	76.02	49360	33140	32942	42162	37736	39836	41056
1.274	76.44	46704	31644	34318	41490	36744	38988	38184
1.282	76.92	42640	32572	32422	40674	35560	38924	36968
1.289	77.34	42736	30108	30974	36794	32840	36428	34584
1.296	77.76	42736	28300	29550	36930	33800	34668	34120
1.303	78.18	41360	29276	28214	34282	31264	34660	33712
1.311	78.66	41328	27020	30886	35834	30448	34324	31856
1.318	79.08	40240	25436	28046	33138	31048	32700	31720
1.325	79.5	38576	25124	28230	32018	27664	32668	29800
1.333	79.98	36592	23108	27174	32570	26376	30260	29440
1.34	80.4	37776	24764	26766	33026	27160	31060	28648
1.348	80.88	36464	24588	22870	30346	25136	30684	27912
1.355	81.3	35952	19596	23518	28778	26128	28668	27048
1.362	81.72	31184	19940	22822	30210	23712	27532	26168
1.37	82.2	30872	19924	21870	26306	24520	26828	26704
1.377	82.62	29848	18540	23694	25282	24592	26428	24016
1.384	83.04	28480	19388	21550	22610	23056	23868	24816
1.392	83.52	26752	19348	20758	25378	21776	22660	25600
1.399	83.94	27872	16820	20054	23762	21296	23388	24408
1.406	84.36	27040	16652	17878	23274	21960	21380	21272
1.414	84.84	27384	16540	18502	26314	24608	23868	21712
1.421	85.26	28432	15268	17310	21690	21592	22876	19600
1.428	85.68	25808	15188	15998	22226	17488	20036	20104
1.436	86.16	25136	15188	16718	20706	15216	20132	19496
1.443	86.58	23328	13580	15582	17706	14872	19236	18712
1.45	87	24008	13116	15686	18618	14376	17396	17208
1.458	87.48	22832	14020	14366	16986	14536	16876	15968
1.466	87.96	21456	13212	13118	16674	14032	17420	15984
1.473	88.38	19632	10508	14710	16250	14664	17348	16488
1.48	88.8	19856	12220	12974	15018	15440	14684	14424
1.487	89.22	19776	12020	13430	17018	15352	14780	14808
1.495	89.7	19456	12228	12350	15626	12640	15188	14672

Appendix 4E Continued

1.502	90.12	18968	10340	12222	13554	12496	13244	13808
1.51	90.6	18976	7444	10734	15090	13776	15180	12264
1.517	91.02	17240	8212	10798	14682	15104	13348	12640
1.524	91.44	18240	8916	11190	13226	13088	14532	12184
1.532	91.92	18888	8788	10006	9138	10792	14492	12224
1.539	92.34	17440	10564	11246	11882	13688	12068	9184
1.546	92.76	16976	8780	10198	11258	10840	10748	11576
1.554	93.24	17080	7972	10526	13106	8936	13468	10192
1.561	93.66	18664	7668	10254	12234	7840	12196	9840
1.568	94.08	18656	6420	9806	10642	10312	11516	11016
1.576	94.56	16000	6164	7470	9498	9328	10148	10000
1.583	94.98	17896	6796	7342	11530	10528	11268	9088
1.59	95.4	14976	3812	6790	10162	9568	10300	7496
1.598	95.88	16704	6228	7518	9826	9176	10548	9544
1.605	96.3	15656	6924	7982	9322	5904	9804	8720
1.612	96.72	12192	6580	8182	8570	6328	10180	8120
1.62	97.2	14176	7364	6118	9394	5992	8124	8440
1.627	97.62	14384	5852	8534	8154	6136	9972	8992
1.634	98.04	12504	4716	6606	10298	5864	6980	7608
1.642	98.52	12592	3972	6406	8506	8232	7500	8176
1.649	98.94	15856	5524	6614	7578	7480	9204	7520
1.656	99.36	14976	5244	6358	8018	7752	7532	6096
1.664	99.84	16216	6196	5318	7682	7056	8308	6520
1.671	100.26	15864	6908	5822	6306	5744	5908	7096
1.678	100.68	11512	3692	4686	6074	4600	4556	5832
1.686	101.16	11808	3540	4902	6274	5200	6300	7872
1.693	101.58	12864	2388	5414	3626	5128	3564	6624
1.7	102	13008	4900	7526	4858	6312	7636	4952
1.708	102.48	13376	3236	7590	2970	4848	5524	4568
1.715	102.9	12920	6148	5422	6378	3552	6908	5104
1.722	103.32	11472	5300	4918	5034	3128	5340	4816
1.73	103.8	12480	4460	1422	6042	5384	4948	4776
1.737	104.22	11816	4388	3198	6186	3632	4612	4624
1.744	104.64	12104	4844	2006	4786	5384	5636	3472
1.752	105.12	11040	3684	4822	3802	5896	4748	6776
1.759	105.54	9184	2956	3350	3642	3664	5700	6600
1.766	105.96	10936	4300	4382	4858	2912	4948	5016
1.774	106.44	10456	3996	2222	4034	5520	5428	5120
1.781	106.86	13280	4076	5254	3242	5504	4996	3520
1.788	107.28	11832	3084	4614	4610	2408	5284	4616
1.796	107.76	9504	4084	3678	4730	3416	6492	4904
1.803	108.18	12856	3484	2182	3010	2720	4468	3480
1.81	108.6	9392	3708	1342	5682	3936	4932	3408
1.818	109.08	10856	3356	2094	4506	4224	4372	2848
1.825	109.5	8848	2612	2238	1778	4280	4700	3544
1.832	109.92	8888	1204	1614	2762	4752	3380	5264
1.84	110.4	8016	1996	2374	3546	3408	2300	4656
1.847	110.82	7120	2324	3302	2882	2520	4996	4424
1.854	111.24	9040	2924	3590	4258	360	2988	4512
1.862	111.72	9808	1180	4078	2970	2552	4420	3984
1.87	112.2	8496	2348	1870	4242	4056	3172	1984

Appendix 4E Continued

1.877	112.62	8992	3388	1286	2642	1928	5052	1960
1.884	113.04	8784	1740	1534	2386	3272	4916	2992
1.892	113.52	6664	1812	2894	2050	872	4108	2248
1.899	113.94	8912	1292	2758	58	2872	2828	3456
1.906	114.36	7472	2564	3334	2130	2504	2996	3416
1.914	114.84	6184	3156	-154	2810	1352	1492	152
1.921	115.26	9280	2756	1742	2890	2584	4148	3680
1.928	115.68	7160	2748	1470	1418	528	2188	2344
1.936	116.16	7128	4044	2910	1426	2440	1788	2280
1.943	116.58	9224	1724	2374	2266	2848	4212	944
1.95	117	8248	588	2734	3314	5424	4964	1384
1.958	117.48	9512	4076	1934	3362	3696	3148	1736
1.965	117.9	7240	2212	2726	2074	3496	1268	3520
1.972	118.32	7632	1972	158	3642	672	2316	3936
1.98	118.8	8344	948	1366	3674	1136	1468	4688
1.987	119.22	9176	1636	1870	2058	-632	1364	1624
1.994	119.64	8040	2772	2750	2538	3728	2620	2176
2.002	120.12	7504	3180	3030	2162	-296	2556	3992
2.009	120.54	8976	3220	4766	2770	1536	2028	3712
2.016	120.96	9440	1948	2958	1482	3560	3796	2864
2.024	121.44	9024	644	3374	2114	688	2492	2544
2.031	121.86	9816	268	1686	970	1624	3164	2840
2.038	122.28	10096	1116	782	754	2152	3764	1144
2.046	122.76	10064	2140	1390	1786	224	900	2192
2.053	123.18	7664	316	806	1530	1392	1268	3816
2.061	123.66	7184	1068	1774	730	1632	2492	1504
2.068	124.08	7088	1668	3198	2098	2776	1780	4432
2.075	124.5	6440	1548	2814	1930	1920	2508	816
2.083	124.98	7400	2484	1542	3058	920	1692	2448
2.09	125.4	7456	1996	534	2818	-776	2540	1136
2.097	125.82	8304	1868	622	-70	680	4036	824
2.105	126.3	5544	428	1670	3826	1112	3908	1216
2.112	126.72	5944	1036	1486	1986	2216	6908	1336
2.119	127.14	7568	1316	342	2802	1368	5308	1296
2.127	127.62	6568	-28	622	1274	1424	4988	3096
2.134	128.04	6936	-180	-754	1850	3728	5292	960
2.141	128.46	5048	1068	2806	2114	536	5132	528
2.149	128.94	6104	-836	4454	2386	2280	5276	2904
2.156	129.36	8936	-84	414	2522	1200	5908	448
2.163	129.78	9392	324	2486	3642	1088	4956	4040
2.171	130.26	6696	92	2150	3642	2728	4540	2576
2.178	130.68	6304	-324	1374	1858	1680	4828	2704
2.185	131.1	6784	1540	574	2250	1296	4596	5392
2.193	131.58	4680	1604	366	658	1272	1756	712
2.2	132	6288	3620	-586	402	704	2572	2464
2.207	132.42	5080	2348	-1162	1658	144	4924	2168
2.215	132.9	8048	2020	206	3002	-848	1796	520
2.222	133.32	7408	1508	998	658	1136	1308	824
2.229	133.74	6680	2388	862	1274	1232	2260	-248
2.237	134.22	5808	3532	758	562	-1616	3868	272
2.244	134.64	7248	252	846	2066	88	2860	1120

Appendix 4E Continued

2.251	135.06	7104	196	2518	2114	1200	3300	1176
2.259	135.54	6920	820	-338	666	520	4148	1680
2.267	136.02	6336	2292	-234	450	176	3236	2136
2.274	136.44	1440	1532	-34	1138	-936	2164	1208
2.281	136.86	4064	900	950	2874	1368	3036	1680
2.289	137.34	5520	724	1262	1898	-432	2324	3864
2.296	137.76	4480	-348	1102	762	504	548	632
2.303	138.18	3504	2060	262	-1190	1504	2860	1640
2.311	138.66	3288	2180	3726	1938	-96	2300	1760
2.318	139.08	5504	716	958	1842	3520	3044	1184
2.325	139.5	8136	2324	-250	202	-232	3260	-1104
2.333	139.98	5376	596	1478	338	832	2196	712
2.34	140.4	4424	924	-210	1186	920	1796	1760
2.347	140.82	6008	956	870	-326	304	2172	1360
2.355	141.3	3368	340	1550	-70	848	1244	2888
2.362	141.72	5520	892	-250	282	-776	188	2688
2.369	142.14	4088	1564	1478	922	1320	-628	1592
2.377	142.62	7008	1156	1630	482	2632	3604	1632
2.384	143.04	5664	-340	-26	-198	1520	2452	1600
2.391	143.46	3768	1660	-250	1194	-128	3452	944
2.399	143.94	6432	-1876	3142	-502	24	3668	688
2.406	144.36	5536	-1292	-50	-230	1504	3012	760
2.413	144.78	4912	1108	214	1498	-944	2572	1136
2.421	145.26	4816	-324	-1530	546	-3256	1524	1544
2.428	145.68	3568	-740	-466	-342	432	1316	984
2.435	146.1	2408	-1140	1310	650	-96	2340	2488
2.443	146.58	5656	-892	198	1554	608	1540	832
2.45	147	5104	2460	-114	3354	1432	2668	1160
2.457	147.42	5544	2428	3254	258	-232	4	-712
2.465	147.9	4256	684	1086	-438	1496	2700	624
2.472	148.32	4032	828	-578	1306	1432	2044	2464
2.479	148.74	1968	132	550	170	1272	1508	64
2.487	149.22	4856	892	-602	1618	1384	2036	816
2.494	149.64	4920	916	-506	1266	-1784	3540	2384
2.501	150.06	4256	-892	-922	-718	208	1188	2904
2.509	150.54	4424	1044	-18	178	1160	708	2384
2.516	150.96	4304	1092	526	866	1224	-324	928
2.524	151.44	3952	1612	230	1338	312	2164	-160
2.531	151.86	4936	1780	430	762	96	-564	1464
2.538	152.28	5864	652	790	-694	-1304	988	960
2.546	152.76	5176	6260	550	1314	-1080	2092	640
2.553	153.18	4928	15516	-826	-398	-560	1852	520
2.56	153.6	4432	26796	782	1202	952	1988	3800
2.568	154.08	6464	34076	1686	50	2336	1956	200
2.575	154.5	5056	37604	462	-798	3456	1068	1904
2.582	154.92	3360	42572	-138	-510	3616	292	1520
2.59	155.4	3160	44756	-626	1226	488	2204	2008
2.597	155.82	2520	46308	206	-1054	1280	2828	1776
2.604	156.24	5896	46060	-634	-30	-648	2100	1192
2.612	156.72	1232	43084	358	1738	1176	3052	-1112
2.619	157.14	3944	44892	1030	962	696	2988	152

Appendix 4E Continued

2.626	157.56	4088	46876	854	-238	1088	1428	1496
2.634	158.04	2936	48156	1678	322	1552	1260	328
2.641	158.46	5536	47596	-490	578	1416	1380	-1656
2.648	158.88	2992	46732	-562	-174	-1400	1236	-240
2.656	159.36	3784	44756	-2474	1906	2352	1308	560
2.663	159.78	4536	42884	-826	-358	3248	1276	2728
2.671	160.26	2776	41676	974	-6	1288	-196	1680
2.678	160.68	2096	39732	-290	850	2560	2364	-736
2.686	161.16	1456	39460	1254	-2158	2264	1908	1464
2.693	161.58	2112	38956	-162	202	2368	2068	888
2.7	162	4056	39612	-418	298	1216	2068	2256
2.708	162.48	5480	39780	-42	1090	1264	1564	2160
2.715	162.9	4064	39700	-34	-726	2184	3108	1296
2.722	163.32	3640	37012	-1154	-2822	-112	2076	560
2.73	163.8	4336	34692	-2058	2362	2464	52	1336
2.737	164.22	3024	32980	-162	1482	480	956	-584
2.744	164.64	3008	32804	-410	1394	1688	1588	-592
2.752	165.12	1848	32564	478	1554	1312	1036	3624
2.759	165.54	1920	33156	-442	-710	1000	940	88
2.766	165.96	3512	32204	-242	282	-480	3660	-880
2.774	166.44	3888	30212	-1058	546	2176	1876	512
2.781	166.86	4288	29564	-1034	1154	3384	1204	-360
2.788	167.28	4792	27380	-514	794	128	220	-584
2.796	167.76	1760	26468	-1090	170	-888	844	512
2.803	168.18	1888	25252	-2122	-166	456	764	952
2.81	168.6	2360	26652	-2106	-342	-1888	2228	592
2.818	169.08	3152	23892	-498	-2590	1640	-1436	-240
2.825	169.5	1896	25212	-1242	-518	-592	-300	-352
2.832	169.92	2696	24116	1870	-1246	-1408	-1028	1200
2.84	170.4	2872	25092	742	-1046	-392	2348	1016
2.847	170.82	4328	23164	-1474	1170	880	2644	688
2.854	171.24	4072	24652	622	26	1048	-140	-1184
2.862	171.72	2408	23052	830	722	928	-244	1176
2.869	172.14	3152	23212	1838	-62	-1376	1604	2136
2.876	172.56	1752	20508	-1114	890	1048	1316	-312
2.884	173.04	3536	20348	-2514	-1126	1216	1420	-1264

Appendix 4E Continued

5.98	4.99	3.91	2.99	2.49	2.05	1.59	1.32
-1096	9364	23346	6274	15811	25382	29318	-4214
1304	10740	27178	6930	18099	28174	32542	-2742
2080	11676	27066	7386	15987	26990	32806	-4310
2120	12508	27050	7586	17931	28198	30614	-3302
1192	11924	25178	7874	15707	27902	31646	-2846
1704	10260	26258	6154	17419	28302	29326	-2982
-712	11700	27994	7258	17115	27086	30390	-2622
2232	12876	27282	7138	16595	27942	30870	-3470
2600	21932	25178	6970	16779	27014	31422	-3806
3384	39380	27106	7946	17443	28630	28182	-2126
12352	43252	27770	8250	19427	25950	30742	-3782
19824	44540	26154	15634	24443	27998	30974	4730
20368	40540	25954	34490	27723	30822	30318	28770
23440	37884	27610	44362	23755	37022	30662	45890
26440	36652	27762	47842	20963	48574	31726	47730
29440	44660	32898	52042	19971	57982	28286	43522
36632	52348	44226	52018	18803	56630	30534	46202
39008	56724	51346	48866	17947	56582	29814	55674
33160	54956	52258	43762	21699	58470	32134	62250
32104	51412	55050	47674	35763	60182	38486	68370
29672	52556	56882	51226	48067	60118	43078	65658
28392	49156	52834	55386	48835	63958	51086	62274
21144	35212	57922	57546	43467	68502	57942	61074
12592	24908	58850	58362	40635	67270	59350	64378
5360	19868	57210	53538	35931	61646	53734	61074
3192	22212	60802	45402	30891	63638	54318	55586
-944	31844	61962	35962	34083	60630	51782	48274
-3096	39196	54066	26330	44459	45350	52510	45930
-2120	43324	46074	19546	56603	31454	59422	44154
4224	44116	33266	25186	68587	27102	60814	41922
10376	43508	27890	41290	76715	39486	59118	35594
15064	40452	32402	65754	79627	52982	55614	27690
21560	35108	45298	90850	73035	66022	51374	21034
25856	27212	62106	103042	59707	73334	51110	17314
27208	20116	75994	104514	45491	77446	46382	12370
26048	18444	83426	98530	42731	83998	49318	11266
22680	17204	89058	83426	47107	83510	56366	8010
21048	16420	87522	70498	61891	76726	66862	9762
20800	17148	81122	54530	70539	72214	80142	11658
17360	17716	68442	46114	76547	64246	89766	12258
18528	18748	58922	34418	74699	51942	94030	12338
15056	19844	50426	26610	67803	44118	90518	13442
14760	19404	37498	23450	57627	37990	77382	13290
15776	18060	31730	19426	48779	34038	63790	13754
13584	18396	27842	17570	39043	26670	53102	11698
15104	17708	25922	15266	31643	23118	43830	10586
16088	18732	22610	14234	25419	22702	37534	10218

Appendix 4E Continued

24552	29884	18226	12490	22603	17590	30142	10506
38872	45980	17514	10858	20051	16238	25742	8794
56616	68148	17738	10458	19331	15478	23870	8962
74080	86476	18186	10434	25627	16206	21622	11058
94824	97260	14434	14098	35659	25214	19390	13730
113960	103884	17546	22562	53715	48254	19246	24258
125832	106836	24114	39258	76251	87910	19654	36386
133064	111540	37706	64690	93987	134142	17190	52690
134408	105804	55250	96834	102627	187398	19606	78082
131400	103996	71410	127458	111571	218598	25158	119474
129544	106692	87010	152002	123827	246438	37174	193874
126216	104060	106298	169730	144459	275798	59926	290642
122952	107932	122050	179650	174251	298230	89710	394418
125512	121092	135842	187874	213899	320662	123470	487922
118536	132708	146210	187266	240011	332726	166094	549394
117768	144804	152130	187330	264107	338550	197582	601810
112232	159268	153890	182882	281771	336566	223534	617842
106536	157732	150850	175682	283563	341750	232718	632914
104360	163876	148450	171330	282539	334710	242926	643890
101448	161604	150018	168674	278027	323478	252014	641778
100680	158852	142434	159138	270731	313814	257198	634098
98408	153956	141506	159298	263371	297846	259406	622674
94888	148004	135010	151266	256939	292950	265198	601170
88168	145156	132130	145890	243947	278806	263790	588274
85768	136900	122882	138594	238539	262998	264078	566482
82664	133156	120322	132354	229195	244630	257198	550098
78568	128580	115746	123170	219051	230774	243662	519410
79624	124612	108706	116610	204075	213718	238510	496562
75016	120580	106178	111778	196043	205206	231150	464082
73544	118628	99394	104290	187403	183094	211886	438258
68520	110180	94914	99362	177803	169814	197166	402866
66024	106628	89634	91010	165515	161206	183470	372466
62696	104644	85378	83810	157963	147542	168558	342226
60808	98724	84066	78626	145419	136214	153998	313682
58312	94180	79106	73122	136843	128950	136494	282930
55144	90148	74818	68610	130155	110838	124078	258514
54760	87140	71554	65826	118243	100150	109902	232850
53736	83716	65442	59458	113675	87862	102686	214034
52584	79876	62674	53442	102187	77718	90310	191626
50024	76164	59114	49258	92659	69718	80910	171610
47432	75236	55354	47402	83547	64950	81750	162370
48968	73636	52234	43402	73723	57406	73238	154522
47464	73860	49186	41282	69027	54606	60486	134970
47368	70084	46858	37834	63211	48526	52950	117186
46856	65732	46210	34258	60403	44550	46166	101330
45288	64772	44442	31146	55771	42622	38694	89210
45512	61156	40394	32306	50443	36422	36014	77346
47432	59044	40306	29730	44571	31398	30718	70466
46280	56644	38266	28386	46507	28614	28886	61298
46248	56420	37066	26058	40811	24558	26222	53282
46152	53956	37186	22642	36379	22062	24734	49082

Appendix 4E Continued

48328	54052	34722	22802	33643	22646	22454	45098
47688	55460	32738	21474	30291	22190	21878	37290
49544	54724	34162	22418	27827	22694	16766	33290
47656	54116	32610	23146	27635	20822	16110	38794
47624	55044	32994	22802	26603	18270	17326	35634
51784	52612	33434	22490	25171	18990	13598	27786
50536	51428	34370	20898	25739	18590	12038	21482
49896	51972	31594	19794	23539	15878	12510	19114
49288	53348	32978	21890	23755	15158	11886	17210
52200	54052	33226	22730	26435	15502	12310	14250
53800	54692	34386	21594	23203	11846	11574	13522
53768	54948	34642	21450	23571	14990	10974	14026
53160	55588	33442	23202	22859	14542	10878	14034
52968	55716	34170	22834	23027	18446	8318	14090
51464	57124	35754	21882	23139	19678	10230	12962
56136	58212	36922	24290	24483	18294	10038	10298
57128	58468	38442	23066	23747	17830	8686	12930
58184	57508	38922	25058	23779	18318	10942	11666
56616	59396	36818	25634	25115	16742	9534	12946
58728	58404	36266	26082	23651	16062	10062	14018
59240	57828	40610	26026	24691	16374	10766	14490
60680	60740	39058	25738	25779	19806	13334	10810
62792	63172	40058	25434	23467	20142	12486	9746
59944	62692	38946	27154	25491	15702	14254	11474
62600	65060	44258	27458	23451	20126	13550	14282
65128	65412	42570	28330	24419	20966	11694	10930
65288	65700	44106	29218	26403	20518	12350	10010
67080	65700	44930	28970	28323	21534	12270	12474
66856	70500	45274	28738	26179	20854	11342	11890
64200	68516	43554	30010	28987	21438	11902	13922
67080	67044	44482	31954	30315	19654	13510	10698
68776	69316	47122	31794	29275	21182	15662	11530
68296	67108	46394	32634	30347	21894	16046	10530
70344	69604	47810	34226	28699	21726	17894	12178
68776	71940	48754	33474	30947	22318	14702	11898
69224	71524	50002	33682	29771	23502	15894	14578
70248	73668	49098	34026	28907	20942	15830	12370
68616	73476	51466	35442	30411	21758	16494	10666
70152	74212	51186	35242	29883	23222	16270	11706
68872	74916	49978	34410	31115	24862	17550	14706
70152	75972	50234	35138	32179	22438	15142	13178
69320	74916	51658	36714	33851	23598	18374	14770
68648	76932	51834	35930	32979	24206	16214	15146
68744	76932	53522	35482	32899	25350	16678	14250
68904	77444	52970	38858	33275	25278	18414	15058
69384	78372	52778	35506	32747	23350	19614	14234
68552	78148	52474	38498	34243	24134	18990	15194
68616	75620	52434	37594	32907	23894	19110	16010
68392	78596	52818	37858	32171	25446	17558	15690
64552	74628	53218	38282	33851	25502	19830	16922
68584	77412	55130	38074	33331	25430	19510	14362

Appendix 4E Continued

64616	77220	52522	37378	35115	25366	17862	12722
65192	78276	52234	36586	34163	22470	18262	15802
64264	77380	53138	38418	32443	21478	21462	16834
62856	75396	48466	37370	34091	26918	20734	17026
60616	78180	54730	38786	35171	24598	19126	16010
61384	77604	48298	35874	32011	23654	20390	16010
60040	75556	53154	38058	32435	27390	19742	16266
60328	76836	54938	36818	33579	26646	18558	17354
58600	74148	51778	38250	32699	26766	18830	18362
56104	73604	49730	36986	32243	25766	18382	18586
56200	72708	49122	36010	31867	24006	17910	18730
53384	73444	50650	33666	31043	23486	18702	17194
54536	71844	46306	36482	33075	21838	20126	16010
51816	72068	46250	35794	31219	22462	18382	15650
50888	71844	44954	36714	30715	24318	21166	18226
49192	68868	43786	35986	32299	23550	18830	18386
48680	66628	46746	33610	32587	21574	19206	19018
46952	67812	46306	34338	29163	24446	19718	16602
46472	67492	43954	34098	30483	23790	19414	17082
44136	66596	44682	33562	28403	21278	17022	18618
45352	65316	41842	34098	30115	20942	17566	19762
42592	64132	42426	32810	29403	23702	17798	16538
42824	61828	42098	32562	28891	20878	17670	20282
42312	62500	40218	31186	29955	20302	16654	19906
41712	60740	40666	30234	28355	17814	14430	16682
40752	57092	38658	29298	26555	19414	16174	16770
38736	59076	36266	27818	26283	17982	17038	17378
37496	58852	33618	27586	25875	16974	15518	18274
36360	60068	38234	28050	25947	20038	17486	18210
35192	56164	35642	27402	23515	18654	16030	19402
34776	56260	35018	25706	22339	17342	16726	17050
34304	53700	34754	25698	23843	19046	16822	15714
35248	52004	34730	25058	22659	14454	15390	16626
33784	50500	32786	25666	22723	17494	14278	16426
30672	48156	32922	25138	19771	15702	16086	13986
30048	46716	30362	22154	23315	13646	12902	14842
28880	46420	29482	23098	22747	15790	13478	14714
28016	45828	29850	20626	21907	14758	15006	14930
26656	46524	27338	20474	20707	12470	15046	14458
25864	44588	28338	20162	19555	14222	15998	17554
24880	43956	28082	21290	20483	14878	14078	14738
26216	42636	27946	20266	18971	11718	12710	13898
23328	44132	28362	21106	17059	12518	12062	16706
21544	40756	25170	19202	17747	10374	11662	16314
22232	39596	24522	18426	16643	10862	12582	15698
22168	36780	23954	17794	16019	10022	10558	15394
22664	36836	21978	15746	17411	9350	8502	13474
19832	31036	19994	15730	15987	11342	11414	12234
18752	35460	19754	15170	14755	11774	13206	13154
19944	31604	20898	15706	17851	11806	11406	13010
18712	34556	20826	15506	13107	11542	12574	12834

Appendix 4E Continued

16168	31620	18474	13994	12971	10814	11262	13706
17368	30300	23010	14394	13691	8486	10014	12114
17288	31692	18866	14154	13531	11534	10046	13666
16112	31884	19122	13874	11963	9742	8534	13938
15688	30412	20106	13418	11915	8934	10030	11746
14752	27284	15914	11106	10867	7542	10998	12602
15096	26716	16354	11122	10379	5702	7622	11258
17368	25164	14914	11882	9787	7302	10878	11498
14904	21700	15298	9338	9907	6614	11206	11730
13536	22092	12690	8890	10251	7742	10182	9402
13944	24836	14850	9202	9331	10270	7910	7874
12720	24220	13986	11210	8331	8478	7326	8802
13680	24564	11914	10194	7931	7350	9710	8282
11312	22380	11914	10386	5947	7182	8110	9266
13600	21644	14986	10474	8747	5790	7430	10338
12656	20684	12666	9210	7739	5894	5870	8386
11512	19508	13410	7914	9019	6046	7486	9922
12328	20020	11330	7914	7347	4326	6038	8578
10600	18924	10066	7130	7779	5454	6766	9658
9544	17100	10674	6274	5475	5382	6398	7762
10600	15580	9458	6690	6027	6478	5774	8034
9760	16564	10226	4978	6611	6182	7246	8882
9424	17212	9674	7930	4987	4038	8006	8530
9072	15676	10434	6450	3915	4670	6742	6514
7784	19068	6402	6386	3691	6166	7654	7194
10064	16308	10162	5986	1859	3958	5422	7146
9280	15148	9138	6114	4987	5430	5662	6442
9720	13388	9178	6138	5859	5046	4870	6650
7752	14444	8194	6578	5283	558	2766	6546
8728	10948	6754	5578	5859	2214	7614	6106
8400	12444	8634	2994	5163	3998	5606	5226
9000	12204	7258	5042	3691	5062	4774	4570
9624	11204	6466	4250	5155	6326	6318	4986
8760	9172	8106	5346	5459	4358	4494	3850
8488	11372	7386	4202	3899	5350	5678	4138
10208	12748	4034	3930	3955	3406	5462	3546
8488	12204	6370	4266	1195	4886	3822	2890
7224	12372	5794	5786	3747	4646	2766	2858
9504	10340	5522	2914	1395	2462	3782	5010
7784	10340	4786	2082	2811	2702	3070	4386
5768	8932	6218	2178	3491	2078	5686	4994
8744	7764	5218	3418	2851	2198	5550	6114
5392	6140	5058	2234	3171	3150	5510	6082
5912	8268	7194	2450	4235	3030	7286	5250
4832	9116	6466	2866	3995	2462	4374	3522
6608	5868	5242	2330	2723	4382	2886	3602
5200	8356	5706	2354	443	1182	4126	4066
6312	8532	4442	3946	987	1022	3054	2874
5936	7164	4714	2506	1523	134	3310	2426
5328	7284	2418	2946	1699	2742	4302	1562
5912	7628	5114	1202	1219	1462	-10	1346

Appendix 4E Continued

3656	8748	5298	3362	1187	3134	4526	1362
6648	7012	4362	2802	1635	838	4582	2354
7520	5708	3946	2346	827	2542	5222	842
4136	6132	4978	2626	515	3102	5438	3698
6384	4476	3938	1786	2747	3526	4342	4106
3800	7356	3810	1042	1587	2286	3702	2474
4760	5212	3578	2706	1587	2078	1494	2754
5368	4388	5346	4274	1515	1406	2646	442
4440	8692	4778	3018	1459	1398	3534	1610
3360	6340	3234	1602	363	486	2502	2106
4248	6172	2298	2034	1875	2030	742	2490
3680	5308	4578	3130	1851	2398	3366	-446
4352	5132	4826	482	1355	718	3246	-1166
2696	6700	3202	1338	1731	1638	1862	1162
4136	6516	2570	-1166	-125	3182	4646	3730
4912	4284	3554	1370	659	2502	3734	3050
2608	3916	6178	1930	-1021	2558	2494	2986
3536	4172	6186	338	435	2302	3350	2730
3040	2372	3538	3050	-317	214	2606	1018
2904	6996	4538	3066	-1029	1582	1374	362
2624	4380	2786	1810	923	1286	1950	946
2800	5108	3210	962	1339	1206	-650	178
5432	3436	3330	1578	947	3326	2590	178
4104	3420	2018	1610	-365	1326	2062	578
3096	4716	2066	2498	35	4102	3190	306
5392	1660	3218	1146	619	2134	2574	618
2624	1932	2402	2138	-181	2926	1998	242
4288	3852	3818	1826	1339	3958	3374	970
4872	3956	4458	778	-141	302	4422	2706
3792	3580	2794	2690	1659	550	2590	2610
2584	2044	2282	2226	-1181	582	3838	2786
3704	3612	1786	2162	307	-1242	3598	1194
2888	4124	1626	1570	1315	926	102	938
4176	3524	2394	34	-125	1590	3294	-342
4528	2844	3506	-278	931	1022	3606	1482
4344	3060	1522	-158	-1069	2030	3758	-342
3816	3340	4826	834	323	2214	4142	-774
4840	2420	3850	-894	123	2606	2414	58
2736	1948	2730	1986	1531	1518	3126	458
1696	4228	1850	914	2211	926	334	-1670
3344	2500	3202	1634	899	222	-34	-1190
2528	3612	1698	2954	-1541	1926	1486	634
3744	4076	3090	1834	-565	1974	3126	450
3136	3340	2770	1026	-661	350	1878	1130
1616	2756	1234	250	1443	606	2510	-278
3328	2316	2698	26	883	702	2630	1330
3472	2724	1602	2746	171	1726	2998	1738
5008	3444	3770	1098	1299	1790	5046	58
3528	4172	4362	-758	-893	3070	1782	-918
3448	180	4250	354	1955	2846	2462	-918
4456	2132	1850	1618	51	2958	2878	-1670

Appendix 4E Continued

2584	1444	1698	906	635	790	926	290
2896	1716	2426	2130	-805	-26	3942	-2550
1792	2388	434	1066	2723	646	2446	762
2104	2380	2418	762	1051	478	1566	-406
3448	2596	1674	-606	-133	-1906	2310	618
2640	3796	1882	1794	739	-378	1478	682
6936	2700	1714	442	-1421	2998	1726	146
5016	1516	3354	-22	523	654	4502	-566
3816	3132	2714	-854	1451	2822	4182	-894
3304	2668	4186	1706	283	726	2694	-582
3816	-428	2450	3394	-125	630	1918	18
3960	2836	162	1602	1219	598	-2122	-686
2480	1428	1058	1314	-509	1038	2246	-382
2480	3164	1426	634	-45	606	1078	-1254
1928	3452	3042	2938	1243	1062	1190	-22
3232	2756	2330	1266	-461	-1314	3054	-358
4928	1588	2650	-958	-109	2502	4638	50
4912	780	2050	2050	1355	3182	3382	698
2824	1716	1650	2330	499	-242	3230	-1006
4792	3028	2178	-206	1059	990	2294	-582
2080	3668	2482	1306	-1453	254	2966	-206
3576	2572	8458	1690	-301	694	2510	1090
3792	2908	2194	1186	851	2094	2198	-142
2000	2292	2266	1794	-293	918	2174	-1390
3136	4460	2426	1170	99	1102	3830	-1438
2336	3108	2522	642	2251	2366	4406	-446
3776	1460	3162	482	1731	2014	4758	-486
4568	1268	3114	-70	2083	1110	2414	-78
4080	1132	1394	-582	619	1550	1126	298
4224	684	1938	538	147	1350	4238	-1030
3264	2276	1554	642	283	2222	1766	138
4208	1932	2138	234	-613	2446	3814	442
2512	1300	2970	330	1451	-586	2326	-918
2248	1564	1346	1874	3323	22	2350	-342
4224	1380	2586	1810	-685	830	2670	314
3552	1348	2770	-110	675	-1138	2726	-534
3680	3164	2682	618	1043	-826	3798	-1190
3344	1964	2394	1722	-405	582	1606	-750
4416	-84	970	218	-309	1358	3278	378
3104	1772	2994	1154	451	1878	3086	-118
1984	1812	2586	66	-1717	3006	3230	562
3432	548	2626	986	-253	550	2782	370
2368	2468	3378	1322	531	966	4486	-54
1256	1700	2042	818	-821	1046	1950	402
856	1548	-750	-166	243	566	1830	1818
4256	4332	818	2410	723	-618	366	-878
1568	3092	1946	1890	-1141	-2794	1982	-318
3224	1348	1770	1754	-1021	-146	3454	-222
2192	3572	2266	1042	-381	2006	4086	-334
1616	2180	-398	1170	-453	2670	2382	-598
1112	1388	2498	1050	1123	1230	2414	-1030

Appendix 4E Continued

1632	2268	2994	1082	-893	2686	2966	114
448	876	2826	1314	283	-282	1798	-1350
2856	-524	3890	-446	259	670	2198	754
1544	1268	2946	778	-1589	-274	1206	842
1464	1508	2834	586	1907	446	1974	850
2472	2788	1186	1010	1211	222	486	-334
2952	2468	1266	650	-1757	-490	2150	-550
5280	1844	3082	-510	-125	1646	4350	-70
4368	956	1634	1034	-1357	166	2574	642
2400	1732	1346	1234	11	2046	2510	890
504	876	2338	386	-981	1478	1790	482
2424	20	2074	-46	-405	1782	4006	-494
1792	-708	1538	1618	-1445	1526	4710	202
1240	396	3410	714	603	974	1854	-966
1584	964	2106	650	-477	1782	1206	-3014
2712	260	1538	746	43	558	2334	818
4336	1676	74	2602	443	-226	2934	-318
3000	236	2442	3130	-877	1902	2326	-1846
3312	580	3066	698	139	-554	3238	1298
3152	3764	1034	82	-1037	1366	1358	402
312	332	674	794	339	1222	2454	-606
1800	3380	122	-174	1499	2270	934	-1006
-584	1732	3178	-950	-141	2126	3142	-446
976	2180	682	-150	-1389	902	4078	426
1504	844	1362	922	2099	-42	3870	802
2616	1716	2490	1826	-309	3390	1374	738
2568	532	2786	-1054	1531	1654	4086	378
4864	-580	2986	2114	1963	582	1974	-2310
3800	1868	2970	1546	-2525	-722	2054	514
2760	1724	2802	2330	131	-186	3806	-46
3272	1636	2178	-70	35	-98	2078	634
3352	3140	1330	3154	2603	974	1958	970
2256	2372	2378	2074	2075	1846	2750	-470
1544	1476	1690	1002	-797	1726	4478	626
3384	3436	3050	1010	-1301	622	2814	-414
2568	3396	1378	-678	-389	1526	4262	-390

Table 4F - King Site ground water chemistry used for calculations in Chapter 4 (SRC Analytical Laboratories). Al, Cd, Cr, and Au were below detection limit (b.d.l.) for all samples.

		B 7.5	B 10	B 15	B 20	B 25	B 30	B 35	B 40	B 45
pH	units	7.96	7.97	8.17	8.05	8.17	8.1	8.18	8.14	7.99
SpC	uS/cm	36500	41300	28400	23100	18600	14800	13300	8450	6160
HCO3-	mg/L	670	769	836	954	992	928	989	764	680
Alk -tot	mg/L	549	630	685	782	813	761	811	626	557
Ca	mg/L	400	410	370	400	420	410	400	380	410
Cl	mg/L	42	31	21	31	49	74	123	162	188
K	mg/L	82	88	56	52	48	37	34	23	19
Mg	mg/L	5900	7200	3700	3100	2020	1300	1010	370	220
NO3-	mg/L	1.2	0.75	0.75	0.35	0.97	0.97	1.5	3.7	6.3
Na	mg/L	8900	10400	6600	4600	3630	2850	2690	1580	1000
SO42-	mg/L	41200	49500	27700	21000	15400	10900	9300	4900	3200
Zn	ug/L	45	50	70	30	40	18	21	53	42
Ba	ug/L	8	11	8	8	6	6	7	6	7
Be	ug/L	470	420	290	320	440	570	660	760	830
B	ug/L	470000	420000	290000	320000	440000	570000	660000	760000	830000
Co	ug/L	b.d.l.	b.d.l.	b.d.l.	b.d.l.	b.d.l.	4	4	1	b.d.l.
Cu	ug/L	69000	150000	43000	11000	12000	17000	16000	21000	12000
Fe	ug/L	b.d.l.	b.d.l.	b.d.l.	b.d.l.	b.d.l.	b.d.l.	b.d.l.	2	b.d.l.
Pb	ug/L	b.d.l.	b.d.l.	b.d.l.	b.d.l.	b.d.l.	3	4	b.d.l.	b.d.l.
Mn	ug/L	7	142	470	1900	1400	1110	1290	950	7
Mo	ug/L	240	250	270	91	100	88	140	16	3
Ni	ug/L	38	36	73	41	300	210	190	53	5
P	ug/L	140	160	120	210	330	200	200	40	100
Si soluble	mg/L	22.5	26	29	30	31	29	25.7	27.9	28.2
Sr	ug/L	7490	10100	8200	12400	11700	8450	7430	4310	3240
Ti	ug/L	2	b.d.l.	b.d.l.	b.d.l.	b.d.l.	2	3	1	1
V	ug/L	b.d.l.	b.d.l.	b.d.l.	b.d.l.	b.d.l.	b.d.l.	b.d.l.	b.d.l.	b.d.l.
Zr	ug/L	3	6	b.d.l.	b.d.l.	b.d.l.	b.d.l.	b.d.l.	b.d.l.	b.d.l.
U	ug/L	556.2	788.5	582.8	491.1	349.5	302	224	53.7	23.4

Appendix 4G - Data used for Uranium and Zinc kinetic experiment in Chaper 4.

Uranium				
	time	**Area (A)**	**A/Ao**	
Stock A	**0**	2225604	1.012	**Stock solution Average (Ao)**
T0	**4**	1408040	0.640	2198510.6
T1	**16**	1235856	0.562	
T2	**49**	1163729	0.529	
Stock B		2346751		
T3	**104**	1158694	0.527	
Stock C		2203095		
T4	**178**	1158331	0.527	
Stock D		2104532		
T5	**967**	1160167	0.528	
Stock E		2112571		

Zinc				
	time	**areas**	**A/Ao**	
Stock A	**0**	18556	1.006	**Stock solution Average (Ao)**
T0	**4**	10965	0.594	18446
T1	**16**	9652	0.523	
T2	**49**	8719	0.473	
Stock B		17613		
T3	**104**	8583	0.465	
Stock C		19390		
T4	**178**	8626	0.468	
Stock D		17728		
T5	**967**	8589	0.466	
Stock E		18945		

APPENDIX 5 Supplementary data for Chapter 5.

Appendix 5A – Diffusion cell data.

Appendix 5B – AsFlFFF fractograms for Warman Site ground water.

Appendix 5C – AsFlFFF fractograms for Mexico City ground water.

Appendix 5D – AsFlFFF fractograms for King Site WTW ground water.

Appendix 5E – Diffusion cell models for Chloride, PSS 4800, 6500, and 15450.

Appendix 5A - Diffusion Cell Data.

PSS 910

Measured			Modeled		
Day	**Collection C/Co**	**Source C/Co**	**Day**	**Collection C/Co**	**Source C/Co**
1	0.040	0.999	0	0.000	1.000
3	0.030	0.952	1	0.000	0.954
4	0.038	0.933	2	0.000	0.935
5	0.027	0.952	3	0.000	0.921
6	0.033	0.871	10	0.007	0.861
7	0.029	0.871	20	0.036	0.811
8	0.004	0.917	30	0.069	0.773
9	0.032	0.870	40	0.099	0.740
10	0.012	0.787	50	0.128	0.709
11	0.019	0.870	75	0.188	0.646
16	0.007		100	0.236	0.596
18	0.032	0.833	150	0.302	0.525
20	0.048	0.795	200	0.344	0.482
23	0.030	0.814	250	0.369	0.455
29	0.055	0.757	300	0.385	0.438
36	0.108	0.733	350	0.395	0.428
48	0.140	0.696	400	0.401	0.421
68	0.196	0.633	450	0.405	0.417
98	0.256	0.562	550	0.408	0.413
107	0.282	0.552			
125	0.296	0.533			
160	0.304	0.518			
188	0.318	0.495			
216	0.322	0.486			
231		0.469			

Model Fit

r^2	*error*	
0.983	0.0381	**source**
0.975	0.4362	**collection**
0.995	0.3035	**total**

Appendix 5A Continued

ground water DOC

Measured					Modeled		
Day	**Collection**		**Source**		**Day**	**Collection**	**Source**
	C/Co	**std dev**	**C/Co**	**std dev**		**C/Co**	**C/Co**
1	0.002	0.008	0.957	0.009	0	0.000	1.000
2	0.010	0.005	0.895	0.020	1	0.000	0.969
3	0.007	0.011	0.918	0.019	2	0.000	0.952
4	0.012	0.002	0.969	0.007	3	0.000	0.938
5	0.017	0.073	0.905	0.017	10	0.000	0.876
6	0.020	0.038	0.856	0.017	20	0.002	0.824
7	0.012	0.025	0.908	0.016	30	0.010	0.787
8	0.015	0.078	0.935	0.016	40	0.021	0.758
9	0.022	0.005	0.849	0.022	50	0.034	0.733
10	0.014	0.026	0.888	0.017	75	0.070	0.684
12	0.017	0.002	0.982	0.022	100	0.106	0.644
17	0.021	0.008	0.848	0.019	150	0.166	0.580
19	0.017	0.016	0.823	0.016	200	0.212	0.531
21	0.016	0.035	0.893	0.016	250	0.248	0.493
23	0.016	0.003	0.853	0.017	300	0.276	0.464
31	0.020	0.022	0.801	0.017	350	0.297	0.442
38	0.041	0.027	0.809	0.022	400	0.313	0.425
55	0.078	0.028	0.769	0.028	450	0.326	0.412
64	0.081	0.021	0.757	0.015	550	0.343	0.394
73	0.122	0.015	0.714	0.023			
82	0.110	0.015	0.694	0.023			
99	0.147	0.015	0.654	0.018			
113	0.146	0.015	0.634	0.025			
134	0.169	0.015	0.605	0.016			
155	0.194	0.031	0.564	0.019			
183	0.220	0.041	0.546	0.022			
210	0.238	0.024	0.503	0.016			
246	0.256	0.021	0.483	0.017			
293	0.281	0.011	0.463	0.014			
375	0.321	0.010	0.420	0.020			
457	0.341	0.014	0.421	0.014			
547	0.350	0.017	0.416	0.014			

Model Fit

r^2	*error*	
0.985	0.7773	**source**
0.987	0.0358	**collection**
0.996	0.5339	**total**

Appendix 5A Continued

PSS 1430

Measured		
Day	**Collection C/Co**	**Source C/Co**
1	0.013	0.979
2	0.009	1.003
3	-0.003	0.939
4	-0.014	0.919
5	0.013	0.895
6	-0.012	0.964
7	0.014	0.951
8	-0.002	0.941
9	-0.007	0.847
10	-0.011	0.899
11	0.017	0.860
16	0.007	0.873
18	0.006	0.860
20	0.008	0.832
23	0.001	0.832
29	0.008	0.787
36	0.000	0.832
48	0.046	0.782
68	0.065	0.710
98	0.104	0.720
107	0.098	0.678
125	0.111	0.675
160	0.137	0.651
188	0.145	0.625
216	0.168	0.586
231	0.176	0.604

Modeled		
Day	**Collection C/Co**	**Source C/Co**
0	0.000	1.000
1	0.000	0.968
2	0.000	0.953
3	0.000	0.942
10	0.000	0.895
20	0.001	0.854
30	0.006	0.825
40	0.013	0.802
50	0.022	0.782
75	0.050	0.741
100	0.078	0.708
150	0.129	0.652
200	0.172	0.607
250	0.208	0.569
300	0.238	0.538
350	0.263	0.512
400	0.284	0.490
450	0.301	0.472
550	0.327	0.445

Model Fit

r^2	*error*	
0.970	0.6346	**source**
0.952	0.0298	**collection**
0.997	0.4409	**total**

Appendix 5A Continued

PSS 4800

Measured Day	Collection C/Co	Source C/Co
2	0	
3	0	
4	0	1.013
5	0	0.960
6	0	1.004
7	0	
8	0	
9	0	0.956
10	0	0.947
12	0	
17	0	0.851
19	0	0.743
21	0	0.876
23	0	0.838
31	0	0.762
38	0	0.724
55	0	0.629
64	0	0.613
73	0	0.617
73	0	0.634
82	0	0.591
99	0	0.571
113	0	0.558
134	0	0.505
155	0	0.503
183	0	0.491
210	0	0.476
246	0	0.457
293	0	0.422
375	0	0.419
457	0	0.418
547	0	0.408

PSS 6500

Measured Day	Collection C/Co	Source C/Co
1	0	1.000
2	0	0.931
3	0	0.966
4	0	0.925
5	0	0.972
6	0	0.952
7	0	0.931
8	0	0.927
10	0	0.910
15	0	0.862
17	0	0.867
19	0	0.861
21	0	0.746
29	0	0.776
36	0	0.789
53	0	0.690
62	0	0.690
71	0	0.655
80	0	0.634
97	0	0.621
111	0	0.586
132	0	0.552
153	0	0.534
181	0	0.517
208	0	0.500
244	0	0.517
291	0	0.479
375	0	0.466
455	0	0.467
545	0	0.469

Appendix 5A Continued

PSS 15450

Measured Day	Collection C/Co	Source C/Co
1	0	0.972
2	0	0.995
3	0	0.972
4	0	0.995
5	0	0.948
6	0	0.931
7	0	0.900
8	0	0.900
9	0	0.900
10	0	0.900
12	0	0.900
17	0	0.900
19	0	0.829
21	0	0.818
23	0	0.806
31	0	0.829
38	0	0.782
55	0	0.782
64	0	0.711
73	0	0.735
82	0	0.689
99	0	0.693
113	0	0.615
134	0	0.616
155	0	0.592
183	0	0.569
210	0	0.592
246	0	0.545
293	0	0.511
457	0	0.491
547	0	0.486

SRFA

Measured Day	Collection C/Co	Source C/Co
1	0.008	1.000
2	0.001	0.875
3	0.002	0.741
4	0.009	0.688
5	0.010	0.582
6	0.008	0.650
7	0.004	0.586
8	0.005	0.659
9	0.003	0.566
10	0.007	0.526
11	0.001	0.538
16	0.002	0.460
18	0.007	0.386
20	0.002	0.404
23	0.000	0.342
29	0.007	0.314
36	0.002	0.314
48	0.006	0.253
68	0.025	0.240
98	0.035	0.186
107	0.037	0.194
125	0.042	0.167
160	0.046	0.161
188	0.048	0.123
216	0.053	0.122
231	0.053	0.135

Appendix 5A Continued

SRHA

Measured Day	Collection C/Co	Source C/Co
1	0	1.001
2	0	0.547
3	0	0.725
4	0	0.670
5	0	0.651
6	0	0.564
7	0	0.359
8	0	0.417
9	0	0.477
10	0	0.435
11	0	0.359
16	0	0.349
18	0	0.216
20	0	0.171
23	0	0.189
29	0	0.181
36	0	0.165
48	0	0.134
68	0	0.099
98	0	0.067
107	0	0.079
125	0	0.071
160	0	0.073
188	0	0.074
216	0	0.077
231	0	0.078

Appendix 5B - AsFlFFF fractograms for Warman Site aquitard porewater samples
Results of molecular weight calculations at end of table.

Time sec.	MW daltons	D_H nm	8903F	8522E	8522D	8522C
0	0	0.06	1.3614	0.1527	-0.1401	0.4173
1	2	0.12	1.3596	0.1527	-0.1401	0.4173
2	4	0.18	1.3584	0.1527	-0.1401	0.4173
3	7	0.24	1.3567	0.1527	-0.1401	0.4173
4	11	0.30	1.3549	0.1527	-0.1401	0.4173
5	17	0.36	1.3537	0.1527	-0.1401	0.4173
6	23	0.42	1.3519	0.1527	-0.1401	0.4173
7	31	0.48	1.3502	0.1527	-0.1401	0.4173
8	40	0.54	1.3490	0.1527	-0.1401	0.4173
9	50	0.60	1.3472	0.1527	-0.1401	0.4173
10	62	0.65	1.3454	0.1527	-0.1401	0.4173
11	74	0.71	1.3443	0.1527	-0.1401	0.4173
12	88	0.77	1.3425	0.1518	-0.1408	0.4153
13	104	0.83	1.3413	0.8255	1.4338	1.3817
14	120	0.89	3.2060	2.5808	3.3384	3.5246
15	138	0.95	3.9511	3.0416	4.0686	4.3861
16	158	1.01	4.0635	2.9686	4.1404	4.5434
17	178	1.07	3.8861	2.7351	3.9351	4.3866
18	200	1.13	3.5608	2.4820	3.6425	4.0770
19	224	1.19	3.2119	2.2453	3.3334	3.6838
20	249	1.25	2.8866	2.0299	2.9947	3.2808
21	275	1.31	2.5673	1.8442	2.6809	2.8876
22	303	1.37	2.4017	1.6766	2.3988	2.5366
23	332	1.43	2.1296	1.5336	2.1387	2.2460
24	362	1.49	1.9049	1.4104	1.9171	1.9826
25	394	1.55	1.7570	1.3152	1.7366	1.8167
26	428	1.61	1.6506	1.2347	1.6080	1.7625
27	463	1.67	1.5441	1.1691	1.5025	1.7272
28	499	1.73	1.4673	1.1174	1.4285	1.6233
29	537	1.79	1.4022	1.0748	1.3623	1.5046
30	577	1.85	1.3253	1.0387	1.2874	1.4049
31	618	1.90	1.2898	1.0109	1.2183	1.3415
32	660	1.96	1.2307	0.9889	1.1761	1.2617
33	704	2.02	1.1834	0.9759	1.1318	1.1776
34	749	2.08	1.1479	0.9678	1.0925	1.1382
35	796	2.14	1.1124	0.9672	1.0685	1.0939
36	845	2.20	1.0769	0.9682	1.0540	1.0569
37	895	2.26	1.0592	0.9757	1.0367	1.0324
38	947	2.32	1.0355	0.9825	1.0166	1.0154
39	1000	2.38	1.0237	0.9892	1.0011	0.9999
40	1055	2.44	1.0060	0.9951	0.9858	0.9993
41	1111	2.50	1.0001	0.9986	0.9858	0.9740
42	1169	2.56	1.0001	1.0004	0.9991	0.9528
43	1228	2.62	0.9941	0.9997	0.9761	0.9325
44	1290	2.68	0.9705	0.9983	0.9416	0.9170
45	1352	2.74	0.9646	0.9910	0.9328	0.8941
46	1417	2.80	0.9409	0.9756	0.9021	0.8763

Appendix 4B Continued

47	1482	2.86	0.9232	0.9527	0.8637	0.8418
48	1550	2.92	0.8877	0.9290	0.8214	0.8230
49	1619	2.98	0.8581	0.8987	0.7725	0.8010
50	1690	3.04	0.8167	0.8644	0.7245	0.7790
51	1762	3.10	0.7753	0.8259	0.6851	0.7495
52	1836	3.15	0.7162	0.7841	0.6390	0.7217
53	1912	3.21	0.6689	0.7440	0.5978	0.6773
54	1989	3.27	0.6334	0.7005	0.5612	0.6255
55	2068	3.33	0.5979	0.6522	0.5142	0.5886
56	2149	3.39	0.5624	0.6054	0.4681	0.5335
57	2231	3.45	0.5210	0.5612	0.4373	0.4941
58	2315	3.51	0.4796	0.5153	0.3999	0.4490
59	2400	3.57	0.4264	0.4718	0.3567	0.4219
60	2488	3.63	0.3850	0.4300	0.3087	0.3941
61	2577	3.69	0.3436	0.3890	0.2732	0.3440
62	2667	3.75	0.3140	0.3514	0.2395	0.3261
63	2759	3.81	0.2726	0.3153	0.2078	0.2833
64	2853	3.87	0.2372	0.2843	0.1810	0.2638
65	2949	3.93	0.2135	0.2507	0.1540	0.2302
66	3046	3.99	0.2017	0.2229	0.1319	0.1808
67	3145	4.05	0.2490	0.1976	0.1041	0.1688
68	3246	4.11	0.2135	0.1722	0.0858	0.1492
69	3349	4.17	0.1780	0.1510	0.0647	0.1470
70	3453	4.23	0.1603	0.1314	0.0522	0.1308
71	3559	4.29	0.1484	0.1168	0.0531	0.1037
72	3666	4.35	0.1189	0.0997	0.0511	0.1015
73	3776	4.40	0.0952	0.0850	0.0492	0.0721
74	3887	4.46	0.0716	0.0745	0.0434	0.0599
75	4000	4.52	0.0716	0.0665	0.0386	0.0527
76	4114	4.58	0.0656	0.0584	0.0376	0.0407
77	4230	4.64	0.0656	0.0520	0.0337	0.0351
78	4348	4.70	0.0597	0.0464	0.0270	0.0362
79	4468	4.76	0.0479	0.0457	0.0231	0.0440
80	4590	4.82	0.0538	0.0410	0.0221	0.0409
81	4713	4.88	0.0479	0.0362	0.0182	0.0429
82	4838	4.94	0.0361	0.0314	0.0173	0.0522
83	4965	5.00	0.0302	0.0291	0.0143	0.0434
84	5093	5.06	0.0242	0.0260	0.0133	0.0429
85	5223	5.12	0.0242	0.0237	0.0105	0.0431
86	5356	5.18	0.0183	0.0222	0.0152	0.0426
87	5489	5.24	0.0124	0.0199	0.0104	0.0379
88	5625	5.30	0.0183	0.0184	0.0027	0.0283
89	5762	5.36	0.0242	0.0153	0.0160	0.0252
90	5902	5.42	0.0242	0.0146	0.0179	0.0305
91	6043	5.48	0.0302	0.0131	0.0131	0.0390
92	6185	5.54	0.0242	0.0174	0.0025	0.0475
93	6330	5.60	0.0302	0.0183	0.0111	0.0512
94	6476	5.65	0.0361	0.0152	0.0150	0.0481
95	6624	5.71	0.1780	0.0146	0.0197	0.0401
96	6774	5.77	0.1366	0.0147	0.0158	0.0297
97	6926	5.83	0.0952	0.0165	0.0119	0.0357

Appendix 5B Continued

98	7080	5.89	0.0716	0.0183	0.0109	0.0260
99	7235	5.95	0.0597	0.0160	0.0071	0.0272
100	7392	6.01	0.0538	0.0170	0.0089	0.0274
101	7551	6.07	0.0302	0.0164	0.0118	0.0211
102	7712	6.13	0.0242	0.0157	0.0099	0.0322
103	7874	6.19	0.0242	0.0159	0.0031	0.0440
104	8039	6.25	0.0183	0.0193	0.0040	0.0475
105	8205	6.31	0.0183	0.0187	-0.0008	0.0495
106	8373	6.37	0.0124	0.0205	-0.0028	0.0522
107	8543	6.43	0.0124	0.0182	0.0059	0.0484
108	8715	6.49	0.0065	0.0175	0.0020	0.0528
109	8889	6.55	0.0065	0.0160	-0.0029	0.0613
110	9064	6.61	0.0006	0.0154	-0.0029	0.0599
111	9241	6.67	0.0006	0.0139	0.0096	0.0619
112	9420	6.73	0.0006	0.0149	0.0105	0.0638
113	9601	6.79	0.0124	0.0159	0.0162	0.0641
114	9784	6.85	0.0124	0.0160	0.0220	0.0660
115	9969	6.90		0.0195	0.0161	0.0622
116	10155	6.96		0.0172	0.0180	0.0633
117	10344	7.02		0.0149	0.0123	0.0702
118	10534	7.08		0.0142	0.0045	0.0688
119	10726	7.14		0.0144	0.0045	0.0691
120	10920	7.20		0.0129	0.0036	0.0710
121	11116	7.26		0.0130	-0.0004	0.0704
122	11314	7.32		0.0140	-0.0033	0.0749
123	11513	7.38		0.0150	-0.0042	0.0768
124	11715	7.44		0.0151	0.0024	0.0762
125	11918	7.50		0.0145	-0.0014	0.0691
126	12124	7.56		0.0163	-0.0024	0.0825
127	12331	7.62		0.0165	-0.0063	0.0698

	8903F	**8522E**	**8522D**	**8522C**
Peak Diam. (nm)	**2.56**	**2.56**	**2.56**	**2.56**
MW (peak)	**1170**	**1170**	**1170**	**1170**
Mw (calc.)	**1639**	**1654**	**1539**	**1618**
***Mn* (calc.)**	**1387**	**1411**	**1331**	**1376**
Mn /Mw	**1.18**	**1.17**	**1.16**	**1.18**

Appendix 5C - AsFlFFF fractograms for Chalco Aquitard porewaters, Mexico City, Mexico. Results of molecular weight calculations at end of table.

Time sec.	MW daltons	D_H nm	MC N10 - 02	MC N10 - 03	MC N10 - 04	MC N10 - 05
1	0	0.00	-0.0120	0.0084	-0.0097	0.0407
2	2	0.04	-0.0120	0.0092	-0.0097	0.0447
3	4	0.08	-0.0120	0.0072	-0.0097	0.0397
4	8	0.13	-0.0120	0.0058	-0.0097	0.0304
5	13	0.17	-0.0120	0.0086	-0.0097	0.0431
6	19	0.21	-0.0120	0.0100	-0.0097	0.0515
7	27	0.25	-0.0120	0.0091	-0.0097	0.0502
8	35	0.29	-0.0120	0.0066	-0.0097	0.0424
9	46	0.33	-0.0120	0.0035	-0.0097	0.0310
10	58	0.38	-0.0120	0.0000	-0.0097	0.0183
11	71	0.42	-0.0120	-0.0036	-0.0097	0.0048
12	86	0.46	-0.0120	-0.0075	-0.0099	-0.0091
13	102	0.50	-0.0126	0.0042	-0.0067	-0.0118
14	120	0.54	0.3522	0.5239	0.4863	0.4792
15	139	0.59	1.1303	1.2514	1.3807	1.3954
16	160	0.63	1.4594	1.6700	1.8693	1.8892
17	183	0.67	1.4594	1.5800	1.9000	1.9599
18	207	0.71	1.4527	1.4200	1.7800	1.8470
19	233	0.75	1.3488	1.3000	1.6766	1.6944
20	260	0.79	1.2217	1.2514	1.5390	1.5554
21	289	0.84	1.1203	1.2483	1.4239	1.4391
22	320	0.88	1.0416	1.1633	1.3286	1.3427
23	352	0.92	0.9814	1.0953	1.2209	1.2645
24	386	0.96	0.9356	1.0432	1.1555	1.2010
25	422	1.00	0.9013	1.0042	1.1041	1.1497
26	460	1.05	0.8768	0.9755	1.0639	1.1073
27	499	1.09	0.8602	0.9555	1.0334	1.0733
28	540	1.13	0.8505	0.9430	1.0107	1.0467
29	583	1.17	0.8467	0.9365	0.9949	1.0268
30	628	1.21	0.8476	0.9351	0.9855	1.0125
31	674	1.25	0.8530	0.9380	0.9814	1.0028
32	722	1.30	0.8624	0.9442	0.9816	0.9971
33	772	1.34	0.8746	0.9531	0.9847	0.9939
34	824	1.38	0.8901	0.9634	0.9894	0.9928
35	877	1.42	0.9078	0.9742	0.9943	0.9926
36	933	1.46	0.9258	0.9842	0.9982	0.9916
37	990	1.51	0.9429	0.9928	0.9997	0.9893
38	1049	1.55	0.9582	0.9983	0.9985	0.9848
39	1110	1.59	0.9705	0.9999	0.9934	0.9779
40	1173	1.63	0.9788	0.9975	0.9841	0.9681
41	1238	1.67	0.9825	0.9894	0.9696	0.9531
42	1304	1.71	0.9809	0.9753	0.9497	0.9322
43	1372	1.76	0.9737	0.9554	0.9234	0.9048
44	1443	1.80	0.9606	0.9299	0.8965	0.8727
45	1515	1.84	0.9415	0.8987	0.8537	0.8354
46	1589	1.88	0.9170	0.8626	0.8133	0.7942

Appendix 5C Continued

47	1665	1.92	0.8876	0.8220	0.7684	0.7494
48	1743	1.97	0.8542	0.7780	0.7210	0.7028
49	1823	2.01	0.8167	0.7314	0.6715	0.6538
50	1905	2.05	0.7759	0.6830	0.6212	0.6050
51	1989	2.09	0.7328	0.6338	0.5710	0.5558
52	2074	2.13	0.6878	0.5848	0.5216	0.5075
53	2162	2.18	0.6418	0.5368	0.4733	0.4611
54	2252	2.22	0.5956	0.4899	0.4272	0.4163
55	2343	2.26	0.5500	0.4448	0.3833	0.3736
56	2437	2.30	0.5054	0.4009	0.3420	0.3340
57	2533	2.34	0.4627	0.3605	0.3038	0.2968
58	2630	2.38	0.4218	0.3220	0.2683	0.2632
59	2730	2.43	0.3831	0.2860	0.2360	0.2322
60	2831	2.47	0.3469	0.2529	0.2067	0.2041
61	2935	2.51	0.3132	0.2230	0.1801	0.1796
62	3040	2.55	0.2820	0.1957	0.1565	0.1570
63	3148	2.59	0.2532	0.1712	0.1355	0.1370
64	3258	2.64	0.2269	0.1492	0.1166	0.1195
65	3369	2.68	0.2031	0.1299	0.1001	0.1045
66	3483	2.72	0.1813	0.1127	0.0858	0.0916
67	3599	2.76	0.1614	0.0977	0.0731	0.0800
68	3717	2.80	0.1436	0.0845	0.0620	0.0701
69	3836	2.84	0.1272	0.0728	0.0528	0.0620
70	3958	2.89	0.1128	0.0624	0.0451	0.0547
71	4082	2.93	0.0999	0.0539	0.0381	0.0488
72	4208	2.97	0.0881	0.0463	0.0318	0.0435
73	4336	3.01	0.0777	0.0398	0.0270	0.0388
74	4466	3.05	0.0683	0.0342	0.0226	0.0350
75	4599	3.10	0.0599	0.0294	0.0191	0.0319
76	4733	3.14	0.0526	0.0253	0.0159	0.0289
77	4869	3.18	0.0460	0.0217	0.0131	0.0266
78	5008	3.22	0.0403	0.0188	0.0111	0.0245
79	5149	3.26	0.0353	0.0161	0.0093	0.0224
80	5291	3.30	0.0308	0.0140	0.0075	0.0209
81	5436	3.35	0.0268	0.0121	0.0062	0.0196
82	5583	3.39	0.0233	0.0105	0.0052	0.0186
83	5732	3.43	0.0203	0.0092	0.0043	0.0175
84	5883	3.47	0.0176	0.0080	0.0036	0.0164
85	6036	3.51	0.0152	0.0069	0.0030	0.0156
86	6192	3.56	0.0130	0.0062	0.0024	0.0152
87	6349	3.60	0.0114	0.0054	0.0018	0.0148

	MC N10 - 02	**MC N10 - 03**	**MC N10 - 04**	**MC N10 - 05**
Peak Diam. (nm)	**1.67**	**1.59**	**1.51**	**1.51**
MW (peak)	**1238**	**1110**	**990**	**990**
Mw (calc.)	**1635**	**1527**	**1473**	**1474**
***Mn* (calc.)**	**1337**	**1266**	**1230**	**1227**
Mn /Mw	**1.22**	**1.21**	**1.20**	**1.20**

Appendix 5D - AsFlFFF fractograms for King Site water table monitoring well. Results of molecular weight calculations at end of table.

Time sec.	MW daltons	D_H nm	WTW June 6, 06	WTW July 11, 06	WTW Sept 29, 06	WTW Oct 16, 06
0	0	0.06	0.1328	-0.0911	0.1090	-0.0706
1	2	0.12	0.1328	-0.0911	0.1090	-0.0706
2	4	0.18	0.1328	-0.0911	0.1090	-0.0706
3	7	0.24	0.1328	-0.0911	0.1090	-0.0706
4	11	0.30	0.1328	-0.0911	0.1090	-0.0706
5	17	0.36	0.1328	-0.0911	0.1090	-0.0706
6	23	0.42	0.1328	-0.0911	0.1090	-0.0706
7	31	0.48	0.1328	-0.0911	0.1090	-0.0706
8	40	0.54	0.1328	-0.0911	0.1090	-0.0706
9	50	0.60	0.1328	-0.0911	0.1090	-0.0706
10	62	0.65	0.1328	-0.0911	0.1090	-0.0706
11	74	0.71	0.1328	-0.0911	0.1090	-0.0706
12	88	0.77	0.1328	0.1264	0.1090	0.2385
13	104	0.83	1.5031	1.5080	1.4592	1.6834
14	120	0.89	2.4368	2.4325	2.3872	2.5055
15	138	0.95	2.5681	2.5614	2.5283	2.5644
16	158	1.01	2.3814	2.3828	2.3540	2.3569
17	178	1.07	2.1393	2.1460	2.1190	2.1068
18	200	1.13	1.9185	1.9249	1.9016	1.8843
19	224	1.19	1.7353	1.7413	1.7203	1.7002
20	249	1.25	1.5848	1.5880	1.5679	1.5491
21	275	1.31	1.4605	1.4605	1.4451	1.4269
22	303	1.37	1.3540	1.3525	1.3406	1.3244
23	332	1.43	1.2653	1.2589	1.2517	1.2368
24	362	1.49	1.1907	1.1833	1.1783	1.1638
25	394	1.55	1.1290	1.1156	1.1141	1.1033
26	428	1.61	1.0757	1.0624	1.0612	1.0506
27	463	1.67	1.0331	1.0206	1.0181	1.0153
28	499	1.73	0.9976	0.9832	0.9835	0.9776
29	537	1.79	0.9685	0.9565	0.9553	0.9471
30	577	1.85	0.9465	0.9349	0.9355	0.9226
31	618	1.90	0.9302	0.9205	0.9221	0.9107
32	660	1.96	0.9217	0.9126	0.9144	0.9030
33	704	2.02	0.9202	0.9119	0.9130	0.9025
34	749	2.08	0.9217	0.9155	0.9151	0.9158
35	796	2.14	0.9295	0.9241	0.9235	0.9226
36	845	2.20	0.9394	0.9342	0.9327	0.9323
37	895	2.26	0.9522	0.9464	0.9447	0.9443
38	947	2.32	0.9650	0.9601	0.9588	0.9583
39	1000	2.38	0.9770	0.9731	0.9715	0.9740
40	1055	2.44	0.9863	0.9846	0.9835	0.9849
41	1111	2.50	0.9962	0.9925	0.9913	0.9940
42	1169	2.56	1.0019	0.9976	0.9969	0.9995
43	1228	2.62	0.9998	0.9976	0.9998	0.9996
44	1290	2.68	0.9934	0.9940	0.9962	0.9955
45	1352	2.74	0.9848	0.9853	0.9878	0.9860

Appendix 5D Continued

46	1417	2.80	0.9706	0.9702	0.9744	0.9711
47	1482	2.86	0.9472	0.9508	0.9532	0.9514
48	1550	2.92	0.9217	0.9248	0.9278	0.9251
49	1619	2.98	0.8925	0.8939	0.8974	0.8941
50	1690	3.04	0.8563	0.8586	0.8636	0.8588
51	1762	3.10	0.8187	0.8190	0.8255	0.8216
52	1836	3.15	0.7747	0.7780	0.7831	0.7792
53	1912	3.21	0.7307	0.7333	0.7365	0.7355
54	1989	3.27	0.6874	0.6887	0.6900	0.6882
55	2068	3.33	0.6412	0.6426	0.6413	0.6415
56	2149	3.39	0.5922	0.5951	0.5947	0.5924
57	2231	3.45	0.5446	0.5476	0.5453	0.5457
58	2315	3.51	0.4978	0.5029	0.4973	0.4990
59	2400	3.57	0.4523	0.4576	0.4528	0.4523
60	2488	3.63	0.4105	0.4158	0.4105	0.4087
61	2577	3.69	0.3707	0.3755	0.3710	0.3661
62	2667	3.75	0.3345	0.3366	0.3329	0.3278
63	2759	3.81	0.3004	0.3013	0.2983	0.2920
64	2853	3.87	0.2706	0.2711	0.2672	0.2585
65	2949	3.93	0.2415	0.2423	0.2390	0.2280
66	3046	3.99	0.2138	0.2178	0.2122	0.2011
67	3145	4.05	0.1861	0.1933	0.1875	0.1778
68	3246	4.11	0.1683	0.1732	0.1685	0.1533
69	3349	4.17	0.1478	0.1559	0.1508	0.1354
70	3453	4.23	0.1314	0.1400	0.1339	0.1193
71	3559	4.29	0.1194	0.1249	0.1198	0.1026
72	3666	4.35	0.1073	0.1120	0.1085	0.0901
73	3776	4.40	0.0966	0.1019	0.0972	0.0794
74	3887	4.46	0.0874	0.0932	0.0880	0.0700
75	4000	4.52	0.0782	0.0860	0.0795	0.0628
76	4114	4.58	0.0718	0.0788	0.0753	0.0575
77	4230	4.64	0.0647	0.0731	0.0682	0.0535
78	4348	4.70	0.0583	0.0680	0.0633	0.0488
79	4468	4.76	0.0540	0.0637	0.0584	0.0447
80	4590	4.82	0.0505	0.0594	0.0534	0.0406
81	4713	4.88	0.0498	0.0558	0.0492	0.0365
82	4838	4.94	0.0462	0.0536	0.0457	0.0336
83	4965	5.00	0.0420	0.0508	0.0421	0.0301
84	5093	5.06	0.0384	0.0479	0.0407	0.0272
85	5223	5.12	0.0413	0.0457	0.0393	0.0261
86	5356	5.18	0.0405	0.0428	0.0365	0.0244
87	5489	5.24	0.0377	0.0414	0.0358	0.0233
88	5625	5.30	0.0370	0.0414	0.0358	0.0229
89	5762	5.36	0.0370	0.0414	0.0330	0.0224
90	5902	5.42	0.0356	0.0400	0.0337	0.0212
91	6043	5.48	0.0334	0.0378	0.0337	0.0208
92	6185	5.54	0.0313	0.0385	0.0323	0.0203
93	6330	5.60	0.0327	0.0371	0.0315	0.0186
94	6476	5.65	0.0320	0.0371	0.0308	0.0175
95	6624	5.71	0.0334	0.0356	0.0315	0.0176
96	6774	5.77	0.0334	0.0349	0.0308	0.0165

Appendix 5D Continued

97	6926	5.83	0.0356	0.0335	0.0287	0.0160
98	7080	5.89	0.0356	0.0328	0.0280	0.0155
99	7235	5.95	0.0370	0.0320	0.0273	0.0156
100	7392	6.01	0.0363	0.0299	0.0266	0.0151
101	7551	6.07	0.0370	0.0284	0.0266	0.0140
102	7712	6.13	0.0377	0.0292	0.0259	0.0154
103	7874	6.19	0.0349	0.0292	0.0266	0.0161
104	8039	6.25	0.0363	0.0284	0.0259	0.0161
105	8205	6.31	0.0363	0.0292	0.0252	0.0175
106	8373	6.37	0.0363	0.0306	0.0245	0.0182
107	8543	6.43	0.0363	0.0299	0.0245	0.0177
108	8715	6.49	0.0363	0.0299	0.0252	0.0178
109	8889	6.55	0.0356	0.0292	0.0273	0.0191
110	9064	6.61	0.0363	0.0292	0.0266	0.0192
111	9241	6.67	0.0349	0.0284	0.0273	0.0187
112	9420	6.73	0.0349	0.0292	0.0280	0.0176
113	9601	6.79	0.0370	0.0284	0.0273	0.0189
114	9784	6.85	0.0370	0.0277	0.0273	0.0184
115	9969	6.90	0.0377	0.0284	0.0273	0.0179
116	10155	6.96	0.0370	0.0284	0.0266	0.0169
117	10344	7.02	0.0363	0.0284	0.0266	0.0164
118	10534	7.08	0.0370	0.0292	0.0259	0.0158
119	10726	7.14	0.0363	0.0299	0.0259	0.0154
120	10920	7.20	0.0370	0.0292	0.0266	0.0149
121	11116	7.26	0.0363	0.0284	0.0259	0.0138
122	11314	7.32	0.0370	0.0284	0.0245	0.0127
123	11513	7.38	0.0377	0.0284	0.0245	0.0134
124	11715	7.44	0.0377	0.0277	0.0245	0.0129
125	11918	7.50	0.0363	0.0277	0.0238	0.0130
126	12124	7.56	0.0363	0.0277	0.0238	0.0137
127	12331	7.62	0.0342	0.0284	0.0238	0.0139

	June 6, 06	**July 11, 06**	**Sept 29, 06**	**Oct 16, 06**
Peak Diam. (nm)	**2.62**	**2.62**	**2.62**	**2.62**
MW (peak)	**1228**	**1228**	**1228**	**1228**
Mw (calc.)	**1561**	**1569**	**1564**	**1548**
***Mn* (calc.)**	**1281**	**1286**	**1284**	**1278**
Mn /Mw	**1.22**	**1.22**	**1.22**	**1.21**

Appendix 5E - Diffusion Cell Models for Chloride, PSS 4800, 6500, and 15450.

Chloride

Modeled Day	Collection C/Co	Source C/Co
0	0.000	1.000
1	0.000	0.968
2	0.000	0.953
3	0.000	0.941
10	0.014	0.891
20	0.049	0.845
30	0.084	0.807
40	0.117	0.773
50	0.146	0.742
75	0.208	0.676
100	0.257	0.625
150	0.325	0.552
200	0.367	0.508
250	0.393	0.480
300	0.409	0.463
350	0.419	0.452
400	0.425	0.446
450	0.429	0.442
550	0.433	0.438

PSS 4800

Modeled Day	Collection C/Co	Source C/Co
0	0.000	1.000
1	0.000	0.962
2	0.000	0.939
3	0.000	0.921
10	0.000	0.840
20	0.000	0.772
30	0.000	0.725
40	0.000	0.689
50	0.000	0.660
75	0.000	0.603
100	0.000	0.562
150	0.000	0.502
200	0.000	0.459
250	0.000	0.427
300	0.000	0.401
350	0.000	0.380
400	0.000	0.361
450	0.000	0.346
550	0.001	0.320

PSS 6500

Modeled Day	Collection C/Co	Source C/Co
0	0.000	1.000
1	0.000	0.968
2	0.000	0.951
3	0.000	0.937
10	0.000	0.871
20	0.000	0.814
30	0.000	0.773
40	0.000	0.741
50	0.000	0.714
75	0.000	0.662
100	0.000	0.622
150	0.000	0.564
200	0.000	0.522
250	0.000	0.489
300	0.000	0.462
350	0.000	0.440
400	0.000	0.421
450	0.000	0.404
550	0.000	0.376

PSS 15450

Modeled Day	Collection C/Co	Source C/Co
0	0.000	1.000
1	0.000	0.972
2	0.000	0.956
3	0.000	0.944
10	0.000	0.888
20	0.000	0.837
30	0.000	0.799
40	0.000	0.770
50	0.000	0.745
75	0.000	0.695
100	0.000	0.657
150	0.000	0.601
200	0.000	0.559
250	0.000	0.526
300	0.000	0.499
350	0.000	0.476
400	0.000	0.456
450	0.000	0.439
550	0.000	0.410